Histology and Histopathology

From Cell Biology to Tissue Engineering

Volume 34 (Supplement 1), 2019

http://www.hh.um.es

XX CONGRESO DE LA SOCIEDAD ESPAÑOLA DE HISTOLOGÍA E INGENIERÍA TISULAR

VIII INTERNATIONAL CONGRESS OF HISTOLOGY AND TISSUE ENGINEERING

VI CONGRESO IBEROAMERICANO DE HISTOLOGÍA

September 4-6, 2019, Murcia, Spain

Organizan:

UNIVERSIDAD DE MURCIA

CAMPUS MARE NOSTRUM 37 38

Sociedad Española de Histología e Ingeniería Tisular

Patrocina:

f SéNeCa (+)
Agencia de Ciencia y Tecnología
Región de Murcia

Apoya:

Comité Iberoamericano de Histología
Tendiendo puentes, creando redes

Colaboran:

PROQUILAB s.a.

EDITORIAL MEDICA panamericana

Wolters Kluwer

HISTOLOGY AND HISTOPATHOLOGY

http://www.hh.um.es

This Journal publishes original and review articles in all fields of microscopical morphology, cell biology and tissue engineering; high quality is the overall consideration.

HISTOLOGY AND HISTOPATHOLOGY is an peer-reviewed international journal, the purpose of which is to publish original works in English in histology, histopathology and cell biology. Its format is the standard international size of 21 x 27.7 cm. One volume is published every year. Each volume consists of 12 numbers published monthly online. The printed version of the journal includes 4 books every year; each of them compiles 3 numbers previously published online. The **price** per volume 34 (2019) is 750 euros (only-online) or 800 euros (print+online+postage by surface mail). Impact factor: 2.015. Journal Citation Report® 2017, published by Thomson Scientific. SJR: 0.672 according to Scimago Journal Rank powered by Scopus® database 2017.

Subscriptions should be addressed to:

HISTOLOGY AND HISTOPATHOLOGY, Lorenzo Pausa 3, Entlo.B, E-30005 Murcia. Spain

NOTICE TO CONTRIBUTORS:

1. Submission of a paper to **HISTOLOGY AND HISTOPATHOLOGY** must be based on the tacit assurance that no similar paper, except for a preliminary report, has been or will be submitted for publication elsewhere. The decision on acceptance of manuscripts will be made on the basis of a peer review system.

2. **The first page** should contain the full title, the author's name(s), place of work, postal and e-mail addresses for correspondence and a short running title (no more than 40 spaces).

3. For indexing purposes, a small number of “key words” (no more than 5) must be supplied.

4. **The text** should be preceded by a short summary not exceeding 250 words and should then proceed to sections of Introduction, Materials and methods, Results, Discussion, Acknowledgements and References.

5. Do not divide words at the end of lines. Pages should be numbered consecutively in arabic numerals. Tables, footnotes and figure legends including magnifications, should be submitted on separate sheets. Tables and figures should be referred in the text as (Table 1), (Fig. 1)...

6. **References** to the literature should be cited in the text by the name of the author(s) followed by the year of publication. In cases in which there are more than two authors, only the first is named, followed by “et al.”. Examples: Smith (1980) reported that...; (Smith, 1980, 1982); (Smith and Tanaka, 1980); (Smith et al., 1980). Suffixes a, b, etc., should be used following the year to distinguish two or more papers by the same author(s) published in the same year; example (Smith, 1981a). When two or more references are included in the same bracket, they must be quoted in the chronological order; example (Smith, 1980; Bell et al., 1984).

7. The reference list should be in alphabetical order. References to articles in periodical publications must include: Names and initials of all authors, year of publication, complete title of paper, name of journal (abbreviated in accordance with PubMed), number of volume, and first and last page numbers. Example:

Morita T., Suzuki Y. and Churg J. (1973). Structure and development of the glomerular crescent. Am. J. Pathol. 72, 349-368.

Reference to books must include: Name and initials of authors, year of publication, full title, edition, editor, publisher, place of publication and page numbers. Example:

Powell D. and Skrabanek P. (1981). Substance P. In: Gut Hormones. 2nd ed. Bloom S.R. and Polak J.M. (eds). Churchill Livingstone. Edimburgh. pp 396-401.

8. **Illustrations** should not exceed 17.8 x 22.2 cm. The Editor reserves the right to reduce or enlarge the illustrations. Apply figure numbers to the lower left-hand corner of each photograph and the scale bar at the lower right-hand corner. Images should be TIFF file format, preferentially, although other formats could be useful (jpg, ppt, etc). Black and white figures must be at gray scale. Color figures should be preferentially in CMYK, but RGB is also allowed. Line art files must have a 500dpi resolution, while other images must have a 300dpi resolution.

9. **Charges to authors**: The authors are requested to cover part of the publication cost (each article with black and white figures: 600 euros; articles with color pages: 900 euros for one color page + 50 euros per additional colour page). **Open access** publication is available at a additional rate of 1,000.00 euros (the paper will be published on the Creative Commons CC-BY license). The authors receive **25 reprints** free of charge. The charge for reprints exceeding this number is 25 ¢ per page each copy.

10. **Electronic submission.** The articles must be uploaded to http://www.editorialmanager.com/hh, The text document must be saved as Word or rtf format. Tables must be included in the text document. Figures must be saved in the formats and at the resolution indicated in point 8 (Illustrations).

Committees

Honor Committee

Chairman
Su Majestad el Rey Don Felipe VI

Members
Sr. D. Pedro Duque Duque
Ministro de Ciencia, Innovación y Universidades

Sr. D. José Francisco Ballesta Germán
Alcalde del Excmo. Ayuntamiento de Murcia

Sr. D. José Luján Alcaraz
Rector Magnífico de la Universidad de Murcia

Sra. Dña. Carmen Robles Moreno
Decana de la Facultad de Medicina Universidad de Murcia

Sr. D. Pablo Ramírez Romero
Director del Instituto Murciano de Investigación Biosanitaria Virgen de la Arrixaca

Organizing Committee

Chairmen
Luis Miguel Pastor García and Juan Francisco Madrid Cuevas

Vicechairwoman
Ester Beltrán Frutos

Secretary
Vicente Seco Rovira

Members
Manuel Avilés Sánchez
María José Izquierdo Rico
María Jiménez Movilla
María Teresa Castells Mora
José Ángel Martínez Menarguez
Jesús Martínez Hernández
Marisa Serrano Sánchez
Enrique Poblet Martínez

Scientific Advisory Committee

Chairwoman

Concepción Ferrer Cazorla

Secretary

Emma Martínez Alonso

Members

Alaminos Mingorance, Miguel (Universidad de Granada, España)
Alonso Varona, Ana (Universidad del País Vasco, España)
Álvarez Vázquez, Pilar (Universidad Complutense, España)
Arévalo Gómez, Miguel Ángel (Universidad de Salamanca, España)
Arriazu Navarro, Riánsares (Universidad CEU-San Pablo, España)
Bernabé Salazar, Antonio (Universidad de Murcia, España)
Buján Varela, Julia (Universidad de Alcalá, España)
Calvo Martín, Juan José (Universidad de la República, Uruguay)
Campos Muñoz, Antonio (Universidad de Granada, España)
Crespo Ferrer, Pascual Vicente (Universidad de Granada, España)
De Juan Herrero, Joaquín (Universidad de Alicante, España)
Díaz-Flores Feo, Lucio (Universidad de La Laguna, España)
García Caballero, Tomás (Universidad de Santiago de Compostela, España)
García Honduvilla, Natalio (Universidad de Alcalá, España)
García Lorenzana, Mario (Universidad Autónoma de Metropolitana, México)
Garrido Fariña, Germán Isauro (Universidad Nacional Autónoma de México, México)
Garrosa García, Manuel (Universidad de Valladolid, España)
Gayoso Rodríguez, Manuel (Universidad de Valladolid, España)
Gómez Torres, María José (Universidad de Alicante, España)
Guzmán García, Xochitl (Universidad Autónoma Metropolitana, México)
Hilario Rodríguez, Enrique (Universidad del País Vasco, España)
Kierszenbaum, Abraham (City University of New York, USA)
Martín Lacave, Inés (Uniersidad de Sevilla, España)
Martínez Ramírez, Alfredo (CIBIR, España)
Montuenga Badía, Luis (Universidad de Navarra, España)
Morales, Carlos R (McGill University, Canada)
Moreno Durán, Carmen Helena (Univesidad Distrital Francisco José de Caldas, Colombia)
Navarro Incio, Ana María (Universidad de Oviedo, España)
Noguera Salvá, Rosa (Universidad de Valencia, España)
Parrado Romero, Concepción (Universidad de Málaga, España)
Peinado Herreros, María de los Ángeles (Universidad de Jaén, España)
Peña Amaro, José (Universidad de Córdoba, España)
Redondo García, Eloy (Universidad de Extremadura, España)
Romero Díaz, Viktor (Universidad Autónoma de Nuevo León, México)
Ruiz Saurí, Amparo (Universidad de Valencia, España)
Sáez Crespo, Francisco José (Universidad del País Vasco, España)
Salido Pericaula, Mercedes (Universidad de Cádiz)
Santafé Martínez, Manel (Universidad Rovira y Virgili, España)
Santamaría Solís, Luis (Universidad Autónoma de Madrid, España)
Sanz-Ochotorena, Ana (Universidad de La Habana, Cuba)
Trejo Iriarte, Cynthia (Universidad Autónoma de México, México)
Zaidan Dagli, María Lucía (Universidad de Sao Paulo, Brasil)
Rodriguez-Martinez, Heriberto (Universidad de Linköping, Suecia)
Zaccone, Giacomo (Universidad de Messina, Italia)

Index

Plenary Conferences

Opening Conference

Marco G. Alves
Department of Microscopy, Laboratory of Cell Biology, Abel Salazar Institute of Biomedical Sciences (ICBAS), Unit for Multidisciplinary Research in Biomedicine, Abel Salazar Institute of Biomedical Sciences (UMIB-ICBAS), University of Porto, Portugal

Plenary Conference

Lucio Díaz-Flores
Department of Basic Medical Sciences, Faculty of Medicine, University of La Laguna, Tenerife, Spain

Closing Conference

Ana Belén Sanz Bartolomé
Laboratorio de Nefrología, IIS-Fundación Jiménez Diaz-UAM, Madrid

Histology and Histopathology
From Cell Biology to Tissue Engineering

Sertoli cell: New perspectives

Alves M.G.
Unity for Multidisciplinary Research in Biomedicine & Institute of Biomedical Sciences Abel Salazar, University of Porto, Portugal

In the 19th century, Enrico Sertoli described the testicular somatic cells with irregular shape that are nowadays known as Sertoli cells (SCs). These cells were proven to form intercellular connections that were later known as the blood-testis barrier. This barrier separates the interstitial from the intratubular fluid where developing germ cells are bathed in an immune-privileged environment. Thus, Sertoli cells control the passage of substances and metabolites for the compartment where germ cells develop. One of the most relevant mechanisms for spermatogenesis is the metabolic cooperation that is established between SCs and developing germ cells. In brief, the former produce the lactate consumed by the latter that can only use that substrate as energy source. In addition, the distinct energetic needs during the different stages of spermatogenesis are also controlled by SCs. This topic has been somewhat overlooked but the worldwide considerable decrease in sperm quality, associated with the pandemic increase of metabolic diseases, has brought it into spotlight. Indeed, the pandemic increase of overweight/obese and (pre)diabetic individuals has been consistently followed by a decrease on male fertility.

The majority of studies aiming to correlate metabolic diseases with male infertility are focused on sperm quality as the most relevant outcome. Nevertheless, the impact of hormonal dysfunction and metabolite shifting caused by those diseases in the testis, particularly in SCs, remain largely unknown. New evidences show that in both cases, the nutritional support of spermatogenesis can be severely altered. From a histological perspective, alterations are well reported but the molecular mechanisms responsible for such alterations remained unknown until recently. Signalling pathways, such as the mammalian target of rapamycin (mTOR), have emerged as crucial mediators for the energetic status of the individuals and their reproductive potential pinpointing a clinical significance for those pathways. Nevertheless, these remarkable cells present some unique features that go far beyond the physical and nutritional support of spermatogenesis.

New techniques and novel ways to study SCs physiology and function will be discussed. For instance, 3D co-culture systems with SCs:germ cells or molecular approaches performed in human SCs derived from testicular biopsies can provide us further knowledge on the molecular mechanisms controlled by these cells and with relevance for spermatogenesis. On one hand, new data can provide essential information to improve the fertility of males; on the other hand, it can identify specific targets to the development of an effective male contraceptive. Overall, the study of SCs is an emerging field of research for researchers interested in the understanding of the molecular mechanisms responsible for male (in)fertility. Ultimately, those studies may highlight new therapeutic targets for the control of male fertility.

Histology and Histopathology
From Cell Biology to Tissue Engineering

Intussusceptive angiogenesis and lymphangiogenesis

Díaz-Flores L.
Department of Basic Medical Sciences, Faculty of Medicine, University of La Laguna, Tenerife, Spain

Intussusceptive angiogenesis (IA) can be defined as the processes by which blood vessels split and remodel through the formation of transluminal small pillars/posts (diameter ≤2.5 μm), large pillars (diameter >2.5 μm), and folds, which form pillars when spanning opposite vessel walls. The presence of these intravascular structures is the principal indicator of IA (pillars hallmarks of intussusception). This process leads to expansion (intussusceptive microvascular growth), arborisation (intussusceptive arborisation), branching remodelling (intussusceptive branching remodelling) and/or segmentation of the vasculature. In this field, we have demonstrated the role of IA in vascular diseases, including intravascular papillary endothelial hyperplasia (IPEH), dilated hemorrhoidal veins in hemorrhoidal disease, sinusoidal hemangioma and in experimental conditions. Also, we contribute the role of IA in lobular capillary hemangioma. In all these processes, in addition to the expansion of the microvasculature, IA has a morphogenic action of the lesions. We also demonstrate the involvement of intussusception in lymphatic vessels: intussusceptive lymphangiogenesis (IL), which has been largely ignored. These studies on IL, using immunohistochemical procedures, serial histologic sections and confocal microscopy, were undertaken in the sinuses of developing human foetal lymph nodes, in lymphatic pathological conditions (lymphangiomas / lymphatic malformations) and vascular transformation of lymph node sinuses. Consequently, new roles are given to vessel intussusception, including the modulation of lymphatic lesions and the formation of the meshwork of intraluminal processes in LN sinuses, with a known important immunological function.

Histology and Histopathology
From Cell Biology to Tissue Engineering

Mechanisms of programmed necrosis in kidney diseases

Martin-Sánchez D., Fontecha-Barriuso M., Ortiz A. and Sanz A.B.
Laboratorio de Nefrología, IIS-Fundación Jiménez Diaz-UAM, Madrid

Acute kidney injury (AKI) results in a usually transient decrease in renal function. AKI increases mortality and chronic kidney disease progression. However, therapy is only symptomatic. Pathogenesis-based therapy is needed. Inflammation and cell death are key features of AKI. In recent years, our understanding of the mechanisms of tubular cell death has improved but there are ongoing discussions on the timing or molecular regulators involved. Morphologically, both apoptosis and necrosis were observed. Apoptosis, as a regulated form of cell death, was an attractive therapeutic target. However, no therapy targeting apoptosis is in clinical use. More recently, interventional evidence of the involvement of different forms of regulated necrosis in experimental AKI has emerged. Contrary to apoptosis, regulated necrosis is immunogenic and pro-inflammatory as dying cells release DAMPs, amplifying sterile inflammatory responses. Of regulated necrosis pathways potentially involved in AKI (necroptosis, ferroptosis, pyroptosis, mitochondria permeability transition-regulated necrosis), there is strong evidence for the involvement of ferroptosis and fnecroptosis. Now, we review the specific role of different cell death pathways during AKI and their contribution to renal inflammation with emphasis on the timing of event, a key feature that will influence potential diagnostic and therapeutic implications. We recently showed that experimental AKI is characterized by an early wave of ferroptosis. AKI is prevented by pre-treatment with ferroptosis inhibitors. However, AKI is usually diagnosed AFTER damage and decreased kidney function have occurred. Ferroptosis triggers local inflammation and an inflammation-dependent secondary wave of necroptosis. Continuous targeting necroptosis was protective even when started after induction of AKI.

Simposiums

Histology Applied to Experimental Pathology

Histology and Animal Reproduction

Histology and Aging

Histology in Regenerative Medicine and Tissue Engineering

Innovation in Histology Teaching

Simposium:

Histology Applied to Experimental Pathology

Luis Santamaría Solís
Department of Anatomy, Histology, and Neurosciences, School of Medicine, UAM, Madrid, Spain

Pablo Pelegrin
Scientific Deputy Director & Principal Investigator BioMedical Research Institute of Murcia (IMIB-Arrixaca), Hospital Virgen de la Arrixaca de Murcia, Murcia, Spain

Alfonso Calvo Gonzalez
Researcher Laboratory 2.03, Solid Tumors and Biomarkers Program Center for Applied Medical research (CIMA), Universidad de Navarra, Pamplona, Spain

Francisco Guardiola Abellán
Department of Cell Biology and Histology, Faculty of Biology, University of Murcia, Murcia, Spain

Histology and Histopathology
From Cell Biology to Tissue Engineering

Estimate of patterns of nuclear distribution and tissue heterogeneity using second-order stereology in ventral rat prostate in a pharmacological castration model

Santamaría L.

Department of Anatomy, Histology, and Neurosciences, School of Medicine, UAM, Madrid, Spain

The comparison between global and local changes in the spatial patterns of histological lesions has aroused increasing interest in some fields. However, there is little data on this subject in the field of prostatic pathology. Recently, several studies have estimated acinar or stromal parameters at the local level in normal and pathological human prostate, using stereological methods of second order. For example: the analysis of the population distribution of cell nuclei and the isotropy of prostatic acini in cancer, etc. The present study deals with the application of second-order stereology methods to investigate changes in the spatial distribution of acini and nuclei of the acinar epithelium in prostate from normal rats and from animals subjected to pharmacological castration by treatment with cyproterone acetate. The androgen deprivation causes in the prostate of the rat regressive alterations due to the decrease of the epithelial cells by apoptosis and to the stromal reorganization. In this regard, cyproterone acetate (CA), currently used in anti-androgenic therapy for prostate cancer, is a potent and specific antagonist of androgens in competition with dihydrotestosterone in binding with its specific receptors. In addition, CA has antigonadotropic action due to the chemical similarity with progesterone, which causes a decrease in the supply of luteinizing hormones and, therefore, the decrease in testicular testosterone production.

Two stereological parameters related to the distribution of the epithelial nuclei and to the conformation of the prostatic acini were used, both in normal (control cases) and treated (pharmacologically castrated) rats. On sections stained with hematoxylin-eosin the following parameters were estimated: 1) Function K: K (r) evaluates the distribution of the centers of mass of the cell nuclei as a function of the internuclear distance (r). 2) Lacunarity: Λε, evaluates the heterogeneity of the distribution of tissue structures by evaluating the pattern of the hole arrangement between these structures.

The following results have been obtained: 1) Both in the control animals and in the rats treated with CA, the arrangement of the nuclei of the prostatic acinar epithelium follows a significantly different grouping pattern of a CSR (complete spatial randomness) distribution. 2) However, this pattern tends to a CSR distribution in internuclear distances greater than 150 μm. 3) The pattern of attraction of the nuclei (clustering) is significantly higher in control rats compared to those castrated in a range of distances between 25 and 90 μm. In this interval of internuclear distances it seems that the epithelial cells of the prostatic acini treated with CA tend to distribute more CSR-like than the controls. 4) These changes in the distribution of nuclei do not seem to significantly affect the acinar architecture: the tissue heterogeneity estimated by lacunarity is similar in controls and treated animals.

Histology and Histopathology
From Cell Biology to Tissue Engineering

Cellular morphological features of inflammasome activation and pyroptotic cell death

Pelegrín P.
Instituto Murciano de Investigación Biosanitaria IMIB-Arrixaca, Murcia, Spain

Pyroptosis has been classically defined as an inflammasome-dependent type of cellular necrotic death and an effector mechanism of the inflammasome as a consequence of the activation of inflammatory caspases (namely caspase-1/-4/-5/-11). The term pyroptosis was chosen, from the Greek 'pyro' (meaning fire or fever) and 'ptosis' (meaning to fall), to underline the pro-inflammatory nature of this type of cell death, and its link to the release of mature IL-1ß and IL-18 cytokines. However, recently it is known that pyroptosis is not necessarily linked to the release of cytokines, since the identification of gasdermin D as the pyroptosis executor, has demonstrated that pyroptosis could be induced without the need of caspase activation. Gasdermin D belongs to the gasdermin family of proteins, and all the members of this protein family are able to induce pyroptotic cell death, uncoupled to inflammasome, inflammatory caspases and cytokine release. Therefore, the term pyroptosis is nowadays redefined as a 'gasdermin-induced necrotic cell death', and applies to all gasdermin family members that cause cell death by membrane permeabilization. The gasdermins are a new family of cell death effectors that consist of a cytotoxic N-terminal domain and a C-terminal repressor domain connected by a flexible linker. Proteolytic cleavage between these two domains releases the intramolecular inhibition on the cytotoxic domain, allowing it to insert into cell membranes and to form large oligomeric membrane pores, which disrupt ion homeostasis and induce cell death. Pyroptosis execution is linked to specific morphological features that have been described in recombinant cellular systems as well as immune-related cells. Morphological changes of pyroptosis in cells include plasma membrane permeabilization, presence of a big cellular bleb, mitochondrial swelling, and the presence of large intracellular protein oligomers in the case of inflammasome activation. These features, will help to identify pyroptotic cells in tissues.

Histology and Histopathology
From Cell Biology to Tissue Engineering

Multispectral immunophenotyping for the study of tumor microenvironment and response to immunotherapy

Calvo A.
IDISNA and Program in Solid Tumors, Center for Applied Medical Research (CIMA) and Department of Pathology, Anatomy and Physiology, School of Medicine, CIBERONC, ISC-III, Spain

Multiplexed platforms to detect and quantify simultaneously several markers in paraffin-embedded tissue sections have been recently developed. Multiplexed assays provide a high volume of tumor biological information through multidimensional data on tissue architecture, spatial distribution of multiple cell phenotypes and co-expression of markers. These technologies are extremely useful to identify immune subpopulations within tumors in order to understand better how the tumor microenvironment (TME) affects cancer growth and to identify predictors of response to immunotherapy. Among the different multiplex platforms, Vectra Polaris (Akoya/Perkin Elmer) developed a workflow that uses Opal fluorochromes conjugated with the Tyramide signal amplification (TSA) system, which allows the simultaneous fluorescent labelling of up to 6 markers plus DAPI (for nuclear staining). This method can be applied in an automated fashion using the Leica Bond RX or another autostainer to evaluate clinical samples. Using multispectral image analysis with Inform software™ involves tissue segmentation, cell segmentation and phenotyping to quantify the number of cells with a particular phenotype. We are applying this technology to study tumor infiltrating lymphocytes (TILs) in lung cancer specimens in association with genetic alterations determined by next generation sequence (NGS).

Recent studies have shown the advantages of using this technology for the identification of immune cell phenotypes that can be used as biomarkers of response to immunotherapy in cancer. Such studies can also be performed in mouse models of cancer in order to evaluate the TME in relation to certain genetic mutations and to assess the effectiveness of novel immunotherapeutic regimes. For example, our studies show that certain genetic alterations in lung adenocarcinomas are associated with a significant increase in the number of CD3+/CD8+ immune cell infiltration when anti-PD-1 immunotherapy is administered in these mice. We are also investigating mechanisms of resistance to immunotherapy in murine models due to mutations of lung cancer-related genes.

In conclusion, multispectral immunophenotyping in paraffin-embedded tissues is a very promising technique to study the TME and for the identification of biomarkers of response to immunotherapy.

Histology and Histopathology
From Cell Biology to Tissue Engineering

Histopathological study in the European eel (*Anguilla anguilla* L.) challenged with *Vibrio anguillarum* and *Tenacibaculum soleae*

Guardiola F.A.[1,2], Conforto E.[3], Vílchez-Gómez L.[1], Esteban M.A.[1] and Cammarata M.[3]

[1]Department of Cell Biology and Histology, Faculty of Biology, University of Murcia, 30100, Murcia, Spain, Campus of International Excellence, *Campus Mare Nostrum*, [2]Interdisciplinary Centre of Marine and Environmental Research (CIIMAR), University of Porto, Terminal de Cruzeiros do Porto de Leixões, Portugal, [3]Marine Immunobiology laboratory, Department of Earth and Marine Sciences, University of Palermo, Palermo, Italy
faguardiola@um.es

European eel (*Anguilla anguilla*) is a traditional consumer food on the Mediterranean coast of Spain. At the production level, one of the most important factors that affect the European eel culture is the incidence of various diseases, especially those caused by bacterial pathogens. In recent years, studies on the prevention of their diseases have focused on the isolation of pathogens and medical treatment. However, little attention has been paid to histological alterations in the main defense barriers (e.g. skin and gills) of European eel.

European eels were randomly divided into three experimental groups of 8 specimens each stored in six tanks (50 L): *i)* control group was injected intraperitoneally with sterile medium TSB; *ii)* and *iii)* groups were injected intraperitoneally with *Vibrio anguillarum* and *Tenacibaculum soleae* [10^7 Colony Forming Unit (CFU) ml^{-1}]. At 72 hours, the fish of each tank were sacrificed. The skin, gills and liver were fixed (Bouin's solution, 24 h). After serial dehydration steps in alcohol, the samples were embedded in paraffin, sectioned (6 µm), mounted and stained with haematoxylin and eosin (H&E) and Gomori trichrome. Slides were analysed by a light microscope (Leica DM750) and images were acquired with a Leica MC170 digital camera for analysis.

In the gills of specimens infected with *V. anguillarum* was observed vasodilation with blood congestion, epithelial uplift, lamellar disorganization and aneurysm of the primary filament. In the case of fish challenged with *T. soleae*, cellular hypertrophy, cellular hyperplasia and partial fusion of secondary lamellae. In the specimens infected with *V. anguillarum* an overall loss of hepatic tissue structure can be seen with an increase in hepatic sinusoidal spaces and the presence of some hepatocytes with pyknotic nuclei. The liver of specimens infected with *T. soleae* shows hepatocytes with irregularly nuclei, sometimes hypertrophic. In particular, we observed a strong presence of goblet cells on the epidermis surface in the specimens inoculated with both pathogens. Therefore, the present study provides a baseline about the histological alterations caused by these bacteria in European eel.

F.A. Guardiola thanks the *Fundación Séneca de la Región de Murcia* (Spain) for his grant (Saavedra Fajardo program, Grant no. 20407/SF/17). This work was supported by the MINECO (grant no. AGL2014-51839-C5-1-R) co-funded by the European Regional Development Funds (ERDF/FEDER) and *Fundación Séneca de la Región de Murcia* (Grupo de Excelencia grant no. 19883/GERM/15).

Simposium:

Histology and Animal Reproduction

Francisco J. Barrionuevo Jiménez
Department of Genetic, Faculty of Sciences, University of Granada, Granada, Spain

Jordi Roca Aleu
Department of Medicine and Animal Surgery, Faculty of Veterinary, University of Murcia, Murcia, Spain

Marc Yeste
Unit of Cell Biology, Department of Biology, Univerisity of Girona, Girona, Spain

Histology and Histopathology
From Cell Biology to Tissue Engineering

Role of the microRNA cluster mir-106b-25 and its paralogue mir-17-92 in the regulation of the spermatogenic cycle

Hurtado A.[1], Palominos-Morales R.[2], Georg I.[3], Lao M.[1], Real F.M.[1], Carmona F.D.[1], Burgos M.[1], Jiménez R[1]. and Barrionuevo F.[1]

[1]Departamento de Genética, Universidad de Granada, Granada, Spain, Instituto de Biotecnología, Centro de Investigación Biomédica, Universidad de Granada, Armilla, Granada, Spain, [2]Departamento de Bioquímica y Biología Molecular I, Universidad de Granada, Granada, Spain, Instituto de Investigación Biosanitaria de Granada, Universidad de Granada, Centro de Investigación Biomédica, Armilla, Granada, Spain, [3]Centro de Genómica e Investigación Oncológica (GENYO), Pfizer-Universidad de Granada-Junta de Andalucía, PTS, Granada, Spain

Micro-RNAs (miRNAs) are small non-coding RNAs (~22 nucleotides) that regulate gene function at the post-transcriptional level. The *miR-17-92* cluster is a polycistronic miRNA gene encoding six members. In human and mice, two paralog clusters exist, the *miR-106a-363* cluster, comprising 6 miRNAS, and the *miR-106b-25* cluster, with 3 members. The members of the *miR-17-92* and *miR-106b-25* cluster are highly conserved in vertebrates, expressed in practically all tissues analyzed, and its absence is associated to developmental disorders and cancer. They are also expressed in germ cells of the testis and conditional inactivation of the *miR-17-92* cluster in either embryonic germ cells or the whole adult testis resulted in spermatogenic defects. In contrast, *miR-106b-25* null mice are fertile and no testicular phenotype was previously described.

We have performed a detailed histological, hormonal and molecular analysis of the testicular function of *miR-106b-25* mutant mice. We also generated double *miR-106b-25* and *miR-17-92* knockout mice to study a possible functional redundancy of both clusters during testicular function.

We found a 30% reduction of the testis mass and a 40% reduction in the epididymal sperm content in *miR-106b-25*$^{-/-}$ mice when compared to controls. Accordingly, we obtained an average Johnsen's score of 9.2 and 7.5 in control and mutant testes, respectively. We also checked DMC1, a marker of leptotene to pachytene spermatocytes and found a similar pattern of positive and negative DMC1 tubules in both control and mutant mice. However, the percentage of DMC1 positive tubules was almost two fold in the mutant when compared to the control. RNA-seq analysis of mutant and control testes showed that replicate samples of the same condition clustered together, indicating that a significant and consistent alteration of the testis transcriptome takes place when *miR-106b-25* is deleted. We identified more than 2000 deregulated genes and a Gene Ontology analysis of these genes showed enrichment in categories such as cell cycle and reproduction, microtubule process, mRNA processing and ubiquitination and catabolism. Subsequently, we performed *in vitro* and *in silico* assays to check the extent of the alterations in these pathways. Despite these alterations in the spermatogenic cycle, fertility appeared to be normal in *miR-106b-25* null mice. Interestingly, the expression of *miR-17-92* was upregulated in the testes of these mice, indicating that *miR-17-92* could compensate for the absence of *miR-106b-25.* To test this hypothesis, we generated *miR-106b-25* and *miR-17-92* double knockout mice, which showed a significant idiopathic weight reduction. Testis mass, epididymal sperm content and Johnsen's score were reduced in the double mutants when compared to controls. Finally, monitored mating experiments showed that fertility was severely reduced in the double mutants.

Our studies show that the *miR-106b-25* cluster is necessary for proper function of the spermatogenic cycle and that, together with *miR-17-92,* is required for the maintenance of the fertility.

Histology and Histopathology
From Cell Biology to Tissue Engineering

Transforming growth factor -β1, -β2, and -β3 in the male reproductive tract: findings from the pig animal model

Roca J.[1], Barranco I.[1], Padilla L.[1], Martínez-Hernández J.[2], Álvarez-Rodríguez M.[3], Martínez E.A.[1], Pastor L.M.[2], Rodríguez-Martínez H.[3] and Parrilla I.[1]

[1]Department of Medicine and Animal Surgery, [2]Department of Cell Biology and Histology, IMIB-Arrixaca, Regional Campus of International Excellence "Campus Mare Nostrum", University of Murcia, Spain, [3]Department of Clinical and Experimental Medicine, Linköping University, Sweden

The transforming growth factor-β (TGF-β) is a superfamily of polypeptides involved in regulating fundamental cell roles such as proliferation, differentiation, migration, survival/apoptosis and immune response. Three TGF-β isoforms, specifically β1, β2, and β 3, are ubiquitous in mammalian tissues. Particularly abundant in reproductive tissues, they are involved in their development and cyclic remodeling, as in germ-cell proliferation and differentiation. Their imbalance in bioavailability results in reproductive disorders, including infertility. This overview aims to evidence the synthesis and bioavailability of TGF-β1, -β2 and -β3 in the reproductive tract of adult, healthy and fertile male pigs used for producing semen doses for artificial insemination (AI). The swine species is an excellent animal model for human, and breeding boars, routinely replaced by younger males with superior genetics when still healthy and fertile, makes it possible to collect healthy reproductive organs at the abattoir and compare source of synthesis with semen bioavailability within the same male. Moreover, with each boar producing AI-doses to inseminate more than 5,000 sows per year, provides accurate measurements of fertility and prolificacy (litter size).

Immunohistochemistry, using polyclonal primary antibodies, in samples from the testis, epididymis (caput, corpus and cauda segments) and accessory sex glands (seminal vesicles, prostate and bulbourethral), evidenced that the three TGF-βs were expressed throughout the genital organs, without clear differences in expression among males. The TGF-βs were most specifically localized in Leydig cells, the principal cells and the surrounding smooth muscle of the entire epididymis and in the glandular cytoplasm of accessory sexual glands, mainly the seminal vesicles. The secreted TGF-βs are measurable in semen, in both spermatozoa and seminal plasma (SP). Immunohistochemistry and imaging flow cytometry have revealed that mature spermatozoa retrieved from the cauda epididymis and the ejaculate expressed the three TGF-βs, depicting differential staining patterns in head, midpiece and tail. The TGF-βs in SP flow free or within extracellular vesicles. A pre-coated magnetic beads assay kit demonstrated that pig SP is rich in TGF-βs, particularly in β1 and β2, whose availability differed among males. Using the same kit, it was also demonstrated that SP extracellular vesicles, either exosomes or microvesicles, carried TGF-βs.

The seminal TGF-βs would be involved in reproductive success once delivered into the female reproductive tract, linked to their role in regulating local immune responses of female reproductive tissues towards maternal tolerance of foreign spermatozoa and SP-proteins. In this way, they would facilitate both sperm survival into the female reproductive tract and subsequent embryo development and implantation, an assumption supported by the documented positive relationship between pig seminal TGF-β1 and in vivo fertility (both farrowing rate and litter size).

The experiments leading to the above results were funded by MINECO & FEDER UE-Funds (BES-2016-07604, AGL2015-69738-R), Madrid; Seneca Foundation (19892/GERM/15), Murcia, Spain; and FORMAS (2017-00946), Stockholm, Sweden.

Histology and Histopathology
From Cell Biology to Tissue Engineering

Presence, function and relevance of aquaporins in the reproductive tract, gametes and embryos

Delgado-Bermúdez A.[1], Rivera del Álamo M.M.[2], Llavanera M.[1], Catalán J.[2], Recuero S.[1], Mateo Y.[1], Barranco I.[1], Fernandez-Fuertes B.[1], Rodríguez-Gil J.E.[2], Bonet S.[1], Miró J.[2] and Yeste M.[1]

[1]Unit of Cell Biology, Department of Biology, University of Girona, Spain, [2]Unit of Animal Reproduction, Department of Animal Medicine and Surgery, Autonomous University of Barcelona, Spain

Aquaporins (AQPs) are integral, transmembrane proteins that were discovered by Peter Agre's group in 1992. Since then, several studies identified up to 13 AQPs, and demonstrated that they play a crucial role for the transport (facilitated diffusion) of water and solutes across cell membranes. These 13 AQPs are classified into three different subfamilies according to their sequence and substrate selectivity: orthodox AQPs, aquaglyceroporins and superaquaporins. In the case of reproductive physiology, previous research showed that AQPs are ubiquitously expressed in the reproductive tissues and organs (including testis, efferent ducts, epididymis, endometrium and placental transference zone, amongst others), gametes and embryos. The precise function of each AQP relies on the cell type, but in most cases, they are involved in the regulation of cell volume and/or in the composition of luminal fluids. For example, AQP1 and AQP9 are involved in the secretion/reabsorption dynamics of luminal fluid during sperm transport and maturation in the efferent ducts and epididymis. On the other hand, the distribution of AQP2 and AQP8 in the female tract appears to play a crucial role during pregnancy and relies on serum progesterone levels. In gametes and embryos, aquaglyceroporins, which do not only allow water but also cryoprotectants to pass through cell membranes appear to be related to cell cryotolerance. In the case of mammalian spermatozoa, previous studies conducted in human, mouse, boar, bull and stallion spermatozoa have demonstrated that aquaglyceropins AQP3 and AQP7, orthodox AQP8 and superaquaporin AQP11 are the main sperm-AQPs and are mostly implied in the regulation of sperm volume, which is crucial during spermatogenesis and sperm transport throughout male and female reproductive tracts. Interestingly, AQP3, AQP7 and AQP11 have been identified as cryotolerance markers in boar, bull and stallion spermatozoa, and recent studies using different inhibitors have suggested that aquaglyceroporins rather than orthodox AQPs are involved in the transport of glycerol and are related to sperm cryotolerance. In the case of oocytes, it has been demonstrated that exogenous expression of AQP3 and AQP7 increase their permeability to water and cryoprotectants, and improves cell survival after vitrification/warming. Finally, AQP3 has also been identified to be crucial for embryo cryotolerance. All these data support that AQPs are involved in a myriad of functions that are crucial for reproductive physiology. Furthermore, the fact that aquaglyceroporins are related to cell cryotolerance suggest that further knowledge on these proteins may increase the yield of cryopreservation protocols for reproductive tissues, gametes and embryos, which are a crucial strategy for fertility preservation not only in humans, but also in livestock species and other animal models.

Simposium:

Histology and Aging

Marta Agudo-Barriuso
Department of Ophthalmology, School of Medicine, University of Murcia, Experimental Ophthalmology Group, IMIB-Arrixaca, Murcia, Spain

Jorge Luis Tolivia Fernández
Department de Morphology and Cell Biology, Faculty of Medicine and Health Sciences, University of Oviedo, Spain

María Luisa Cayuela Fuentes
Telomerase, Cancer and Aging, Surgery Department, IMIB-Arrixaca, Murcia, Spain

Histology and Histopathology
From Cell Biology to Tissue Engineering

The senescence of the rat retina: from function to anatomy

Nadal-Nicolás F.M.*, Valiente-Soriano F.J., DiPierdoménico J., Vidal-Sanz M. and Agudo Barriuso M.

Grupo de Oftalmología Experimental, Instituto Murciano de Investigación Biosanitaria-VIRGEN DE LA ARRIXACA (IMIB-Arrixaca) and Departamento de Oftalmología Facultad de Medicina, Universidad de Murcia, Murcia, Spain

*Present address: Retinal Neurophysiology Section, National Eye Institute, National Institutes of Health, 20892-0608, Bethesda, MD, USA

Aging is one of the main risks factors associated to several human ophthalmic diseases. Because age and these diseases are tangled is difficult to ascribe a given decline to normal senescence or to a given disorder. Studying the effects of aging in experimental animals under a controlled environment will provide valuable information about the functional and anatomical impairment caused by senescence alone. The aged rat retina shows a functional decline and loss of some neuronal types, although controversial conclusions have been reported for the innermost retina. Here we have studied the retina and its retinorecipient areas in the brain of albino and pigmented rats along the life span of this species.

Weaned, young adult, adult, middle-aged and old albino and pigmented rats were used in this work. The functionality of the retina was studied using electroretinographic recordings. Anatomical analyses were done *in vivo* using optical coherence tomography, and *ex vivo* using immunohistofluorescence and retrograde tracing. Neuronal populations in the retina were quantified automatically, and their distribution assessed by topographical maps.

Our analyses show that independently of age, the electroretinographic recordings, the area of the superior colliculi innervated by retinal ganglion cells, and the volume of the retina and its layers are smaller in the albino than in the pigmented rat. Comparing young *vs.* old animals, we show that: i/ the retina grows linearly with time, causing a concomitant diminution of cell density; ii/ there is no loss of retinal ganglion cells, nor of other cells in the ganglion cell layer; iii/ while in aged albino animals, is observed cell loss in both inner and nuclear layers, only in the pigmented strain there is a decrease of cone photoreceptors; iv/ retinal function is impaired in aged animals of both strains, with a reduction of the cone- and rod- mediated responses, and an increase of the implicit time of response; v/ aged superior colliculi, the main projection area in rodents, show signs of gliosis and microglial activation, and a diminution of the area innervated by retinal ganglion cells, and, finally, vi/, the retinal pigmented epithelium shows signs of impaired phagocytosis in aged animals

The present study provides the baseline to understand better the real implication of aging in rat models of human pathologies that are closely related with senescence, such as glaucoma, aged-related macular degeneration or diabetes.

Histology and Histopathology
From Cell Biology to Tissue Engineering

Aging, Alzheimer and apolipoprotein D

Tolivia J., Navarro A., Martínez Pinilla E., del Valle E. and Astudillo A.
Department de Morphology and Cell Biology, Faculty of Medicine and Health Sciences, University of Oviedo, Spain, Instituto de Neurociencias del Principado de Asturias (INEUROPA), Spain, Instituto de Salud del Principado de Asturias (ISPA), Spain

Normal brain ageing is characterized, among other factors, by neuronal loss in certain areas (cerebellum), loss of synapses and the presence of neuropathological lesions similar to those observed in Alzheimer's disease (AD). However, these age-related changes are less frequent and are located in restricted regions of the cerebral cortex.

Sporadic AD is the most common form of dementia and is characterized clinically by a fatal, irreversible and progressive loss of memory and cognitive abilities. From an anatomopathological point of view it is characterized by loss of neurons, neurites and synapses, and the presence of senile plaques in the neuropile and neurofibrillary tangles in neurons. The presence of these tangles begins in the entorhinal cortex and hence extends to the limbic system and subsequently to other regions of the neocortex with a dispersion pattern that has been exhaustively characterized by Braak and Braak (1995).

Apolipoprotein D (Apo D) is a small glycoprotein of extracellular secretion, detected for the first time in human blood plasma and isolated from high-density lipoproteins (HDL). In the central nervous system (CNS) it can be synthesized by neurons, astrocytes and mainly oligodendrocytes postulating, according to the most of the studies, as a neuroprotective and antioxidant protein during normal ageing and in various neuropathologies. In this sense, our research group has focused basically on the role of Apo D in some processes that take place in both normal brain aging and certain neurodegenerative diseases as AD.

In relation to aging of the CNS, we have found that Apo D expression varies depending on the brain region studied. Thus, its expression shows a significant increase with age in the newest evolved parts of the mammalian brain, such as the neocortex, but without apparent gender differences. Apo D overexpression seems to be directly related to the high levels of oxidative stress that characterized neocortex. It is important taken into account that no changes in neuronal density during ageing were observed for this brain area. In oldest brain centers, from a evolutionarily point of view, such as the medulla oblongata, we have found that increase of Apo D expression begins at early ages and is maintained throughout the individual's life. Once again, the neuronal loss in the nuclei of this area is practically non-existent.

Regarding to AD, our group was the first to detect the presence of Apo D in senile plaques. Subsequent studies have highlighted the absence of its expression in neurons in degenerative phase. . We have also found a gender difference, both in the loss of the number of neurons and the expression levels of Apo D. Likewise, its expression in relation to the Apo E was totally antagonistic, having a different location in plaques and vessels with amyloidosis. In contrast when we compare Apo D with Apo J expression we found a parallel increase during the development of the disease.

All our results together with those found in the literature seem to unequivocally demonstrate the neuroprotective role of Apo D in aging and neurodegenerative diseases.

This study has been funded by Instituto de Salud Carlos III though the project (PI15/00601) (Co-funded by European Regional Development Fund/European Social Fund "Investing in your future").

Histology and Histopathology
From Cell Biology to Tissue Engineering

Zebrafish: New model for aging and rejuvenation

Roca M.[1], Fernández-Silva D.[1,2], Fernández-Lajarin M.[1,3], Martínez-Balsalobre E.[1,3], Naranjo E.[1,3], García-Castillo J.[1], López-Maya I.[1], Conde-Garrosa R.[1], Mulero V.[1,3], Pérez-Sánchez H.[2], Alcaraz-Pérez F.[1,3] and Cayuela M.L.[1]

[1]Telomerase, Cancer and Aging, Surgery Department, Instituto Murciano de Investigación Biosanitaria-VIRGEN DE LA ARRIXACA (IMIB-Arrixaca), Murcia, [2]Bioinformatics and High-Performance Computing Research Group (BIO-HPC), Computer Science Department, Universidad Católica San Antonio de Murcia (UCAM), [3]Department of Cell Biology and Histology, Faculty of Biology, University of Murcia, Murcia, Spain

The aging is a biological process produced by an accumulation of physiological and molecular damages which lead to symptoms related to age related diseases. Telomere dynamics have been found to be better predictors of survival and mortality than chronological age. Telomeres, the caps that protect the end of linear chromosomes, are known to shorten with age, promoting aging. Telomerase is the enzyme necessary to restore telomeres to continue division and reproduction. Telomerase is a ribonucleoprotein with two main subunits: telomerase reverse transcriptase (TERT) and telomere RNA (*TERC* or *TR*).

In this study, we use the zebrafish (*Danio rerio*) as a key vertebrate model in aging biology. In fact, during the last decade, several zebrafish studies about the role of the TERT complex in aging, cancer and regeneration have contributed to deciphering the mechanisms of aging, and in developing preventive and therapeutic strategies to prolong the productive lifespan ('healthspan') in humans and postpone aging.

Wild type and *tert* and *terc* mutant zebrafish from different ages were used in this work. The aging analysis and telomeres was studied using histological analysis, telomere length and telomerase activity techniques. Memory and locomotion test were performed and analysis of gene expression by RT-qPCR were carried out. Screening of several rejuvenation compounds were also performed

In the present study, a Tert-deficient zebrafish was characterized. This model shows signs of premature aging, including spinal curvature, infertility and reduced lifespan in the first generation. Furthermore, the zebrafish mutants display activation of p53 in response to telomere attrition and show the anticipation phenomenon (the onset of disease at a younger age in the next generation) due to telomerase haploinsufficiency, providing further evidence that telomerase dosage is essential. Crucially, reintroduction of telomerase is able to rescue telomere shortening and longevity in the zebrafish, what has clinical implications. These characteristics together with the feasibility of zebrafish for high-throughput chemical screening underlines the usefulness of this animal model for the identification of new therapeutic drugs. We carried out a proof of concept of rejuvenation screening using drugs known to affect telomerase.

Zebrafish, whose telomeres are of a similar length to human telomeres, has recently emerged as an excellent model for high-throughput chemical and genetic screening. The present study paves the way to better understand the role of telomere dynamic in aging and for the identification of new therapeutic drugs able to rejuvenate.

Simposium:

Histology in Regenerative Medicine and Tissue Engineering

David García Bernal
Hematopoietic Transplant and Cellular Therapy Unit, IMIB-Arrixaca, and Internal Medicine Department, Medicine School, University of Murcia, Murcia, Spain

Fernando Campos Sánchez
Department of Histology, Tissue Engineering Group, University of Granada, Granada, Spain

Sebastián San Martín
Centro de Investigaciones Biomédicas, Escuela de Medicina. Universidad de Valparaíso, Chile

Histology and Histopathology
From Cell Biology to Tissue Engineering

Histology of murine acute graft-versus-host disease (aGvHD) and the effect of mesenchymal stem cells (MSCs) on the inflammatory response

García-Bernal D.[1,2], Blanquer M.[1,2], Martínez C.M.[3], García-Guillén A.I.[1], García-Hernández A.M.[1,2], Algueró M.C.[1], Yañez R.[4,5], Lamana M.L.[4,5], Moraleda J.M.[1,2] and Sackstein R.[6]

[1]Hematopoietic Transplant and Cellular Therapy Unit, Instituto Murciano de Investigación Biosanitaria IMIB-Arrixaca, Virgen de la Arrixaca University Hospital, University of Murcia, Spain, [2]Internal Medicine Department, Medicine School, University of Murcia, Murcia, Spain, [3]Experimental Pathology Unit, Instituto Murciano de Investigación Biosanitaria IMIB-Arrixaca, Spain, [4]Hematopoietic Innovative Therapies Division, Centro de Investigaciones Energéticas, Medioambientales y Tecnológicas (CIEMAT) and Centro de Investigación Biomédica en Red de Enfermedades Raras (CIBER-ER), Madrid, Spain, [5]Advanced Therapies Mixed Unit, Instituto de Investigación Sanitaria-Fundación Jiménez Díaz (IIS-FJD), Madrid, Spain, [6]Department of Translational Medicine, Herbert Wertheim College of Medicine, Florida International University, Miami, Florida, USA

Mesenchymal stem cells (MSCs) are distributed in all tissues. *In vitro*, MSCs display potent anti-inflammatory/immunomodulatory properties, however, their immunobiology *in vivo* is obscure because MSCs are sessile, incapable of infiltrating distant inflammatory sites. In a recent work, we have examined how MSC tissue colonization impacts concurrently evolving immunopathology in a murine model of acute graft-versus-host disease (aGvHD) coupled with intravascular administration of host-derived MSCs. Targeted tissue recruitment of MSCs was achieved by enforced expression of HCELL, a CD44 glycoform that is a potent E-selectin ligand. Compared to mice receiving HCELL- MSCs, recipients of HCELL+ MSCs had increased MSC density within aGvHD-affected site(s), decreased leukocyte infiltrates, lower systemic inflammatory cytokine levels, superior tissue preservation, and markedly improved survival. Mechanistic studies in vitro reveal that HCELL/CD44 engagement potentiates MSC immunomodulatory activity. These findings indicate that MSCs counteract immunopathology *in situ*, and provide evidence that CD44 ligation unleashes MSC immunobiologic properties serving to maintain/establish tissue immunohomeostasis.

Histology and Histopathology
From Cell Biology to Tissue Engineering

Biomimetic artificial tissues. Models and applications

Campos F.

Department of Histology, Tissue Engineering Group, University of Granada, Granada, Spain

Generation of increasingly biomimetic and biocompatible artificial tissues is the basic objective of tissue engineering. The process of biofabrication and functionalization of biomaterials used for the construction of artificial tissues is an important research goal, since biomaterials are essential active components influencing the properties of the new tissues.

In this presentation, different biofabrication methods suitable for hydrogels are considered, since these methods could contribute to designing biomimetic tissue- like structures that can be applied to tissue engineering protocols.

Three different procedures have been developed by our research group in order to generate biomaterials with specific architectural and biomechanical properties: nanostructuration, chemical cross-linking and incorporation of different types of nanoparticles. Nanostructuration is based on a plastic compression process a combining dehydration and mechanical compression applied in order to modify the properties and structure of the biomaterial. Uniform mechanical pressure is applied to the hydrogels until they reach the weight corresponding to the desired water content percentage. In the case of chemical cross-linkers, these agents are able to induce the generation of molecular interactions among the biomaterial molecules, thus modifying their biomechanical and structural properties. Finally, magnetic nanoparticles have been used to develop innovative magnetic biomaterials in which the fibers and molecules can be aligned and oriented by using a definite magnetic field, resulting in an ordered fibrillar pattern.

The results show that the application of these methods, whether independently or as a combination of methods, allowed us to generate novel biomaterials whose porosity can be controlled and tuned in most of hydrogel models. This resulted in a controlled improvement of the stiffness modulus (G) of these biomaterials, with an increase of the elastic modulus (G') respect to the viscous modulus (G''). Cell viability analyses showed that cells were viable and functional in these novel biomaterials, although some specific differences were detected. This should be taken into account to select the best choice to be implemented in tissue engineering protocols.

The generation of different artificial tissue models by the application of these biofabrication processes -nanostructuration, chemical crosslinking and incorporation of magnetic nanoparticles- allows the design of versatile artificial tissue models such as the human nerve, cornea, sclera, cartilage, oral mucosa or skin, with biomimetic structural patterns. The porosity and biomechanical patterns (stiffness, elasticity and viscosity) can be tuned according to the tissue to be reproduced. These results could be applied to different tissue engineering protocols.

Supported by the Spanish Plan Nacional de Investigación Científica, Desarrollo e Innovación Tecnológica (I+D+i) from the Spanish Ministry of Economy and Competitiveness (Instituto de Salud Carlos III), Grants FIS PI17/0391 and PI17/393 (cofinanced by FEDER funds, European Union) and by SAS PI-400-2016 and CS PI-0257-2017 by the Regional Ministry of Health, Junta de Andalucia, Spain.

Histology and Histopathology
From Cell Biology to Tissue Engineering

Human amniotic membrane, from basic research to clinical applications

San Martin S.[1], Garrido M.[1,2], Riegel M.[1] and Montedonico S.[1,2]

[1]Centro de Investigaciones Biomédicas, Escuela de Medicina, Universidad de Valparaiso, Chile, [2]Unidad de Cirugía Pediátrica y Servicio de Maternidad, Hospital Carlos Van Buren de Valparaíso, Chile

Amniotic membranes are usually discarded following birth and their use do not elicit ethical debate. This tissue is a good choice for regenerative medicine because of both their phenotypic plasticity and immunomodulatory capability and has been effectively used in both clinical and experimental setting.

We describe different uses of amniotic membrane: as a therapeutic tool in an animal model of liver fibrosis and as an alternative to ocular bullous keratopathy (BK).

Animal model: Sprague-Dawley rats were randomly divided into three groups: sham surgery, bile duct ligature (BDL) (liver fibrosis model) and bile duct ligature plus amniotic membrane on liver (BDL+AM). The animals were sacrificed on the 2nd, 4th, and 6th postoperative weeks. Histopathological examination of liver tissue was performed with hematoxilyn-eosin and Sirius red stainings. Clinical Trial I: Adults patients with bullous keratopathy were from the Ophthalmology Unit of Hospital Carlos Van Buren in Valparaíso, Chile. They were randomized into 2 groups: amniotic membrane and therapeutic contact lenses. Eye pain severity (visual analogue scale) was compared among the two groups mentioned, for a period of 6 months.

On animal model at 6th postoperative week, ductular reaction, portal fibrosis and bile plugs were markedly reduced in the BDL+AM compared to the BDL group on histopathological examination. Collagen surface area was 26.96 ± 11.63% in BDL group versus 14.57±9.37% in BDL+AM group (p<0.01). On clinical assays I, 20 patients with BK awaiting corneal transplant were studied. Pain from the surgery was statistically significant lower at 7 (p=0.005) and 30 days (p=0.002) but higher at 90 days (p=0.042).

Our studies demonstrate that Amniotic Membrane constitutes an efficient and safe therapy to the preclinical and clinical assays.

Financial support : CI 05/2006 (Universidad de Valparaíso, Chile).

Simposium:

Innovation in Histology Teaching

Catalina Guerrero Romera
Department of Theory and History of Education, Faculty of Education, University of Murcia, Murcia, Spain

Francisco José Sáez Crespo
Department of Cell Biology and Histology, School of Medicine and Nursing, University of the Basque Country UPV/EHU, Vizcaya, Spain

Germán Isauro Garrido Fariña
Department of Biological Sciences, FES-Cuautitlán, Universidad Nacional Autónoma de México, México

Histology and Histopathology
From Cell Biology to Tissue Engineering

Teaching innovation and quality in Higher Education

Guerrero C.
Department of Theory and History of Education, Faculty of Education, University of Murcia, Murcia, Spain

This paper analyzes some of the keys and trends in teaching innovation in university education and reflects on the possibilities that innovative technologies and pedagogies have in teaching practices in order to assess the quality and impact of projects and actions of innovation that are carried out in higher education, and that allows us to detect good innovation practices. It also reviews existing trends and models to assess the quality of innovation in university education in terms of the dimensions and indicators they propose (Guerrero, 2019).

It also presents a project initiated within the framework of the Campus of International Excellence Mare Nostrum Campus that has had the objective of reflecting on teaching innovation projects and actions, as well as exchanging experiences between representatives of different universities and international networks (RELFIDO Network, international network of scientific and technical cooperation at European and Latin American level in the field of teacher training and innovation, OBIP International Observatory of the Teaching Profession, Virtual Campus Network and Research Network for Teaching Innovation at UNED). Among the most outstanding results of this project was a forum and a dynamic unit of knowledge about innovations in the teaching field especially for the promotion of their quality, as well as in international cooperation and continuous innovation of the teaching processes On the other hand, an elaborated and validated instrument for the evaluation and improvement of the projects and actions of university teaching innovation consisting of 4 dimensions, several subfactors and 52 indicators is described.

This is intended to advance in the evaluation of the quality and impact of these actions and in the detection and analysis of good teaching innovation practices based on the analysis and discussion of these practices in different fields and contexts, in order to enhance the ability of teachers to develop and implement in their subjects new methodologies and innovation processes in the current digital context, as well as detect the training needs of teachers.

Histology and Histopathology
From Cell Biology to Tissue Engineering

A flipped classroom model for the teaching of Histology using thematic videos

Sáez F.J. and Badiola I.
Department of Cell Biology and Histology, School of Medicine and Nursing, University of the Basque Country/Euskal Herriko Unibertsitatea UPV/EHU, Leioa (Vizcaya), Spain

The flipped classroom is a teaching method in which the lectures are used to reinforce the previous autonomous study of the students.
Three teaching modalities are carried out In the Human Histology subject of the first degree of dentistry at the UPV/EHU: lectures, classroom practices and laboratory practices. For some years, we have already carried out both classroom practices and laboratory practices based on the student's previous study. Now, our objective was to implement the flipped classroom in the lectures. To introduce the flipped classroom method in the lectures, we needed three things: 1) Provide students with materials for autonomous study, 2) Prepare materials to work in face-to-face classes, 3) Establish an active working method for classroom sessions.

We have prepared different materials to support teaching. For autonomous study, we have published a handbook of Histology that explains the twenty-three topics of the subject. In addition, we have produced twenty-three videos to support teaching, one for each topic of the subject. We have also prepared self-assessment and evaluation tests. The videos and tests were available on the eGela (Moodle) platform for teaching support of the UPV/EHU.
The completion of each video followed the following process: 1) Preparation of a presentation with the PowerPoint 2016 software; 2) Elaboration of an explanatory text of each slide; 3) Conversion of text into sound (mp3 files) using the web fromtexttospeech.com, 4) Adding the sound file on each slide; 5) Record the PowerPoint presentation with the option "Record slide show", including the use of the laser pointer that facilitates the program; 6) Save the presentation as MPEG-4 video (.mp4).

We have produced videos of ten to twenty minutes in length, one for each topic of the subject. Each video explains the most important concepts of each topic. The videos have been stored in Google Drive and the link for downloading was available on eGela platform. We have also prepared materials for face-to-face classes. The first ones were interactive quizzes using a student response formative assessment system (SOCRATIVE or similar). Moreover, we have also made printed review exercises for each topic.
The working method used was as follows:
Before the lecture, each student did an autonomous work on the subject:

1) Each student studied using the handbook and the thematic videos.
2) The student reviewed his knowledge by answering the self-assessment and evaluation tests in eGela.

In the classroom, during the lecture:

1) The professor posed questions in interactive quizzes (SOCRATIVE), each student responded using his electronic device (cellular, laptop or tablet).
2) The professor resolved the misconceptions.
3) To finish, the students answered in groups a printed review exercise on the topic.

It is possible to develop a flipped classroom method meeting the following requirements: 1) Prepare materials that guarantee that the student can study each topic autonomously before the face-to-face class. 2) Carry out active methodologies in the face-to-face class that review the main concepts of each topic, resolve the misconceptions and reinforce autonomous learning.

Histology and Histopathology
From Cell Biology to Tissue Engineering

Higher education in Mexico: can it still be a paradigm of transformation and renovation?

Dr. German Isauro Garrido Fariña.
Departamento de Ciencias Biológicas, Facultad de Estudios Superiores Cuautitlán, Universidad Nacional Autónoma de México, México

In the globalization, higher education have to deal with the creation of new paradigms, as a result of the increase in students enrollment, skills diversification, large number o university and colleges options and a civilization in constant changing. Understanding the historical context of our countries and of an increasingly interconnected environment, may allow educational institutions to influence the delicate balance of the organization of new social, economic and political systems.

Mexico began in 1551 with the foundation of the Royal and Pontifical University of Mexico, through the cedula gifted in 1547, by His Majesty Felipe II of Spain. In 1867, by decree of Don Benito Juarez García, the law to orient and regulate education was published, taking as a guiding principle the preparatory or highschool intruction. In 1910, Don Porfirio Díaz Mori promulgates the law that constitutes the University as National. The Autonomy is registered for the first time in the organic law of the National Autonomous University of Mexico (UNAM) in 1929, but it is only until 1980 that this autonomy for all universities earn Constitutional rank.

In parallel and whit the law of 1867, technical education in Mexico began with the creation of different fundamental institutions, namely: The Royal Mining Seminary in 1783 and later was transformed into the Special school of engineers in 1883. The Royal Academy of Noble Arts of San Carlos, founded in 1781. The heroic Military College founded in 1838. The Commercial Institute in 1845. And in1916 the Practical School of Mechanical and Electrical Engineers was established. These institutions and their students laid the basis for the creation of the schools that would be part of the Department of Industrial and Commercial Technical Education created in 1922 and later were transformed on to the Instituto Pilitécnico Nacional (IPN), created by General Lázaro Cárdenas del Río in 1936. Finally in this way comes the creation of the Council of the National System of Technological Education in 1978.

The history of basic education or “first letters” in Mexico, is inheritance of the Bourbon laws in the 18th century, but its development was the transition from rudimentary rural education, to modernization through state school networks and private schools. At the end of the 18th century, the normalist teachers appeared, the concept of “pupilo” or “educando” and an organization controlled by the liberal postrevolutionary State was developed. It was declared mandatory in 1917.

Although secondary or middlescholl education acquire some importance since 1848 was institutionalized in the instruction law of 1865, and consciously promoted in 1925. Whit the centralitation and administered by the state in 1935 had a popular and socialist goal, but shortly after in the hands of Mr. Jaime Torres Bodet, acquires its humanistic, formative, rational and experimental condition, he create in 1958 the technical secondary, that included technical activities, finally the “Telesecundaria” and the technological schools sistem basis were created. Only until 1993 was mandatory.

The highschool middleschool or “Bachiller” level, obtains official character in the Organic Law of Public Instruction in México Federal District of 1867, with the stablishment of the Escuela Nacional Preparatorias. In 1910 it is integrated under presidential decree to the recently created National University. General Plutarco Elías Calles Campusano signed in 1925 the decree for the separation of secondary, high school and university. The UNAM creates the National Preparatory School and the IPN the vocational schools. In the decade of the 70s, the great demand brought to the creation of different middleschool options: Clegio de Ciencias y Humanidades, Colegio de bachilleres and centers of scientific and technological studies, as well as the CONALEP, Colegio Nacional de educación profesional Técnica.

This era in which we live, forces us to consider: ¿What should guide the transformation of our educational systems? -The needs of the system for which they work; -Transformations according to the changes of the society in which it is developed; -The possibility of open educational systems, where the individual, the community where lives and globalization, can be integrated again into the humanistic-universal education resembling some of first European universities and colleges.

Oral Presentations

Oral Presentations

Session 1

Thursday, 12-14 hours

Oral presentation: Session 1. Room A. Code: 5016

Histology and Histopathology
From Cell Biology to Tissue Engineering

BRAF mutation in thyroid papillary carcinoma and its relation with the morphological changes

Cabrera Galván J.J.[1,3], Martínez-Martín M.S.[1,3], Araujo-Ruano E.J.[3], Galán-García M.E. [1] and Salido-Ruiz E.[2]

[1]Servicio de Anatomía Patológica del Complejo Hospitalario Universitario Insular-Materno Infantil de Las Palmas de Gran Canaria, [2]Hospital Universitario de Canarias-Tenerife, [3]Unidad de Anatomía Patológica Departamento de Morfología ULPGC

Papillary Thyroid Carcinoma (PTC) is one of the most common endocrine tumours, and constitutes 80-90% of all thyroid tumours and is virtually responsible for the increase of this pathology. BRAF somatic mutation affects 45% of CPT and 25% of Anaplastic Carcinomas, being absent in Follicular Carcinoma, Medullary Carcinoma and benign thyroid tumours. By aberrant and constitutive activation of the Ras-Raf-Mapkinase/ERK pathway, the resulting BRAF 600E Kinase mutation is potentially oncogenic. Morphological features relating CPT to the BRAF mutation have been described and shown to be predictive. Likewise, the percentage of this mutation has been related to prognostic factors. However, little is known about the combination of both possibilities; this being the objective of this work.

We selected a total of 60 cases of Papillary Thyroid Carcinoma that have undergone surgery in the last 10 years at the Hospital Insular Materno Infantil of Las Palmas. The paraffin blocks were cut at 10um each and after the macrodissection, the DNA was extracted and the BRAF gene was amplified by PCR using primers, quantified and evaluated in agarose gel. This product was subjected to Pirosecuenciónde Quiagen® for mutation T1799A/ V600E. Finally, all established variables were statistically evaluated by Multivariate Analysis and Median QR for the percentage trend.

We found a relationship between prognosis and CPT morphological prediction for the variables Infiltration of tumour limits $p<0.001$ independent and significant for eosinophilic cytoplasmic changes or “Pink-atipia”, Stage >1, fibrosis and tumour desmoplasia, which were equally significant by means of the statistical study of the percentage of mutated alleles. We detected a significantly opposite relationship between fibrosis and tumour desmoplasia with respect to the BRAF mutation, favourable to the latter.

This allows us to conclude that the morphological changes cited can predict in advance that this CPT has an almost 87% chance of presenting the BRAF mutation.

Oral presentation: Session 1. Room A. Code: 5695

Histology and Histopathology
From Cell Biology to Tissue Engineering

The synthetic cannabinoid URB447 reduces cell death, white matter demyelination and reactive astrogliosis in the neonatal rat brain

Carloni S.[1], Duranti A.[1], Pintor-Rial A.[2], Pacho M.[2], Álvarez A.[2], Hilario E.[2], Balduini W.[1] and Alonso-Alconada D.[2]

[1]Department of Biomolecular Sciences, University of Urbino "Carlo Bo", Urbino, Italy, [2]Department of Cell Biology and Histology, School of Medicine and Nursing, University of the Basque Country (UPV/EHU), Leioa, Bizkaia, Spain

Neonatal hypoxia-ischemia is a devastating condition that may result in death or severe neurologic deficits in children. After the onset of the injury, every single brain cell can be affected, displaying a wide range of molecular and morphological changes depending on the type of cell lineage. Neurons, with their high-energy demand, cannot afford the lack of ATP and may die through necrosis and/or apoptosis. As astrocytes are less susceptible to injury, those that survive adjacent to the injured tissue are able to re-establish neuronal integrity. Oligodendroglial injury (leading to myelination deficiency) and microglial activation will produce adverse effects on axonal function and neuronal survival, resulting in long-term cognitive impairment. Our aim was to evaluate histologically the protective effect of the synthetic cannabinoid URB447 on neurons, astrocytes, oligodendrocytes and microglia after hypoxic-ischemic brain injury in neonatal rats.

Rat pups at postnatal day seven were anesthetized and the left common carotid artery was isolated, ligated and sectioned. Hypoxia was induced by maintaining the animals in a container perfused with humidified 8% O_2 and 92% /N_2 for 2 h. Three experimental groups (n=10 for all groups) were established for histological evaluation. Control pups had neither artery ligation nor a period of hypoxia (Sham). Hypoxic-ischemic animals (HI) received vehicle (PBS:DMSO), while treated pups a single i.p. dose (1 mg/kg) of the synthetic cannabinoid URB447 3h after hypoxia (HI+URB447). The most effective dose and best administration regimen were evaluated in a previous set of experiments. Seven days after the injury, cellular cytoarchitecture was studied on 5μm paraffin-embedded brain sections using Nissl staining. Regional evaluation of well-preserved neurons was performed in areas commonly affected by HI, like hippocampus and cortex. Using TUNEL technique, we visualized DNA fragmentation. Glial fibrillary acidic protein (GFAP, whose accumulation in response to injury is related to the glial scar) and Ionized calcium binding adaptor molecule-1 (Iba-1, a marker of microglia) were analysed by immunohistochemistry. The expression pattern of myelin basic protein (MBP), the major myelin protein and a hallmark of inflammation-associated diffuse white matter damage in fetal rodents, was evaluated at the level of the mid dorsal hippocampus and thalamus and at the level of the mid-striatum.

Cannabinoid-treated animals maintained the number of morphologically well preserved neurons, reaching values similar to sham group, together with a decrease in cell death (revealed by Nissl staining and TUNEL assay, respectively). Asphyctic animals displayed an important ($p<0.01$) loss in MBP immunostaining pattern in subcortical white matter at the level of the mid dorsal hippocampus and thalamus and at the level of the mid-striatum. The marked loss of axonal processes was evident in the cingulum, external capsule and adjacent striatum, a reduction avoided by URB447 administration ($p<0.01$). Astrogliosis and microglial activation were prominent in the ipsilateral hemisphere of HI animals, in regions surrounding necrotic cells. Cannabinoid reduced the expression of both markers.

The histological evaluation of the protective effect of URB447 after HI reveals its ability to reduce cell death, white matter demyelination and reactive astrogliosis.

Grants: UPV/EHU (GIU17/018).

Oral presentation: Session 1. Room A. Code: 5714

Histology and Histopathology
From Cell Biology to Tissue Engineering

Evaluation of the changes in the extracellular matrix after myocardial infarction by morphometric analysis

Ruiz-Sauri A.[1,2], Rios-Navarro C.[1], Ortega M.[1], Gavara J.[1], Marcos-Garces V.[3], Chorro F.J.[1,3,4,5] and Bodi V[1,3,4,5]

[1]Institute of Health Research-INCLIVA. Valencia, Spain, [2]Pathology Department, Faculty of Medicine, University of Valencia. Valencia, Spain, [3]Cardiology Department. Hospital Clinico Universitario. Valencia, Spain, [4]Medicine Department, Faculty of Medicine, University of Valencia. Valencia, Spain, [5]Centro de Investigación Biomédica en Red – Cardiovascular (CIBER-CV). Madrid, Spain

Extracellular matrix (ECM) is an imbricated network constituted by cells, fibers, and ground substance (mainly composed by glycosaminoglycans, proteoglycans, and adhesion glycoproteins), which play a key role in regulating cell survival, migration, proliferation, apoptosis, and in the inflammatory response. Myocardial infarction (MI) is caused by the thrombotic occlusion of a coronary artery, provoking a massive loss of cardiac cells. In response to the ischemia and reperfusion process following MI, dramatic changes in myocardial ECM components need to take place to heal the infarcted myocardium. The objective of this study was to characterize the myocardial ECM changes from ischemia onset until late phases after coronary reperfusion in a swine model of reperfused MI.

MI was induced in swine by transient 90-min coronary occlusion using angioplasty balloons. One control group and three MI groups were defined: 1) without reperfusion, 2) 1-week, and 3) 1-month reperfusion (n=5, each). Myocardial samples from the infarcted area were isolated and histologically staining to evaluate the presence of collagen type I, collagen type III, elastic fibers, and proteinglycans. Moreover, the presence of laminin, fibronectin, and secreted protein, acidic and rich in cysteine (SPARC) was determined by immunohistochemistry. Ultimately, the cellular component of the ECM (neutrophils, monocytes, T lymphocytes, and myofibroblast) was also assessed by immunohistochemistry. Five independent photographs for each group and each stain were taken and the presence of the different components of the interstitium was morphometrically quantified by using the software ImagePro Plus.

In the no-reperfusion group, an increase in fibronectin, laminin, and elastic fibers were observed, whereas no changes neither in the quantity nor in the organization of collagen-I and collagen-III fibers were detected. In the 1-week and 1-month reperfusion groups, an augmentation in the content of collagen-I, collagen-III, elastic fibers were found. These fibers displayed a more organized pattern compared to control tissue. The quantity of proteinglycans, laminin, fibronectin, and SPARC were also increased. Regarding the cellular component, a peak of neutrophils and monocytes occurred 1-week after reperfusion, whereas the amount of T lymphocytes was maximum 1-month after coronary reperfusion. The quantity of myofibroblasts was elevated in both reperfused MI groups.

ECM remodeling starts after ischemia onset, probably aiming to protect cardiomyocytes from the ischemic damage. After reperfusion, the ECM evolves to constitute a fibrotic scar to maintain a proper cardiac function. ECM changes might be accurately regulated since it could provoke an adverse left ventricular remodelling, consequently impairing patient prognosis.

This study was funded by “Instituto de Salud Carlos III” and “Fondos Europeos de Desarrollo Regional FEDER” (PIE15/00013, PI17/01836, and CIBERCV16/11/00486 grants) and Generalitat Valenciana (GV/2018/116).

Oral presentation: Session 1. Room A. Code: 5720

Histology and Histopathology
From Cell Biology to Tissue Engineering

High expression of mast cells and angiogenesis throughout the PI3k→AKT→AM signaling pathway in human renal cell carcinoma

Ruiz-Saurí A.[1,2], Ríos-Navarro C.[2], García-Bustos V.[3], Sales M.A.[4], Nuñez-Benito E.[1], Martín de Llano J.J.[1,2], Mata M.[1,2], Sancho-Tello M.[1,2], Carda C.[1,2], Llombart-Bosch A.[1,2]

[1]Pathology Department, Faculty of Medicine, University of Valencia. Valencia, Spain, [2]Institute of Health Research-INCLIVA. Valencia, Spain, [3]Internal Medicine Service, University Hospital and Polytechnic La Fe. Valencia, Spain, [4]Pathological Anatomy Service, Hospital Clínico Universitario. Valencia, Spain

Renal cell carcinoma (RCC) is a highly vascular tumor that usually occurs and progresses in a hypoxic environment, suggesting that tumor cells need to induce increased angiogenesis for growth. Histologically, Mast Cells (MCs) are present in the interstitium of normal renal tissue surrounding the blood vessels. Recently, links between RCC, increased MC count and microvessel density (MVD) have been established. MC can be activated through the PI3K/AKT/GSK3β/AM axis.

In the present study, we investigated the possible correlation between increased MC and angiogenesis in RCC, as well as the relationship between MC and the PI3K/AKT/GSK3β/AM signaling pathway in three types of carcinomas: clear cell, papillary, and chromophobe.

Formalin-fixed and paraffin-embedded specimens were collected from 30 patients with RCC (10 clear cell, 10 papillary cell, and 10 chromophobe). All had been treated with radical nephrectomy. Control tissue was obtained from non-tumor areas of the same kidneys. For immunohistochemical staining, the antibodies used were: anti-CD31, C-Kit, PI3Kinase, AKT, PAKT, GSK, PGSK, and AM. The number and intensity of positive cells was counted on 50 consecutive fields at 40x within the intratumoral and peritumoral fields, and in the histologically normal tissue. MVD was evaluated with image analysis software Image-Pro Plus 7.0 in a semi-automatized manner. MVD was calculated as the average measurement in 10 random fields at 20x. The statistical analysis was performed using SPSS 17.0 and statistical significance was considered for two-tailed p-value <0.05.

The mean number of MCs was higher in tumor tissue than in normal kidney tissue and statistically significant in the peritumoral fields ($p<0.001$). The mean number of MCs per field was 3.32±3.78 in peritumoral fields, whereas in normal renal tissue it was 0.33±0.27.

A relationship was observed between the increase in MC density (MCD) and in MVD in the peritumoral fields in the three types of tumors. MCD in AM^+ RCC tissue was higher than in AM^- RCC tissue (4.38±3.33 vs 2.65±3.71). Similarly, MVD in AM^+ RCC tissue was significantly higher than MVD in AM^- RCC tissue: 31.37±20.80 vs 23.27±15.91. MCD and MVD in AKT^+ RCC tissue were higher than in AKT^- RCC tissues (MCD: 4.79±4.22 vs 3.16±2.32; MVD: 10.91±7. vs 9.55±5.92). The present findings show that in RCC, only AKT and AM expression are correlated with MC infiltration and microvessel formation.

In RCC (clear cell, papillary and chromophobe), activation of the PI3K/AKT signal pathway induces AM expression. This increase recruits MC into the tumor and the peritumoral fields, stimulating local angiogenesis and inducing progression of RCC. Controlling this signaling pathway may help develop new therapies to the control of RCC.

Oral presentation: Session 1. Room A. Code: 5757

Histology and Histopathology
From Cell Biology to Tissue Engineering

Migroglial reaction to syngenic and allogenic intravitreous transplant of olfactory ensheathing glia

Norte-Muñoz M.[1,2], Portela-Lomba M.[3], Sobrado-Calvo P.[1,2], Simón D.[4], Di Pierdomenico J.[1,2], Sierra-Isturiz J.[3], Vidal-Sanz M.[1,2], Moreno-Flores M.T.[4] and Agudo-Barriuso M.[1,2].

[1]Departamento de Oftalmología, Facultad de Medicina, Universidad de Murcia, Murcia, Spain, [2]Oftalmología Experimental, Instituto Murciano de Investigación Biosanitaria Virgen de La Arrixaca (IMIB-Arrixaca), Murcia, Spain. [3]Facultad de Ciencias Experimentales, Universidad Francisco de Vitoria, Madrid, Spain. [4]Departamento de Anatomía, Histología y Neurociencia, Facultad de Medicina, Universidad Autónoma de Madrid, Madrid, Spain

Recent studies are focused on pluripotent cell transplantation for their ability to ameliorate the neuronal degeneration caused by central nervous system (CNS) injuries. However, for a therapeutical use transplantation has to be safe. Toxicity assays are scarce thus, we have analyzed *in vivo* the retinal microglial reaction and neuronal survival to allogeneic and syngeneic grafts of olfactory ensheathing glia (OEGs) into the vitreous body.

A dose of 80,000 cells/eye from a fluorescent immortalized OEG line (TEG3-GFP) from Wistar rats, was administered into the right vitreous chamber of albino rats from two strains: Sprague Dawley or Wistar. Animals were sacrificed 7 and 21 days after the injection. Intact retinas+vehicle matched groups were used as controls. TEG3-GFP cells were followed *in vivo* using OCT-SD. Retinas were flatmounted, RGCs and microglia cells immunodetected and RGCs automatically quantified.

TEG3-GFP remained in the vitreous up to 21 days after the transplant, without integrating in the retina. At 7 days post-transplant, TEG3-GFP do not cause retinal ganglion cell (RGC) loss in intact retinas neither in SD (allogeneic) nor in Wistar (syngeneic) rats. However, microglial cells showed signs of activation. At 21 days post-transplant, there is a significant decrease of RGC population in both scenarios. Microglial cells were highly activated compared to the vehicle-treated group. In addition of ameboid active forms, microglial reaction seems to be so potent that they also form aggregations all over the retina. This reaction is observed in both transplants.

The intravitreal syngeneic or allogeneic transplant of OEGs, induces a long-term activation of retinal microglial cells which in turn, has a negative impact on RGCs.

Oral presentation: Session 1. Room A. Code: 6178

Histology and Histopathology
From Cell Biology to Tissue Engineering

Comparative analysis of the neuronal damage and nitrosative stress in the cerebellum and brain stem of rats submitted to global ischemia by cardiac arrest

Hernández R., Blanco S. and Peinado M.A.
Department of Experimental Biology, University of Jaén, Jaén, Spain

Global ischemic hypoxia triggered by cardiac arrest is one of the main causes of mortality and morbidity in the western world. It has been suggested that ischemic episodes do not affect equally the different brain zones. Probably, it is due to the fact that neurons have diverse metabolic responses according to its microenvironment, so it is interesting to compare how ischemia affects neurons depending on their location. Among the complex metabolic reactions responsible for triggering cell damage during ischemic hypoxia, many of them are related to the formation of reactive oxygen species (ROS) and to the degree of oxidative metabolism. The degree of damage to the neurons of each region of the brain can be measured by particular markers, such as the neuron specific enolase (NSE). Under hypoxic conditions, nitric oxide (NO) is produced in large quantities and may react with superoxide anion (O_2^-). Both reactive species can lead to the formation of the potent oxidant peroxynitrite ($ONOO^-$). In this regard, the nitration of the residues of tyrosine (nitrotyrosine, n-Tyr) in proteins has been described as one of the most negative effects of $ONOO^-$, thus altering the structure and functionality of those proteins and cells.

This research aims to compare the neuronal damage and nitrosative stress, both labels of an ischemic episode, in the cerebellum and brainstem of adult rats subjected to an experimental model of global ischemia by cardiac arrest. To achieve this goal, the integrity of the tissues, the expressions of NSE and n-Tyr, as well as the levels of nitrates, nitrites and S-nitroso compounds (NOx) have been analyzed in both cerebral zones.

Histological sections from cerebella and brain stems of rats submitted to an experimental model of cardiac arrest (Pluta et al., 1991)) were stained with cresyl violet acetate to determine the general status of the cerebral tissue. Cerebella and brain stems homogenates from another set of animals were processed by western-blot to ascertain the expressions of NSE and n-Tyr). NOx levels were determined by chemiluminescence (NOA^{TM}), in samples from the same homogenates.

Our results indicate that the experimental model of cardiac arrest increased the expression of NSE and n-Tyr, as well as the levels NOx both in the cerebellum and in the brain stem. Nevertheless, these changes were significantly higher in cerebellum. Concerning the histological study, only some alterations, mainly in the Purkinje neurons of the ischemic cerebellum, were found.

This study indicates that the neuronal damage and the nitrosative stress triggered by an experimental model of global ischemia by cardiac arrest, vary in intensity depending on the zone of the brain studied; the cerebellum being more severely affected than the brain stem.

This work has been funded by the “Aid for First Research Projects” under the R & D & I Support Plan of the University of Jaen for the biennium 2014-2015 (R / 6/2014, Action 6). Ref.: UJA 2014/06/19.

Pluta R., Lossinsky A.S., Mossakowski M.J., Faso L. and Wisniewski H.M. (1991). Reassessment of a new model of complete cerebral ischemia in rats. Meathod of induction of clinical death, pathophysiology and cerebrovascular pathology. Acta Neuropathol. 83, 1-11.

Oral presentation: Session 1. Room B. Code: 5742

Histology and Histopathology
From Cell Biology to Tissue Engineering

Successful outcome of the application of amniotic membrane to difficult wounds. what is it the molecular code behind its effect?

Bernabé-García A.[1], Liarte S.D.[1], Rodríguez-Valiente M.[1,2], Moraleda J.M.[3], Castellanos G.[2] and Nicolás F.J.[1]

[1]Regeneration, Molecular Oncology and TGFß. IMIB-Arrixaca, Murcia, Spain, [2]Chronic wounds and diabetic foot ulcer unit, Hospital Clínico Universitario Virgen de la Arrixaca, Murcia, Spain, [3]Hematology, hematopoietic transplantation and cellular therapy, University of Murcia, Murcia, Spain

The application of Amniotic Membrane (AM) at chronic wounds that have difficulties in the process of wound healing (chronification, diabetic foot ulcer…) has proven a very successful therapy. During wound healing, the migration of keratinocytes onto newly restored extracellular matrix aims to reestablish continuity of the epidermis. The application of AM to chronic, deep traumatic, non-healing wounds has proven successful at stimulating re-epithelialization.

We obtained AM from elective cesareans that had been chriopreserved. Using a cell culture approach, we investigate the effect of Amniotic membrane on human keratinocyte cell line (HaCaTs) by studying protein and gene expression (western blot and qPCR) and cell proliferation (cell cycle by flow cytometry). Additionally, we used wound healing scratch assay to test the effect of amniotic membrane on cell migration. Additionally, we measured by cyto-immunofluorescence staining the expression of important proteins required for cell migration at the wound edge. Results obtained from patient's wound tissue sections support the results obtained in our vitro system.

When applied on epithelial cells on culture, AM activates extracellular signal-regulated kinases 1/2 (ERK1/2) and c-Jun N-terminal kinases 1/2 (JNK1/2), with the overexpression and phosphorylation of c-Jun along the wound edge. Additionally, TGFß plays a very important role for the management and control of the wound healing process of the skin, its fine regulation alteration may end up in a chronification of the wound, impeding its natural healing. We have seen that AM exert a delicate control on TGFß pathway, attenuating its signaling and allowing for a better unfolding of the process. The proper management of the TGFß signaling on cell proliferation together with the stimulation of migration confers the AM the ideal control on different aspects that must be stimulated for the keratinocytes to successfully re-epithelialize the wound. Moreover, behind the control of cell migration by AM an important role in the cytoskeleton and focal adhesions restructuring has been envisaged. Additionally, our lab currently works in the application of AM to other challenging wounds as the foot diabetic ulcer; also, the application of perinatal stem cells from other sources for wound healing improvement using natural materials as scaffolding. Finally, data from AM-treated foot ulcer-patients will be presented.

Amniotic membrane is a successful agent that is able to re-epithelialize complicated wounds. The precise knowledge of the molecular mechanisms involved on the phenomena allow us to improve its application of and to look for successful alternatives based on the use of live cells obtained from AM.

Oral presentation: Session 1. Room B. Code: 5781

Histology and Histopathology
From Cell Biology to Tissue Engineering

Tissue-like biomimetic scleral substitutes as medical products

Campos F.[1], Carriel V.[1], Vizcaíno-López G.[2], González-Gallardo C.[3], Martín-Piedra M.A.[1], Crespo P.V.[1], García J.M.[1] and Sánchez-Montesinos I.[4]

[1]Tissue Engineering Group, Department of Histology, University of Granada and Instituto de Investigación Biosanitaria ibs, Granada, Spain, [2]Department of Histology, Autonomous University of Santo Domingo, Dominican Republic, [3]Division of Ophthalmology, University Hospital San Cecilio, Granada, Spain, [4]Department of Human Anatomy and Embryology, University of Granada, Spain

The sclera is the outer fibrous layer of the eye, which is crucial for the normal physiology of the vision system. Scleral structural injuries are relatively frequent and are commonly repaired with allogenic grafts with variable success rate and several associated drawbacks. In this context, the aim of this study was to evaluate the possibility to use different nanostructured fibrin/agarose-based hydrogels (NFAH) to repair scleral defects in a rabbit model. Furthermore, tissue regeneration was histologically analyzed.

For this approach, 15 adult male New Zealand rabbits were used. In each animal, a scleral defect of 5-mm of diameter was created in the left eye and repaired by using allogenic scleral grafts (positive control), NFAH, NFAH crosslinked with Genipin (NFAH-GP) or with Glutaraldehyde (NFAH-GL) [1,2] or not repaired (negative control) (n=3 each). Right eyes were used as native controls. Animals were euthanized after 40 days for histological and histochemical analyses.

After 40 days, the macroscopic evaluation revealed that all defects were successfully repaired as compared to the negative controls. Histology showed that the use of allogenic scleral grafts covered the defects and these grafts became partially integrated in the host eye. The analysis of crosslinked biomaterials substitutes revealed a partial biodegradation process characterized by the presence of a covering loose connective and an inflammatory tissue which contributed to repair the defects. In the case of the NFAH, histology revealed the presence of a newly formed and immature scleral tissue covering the defects with few phagocytes and no remnants of grafted biomaterials. However, the tissue pattern was not fully comparable to the density and high organization of native tissue.

In this study, we evaluated a biomaterial-based graft to repair a highly dense and poorly vascularized tissue. Our results demonstrated the potential suitability of these biomaterials, especially NFAH, in the repair of scleral defects. In this sense, NFAH, resulted to be highly biointegrated and remodeled, and promoted tissue regeneration without any undesired reaction. However, the regenerated tissue obtained using NFAH was not fully comparable to the pattern of a native tissue. These differences could be related to several factors including the lack of supporting cells and/or growth factors, biomechanical differences between host tissue and grafted biomaterials or the chemical composition or 3D structure of biomaterials used. Further studies are still needed to improve the efficacy of NFAH in scleral repair.

This study was supported by Grant PI-400-2016 from Consejería de Salud y Familias, Junta de Andalucía, Spain.

[1] Campos F, et al. Biomed Mater. 2018;13(2):025021
[2] Campos F, et al. Biomed Mater. 2016;11(5):055004

Oral presentation: Session 1. Room B. Code: 5785

Histology and Histopathology
From Cell Biology to Tissue Engineering

Osteodiferentiation of human dental pulp pluripotential cells

Salazar A.[1], Avelar F.J.[2], Luna F.[3], Moreno A.[1] and Guerrero-Barrera A.L.[1]

[1]Laboratory of Cellular and Tissue Biology, Department of Morphology. Autonomous University of Aguascalientes. Aguascalientes, Mexico, [2]Environmental Sciences Laboratory. Department of Physiology and Pharmacology. Autonomous University of Aguascalientes. Aguascalientes, Mexico, [3]Area of Health Sciences. Autonomous University of Zacatecas. Zacatecas, Mexico

Since the existence of adult mesenchymal stem cells (MSCs) was identified, research has been carried out to know their pluripotentiality characteristics, which allows their differentiation in various cell lineages. MSC's are present in several tissues including skin, adipose tissue, peripheral blood, bone marrow, pancreas, intestine, brain, hair follicles and dental pulp. Dental pulp cells (hDPSCs) derived from the neural crest have the capacity to generate adherent and clonogenic cell clusters when they are sown in the same *in vitro* culture conditions. They are proliferative, pluripotencial and can differentiate into several cell types; hDPSCs are the most viable and promising cell line, due to their biological properties. They are ease to obtain because they are present during almost all the useful life in permanent teeth, being an autologous alternative to treat various diseases of Immune, degenerative or traumatic origin.

With approval of the Ethics Committee and informed consent, primary cultures of hDPSCs of third molars from individuals between 13 and 24 years of both sexes were established. The pulpal tissues were subjected to enzymatic digestion with EDTA/Collagenase Type I. The cells were seeded in Dulbecco's medium with 15% FBS and 1% Pen-Strep/Amphotericin B; they were incubated at 37°C in a humid atmosphere with 5% CO_2. Its viability and cell proliferation were determined by MTT assay. With RT-PCR and RT-qPCR phenotyping of hDPSC's was established with identification of CD14, CD34, CD44 and STRO-1 and the genes of osteoblastic cells COL-I-A, COL2, BSP, ALP and GAPDH. A process of cytodifferentiation to osteoblasts was performed with differentiating medium and staining with Alizarin Red.

Primary cultures of hDPSCs from third molars were obtained and showed optimal growth under the conditions in which they were cultivated. They presented spindle-shaped morphology with cytoplasmic extensions and central oval core. The cell growth followed a stable and ascending pattern in the phases of latency, logarithmic and stationary, correlating with the metabolic activity valued by the MTT test. The hDPSCs positively expressed CD14, CD34, CD44 and STRO-1, as well as the osteoblastic genes COL-IA, BSP, ALP and GAPDH. With the application for 21 days of osteodifferentiating medium and through Alizarin red staining, calcium ions were identified in the cells.

The use of the enzymatic digestion method proved to be efficient for the establishment of primary cell cultures of hDPSCs. Since the hDPSCs were described, it has been possible to deepen their phenotypic, ontogenetic and functional characterization; However, it would be necessary to continue deepening the aspects that allow to expand the knowledge about its biology and pluripotentiality capacity.

Oral presentation: Session 1. Room B. Code: 5796

Histology and Histopathology
From Cell Biology to Tissue Engineering

Fibrosis increases *myod* expression in regenerating muscle fibers

Leiva-Cepas F.[1,2,3*], Ruz-Caracuel Ignacio[1,2**], Gil-Belmonte M.J.[1], López-Espejo M.E.[1], Osuna-Soto J[1], Jimena I.[1,2,3] and Peña J.[1,2,3]

[1]Research Group in Muscle Regeneration, University of Córdoba, Spain, [2]Department Morphological Sciences, Section of Histology, Faculty of Medicine and Nursing, University of Córdoba, Spain, [3]Maimónides Institute for Biomedical Research IMIBIC, Reina Sofia University Hospital, University of Cordoba. Spain

Present address:

* Department of Pathology. Reina Sofia University Hospital, Cordoba, Spain

** Department of Pathology. La Paz University Hospital, IDIPAZ. Madrid, Spain

The regeneration of skeletal muscle is a balanced process between the formation of new muscle fibers and the development of connective tissue. Its imbalance leads to fibrosis and, therefore, affects the development and growth of regenerative muscle fibers. It is established that *MyoD*, a regulatory factor of myogenesis, is under the control of innervation, is expressed in the activation of satellite cells and is essential in the growth of regenerative muscle fibers. Since fibrosis prevents or hinders muscle regeneration, we have analyzed *MyoD* labeling in regenerative muscle fibers in a normal process of regeneration compared to the regenerative muscle fibers that form under a fibrosis situation.

Twelve Wistar rats we used divided into three groups (n=4): Normal control group (NG), regenerative group (RG) in which the animals were injected into the anterior tibial muscle with a myotoxic and a third group in which the fibrosis by extracting a fragment of the middle third of the tibialis anterior muscle (FG). After 28 days, the muscles were extracted and the samples were processed by freezing for study in light microscopy, by staining hematoxylin-eosin, acridine orange, NADH-tr, ATPase, acid phosphatase, desmin, and *MyoD.*

The area occupied by connective tissue in the FG was 70%, compared to 6% in the RG and 3% in a normal muscle. The evaluation of the dyeing characteristics between the regenerative fibers in the RG and FG showed a notable difference in the staining patterns in the regenerative muscle fibers of both groups. In the RG the muscle fibers were completely regenerated showing only the presence of internal nuclei and staining patterns similar with the normal fibers of the NG. No peripheral (0%) or internal (0%) nuclei in the regenerated fibers was positive for *MyoD*.mIn the FG, the microscopic features of the muscle fibers show a remarkable structural and staining variability clearly indicative of an alteration in their growth and maturation. In these fibers there was an important expression of *MyoD* both at the level of both peripheral and central nuclei (52%) or internal (68%).

The persistence of *MyoD* labeling in the nuclei of the regenerative fibers in muscles suffering from fibrosis suggests that, although the development of these fibers is affected, the myogenic program remains activated. This is probably related to difficulties in the reinnervation of regenerative muscle fibers by fibrosis.

Oral presentation: Session 1. Room B. Code: 5824

Histology and Histopathology
From Cell Biology to Tissue Engineering

Identification of novel agarose types as tissue engineering scaffolds with improved biocompatibility

Irastorza-Lorenzo A.[1], Martín-Piedra M.A.[1], de Frutos M.J.[2], Esteban E.[2], Fernández J.[2], Janer A.[2], Campos A.[1] and Alaminos M[1]

[1]Tissue Engineering Group, Department of Histology, University of Granada and Instituto de Investigación Biosanitaria ibs Granada, Spain, [2]Hispanagar, SA, Burgos, Spain

Agarose is a polysaccharide consisting of repeating unit of agarobiose (D-galactose and L-galactopyranose). Due to its property to form hydrogels, agarose has been used for different purposes, including tissue engineering [1]. The excellent biomechanical properties of agarose gels and their biocompatibility make this biomaterial a good scaffold for the generation of bioengineered tissues by tissue engineering. However, different agarose types are available and their specific usefulness in tissue engineering should still be determined. The objective of the present work is to analyze the biocompatibility of hydrogels generated from 5 types of agaroses in order to identify the most adequate agaroses for use in tissue engineering.

Bioartificial human dermis substitutes were generated using human dermis fibroblasts immersed within different agarose hydrogel scaffolds. These scaffolds consisted in 5 agarose types generated by Hispanagar, SA (LM, D2LE, D1LE, MS8 and D5) solved in PBS at a final concentration of 0.3, 0.5, 1 and 3%. These bioartificial tissues were analyzed after 24h of culture ex vivo by using WST-1 metabolic assays. As positive controls, cells cultured in 2D systems were used, whereas cells treated with triton X-100 were used as negative controls.

A positive correlation between cell viability and the agarose concentration was found (p=0,000; r=-0,601), although the correlation with the type of agarose used was not statistically significant (p=0,165; r=-0,054). The highest WST-1 activity corresponded to agarose D5, which was comparable to positive controls at the concentrations of 0.3 and 0.5%. At 0.3%, viability was also high for D1LE and D2LE agaroses, although WST-1 was slightly lower than positive controls and agarose D5 at the same concentration.

These results confirm the high biocompatibility of all types of agarose, although differences among the different agarose types and concentrations exist. These data point out the preference of using D5, D1LE or D2LE, agaroses with the highest biocompatibility, and the need of using the lowest agarose concentrations.

Supported by IDI-20180052 (Agarmatriz), leaded by Hispanagar, SA, Burgos, Spain, through CDTI, Ministry of Economy and Competitiveness, Spain, Programa Operativo Plurirregional de Crecimiento Inteligente (CRIN).

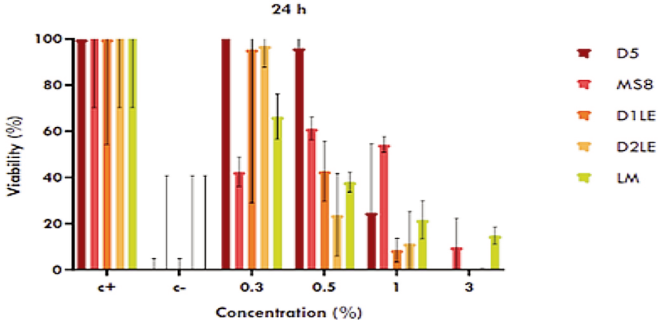

[1] Zarrintaj P, et al. Carbohydr Polym. 2018;187:66-84

Figure 1: WST-1 metabolic activity of the bioengineered skin dermis substitutes generated at different concentrations of 5 different agaroses. C+: positive control cells; C-: negative control cells.

Oral presentation: Session 1. Room B. Code: 5861

Histology and Histopathology
From Cell Biology to Tissue Engineering

A 3D in vitro neuroblastoma model reveal stiffness-dependent vitronectin expression

Monferrer E.[1], Martí-Vañó S.[1,2], Carretero A.[1], García-Lizarribar A.[3], Burgos-Panadero R.[1,2], Navarro S.[1,2], Samitier J.[3,4] and Noguera R.[1, 2]

[1]Department of Pathology, Medical School, University of Valencia / INCLIVA, Valencia, [2]CIBER of Cancer (CIBERONC), Madrid, Spain, [3]Institute for Bioengineering of Catalonia, Barcelona Institute of Science and Technology, Barcelona [4]CIBER-BBN, Madrid, Spain

The benefit of using a 3D in vitro model for biomedical research is the simulation and control of tumor microenvironment biology including the study of the extracellular matrix (ECM) elements. The composition of ECM and its structural and mechanical properties can control cancer cell behavior, favoring the creation of a tumor environment that promotes cell migration and invasion. Vitronectin (VN) is an adhesive ECM glycoprotein with multiple functions, which is involved in tumor progression and its expression has been associated in our previous studies with unfavourable prognostic factors in neuroblastoma (NB) patients. VN can also remodel ECM stiffness and promote cell mobility, so it is being studied as a possible new therapeutic target. This work aims to study the effect of ECM stiffness over the time on the VN expression in NB cells using a 3D cell culture model in order to define the physical cues that promote NB aggressiveness in relation with VN.

Biomimetic hydrogels incorporated 5% of methacrylated gelatin and different percentages of methacrylated alginate (0%, 1% and 2%). Neuroblastic SK-N-BE (2) cells were incorporated into the hydrogels during their fabrication and then were cultured from 2 to 4 weeks. Models were paraffin-embedded, sectioned, automatically immunohistochemically stained with anti-VN antibody (Abcam) and digitalized. VN expression was analyzed applying the HistoQuant module of Pannoramic Viewer software, obtaining the percentage of the VN stained area of each cluster independently. High VN expression was considered when the percentage of the VN stained cell area exceeded the 50% of the cluster cell area. Cell clusters were group as small, medium and large depending on their size (<400 μm^2, 400-2000 μm^2 and >2000 μm^2, respectively) and their VN expressions were compared to each other in all time and stiffness conditions.

VN expression was present in all 3D in vitro model conditions and tended to increase with higher stiffness and larger cluster cell sizes. The VN expression changes were not associated with time of culture.

The largest clusters of malignant neuroblasts would be more susceptible to the physical cues generated by the ECM stiffness resulting in an increased VN expression. The manufacture of 3D cell culture scaffolds, including stromal and/or immune cells, could reveal more accurately which is the effect of VN in cancer cell migration and its future therapeutic use in aggressive NB.

Seed Project Ciberonc-Ciberbbn (2018), PI17/01558, JAP-AECC (2018/150) and Neuroblastoma Foundation.

Oral presentation: Session 1. Room B. Code: 5873

Histology and Histopathology
From Cell Biology to Tissue Engineering

Microtechnologies for cell transfection with controlled cell-cell contact

Azuaje Hualde E.[1,2], Rosique M.[2,3], Calatayud-Sánchez A.[1,4], Ojeda E.[1,4], Benito-Lopez F.[4], Martínez de Pancorbo M.[2] and Basabe-Desmonts L.[1,5]

[1]BIOMICs microfluidics Research Group, Microfluidics Cluster UPV/EHU, Lascaray Research Center, University of the Basque Country UPV/EHU, Vitoria-Gasteiz, Spain, [2]BIOMICs Research Group, Lascaray Research Center, University of the Basque Country UPV/EHU, Vitoria-Gasteiz, Spain, [3]Department of Clinical and Biomedical Laboratory, EGIBIDE "Fundación Diocesanas – Jesús Obrebro Fundazioa", Vitoria-Gasteiz, Spain, [4]Analytical Microsystems & Materials for Lab-on-a-Chip (AMMa-LOAC) Group, Microfluidics Cluster UPV/EHU, Analytical Chemistry Department, University of the Basque Country UPV/EHU, Spain, [5]Basque Foundation of Science, IKERBASQUE, Bilbao, Spain

Gene transfection of cultured cells is a powerful tool in the development of new gene therapies and the generation of new disease models. Genes that express a fluorescent protein, such as green fluorescence protein, (GFP) are commonly transfected as reporters to facilitate the quantification of the transfection efficiency. Flow cytometry analysis or direct fluorescence microscopy observation are commonly used to quantify transfection efficiency [1], however, the cost of the equipment and trained personnel required for flow cytometry and the lack of control on the distribution of cells and cell-cell contacts in adhered cells generates a need in the development of new methodologies for cell transfection and quantification [2]. We propose a new methodology based on substrate micropatterning that allows cell transfection on adhered cells controlling cell-cell contact, reduces sample manipulation and simplifies the quantification of transfection efficiency.

Hair follicle mesenchymal stem cells (hfMSCs) were incubated over fibronectin patterns obtained by microcontact printing on microwell plates [3]. In order to compare the effect of cell-cell contact, we created two types of cell patterns: single-cell arrays, where individual cells are confined in a 20 μm diameter fibronectin dots without contact between cells, and arrays of small groups of cells, confined on 100 μm fibronectin dots, where cells were in contact with other cells. Patterned cells were incubated in the presence of GFP plasmid and lipofectamine, using concentrations optimized on regular cultures analyzed by flow cytometry. Samples were regularly observed, up to 42 h, by brightfield and fluorescence microscopy to quantify the total number of patterned cells and the number of transfected cells respectively. Finally, cell viability was studied after transfection, by changing the serum-free medium to a complete medium (30% fetal bovine serum).

When cells where in contact with other cells, we observed a maximum transfection efficiency of 20% after 24 h, while in samples containing only single cells the maximum efficiency of also 20% was achieved at 18 hours. These results indicated the impact of cell-cell contact on gene transfection. The absolute transfection efficiency (total number of transfected cells) over the course of 42 h in the single cell array was of 24%. After the transfection process, the hfMSCs showed a good viability and the cells formed a new culture as they grew and spread outside of their patterns after renewal of the culture medium.

Micropatterning of substrates enabled a low-cost methodology that simplifies the quantification of transfection efficiency and highlights the impact of cell-cell contact in the transfection process.

1. Homann S. et al. "A novel rapid and reproducible flow cytometric method for optimization of transfection efficiency in cells," Plos One, 2017, 12, 9.
2. Shiu JY. et al. "Observation of enhanced cell adhesion and transfection efficiency on superhydrophobic surfaces," Lab on a Chip, 2010, 10.
3. Hamon C. et al. "Tunable Nanoparticle and Cell Assembly Using Combined Self-Powered Microfluidics and Microcontact Printing," Advance Functional Materials, 2016, 26, 44.

Oral presentation: Session 1. Room B. Code: 5932

Histology and Histopathology
From Cell Biology to Tissue Engineering

Heterogeneity of mesenchymal cells in diverse zones of human amniotic membrane

Serrano-Sánchez M.[1], Cortés S.[2], Beltrán-Frutos E.[1], Martínez-Hernández J.[1], Seco-Rovira V.[1], Delgado J.L.[2], Ferrer C.[1] and Pastor L.M.[1]

[1]Department of Cell Biology and Histology, [2]Department of Surgery, Pediatrics, Obstetrics and Gynecology, IMIB-Arrixaca. School of Medicine, Regional Campus of International Excellence "Mare Nostrum Campus", University of Murcia, Murcia. Spain
bioetica@um.es

There is great interest in the amniotic membrane (AM) for use in regenerative medicine and for its role in membrane rupture during delivery. Recently, we have observed heterogeneity in the population of mesenchymal cells in the AM. The objective of this communication is to determine the distribution of different types of mesenchymal cells in human AM.

AM from five placentas at (37-39+6) weeks of gestation from natural delivery were processed for conventional light microscopy, semithin sections, immunohistochemistry and western blot. AM from the rupture zone (AMR), from next to the umbilical cord (AMC) and from the membrane of the uterine wall (AMU) were used. A semiquantitative study was realized with semithin sections to characterize the distribution of diverse mesenchymal cells.

By light microscopy and semithin sections three types of mesenchymal cells were characterized: type I, poorly differentiated; type II, moderately differentiated; and type III, well differentiated. Although semithin sections also pointed to a fourth type (Hofbaüer cells). In the AMC zone, type II mesenchymal cells were significantly more numerous that other cell types. In all three zones type II and III were significantly more abundant that type I and IV. Type I and II mesenchymal cells were significantly more abundant in the AMC zone that in the other zones. Type III mesenchyma cells were significantly more abundant in the AMR and AMU zones than in AMC. Type IV mesenchymal cells showed similar distribution in all amniotic zones. The expression of fibronectin was significantly higher in AMR that in AMC and AMU. Vimentin expression was significantly higher in AMR that in AMC. TGFβ2 and FGF-2 was found in the amniotic membrane in all zones with no significant differences in their expression among them.

Conclusions: a) Mesenchymal cell types are distributed differently in the amniotic membrane; b) undifferentiated mesenchymal cells are more frequent in the AMC zone while the differentiated cells in the AMR; c) this last observation was confirmed by a higher expression of fibronectin and vimentin in this location, suggesting a fibroblastic differentiation of mesenchymal cells.

Financed: Funded by GERM 19892/15 from Fundación Séneca CARM

Oral presentation: Session 1. Room C. Code: 5701

Histology and Histopathology
From Cell Biology to Tissue Engineering

Identification of proper SPAM1 distribution in selected human sperm by hyaluronic acid test

Sáez-Espinosa P.[1], Manzano-Santiago P.[1], Huerta-Retamal N.[1], Robles-Gómez L.[1], Avilés M.[2], Romero A.[1] and Gómez-Torres M.J.[1,3]

[1]Departamento de Biotecnología, Universidad de Alicante, Alicante, España, [2]Departamento de Biología Celular e Histología, Universidad de Murcia e IMIB-Arrixaca, Murcia, España, [3]Cátedra Human Fertility, Universidad de Alicante, Alicante, España

The failures of binding to the oocyte zona pellucida are commonly attributed to defects in the sperm adhesion molecules. SPAM1 is a hyaluronidase implicated in the dispersion of the cumulus-oocyte matrix and zona pellucida adhesion. However, SPAM1 residues distribution during capacitation remains poorly defined. Here, we evaluated the location of SPAM1 protein in human sperm before capacitation, during different capacitation times and after hyaluronic acid selection test.

Sperm samples were obtained from ten normozoospermic donors and cells were capacitated by swim-up for one and four hours. After capacitation, mature sperm were additionally selected by hyaluronic acid test. Sperm trapped in hyaluronic acid were considered mature and those that traversed it immature. SPAM1 patterns were evaluated by using an anti-SPAM1 antibody produced in rabbit and a secondary antibody against rabbit IgG conjugated to FITC. Cells were observed by microscope fluorescence and SPAM1 patterns percentage were analyzed statistically.

We detected three different SPAM1 fluorescent patterns: label throughout the head (Pattern 1), equatorial segment with acrosomal faith label (Pattern 2), and postacrosomal label (Pattern 3). Non-capacitated sperm condition showed a high subpopulation of cell with SPAM1 Pattern 1 (~50.00%). Conversely, after both capacitation times, results reported a significant increase (p<0.05) in the percentage of cells with Pattern 2 compared to non-capacitated cells, 42.79% after one hour and 44.08% after four hours capacitation. No significant differences in SPAM1 localization were reported between different sperm capacitation times. Otherwise, despite the increase of Pattern 2 during capacitation, the data obtained after selecting the mature sperm by the hyaluronic acid test significantly highlighted the Pattern 1 (label throughout the head) in both capacitation times. Specifically, mature sperm selected after one and four hours capacitation showed a 79.74% and 81.48% of this pattern, respectively. However, immature sperm after selection in both capacitation times displayed a high prevalence of Pattern 2 (~45.00%) and Pattern 3 (~45.00%) and a low presence of pattern 1 (~10.00%).

Our findings reported the existence of sperm subpopulations with different SPAM1 protein locations before and after capacitation. Further, hyaluronic acid test allows identifying that human sperm require the presence of SPAM1 throughout the sperm head (Pattern 1) to proper contact to cumulus-oocyte matrix. Overall, our results provide new insights in the physiological basis of sperm capacitation and could contribute to the improvement of sperm selection techniques.

VIGROB-186 and Cátedra Human Fertility of Universidad de Alicante.

Oral presentation: Session 1. Room C. Code: 5722

Histology and Histopathology
From Cell Biology to Tissue Engineering

Field emission scanning electron microscopy (FE-SEM) technique applied to analyze D-mannose distribution in human sperm

Robles-Gómez L.[1], Padilla-Cámara E.[1], Sáez-Espinosa P.[1], Huerta-Retamal N.[1], Avilés-Sánchez M.[2], Romero A.[1] and Gómez-Torres M.J.[1,3]

[1]Departamento de Biotecnología, Universidad de Alicante, Alicante, España, [2]Departamento de Biología Celular e Histología, Universidad de Murcia e IMIB-Arrixaca, Murcia, España, [3]Cátedra Human Fertility, Universidad de Alicante, Alicante, España

Capacitation includes the reorganization of sperm plasma membrane components and particularly the dramatic modification of sperm glycocalyx occur. The presence of mannose residues and sperm glycocalyx changes during *in vitro* capacitation have been described in humans using Con A lectin. However, little is known about quantitative data of mannose labelling densities on the sperm surface. Field Emission Scanning Electron Microscopy (FE-SEM) allows the detection of surface antigens and the assessment of molecules densities. Moreover, FE-SEM immunochemistry offers the three-dimensional location of receptors along the cell surface and the possibility to analyze surface receptors. The aim of this study was to determine the density and distribution of mannose residues on ejaculated and *in vitro* capacitated human spermatozoa using lectin immunogold-labelling by using FE-SEM.

Samples were obtained from normozoospermic donors and spermatozoa were capacitated by swim-up for 1h and 4h in a buffer containing BSA (5 mg/ml). Spermatozoa were fixed in three different physiological stages. Uncapacitated sperm (UCAP), one-hour capacitated sperm (CAP1) and four-hour capacitated sperm (CAP4). Mannose residues were detected by indirect inmmunogold-labelling using Concavalin A lectin (Con A). A total of 100 FE-SEM images were taken for each physiological stage. Colloidal gold particles were quantified in the acrosomal and postacrosomal regions.

We recorded a significant higher density ($P<0.05$) of Con A receptors in the acrosomal than in the postacrosomal region in UCAP, CAP1 and CAP4. In addition, a significant and progressive reduction in colloidal gold particles were observed in both acrosomal (from ~140 in UCAP to ~100 in CAP1 and ~60 in CAP4) and postacrosomal region (from ~40 in UCAP to ~30 in CAP1 and ~15 in CAP4).

FE-SEM allows us to accurately quantify and locate surface mannose residues simultaneously. The significantly decrease in D-mannose during *in vitro* capacitation is time-dependent.

VIGROB-186 and Cátedra Human Fertility of University of Alicante.

Oral presentation: Session 1. Room C. Code: 5835

Histology and Histopathology
From Cell Biology to Tissue Engineering

Objective diagnosis of thyroid carcinoma using second harmonic microscopy images

Bueno J.M.[1], Hristu R.[2], Párraga D.[1], Stanciu S.G.[2] and Stanciu G.A.[2]

[1]Laboratorio de Óptica, Universidad de Murcia, Murcia, Spain, [2]Center for Microscopy-Microanalysis and Information Processing, University Politehnica of Bucharest, Romania

Papillary carcinoma is the most prevalent type of thyroid cancer. Its diagnosis often requires accurate and subjective analyses carried out by expert pathologists. Although some objective image processing algorithms have been reported in the literature, these usually inform on overall tissue arrangements of the collagen morphology, what might lead to erroneous interpretations. Here we propose a method based on the Hough transform (HT) to detect and objectively determine local structural changes in the collagen of malignant thyroid tumors.

A home-made second harmonic generation (SHG) microscope combining a femtosecond laser and confocal microscope was used for the purpose of the present work. SHG imaging of different non-stained histological sections of thyroid fragment samples were acquired. Tissues corresponded to the healthy thyroid capsule (used as control), and to nodules diagnosed as benign (follicular adenoma, FA) and tumoral (papillary thyroid carcinoma, PTC). The HT was applied to each SHG image to extract numerical information on the orientation of the collagen-based tissues under analysis. This HT is defined as a mathematical algorithm to detect aligned segments and combining them in an accumulator matrix with dimensions associated with the polar coordinates of a straight line. The local maximum values in this matrix provide the preferential orientations found across the image.

SHG images of control samples reveal a wavy collagen distribution with local orientations. On the opposite, in PTC tissues collagen remodeling is produced and these local undulations disappear, turning into an aligned pattern with a global preferential orientation. As detected by the HT, the amount of dominant orientations clearly decreases in tumoral samples. In addition, FA tissues present a partial organization that significantly differs from both normal and PTC specimens.

The procedure here described represents a useful tool to automatically detect changes in collagen distribution in thyroid cancer by combining the HT with SHG imaging microscopy. The collagen realignment quantified by the HT (associated to an absence of local orientations) in PCT samples differs from that occurring in FA tissues. The usefulness of the method lies in the ability to discriminate malign from benign tumors, what might have potential clinical applications in fields such as Oncology and Pathological Anatomy.

Oral presentation: Session 1. Room C. Code: 5854

Histology and Histopathology
From Cell Biology to Tissue Engineering

Histological consequences on placental chamber in women with venous insufficiency in lower limbs

Ortega M.A.[1], Romero B.[1], Bravo C.[2,4], Sainz F.[3], Asúnsolo Á.[2], Coca S.[1], Martínez-Vivero C.[1], Álvarez-Rocha M.J.[1], Sanz M.A.[1,5], De León-Luis J.[6], Álvarez-Mon M.[1,7], Buján J.[1] and García-Honduvilla N.[1]

[1]Department of Medicine and Medical Specialties, Faculty of Medicine and Health Sciences, University of Alcalá, Alcalá de Henares, Networking Biomedical Research Center on Bioengineering, Biomaterials and Nanomedicine (CIBER-BBN), Ramón y Cajal Institute of Sanitary Research (IRYCIS), Madrid, Spain, [2]Department of Surgery, Medical and Social Sciences, Faculty of Medicine and Health Sciences, University of Alcalá. Ramón y Cajal Institute of Sanitary Research (IRYCIS), Madrid, Spain, [3]Angiology and Vascular Surgery Unit, Central University Hospital of Defense-UAH, Madrid, Spain, [4]Service of Gynecology and Obstetrics, Central University Hospital of Defense-UAH, Madrid, Spain. [5]Service of Pathological Anatomy, Central University Hospital of Defense-UAH, Madrid, Spain, [6]Service of Gynecology and Obstetrics, Section of Fetal Maternal Medicine, University Hospital Gregorio Marañón, Madrid, Spain, [7]Immune System Diseases-Rheumatology and Oncology Service, University Hospital Príncipe de Asturias, Alcalá de Henares, Madrid, Spain

The appearance of varicose veins during pregnancy is a symptom of venous hypertension and venous insufficiency of the lower limb (VI). Despite its frequency, it is unknown whether there are histopathological repercussions, as well as the affectation of the placenta and the newborn. The aim of this study is to analyze the impact VI has on the placenta and its consequences.

A total of 62 IV women and 52 healthy controls (C) were studied. We analyzed the presence of markers of hypoxic damage (Hif-1α), oxidative stress (NOX1, NOX2, iNOS, eNOS, MDA) and cell death in placental tissue with immunohistochemistry and RT-qPCR, as well as metabolomic studies. Plasma and placental levels of MDA were determined by colorimetry in the two study times of 32 weeks of gestation and postpartum. In this line, the impact on the elastic component (tropoelastiena, LOX, LOXL-1, Fibulinas, fibrillins) and collagen (Col-I, Col-III) was analyzed.

The placental damage that was found in women VI was characterized by overexpression of markers of hypoxia, oxidative stress and cell death, accompanied by a change in the profile of the metabolites. Pregnant women with VI showed systemic increases in markers of oxidative stress, such as MDA levels in plasma at different times of study. It was observed how there was an increase in the expression of the elastic component (TE, LOX and LOXL-1), as well as a deregulation of the expression of the collagen component. The fetuses of VI women had a significant decrease in their venous pH compared to those of control women.

The presence of venous disease in the lower extremities during pregnancy could be associated with placental damage and systemic repercussions. The present study shows how VI during pregnancy produces histopathological consequences in the placenta of these women.

This work was supported by grants from the National Institute of Health Carlos III (FIS-PI18/00846) and B2017/BMD-3804 MITIC-CM.

Oral presentation: Session 1. Room C. Code: 5856

Histology and Histopathology
From Cell Biology to Tissue Engineering

Venous reflux induces an inflammatory state modulated by PI3K/Akt/mTOR pathway

Ortega M.A.[1], Romero B.[1], Asúnsolo Á.[2], Sainz F.[3], Álvarez-Rocha M.J.[1], Coca S.[1], Álvarez-Mon M.[1,4], Buján J.[1] and García-Honduvilla N.[1]

[1]Department of Medicine and Medical Specialties, Faculty of Medicine and Health Sciences, University of Alcalá, Alcalá de Henares, Networking Biomedical Research Center on Bioengineering, Biomaterials and Nanomedicine (CIBER-BBN), Ramón y Cajal Institute of Sanitary Research (IRYCIS), Madrid, Spain, [2]Department of Surgery, Medical and Social Sciences, Faculty of Medicine and Health Sciences, University of Alcalá. Ramón y Cajal Institute of Sanitary Research (IRYCIS), Madrid, Spain, [3]Angiology and Vascular Surgery Unit, Central University Hospital of Defense-UAH, Madrid, Spain. [4]Immune System Diseases-Rheumatology and Oncology Service, University Hospital Príncipe de Asturias, Alcalá de Henares, Madrid, Spain

Chronic venous insufficiency (CVI) is a multifactorial disease, commonly caused by valvular incompetence (venous reflux). This fact clearly increases with the age of the patients, with aging being considered as one of the risk factors involved. The activity of the PI3K/Akt/mTOR pathway is mentioned as fundamental in vascular pathologies, understanding its involvement would help in the development of possible therapeutic targets.

This is an observational, analytical and prospective cohort study reviewing 110 patients with CVI. They were distributed according to the presence or not of valvular incompetence-venous reflux, being diagnosed clinically with absence of venous reflux (NR=29) or with venous reflux (R=81). Each of the groups was divided according to age, with the cut-off point being fifty years (NR <50=13, NR≥50=16, R <50=32 and R≥50=49).

The implication of the PI3K/Akt/mTOR pathway, as well as HIF-1α, HIF2-α, CD4+, CD8+, CD19+ and mast cells, has been demonstrated by RT-qPCR, immunohistochemistry and histological techniques. The results show how patients R<50 show a significant increase in PI3K/Akt/mTOR activity, as well as HIF-1α, CD4+, CD19+ and mast cell.

These facts give a basis to the possible existence of changes in the activity of the PI3K/Akt/mTOR route in young patients, with a possible accelerated asynchronous aging that is enhanced by the CVI.

This work was supported by grants from the National Institute of Health Carlos III (FIS-PI18/00846) and B2017/BMD-3804 MITIC-CM.

Oral presentation: Session 1. Room C. Code: 5867

Histology and Histopathology
From Cell Biology to Tissue Engineering

Differential distribution of proteoglycans and other extracellular matrix components in the stroma of the zones of normal human prostates from young adults

Monteiro F.G.R, Beltré R.L.R, Mandarim-de-Lacerda C.A. and Cardoso L.E.M.
Laboratory of Morphometry, Metabolism, and Cardiovascular Diseases, Biomedical Center, State University of Rio de Janeiro, Rio de Janeiro, RJ, Brazil
luizemcardoso@gmail.com

The definition of human prostate zones is based on histological features of the glandular tissue (1). These zones are associated with specific diseases, and their extracellular matrix (ECM) is involved in prostatic disorders such as cancer (2) and BPH (3). However, data on the prostate stroma usually derive from samples of unknown age, with associated co-morbidities, and of restricted/unspecified anatomical locations. Thus, the composition of the normal, aging-unaffected stroma of the human prostate is still little known. Our aim was thus to assess the contents of ECM components in the different zones of the normal prostate using samples from young adults.

Prostate samples were obtained during autopsy of 9 adults aged 21.6±3.5 (mean ± SD) years who had died of accidents, and whose bodies had no macroscopic evidences of systemic diseases or of alterations in the genitourinary tract. Prostates weighed 20.6±2.9 g and were histologically normal. Prostates were perfused in situ with 4% buffered formalin, excised, fixed in this fixative, and totally embedded in paraffin for whole-mount preparations. The zones under study were the anterior fibromuscular stroma (AFS), and the transition (TZ), central (CZ), and peripheral (PZ) zones, and their anatomical delimitations and designations followed Weinreb et al. (1). Immunohistochemistry was carried out on whole-mounts of the prostate using primary antibodies against decorin, biglycan, fibronectin, and smooth muscle alpha-actin. Quantitation of the immunolabeling was based on the color deconvolution method (4) and the relative amount of antigen is expressed as a percentage of maximum theoretical labeling. Total collagen concentration in each zone was determined by a biochemical assay and is given as µg hydroxyproline/mg dry tissue. Numerical results are reported as mean and its 95% confidence interval.

For each protein, zones are ordered according to magnitude of the mean. Collagen concentrations were: PZ, 18.77 (15.56-21.98); CZ, 22.57 (16.53-28.61); TZ, 28.16 (24.07-32.25); AFS, 32.28 (29.37-35.20). Smooth muscle alpha-actin: AFS, 17.11 (13.34-20.88); PZ, 18.46 (12.79-24.13); CZ, 19.19 (12.89-25.477); TZ, 20.52 (17.58-23.47). Biglycan: AFS, 6.91 (5.19-8.63); TZ, 12.79 (9.05-16.54); CZ, 13.13 (8.47-17.78); PZ, 14.07 (9.67-18.47). Decorin: AFS, 18.56 (12.36-24.76); PZ, 21.27 (19.28-23.29); TZ, 23.53 (20.17-26.89); CZ, 40.02 (34.10-45.94). Fibronectin: AFS, 9.49 (8.11-10.86); CZ, 9.82 (8.93-10.71); TZ, 11.77 (8.40-15.14); PZ, 13.16 (10.23-16.09).

In line with previous publications showing differences in glandular tissue among prostate zones, the composition of the prostatic ECM also varies markedly according to region. The AFS differs more conspicuously, whereas PZ, which is associated with cancer, has less collagen and decorin. The latter is decreased in prostate cancer, so that lesser amounts of this proteoglycan in the normal, young PZ and TZ might render these zones more prone to proliferative events, both malign and benign.

(1) Weinreb. Eur Urol. 2016;69:16
(2) Binder. Cancer Lett. 2017;385:55
(3) Cardoso. BJU Int. 2004;93:532
(4) Helps et al. Appl Immunohistochem Mol Morphol. 2012;20:82

Oral presentation: Session 1. Room C. Code: 6176

Histology and Histopathology
From Cell Biology to Tissue Engineering

Impaired activity of ecto-nucleotidases in human endometrial pathologies

Martín-Satué M.[1,2], Rodríguez-Martínez A.[1,2], Trapero C.[1,2], Vidal A.[1,2,3], Gómez de Aranda I.[1], Fernández-Montolí M.A.[2,4], Piulats J.M.[2], Coroleu B.[5], Barri P.[5], Tresserra F.[5], Ponce J.[2,4] and Matias-Guiu X.[2,3]

[1]Unit of Histology, Department of Pathology and Experimental Therapeutics, Faculty of Medicine and Health Sciences, University of Barcelona, Bellvitge Campus, Spain, [2]Bellvitge Biomedical Research Institute (IDIBELL), CIBERONC, Spain, [3]Department of Pathology, University Hospital of Bellvitge, Barcelona, Spain, [4]Department of Gynecology and Obstetrics, University Hospital of Bellvitge, Barcelona, Spain , [5]Department of Reproductive Medicine, Dexeus Mujer, University Hospital Quiron-Dexeus, Barcelona, Spain

The levels of extracellular ATP and its derivatives such as adenosine are impaired in the tissue microenvironment during tissue stress conditions such as hypoxia, infection, metabolic stress, tumor transformation and inflammation. Ecto-nucleotidases are the main regulators of extracellular ATP and adenosine levels. The aim of the present work is to upgrade our understanding of the role and location of ecto-nucleotidases in the context of two endometrial pathologies: cancer and endometriosis, as well as to investigate new diagnostic and treatment modalities based on the inhibition of ecto-nucleotidases' activities.

We have analyzed by means of immunolabeling and in situ enzyme histochemistry human endometrial samples from: 1) endometrial tumors, and, 2) eutopic endometria as well as ectopic endometriotic lesions from women with endometriosis. We have also studied endometrial cell cultures to evaluate the consequences of the overexpression of ecto-nucleotidases in their proliferative and invasive phenotypes.

Ecto-nucleotidases showed impaired expression in pathological conditions when compared with non-pathological endometria. This altered pattern includes changes in expression levels and changes in protein localization, mainly a switch between epithelium and stroma. Overexpression of ecto-nucleotidases in endometrial cell cultures lead to changes in the proliferation and invasion rates.

Impaired ecto-nucleotidases activities in endometrium might contribute to the pathogenesis and maintenance of endometrial pathologies with an inflammatory component such as cancer and endometriosis.

This work is supported by grants from the *Instituto de Salud Carlos III* (*FIS PI15/00036, PI18/00541*), co-funded by FEDER funds/European Regional Development Fund (ERDF)-"a Way to Build Europe"- // *FONDOS FEDER "una manera de hacer Europa",* and a grant from the *Fundación Merck Salud* (*Ayuda Merck de Investigación 2016-Fertilidad*), and *Grupos coordinados estables de investigación oncológica* of *Asociación Española Contra el Cáncer* (*AECC*). ARM awarded a fellowship from the *AECC*.

Oral presentation: Session 1. Room D. Code: 5672

Histology and Histopathology
From Cell Biology to Tissue Engineering

Histological characterization of the gametogenic stages of *Melongena melongena* (*Linnaeus, 1758*)

Uría Galicia E. and Espinosa Almanza B.
Instituto Politécnico Nacional, Escuela Nacional de Ciencias Biológicas, Departamento de Morfología, Laboratorio de Histología Animal, Ciudad de México, México
estherqbp@yahoo.com

The coastal lagoons are ecosystems that harbor great quantity of organisms, some species take advantage of the alimentary resources, as well as: oysters, clamps, mussels and snails, which are part of the diet of fishes, aquatic birds and crustaceans, being part of complex trophic chains. The Tampamachoco lagoon it is localized at the coastal plain of the State of Veracruz. The snail *Melongena melongena*, known as "molón" or "nolón", it's distributed from the coast of Florida and west of Alabama, in the United States of America, till the Antilles and South America. In Mexico, it is localized in the states of Veracruz, Campeche and Yucatán, it is a benthic gastropod that is usually buried in the lagoon sediment; it is dioecious with intern fertilization and differentiated reproductive organs. In spite of its ecological importance as representative species from the lagoon, its reproductive cycle is unknown, as in the case of the Chivita snail, *Melongena corona bispinosa* (Philippi, 1844), endemic of the Yucatan Peninsula, Mexico, its reproductive aspects and reproduction cycle are mentioned, so this paper establishes the histological features of the gametogenic stages and made possible to characterize the reproductive cycle of M. melongena, contributing to its conservation in the mentioned lagoon.

In the months of February, April, June and September, which corresponds to each season of the year 2014, was collected samples of this specimens using traps for crab, obtaining a total of 256 samples, of which were selected 40 of both sexes and largest size. In the laboratory, through the inclusion technique in paraffin, 10 specimens of every month were processed, taken the samples from the region of the gonad; sections of 7-10 microns were stained with Harris hematoxylin and contrasted with eosin, then, photographed for their analysis.

The stages were histological characterized: Maturation, spawning and expulsion; based in: gonadic tissue volume, grade of development of the gametogenic cells and the presence and abundance of this. Specimens in gametogénesis stage where not found, because the harvest wasn't made the whole year and the samples were the largest ones of the four months. Constant gamete expulsion was found in the male samples, and spawning fluctuation in the female samples, with these stages: spawning-simultaneous expulsion, exclusively in September.

M. melongena presents during the whole year, gamete emission (spawning and expulsion stages), reproductive pike in September (autumn), where the spawning and gamete expulsion coincides with the rain season which helps to descend the water temperature and the average of salinity, coinciding as well, with some aspects of the gametogenic stages described for *M. corona bispinosa.*

Oral presentation: Session 1. Room D. Code: 5868

Histology and Histopathology
From Cell Biology to Tissue Engineering

Characterization of the sea anemone *Bunodosoma sp.* cnidome, of Tecolutla, Veracruz, Mexico

Cordero-Ramos D.I.[1], Márquez-Ramos J.A.[1], Valdez-Peralta H.I.[1], Matadamas-Guzmán M.F.[1], Hernández-Calderas I.[1], Guerrero-Legarreta I.[2]. Segoviano-Ramírez J.C.[3], Díaz-Larrea J.[4], and Guzmán-García X.[1]

[1]Laboratorio de Ecotoxicología. Departamento de Hidrobiología, División de Ciencias Biológicas y de la Salud, Universidad Autónoma Metropolitana Unidad Iztapalapa, Ciudad de México, México, [2]Laboratorio de Macromoléculas. Departamento de Biotecnología, División de Ciencias Biológicas y de la Salud, Universidad Autónoma Metropolitana Unidad Iztapalapa, Ciudad de México, México, [3]Unidad de Bioimagen. Centro de Investigación y Desarrollo en Ciencias de la Salud, Universidad Autónoma de Nuevo León, Monterrey, Nuevo León. México, [4]Laboratorio de Genética y Ficología aplicada. Departamento de Hidrobiología, División de Ciencias Biológicas y de la Salud, Universidad Autónoma Metropolitana Unidad Iztapalapa, Ciudad de México, México

xochitlguga@gmail.com

Cnidarians are a group of invertebrate organisms, characterized by the presence of urticating's cells, called cnidocytes. These secrete toxins, with important applications in biochemical, pharmaceutical and biotechnological industries, among others. The distribution and type of cnidocytes in sea anemones form the cnidome, its characterization is essential for taxonomic identification. Traditionally, the use of taxonomic keys has been used for species identification, however, the histological identification of sea anemone cnidoma allows an identity approach. The objective of this work was to characterize sea anemone cnidome in organisms from Tecolutla, Veracruz, through histological techniques, leading to taxonomic location and to contribute towars the knowledge of this geographic area biological heritage.

Ten sea anemones were collected in Tecolutla, Veracruz, transported to our laboratory, and kept *in vivo*. Physicochemical and morphometric parameters were registered and controlled. The organisms were anesthetized by two methods: using menthol crystals and cooling down at 1ºC/10 min up to 4°C. Sections of pedal disc, column, oral disc and tentacles were obtained and stained with H-E and H-F. Identification of cnidocytes was performed in an optical microscope fitted with a 100x objective. An average of 11 fields were reviewed for each preparation. Thirty cells of each of cnidocyte type were chosen at random; the length and width were measured using an AxioVision 4.8 program. Subsequently, the frequency of appearance of each cnidocyte was recorded and statistics (mean, standard deviation and range) were calculated. Cnidocyte photo-documentation was processed in two programs: Adobe Lightroom Classic CC 8.1 and Zerene Stacker 1.04. Cnidocyte type was concluding, by comparing our observations to those reported in the literature.

The optimal sedation method for these sea anemones was the gradual temperature reduction. The average physicochemical parameters were: 24°C, pH8.2, 34 ups salinity, 3.4 mg/L dissolved oxygen, 0.02 mg/L and NH3/NH4 ratio These parameters allowed a low mortality rate. In characterizing the cnidome, the following cnidocites were observed: spiral-shaped spirocytes; narrow and elongated basitrichs; and narrow and slightly twisted mastigophores and holigotrics All of these structures take part in processes such as food capture, defense mechanism and adhesion to the substrate. In agreement to previously reports studies, our results showed that the studied anemone has common characteristics with *Bunodosoma cavernatum* species, reported by González- Muñoz (2013).

Cnidome characterization is relevant for sea anemone taxonomic identification. Therefore, tissue technique is an important diagnosis tool, however, it is important to carry out measurements with specialized microscopes. Our study contributed to the knowledge of the tissue composition of sea anemone cnidome, particularly of organisms from Tecolutla, Veracruz and provided an approach on its taxonomic identity.

Gonzales-Muñoz (2013). Sea anemones (Cnidaria, Anthozoa, Actiniaria) from coral reefs in the southern Gulf of Mexico. *Zookeys*. 341, 77-106.

Oral presentation: Session 1. Room D. Code: 5869

Histology and Histopathology
From Cell Biology to Tissue Engineering

Analysis of the histopathological index in the digestive gland of the clam *Polymesoda caroliniana* from Tecolutla, Veracruz, Mexico

Jerónimo-Juárez J.R.[1], Hernández-Calderas I.[1], Segoviano-Ramírez J.C.[2] and Guzmán-García X.[1]

[1]Laboratorio de Ecotoxicología, Histología. Departamento de Hidrobiología. División de Ciencias Biológicas y de la Salud. Universidad Autónoma Metropolitana Unidad Iztapalapa. Ciudad de México, México, [2]Unidad de Bioimagen. Centro de Investigación y Desarrollo en Ciencias de la Salud. Universidad Autónoma de Nuevo León. Monterrey, Nuevo León. México

Histopathological index is a semiquantitative analysis that integrates pathological alterations of a target organ into a single value. This value is constructed from the biological significance and the degree of dissemination of each pathological alteration. Histopathological index has been proposed in pollution monitoring studies since it allows to infer the health status of the organisms. In Mexico, these analyzes have not been carried out on bivalves and they represent an advantage in the evaluation of the effects of contamination. The aim was to evaluate tissue responses in the digestive gland of clam *P. caroliniana* from Tecolutla, Veracruz, in order to determine its state of health through a histopathological index.

Fifty clams of the *P. caroliniana* were collected in Tecolutla Veracruz. The samples were fixed with 10% buffered formalin in PBS 1 mM, pH7.4, three serial histological cuts of 5 µm of the digestive gland were made with a microtome and stained with Hematoxylin-Eosin. The morphological analysis of the tissue sections was performed with an optical microscope. The fields from slides analyzed were randomly chosen by a "zig zag" movement, considering the structure of the tubules. In the tissue description, presence of the covering epithelium, lumen of the tubules, as well as the appearance of the connective

tissue and presence of infiltrations, brown cells, atrophies or parasites were considered. For the analysis of alterations, 18 optical fields (40X) per organism were considered. The values and the histopathological index estimation model were made according to Cuevas et al. (2015) who consider infiltrations, presence of brown cells, atrophies and parasites as histopathological alterations. Later, the prevalence of the alterations was calculated, and values of biological significance were assigned from 1 to 3 (where 1 is minimal significance and 3 is severe) and the degree of dissemination from 0 to 6 (where 0 is absence of the alteration and 6 is diffuse).

Digestive tubules were characterized by presenting simple epithelial tissue with pyramidal cells, central lumen and surrounded by loose connective tissue . Five pathological alterations were observed: brown cells in epithelia and connective tissue, hemocytic infiltrations in intertubular connective tissue, aggregates of lipofuscin, atrophies and parasites. According to the percentage of prevalence of alterations, 90% of the organisms showed brown cells, 70% hemocytic infiltrations, 5% lipofuscin aggregates and atrophies and in 0.5% parasites. The estimated histopathological index showed values between 0.01 and 0.18 in the whole population, that according to what was reported by Costa et al. (2013) do not compromise the state of health of the organisms.

The alterations observed in the digestive gland of the clam and the values obtained in the estimation of the histopathological index suggest that there is no significant pathological compromise in the state of health of these organisms. The histopathological index estimation is a method that can be considered in the semiquantitative evaluation of wild organisms.

We acknowledge to Posgrado en Energía y Medio Ambiente de la Universidad Autónoma Metropolitana Unidad Iztapalapa.

Oral presentation: Session 1. Room D. Code: 6200

Histology and Histopathology
From Cell Biology to Tissue Engineering

Effect of dietary addition of the probiotic *Bacillus pummilus* on the gut and liver of *Aparus aurata*

Albaladejo-Riad N.[1], Jlidi M.[2], Mamdouh Ben Ali M.[2] and Esteban, M.A.[1]

[1]Department of Cell Biology and Histology, Faculty of Biology, Campus Regional de Excelencia Internacional "Campus Mare Nostrum", University of Murcia, Murcia, Spain, [2]University of Sfax, Centre of Biotechnology of Sfax (CBS), Laboratory of Microbial Biotechnology and Engineering Enzymes LMBEE, Sfax, Tunisia

aesteban@um.es

The use of probiotics in aquaculture with the aim of improving feed and thus increasing the survival of the specimens is very common [1, 2]. One of the best known and used probiotics are different species of *Bacillus sp.*, both in aquaculture and in human medicine [3]. There are several studies that support the advantages of using *B. pumilus* as probiotic in humans [4] and, for this main reason, we decided to test the efficacy of *B. pumilus* as a probiotic in farmed fish.

Juvenile gilthead seabream (*Sparus aurata* L.) of 50±25 g body weight were obtained from a local farm (Murcia, Spain) and randomly distributed in 6 tanks (12 fish/tank) of sea water (250 L) at the Marine Fish Facilities of the University of Murcia. The water was maintained at 20±2ºC, 28‰ of salinity and circulating at 900 lh^{-1}. The fish acclimatized for 2 weeks under these conditions and were fed daily at a rate of 2% of their mean tank biomass with a commercial diet (Skretting, Spain). After the acclimatization period, three experimental groups (n=12) were fed for one month with a commercial diet supplemented with one of the three concentrations of *B. pumilus*: 0 (control), 10□ CFU/g and 10□ CFU/g. Half of these specimens (n=6) were randomly sampled after two weeks of experimentation, and the other half after one month of trial.

The full fish were fixed in Bouin and included in paraffin to obtain longitudinal, transverse and sagital sections of them which were stained with Hematoxylin and Eosin. The somatometric parameters were analyzed with MIP-4.5 and the data obtained with ANOVA one way by using SPSS.

The results more evident were in digestive (gut and liver). In this way, for each group, the degree of hepatic steatosis, the length of the intestinal villi, the variation in the diameter of the testicular cords and the area occupied by interstitial space in fractions of the testicle were measured.

It can be concluded that the inclusion of this probiotic in fish diet has a direct effect of gut morphology.

This work was supported by the MINEICO (grant no. AGL2017-83370-C3-1-R) co-funded by the European Regional Development Funds (ERDF/FEDER) and Fundación Seneca de la Región de Murcia (Grupo de Excelencia grant no. 19883/GERM/15).

[1] Irianto A. & Austin B. (2002). Probiotics in aquaculture. *J. Fish Dis*, *25*, 633-642.
[2] Balcázar J.L., De Blas I., Ruiz-Zarzuela I., Cunningham D., Vendrell D. & Muzquiz J.L. (2006). The role of probiotics in aquaculture. Vet. Microbiol.114, 173-186.
[3] Cutting S.M. (2011). Bacillus probiotics. Food Microbiol. 2, 214-220.
[4] Duc L.H., Hong H.A., Barbosa T.M., Henriques A.O. & Cutting S.M. (2004). Characterization of Bacillus probiotics available for human use. Appl. Environ. Microbiol., 70, 2161-2171.

Oral presentation: Session 3. Room B. Code: 5904

Histology and Histopathology
From Cell Biology to Tissue Engineering

Morphological characterization and function of amacrine cells expressing TRPM8 cold-transducing ion channel

Alcalde I.[1], Sánchez C.[1], Artime E.[1], García Fernández J.M.[2], Martín C.[1,3], Quirós L.M.[1,3] and Merayo-Lloves J.[1]

[1]Instituto Universitario Fernández-Vega, Fundación de Investigación Oftalmológica, Universidad de Oviedo, Oviedo, Asturias, [2]Departamento de Morfología y Biología Celular, Universidad de Oviedo, Oviedo, Asturias, [3]Departamento de Biología Funcional, Universidad de Oviedo, Oviedo, Asturias, España
nacho.alcalde@fio.as

TRPM8 is a cold-transducing ion channel expressed characteristically in a supopulation of peripheral sensory neurons, innervating the skin, the cornea of the eye, the tongue and gut. Recently, TRPM8 has been related to the mainteinance of hydration in the ocular surface and also discussed to have a role in body temperature regulation. Novel transgenic mice expressing fluorecent reporters associated to TRP channels have been developed and morphological studies of protein location have been significantly improved. We report here the expression of TRPM8 channels in neurons with no clear exposition to cold stimulus, such as the retina or the brain. This study is aimed to characterize the distribution and function of TRPM8 ion channel in the retina.

Retinas from adult transgenic TRPM8-EYFP and TRPM8-KO mice, in which a fluorescent protein was attached to the promoter sequence of cold-transducing channel TRPM8 were used. A total of ten animals of each genotype was employed. Immunohistochemical techniques against calcium binding proteins (Calretinin, Calbindin, Parvalbumin), and markers to neurotransmitters (Tyrosin-hyroxilase, Cholin acethil transferase, GABA and Glutamate transporters and receptors) were performed on whole mounted retinas and transversal cryostat sections of transgenic eye globes. To establish the cytoarchitecture of isolated amacrine cells dendritic arborization and their IPL contribution, iontophoretic injection of Neurobiotin was performed. Previous to morphological analysis, mice were submmited to an Electroretinography (ERG) study to evaluate the functional role of TRPM8 in the retina. Animals were handled and cared following the guidelines Spanish Goverment (RD 53/2013) and the European Commissions (86/609/EC).

We described a population of TRPM8 positive amacrine cells homogeneously distributed in the central and periferal retina without formation of clusters. These cells were located both at the inner border of the internal nuclear layer and in the ganglion cell layer. They were identified morphologically as amacrine cells, and were never found grouped in clusters. Their dendritic processes were located in two densely packed layers coinciding with sublayers 2 and 4 of the inner plexiform layer (IPL) corresponding to the two outer layers of CR staining. Fluorescent cells were also seen in the ganglion cell layer (GCL), being classified as displaced amacrine cells of the GCL. These cells were $ChAT^+$ and contribute to form the inner $TRPM8^+$ sublayer at the IPL. Amacrine cells in the retina of TRPM8-KO mice did not express TRPM8 protein or mRNA. However, the number of ChAT+ amacrine neurons at the IPL and GCL was similar to that found in wild type mice. Electroretinograph analysis showed a reduced impact of TRPM8 lack in the phisyology of the retinal amacrine layer. The absence of TRPM8 in aged KO mice altered the normal oscillatory potentials and b-wave.

A subtype of amacrine cells expressing TRPM8 channels was identified. It appears unlikely that TRPM8 channels expressed by these neurons is involved in cold detection. In contrast, the expression of ChAT strongly suggests that near a 60% of cells of this new subtype may be starburst-like cells and could be involved in directional selectivity.

Oral Presentations

Session 2

Thursday, 18-19 hours

Oral presentation: Session 2. Room A. Code: 5882

Histology and Histopathology
From Cell Biology to Tissue Engineering

Vitronectin and its receptors: human neuroblastoma 2D *in vitro* characterization

Burgos-Panadero R.[1,2], Monferrer E.[1], Noguera Salvá I.[3], Navarro S.[1,2] and Noguera R.[1,2]

[1]Department of Pathology, Medical School, University of Valencia/INCLIVA, Valencia, Spain, [2]CIBER of Cancer (CIBERONC), Madrid, Spain, [3]Central Support Service for Experimental Research (SCSIE), University of Valencia, Spain

The stiffness of the extracellular matrix (ECM) has been correlated with the aggressiveness of malignant tumor cells. In order to identify new therapeutic targets, we focus on vitronectin (VN), a multifunctional glycoprotein that acts as a link between cells and the ECM through several ligands such as integrins and urokinase plasminogen activator receptor (uPAR). VN has an adhesive role in the provisional matrix of several human tumors participating in tumor growth, angiogenesis and metastasis. Our aim in this work is focused on defining the 2D *in vitro* VN expression and its receptor patterns exhibition in neuroblastoma (NB) cell lines.

SK-N-BE (2) and SH-SY5Y NB cell lines were grown in complete and serum-free media. Cells were cultured in cell chamber slides and in T-75 flasks for VN detection. Using Trypsin/EDTA 0.25% we detached flask cells and deposited onto poly L-lysine coated slides by cytocentrifugation. Cells were fixed with methanol/acetone (1:1) for 10 min at room temperature and immunostained with VN antibody (ab45139, Abcam) using the BenchMark XT automated slide staining system. In addition, for the detection of $\alpha_v\beta_3$ integrin (ab7166, Abcam) and uPAR (ab218106, Abcam) we employed the Dako REAL™ EnVision™ Detection System, Peroxidase/DAB+, Rabbit/Mouse Kit.

Regarding VN presence, when we grew the cells lines in cell chambers slides, we observed that VN pattern expression was as dot drops at cytoplasmic compartment in both cell lines and growth conditions (complete and serum-free media) and in cell prolongations mainly in SK-N-BE (2) cells. We only observed cytoplasmic VN dot drops expression in cytospined cells being higher in SH-SY5Y cells. Additionally, we found diffuse cytoplasmic pattern of $\alpha_v\beta_3$ integrin staining being very low or negative staining in SK-N-BE (2) cells and with several expression degrees in SH-SY5Y cells. Finally, we observed that uPAR expression was as Golgi-like staining pattern with a low expression in SK-N-BE (2) cells and high expression in SH-SY5Y cells.

We highlighted the importance to carry on doing further studies to prove the potential use of VN and its receptors as future therapeutic targets in NB.

Funding: CIBERONC (CB16/12/00484) and FIS (PI17/01558), Institute of Health Carlos III (Madrid) cofounded with ERDF and Neuroblastoma Foundation.

Oral presentation: Session 2. Room A. Code: 5890

Histology and Histopathology
From Cell Biology to Tissue Engineering

Effect of sexual behavior on the histological characteristics of major pelvic ganglion and denervated prostate

Sánchez-Zavaleta V.[1], Mateos-Moreno A.[1], Herrera-Covarrubias D.[2], Aranda-Abreu G.E.[2], Manzo-Denes J.[2] and Hernández-Aguilar M.E.[2]

[1]Doctorado en Investigaciones Cerebrales, Universidad Veracruzana, Veracruz, México, [2]Centro de Investigaciones Cerebrales, Universidad Veracruzana.

The prostate, is a sexual gland responsible for producing prostatic fluid necessary to ensure reproductive success. In the male rat, this gland is regulated by both, hormones and innervation from the Major Pelvic Ganglion (MPG). It is known that sexual behavior is a stimulus that, in addition to inducing an increase in prostatic fluid synthesis, is also believed to be associated with the possibility of not developing prostate cancer. But it is still unknown if this hypothesis is correct and if the nervous system intervenes in the development of diseases in the gland. That is why the objective of this work was to analyze the effect of sexual behavior on the histology of MPG and denervated prostate.

Male Wistar rats of 3 months old were divided into two groups: without sexual experience (WSE) and sexual experience (SE), and grouped into non-manipulated (NM), false surgery (SHAM), denervated from pelvic nerve, denervated from hypogastric nerve and denervated from both nerves, for a period of 15 days.

The dates obtained shown that denervated prostate from WSE subjects, presents histological alterations similar to metaplasia and mild dysplasia, while in the MPG had a decrease in the neuronal area and a more significant presence of SIF cells and fibroblasts. On the other hand, denervated prostate of SE subjects had normal histology and this is similar to the non-manipulated subject, and in the same way, the MPG.

These results indicate that sexual behavior is a stimulus that favors the maturation of both, ganglion and the prostate and suggest that elevation of prolactin and testosterone observed during the execution of the sexual behavior, as well as the activation of the ganglion during the performance of such action, not only control the function of the gland but also promotes a delay in the appearance of diseases in the prostate.

Support: (CONACyT: VSZ 595360 y AMM 595375; UV-CA-304).

Oral presentation: Session 2. Room A. Code: 5746

Histology and Histopathology
From Cell Biology to Tissue Engineering

Rabbit peyer's patches membranous cells (M cells) subcutaneously challenged with ovoalbumin

Roma S.M.[1,2], Pérez F.A.[1] and D'Ottavio A.E.[2]

[1]Cátedra de Histología y Embriología, Facultad de Ciencias Médicas, [2]Consejo de Investigaciones, Universidad Nacional de Rosario República Argentina

Rabbit Peyer's patches (PP) are lined by a simple columnar epithelium associated with the follicle (FAE) where there are numerous membranous cells (M cells) specialized in macromolecular transfer. While the contact of antigens with this internal tissue triggers a harmful inflammatory response, once the noxa has been removed the repair stage starts. Although changes have been published in PP-FAE when the antigen was orally administered, no information was found regarding what could happen when parentally injected. Therefore, this communication reports morphological modifications in rabbit PP- M cells subcutaneously (sc) challenged with ovalbumin (OVA).

Thirty adult New Zealand rabbits were divided into six groups: (1) four groups related with inflammatory stage [A-control; B- subcutaneous administration of complete and incomplete Freund adjuvant (CFA and IFA); C- subcutaneous injection of OVA emulsified in CFA; D - two subcutaneous injections of OVA emulsified in CFA and IFA, and (2) two groups related with reparation stage: [E and F- euthanized 1 and 2 weeks after the second dose of OVA, respectively]. PP samples stained with H&E and immunostained with vimentin (universal and reliable marker for M cells), were studied with specialized software for image analysis (Ipwin4). The areas of FAE and M cell pockets were measured, statistically expressed as arithmetic mean±standard error and analyzed with the ANOVA test, considering a $p<0.05$ as significant.

Results regarding FAE areas were: A-47976.3±3215.7 μm^2; B-45022.67±3557.3 μm^2; C-43154.27±2156.3 μm^2; D-35084.83±4744 μm^2; E-44564.56±1858.8 μm^2 and F-53510.12±2969.8 μm^2 ($p=0.0177$) and regarding M cell pocket areas, were: A-17221.29±1376 μm^2; B-17155.02±387.3 μm^2; C-13763.48±1004.2 μm^2; D-10652.16±1987 μm^2; E-16737.11±1017.4 μm^2 and F-17775.7±950.4 μm^2 ($p=0.0183$). As seen, the parenteral administration of an antigen (peripheral immune system) produces changes in FAE area (mucosal immune system). The immediate decrease in both registered areas after immunization could be related with a lower sensing of the luminal content and a lower stimulation of the secretory immune response. On the other hand, the harmful effect would have ended in E and F groups allowing the recovery of FAE area to control group values and indicating their participation in the immuno-homeostasis.

In conclusion, the obtained results point out an interconnection between the mucosal and peripheral immune systems, and reveal PP changes in rabbits subcutaneously challenged with an antigen, contributing to the knowledge of the mucosal barrier and warning about a possible mechanism weakening it.

Oral presentation: Session 2. Room B. Code: 5895

Histology and Histopathology
From Cell Biology to Tissue Engineering

Evaluation of digital stereology methods for estimating the batch fecundity of the pacific sardine (*Sardinops sagax*) on the west coast of Baja California Sur, Mexico

Torres-Villegas J.R.[1], Ochoa-Báez R.I.[1,2] and Valdez-Montiel U.F. [1]

[1]Centro Interdisciplinario de Ciencias Marinas (CICIMAR-IPN), Instituto Politécnico Nacional (IPN), La Paz, BCS, México, [2]Becaria de la Comisión de Operación y Fomento de las Actividades Académicas del IPN

There is growing concern about the sustainable management of fisheries due to overexploitation of many marine fish species. A key is the fecundity and the control of oocyte production in the breeding population. Histological studies are used to identify spawned females and those with follicular atresia. However, to study the mechanisms of oocyte production in fish, it is necessary to study the recruitment of oocytes between maturity stages, as well as the effect of atresia, both with quantitative assessments. However, to study the mechanisms of oocyte production in fish, qualitative and quantitative estimates of oocytes recruitment among maturity stages and the effect of atresia are required. These issues are little known, particularly in fish species with indeterminate fecundity. We suggest estimates of batch fecundity in Pacific sardine obtained with digital stereology applications.

In this study, we analysed the calibration of batch fecundity assessment obtained by the gravimetric, Weibel-Gomez, and physical dissector methods, when applied to the same group of mature Pacific sardine females (*Sardinops sagax*) a species with indeterminate fecundity, for which the production of oocytes per female can only be estimated each spawning event. In all of the applied methods, digital image processing techniques were used. To apply the Weibel-Gomez method, micrometric estimates of the shape and size of the oocytes were used to preclude the necessity for assumptions regarding any of these parameters. Much of the bias was related to the tissue shrinkage due to the histological technique, so we estimated a correction factor that was applied to all of the batch fecundity estimates. In addition, further bias was introduced in the physical dissector method because the density of intraovaric oocytes at final maturity influences the dissector based on its depth of acquisition, so a geometric system was developed to reduce this bias.

The calibration curves and ANOVA do not indicate significant differences in the results obtained with the three methods; although, there is a non-significant deviation with the estimation of partial fecundity obtained with the thickest physical dissector. Finally, we discuss the ramifications of the use of these calibration curves, in particular, the possible reduction of work given the ability to use digital image processing techniques to support stereology to estimate the batch fecundity of the Pacific sardine, a species with indeterminate fecundity.

Oral presentation: Session 2. Room B. Code: 5896

Histology and Histopathology
From Cell Biology to Tissue Engineering

Oogenesis and spawning in *Cardinops sagax*, B.C.S., Mexico, and *Engraulis encrasicolus*, Mediterranean sea

Ochoa-Báez R.I.[1,2] and Torres-Villegas J.R.[1]

[1]Centro Interdisciplinario de Ciencias Marinas (CICIMAR-IPN), Instituto Politécnico Nacional, La Paz, BCS, Mexico, [2]Becario de la Comisión de Operación y Fomento de las Actividades Académicas del IPN

Oogenesis in teleost fishes has been described in numerous species based on microscopic morphology, this methodology allows to follow the dynamics during the growth of the oocyte, the spawning and the post in each day in the reproductive season. The information produced provides the parameters to estimate the spawning biomass by the daily method egg production, applied in pelagic fish. The Pacific sardine, *Sardiops sagax*, from northwestern Mexico and *Engraulis encrasicolus*, in the Mediterranean Sea, are examples. Both are iteroparous species, characterized by the polymodal distribution of intraovarian oocyte diameter.

The objective of this study is to compare the tissue and cellular changes in the ovary during the maturity of the oocytes and the postovulatory follicles in the circadian cycle, during the season of maximum reproductive activity.

Sardines were collected in winter in purse-seine fishing sets on board the commercial fleet and anchovies in the spring in experimental trawling for anchovies, both at the peak of their spawning season. Due to the logistic of the fishing the samples were collected in different dates and schedules, by logistic of the capture, in schedules and different dates, until completing the scheme hour by hour in the 24 hours of the day. The ovaries were fixed in 10% buffered formaldehyde and the morphometric parameters of each specimen were recorded. The samples were processed with the histological technique by inclusion in paraffin.

The stages of maturity were identified and morphological changes were registered in periods of one hour from oogonia to hydration, spawning, post-spawning and atresia. The frequencies of the stages of the follicles were obtained throughout the cycle, the time of spawning was taken as a reference and a model was constructed to estimate the time elapsed until spawning and post-spawning. With this model, the “age” of the postovulatory follicles of both species is estimated, which coincides approximately with the antecedent of the northern anchovy in California.

With this information, we validate the way to estimate the frequency of spawning females per laying event and the number of spawning during the breed season for these species. On the other hand, the monitoring of oocyte maturity stages provides an idea of the intraovarian dynamics of oocyte recruitment between stages and the possible control of atresia in fecundity, both relevant issues in the sustainable management of fishery resources.

Oral presentation: Session 2. Room B. Code: 5897

Histology and Histopathology
From Cell Biology to Tissue Engineering

Histological comparison of the reproductive system between oviparous and viviparous species of elasmobranchs distributed in the mexican coasts

Soto-López K., Ochoa-Báez R.I. and Galván-Magaña F.

Centro Interdisciplinario de Ciencias Marinas (CICIMAR-IPN). Instituto Politécnico Nacional, La Paz, BCS, Mexico

Reproductive biology information is necessary to contribute to sustainable management for exploited elasmobranch species. Histology is an important tool for validating the maturity, the minimum and average size of capture, as well as the demography of the species. *Mustelus henlei,* a placental viviparous shark and *Raja velezi* an oviparous ray, are commercially targeted on the coasts of the Mexican Pacific.

The aim of this study was to compare by morphophysiological analysis the reproductive system of females and males, of *M. henlei* and *R. velezi*.

For females the ovary and the oviducal gland and for male testicle, epididymis and the seminal vesicle were studied. The organs were fixed in 10% neutralized formaldehyde; inclusions were made in paraplast and thin sections. Staining techniques were made according to the structure: with Mallory's Trichrome to describe the ovary; the oviducal glands the periodic acid-Schiff technique and for the testicles, epididymis and seminal vesicles the Feulgen technique.

The ovary of the two species present a similar histological and cellular structure; *R. velezi* shows an asynchronous development on the distinguishable oocytes in the different stages of oogenesis, as for *M. henlei*, the ovarian development is synchronous. Oviducal glands presents the four characteristic zones in the elasmobranchs (club zone, papillary zone, baffle zone and terminal zone), in both species semen storage occurs in the terminal zone, with different positions according to the storage time. In addition, secretions of mucopolysaccharides were located in *R. velezi* in the baffle zone where the ovigerous capsule is formed. On the other hand, for males, the testes of both species show the spermatogenic development in its different phases, noticing a continuous production of semen. At the level of the epididymis, *R. velezi* shows sperm arrangement in packages, which will be stored in the seminal vesicle. *M. henlei* showing the arrangement in the seminal vesicle forming conglomerate or spermatozeugmata. Given the histological characteristics of the gonads of both species, it was possible to determine the reproductive maturity of the organisms.

In conclusion, the scientific information obtained in the present study is important to contribute to protective measures in the fisheries management of these species. Since the reproductive strategies described can only be validated histologically, such as the semen storage in both males and females, they confirm the need to carry out histological studies in all commercially captured elasmobranch species.

Oral presentation: Session 2. Room C. Code: 5690

Histology and Histopathology
From Cell Biology to Tissue Engineering

Heterogeneity of Wt1 immunoexpression in pericardial tissues

Andrés-Delgado L. and Santamaría L.

Departamento de Anatomía, Histología y Neurociencia, Facultad de Medicina, Universidad Autónoma de Madrid, Spain

The epicardium, the outer mesothelial layer enclosing the myocardium, plays key roles in heart development and regeneration. Also, the epicardial derived cells can differentiate into other cell types such as cardiac fibroblasts or valves. The epicardium derives from the proepicardial organ (PE), a mass of cells that emerges from the dorsal pericardium tissue (DP) close to the venous pole of the heart tube. PE appears around the time of heart looping and after the onset of the beating of the heart. After the PE is formed, the heartbeat generates a pericardial fluid flow that allows the PE cells to detach from DP and bind to the myocardium.

We used the zebrafish model to study the morphogenetic events leading to PE tissue formation. It takes place at 60 hpf (hours post fertilization) in zebrafish, and about 10 cells of the DP suffer a transformation from a mesothelial flat tissue to a protruded cluster of PE tissue. This suggests that an epithelial-mesenchymal-like transition (EMT) process could be taking place. Wt1 has been implicated in regulating the EMT equilibrium in multiple contexts, including kidney and heart development, or cancer. In epicardial derived cells expression of Wt1 is present in the larval zebrafish. We studied whether in zebrafish Wt1 expression is similar in the PE compared to the DP tissue.

Experiments were performed in Zebrafish (*Danio rerio*), using the line Et(-26.5Hsa.WT1-gata2:EGFP)^{cn1}, in which GFP expression is controlled by the regulatory elements of *wilms tumor 1a* (*wt1a*), and recapitulates its expression pattern. Thus, in these animals PE and DP tissue are GFP^{+}. After 60 hpf embryos fixation, they were immunostained with a primary antibody against GFP, and secondary antibody were tagged to an alexa-488 (green). Embryos were imaged with a Zeiss 780 confocal microscope under a 20× objective. Z-stacks of the whole heart cavity were taken every 5 µm of distance. Calculation of tissues volumes were done using stereological Cavalieri's estimator. Intensity quantification of immunofluorescence was calculated in the Wt1-green channel.

PE tissue is rounder than the DP tissue. PE tissue volume is lower than the DP tissue volume. PE tissue present increased Wt1 immunostaining intensity related to DP tissue.

In zebrafish, using a line where GFP recapitulates Wt1 expression, we conclude that Wt1 protein is more expressed in PE than in DP tissue. Wt1 overexpression could be favoring the formation of PE tissue during development in a way resembling to an EMT process.

Oral presentation: Session 2. Room C. Code: 5784

Histology and Histopathology
From Cell Biology to Tissue Engineering

High-resolution microscopy shows a concentration of beta2-adrenergic receptors in the terminal piece of the human sperm flagellum

Girela J.L.[1,2], Francou M.[1,2], De Juan A.[4] and De Juan J.[2,3]

[1]Department of Biotechnology, Faculty of Sciences, [2]Biotechnology Research Group, [3]IUIEG, University of Alicante, Spain, [4]University Hospital, San Juan, Alicante, Spain

Recent studies have shown that spermatozoa have a very complex machinery of cell signalling processes. As part of that signalling machinery, numerous neuroreceptors have been reported in the sperm plasma membrane. Human sperm is regionalised, with several physiological processes restricted to determined areas, being therefore expected that specific molecules involved in those processes should also be restricted to that area. Although indirect methods have determined the presence of the Beta2-adrenergic receptor (ADRB2) in human sperm, there is no direct evidence nor the description of the localisation of that receptor. We design the study by developing new techniques that allow us to use high- resolution microscopes (i.e. Laser Scanning Confocal Microscopy LSCM and Field Emission Scanning Electron Microscopy or FE-SEM) to identify the fine localisation and distribution of ADRB2 in human sperm.

After written consent and ethical approval, semen samples from 7 young, healthy volunteers were used. All the samples were normozoospermic according to WHO 2010 criteria. As positive control, we used the neuroblastoma cell line SH-SY5Y known to express the ADRB2. To identify the presence of the protein we used Western Blot techniques, in both sperm and neuroblastoma cells. As a positive control for western blot techniques, we used tubulin. Immunolabelling techniques were performed by using anti-ADRB2 primary monoclonal antibody produced in rabbit (Abcam, UK) followed by the fluorochrome-conjugated secondary antibody for LSCM or gold conjugated for FE-SEM (Jackson laboratories, USA). Samples were fixed in 4% paraformaldehyde for 5 minutes before depositing them on poly-L-lysine solution coated cover-slide. Negative controls were performed in immunolabelling techniques by omitting the primary antibody. The number of gold nanoparticles in the FE-SEM images of sperm cells (n=70 sperm cells, 10 per sample) as well as in the background was counted to determine the specificity of the technique. The area of the spermatic structure and background was quantified and the result expressed as particle per square micrometer (μm2). Gold nanoparticles per μm2 were expressed as mean ± standard error (SEM). Student's t-test was used to examine the differences.

We confirm the presence of ADRB2 receptors in human sperm in all the samples studied, both by western blot and immunolabelling techniques. LSCM images showed a predominant distribution of the ADRB2 receptor on the sperm flagellum, with a brighter signal at the end piece. ADRB2 receptors were also detected on the sperm head, with a lower intensity in all the cells. The mean number of gold particles/μm2 found in the end piece of the sperm flagellum was significantly higher than the one found in the midpiece and principal piece ($p<0.001$).

The presence of the ADRB2 in the sperm flagellum demonstrated by immunocytochemistry support the participation of this receptor on the regulation of the sperm motility, as was previously suggested in functional studies using agonist and antagonist of this receptor. Due to the possible interaction of ADRB2 with commonly used therapeutics drugs, such those for the treatment of asthma and hypertension, further studies should be performed to determine their implications in male fertility.

Oral presentation: Session 2. Room C. Code: 5874

Histology and Histopathology
From Cell Biology to Tissue Engineering

Taphonomic and paleohistologic analysis in human bone remains from the Cacaramoa archaeological site, Caribbean region of Colombia

Ramos E., Ragua L. and Rodríguez F.

Departamento de Antropología, Laboratorio de ADN Antiguo, Universidad de los Andes, Bogotá, Colombia

Paleohistological analysis provides important information to identify the state of conservation in bone tissue, which allows to understand some of the taphonomic processes that affect the formation of an archaeological site, and also adaptive responses of human beings in the past. In this study, we present the results of the histological analysis in bone tissue samples of individuals recovered during the excavations of a prehispanic cemetery in the Cacaramoa site in the Colombian Caribbean Region. The site has been dated by radiocarbon between 1420 AD-1460 AD. For the Colombian Caribbean Region, there are not taphonomic studies aimed at to understand the histological conservation status of bone. Therefore, in the regional archaeological context, histological studies offer a novel way of analysis, and open the possibility of constructing taphonomic references for later studies in the country. This informarion is essential for interpretations derived from it.

To evaluate diagenetic processes in human skeletal remains, we analyzed sections of approximately 2 cm derived from left tibia and femur in four individuals. Each fragment of bone was subdivided to study the Diagenetic Histological Index (DHI) and the changes in porosity using optical microscope and SEM. Finally, the crystallinity index (carbonate and calcite concentration) was evaluated by Infrared spectroscopy with Fourier transform (FTIR).

The data obtained allowed us to identify that the samples exhibit a high degree of histological alteration, which is evidence of the action of biological agents (fungi and bacteria), which altered the bone tissue through the destruction of collagen and the mineral structure.

According to the macroscopic and microscopic taphonomic analyzes carried out in the sample, it can be deduced that the most important taphonomic agents in the Cacaramoa site are groundwater, microorganisms (bacteria and fungi) and vegetation. To a lesser extent, the effects of the chemical dissolution process were observed, which may also be associated with the action of microorganisms.

Oral presentation: Session 2. Room C. Code: 5902

Histology and Histopathology
From Cell Biology to Tissue Engineering

Bone diagenesis and ancient DNA preservation: a microscopic evaluation from archaeological samples from Sabana de Bogota (Colombia)

Rodríguez F.[1,2,3], Maldondo W.[3] and Rojas C.[3]

[1]Laboratorio de ADN Antiguo, Universidad de los Andes, Bogotá, Colombia, [2]Programa de Arqueología, Universidad Externado de Colombia, Bogotá, Colombia, [3]Laboratorio de Arqueología. Arge de Colombia, Bogotá, Colombia

After death, the bones suffer multiple ultrastructural changes due a different taphonomic and diagenetic processes that limit the bioanthropological studies and the analysis of ancient DNA (DNAa). The multidisciplinary approaches have discussed the relationship between the conservation of bone tissue and the biochemical preservation of ancient DNA. The conservation has been described by the Histological Diagenetic Index (HDI) while to determined DNA preservation are common the quantification or detection DNA by immunohistochemical techniques. The aim of this work is to analyze the relationship between the ultrastructural conservation of bone tissue in archaeological samples from Sabana de Bogotá (Colombia) and the biochemical preservation of ancient DNA.

Sections of human bone tissue were obtained from archaeological samples with an age between 600 to 10000 years old. All procedures were performed in the Ancient DNA Laboratory at the University of Andes. Bricks of bone tissue (1 cm) were immersed in epoxy resin (BioDur®). The thin sections were obtained by polishing technique, and then observed in optical microscope. A second group of samples was subjected to a metallization process (gold coating) and subsequently observed in the scanning electron microscope (SEM). DNA extraction was carried out by combining the Zymo-Spin V kit (Zymo Research®) and the QIAamp® DNA Investigator kit (Qiagen®). DNA quantification was carried out using real-time PCR.

Through ultrastructural analysis in bone tissue was possible to identify altered and unaltered areas and was evaluated the HDI in each sample. A uniform distribution of the HDI categories was not found in the group, or a correlation between the HDI and the age of the sample. However, although in all the samples is possible identify variable presence of diagenetic foci by action of microorganisms (bacteria's, fungis), from samples was possible to extract DNA with different concentrations. Respect to HDI variables and DNA quantification, a positive correlation was observed, so greater bone tissue conservation seems to tend towards higher DNA concentrations.

The results obtained in the present study are compatible with a correlation between the degree of ultrastructural preservation of the tissue and the biochemical preservation of the DNA, as has been suggested by other studies. In this way, paleohistology can become a useful tool for researchers of ancient DNA, identifying those samples that are more likely to preserve DNA.

Oral presentation: Session 2. Room D. Code: 5738

Histology and Histopathology
From Cell Biology to Tissue Engineering

Effect of 3-days magnetic field exposition on pellet cultured human chondrocytes

Salvador-Clavell R.[1], Martín de Llano J.J.[1], Mata M.[1], Milián L.[1], Sancho-Tello M. and Carda C.[1,2]

[1]Department of Pathology and INCLIVA, University of Valencia, Valencia, Spain, [2]CIBER-BBN, Instituto de Salud Carlos III, Spain

Articular cartilage diseases are very important in actual society. Many trauma treatments are implemented, but regeneration index is not high yet. Tissue engineering is an emergent field that can improve these treatments, allowing a better articular cartilage regeneration. In this work, irradiation of a magnetic field is applied on chondrocytes 3D-pellets containing magnetic particles to simulate physiological conditions on articular cartilage.

The device used for magnetic field exposition was designed for maximizing the magnetic flux gradient (1), while its magnitude always ensured the magnetization of the beads. Magnetic ferrite PLA-particles were fabricated by emulsion and solvent evaporation. Human chondrocytes were cultured on 3D-pellets containing magnetic particles. After 3 days, culture media was changed to chondrocyte-differentiation culture media and the irradiation treatment began (A samples). A magnetic field (30 T/m, pulse direction changing every 3 s) was applied at a schedule of 4 treatment sequences of 20 min irradiation/40 min resting time for 3 days. Control samples were maintained inside the cell incubator with the presence (B control) or absence (C control) of magnetic particles, whereas additional non-irradiated controls were kept in the device at room temperature during treatment also with the presence (D control) or absence (E control) of magnetic particles. After 3 days of treatment, samples were processed for molecular biology analysis and real time quantitative PCR was implemented. Chondrocytes in 3D-pellets and 2D-cultures were morphologically characterized after DAPI and phalloidin staining.

The size range of the magnetic spherical shaped particles obtained was from 20 to 70 μm. Chondrocytes staining showed rounded cells with also rounded nuclei on 2D-culture, whereas pellet-culture showed a spheroid structure containing rounded cells. After real time qPCR, irradiated samples (A) showed higher MMP13, TIMP1 and VEGFA gene expression than any of the controls, whereas COL2A1 expression was not detected. D- and E-controls showed lower expression of ACAN, COL1A1, COL2A1, COL10A1, SOX5, SOX6 and SOX9 genes than B- and C-controls. At room temperature, D-controls showed COL2A1, SOX5, SOX6 and MMP1 gene expression higher than E-controls, in a similar way that samples kept inside the cell incubator.

Irradiation treatment did not show an improve of chondrogenic markers expression after 3 days of treatment. Control samples kept at room temperature during the irradiation treatment showed worse properties than those kept inside the cell incubator. Finally, the presence of PLA particles improved chondrogenic cellular culture.

This work was supported by grant MAT2016-76039-C4-2-R from the Ministry of Science, Innovation and Universities of the Spanish Government. CIBER-BBN is funded by the VI National R&D&I Plan 2008-2011, Iniciativa Ingenio 2010, Consolider Program, CIBER Actions and with assistance from the European Regional Development Fund.

(1)Salvador-Clavell R et al., Histology and Histopathology, Volume 32 (Supplement 1), p. 170, 2017.

Oral presentation: Session 2. Room D. Code: 5761

Histology and Histopathology
From Cell Biology to Tissue Engineering

Retinal response to intravitreal or subretinal transplant of mononuclear bone marrow stem-cells into two animal models of photoreceptor hereditary degeneration

Di Pierdomenico J.[1], Rodríguez González-Herrero M.E.[2], García-Ayuso D.[1], Agudo-Barriuso M.[1], Manuel Vidal-Sanz M.[1] and Villegas Pérez M.P.[2]

[1]Departamento de Oftalmología, Optometria, Otorrinolaringología y Anatomía Patología, Universidad de Murcia. Instituto Murciano de Investigación Biosanitaria Virgen de la Arrixaca (IMIB-Arrixaca), Murcia, España, [2]Instituto Murciano de Investigación Biosanitaria Virgen de la Arrixaca (IMIB-Arrixaca), Servicio de Oftalmología Hospital Clínico Universitario Virgen de la Arrixaca, Murcia, España

To determine the safety and effects of intravitreal or subretinal bone marrow mononuclear cell (BMSC) injection in two animal models of hereditary photoreceptor (FR) degeneration.

Homozygous P23H-1 female albino rats and 21-day-old Royal College of Surgeons (RCS) pigmented rats received one intravitreal injection or one subretinal injection of BMSC (5 µl; 50,000 cells/µl). As controls, intact animals of the same strains were used. All animals were immunosuppressed with oral cyclosporine and intraperitoneal dexamethasone. The injected animals were perfused 7, 15, 30 or 60 days after injection. Eyes were cross-sectioned in a cryostat and the sections were immunodetected to visualize BMSCs (α-human CD45), outer segment of cone photoreceptors (α-Opsins S and L/M), all photoreceptors (α-Recoverin), astrocytes and Müller cells (α-GFAP), or microglial cells (α-Iba-1). All nuclei were counterstained with DAPI. Sections were examined under fluorescence and confocal microscopy to study cell morphology and to measure the thickness of the outer nuclear layer.

In the BMSC-treated eyes no macro or microscopic anomalies, tumours, necrosis, inflammation or infection were observed. In the intravitreally injected eyes, BMSC-CD45$^+$ were found in the vitreous and attached to the inner limiting membrane. In the eyes with subretinal injections, BMSC-CD45$^+$ formed a layer between the pigment epithelium and the external segments of the photoreceptors. Compared to control animals, there was a decrease of GFAP expression in the transplanted eyes, indicating a reduction of gliosis. However, there was no increase in the number of photoreceptors nuclei in the outer nuclear layer, suggesting that the transplant does not elicit neuroprotection.

Intravitreal and subretinal injections of human BMSC into two rat models of retinal degeneration, decreased GFAP expression compared to untreated retinas. Finally, these transplants seem to be safe as there were no adverse effects such as tumour formation.

Oral presentation: Session 2. Room D. Code: 5816

Histology and Histopathology
From Cell Biology to Tissue Engineering

Evaluation of chemical crosslinking on decellularized peripheral nerves

García-García O.D.[1], Campos F.[1], El Soury M.[1,2], Chato-Astrain J.[1], Aguilar-Bohórquez E.[3], Llinares-Monllor C.[1], Campos A.[1] and Carriel V.[1]

[1]Tissue Engineering Group, Department of Histology, University of Granada and Instituto de Investigación Biosanitaria ibs, Granada, Spain, [2]Department of Clinical and Biological Sciences, University of Torino, Italy, [3]Andalusian Initative in Advanced Therapies, Seville, Spain

Implant of nerve autografts is the gold standard technique for the repair of critical nerve defects. Unfortunately, this method has several well-known disadvantages and new therapeutic alternatives are needed. In this sense, tissue decellularization has emerged as a promising alternative in peripheral nerve repair. However, this process often affects the structure, molecular composition and mechanical properties of decellularized nerves [1, 2]. Recently, Genipin (GP) demonstrated to be an efficient agent to increase the biomechanical properties of hydrogels in tissue engineering [3], being an attractive alternative to be combined with decellularized nerves. In this regard, the aim of this study was to investigate the possibility to improve the structural and biomechanical properties of decellularized nerves using GP cross-linking.

Wistar rat sciatic nerves were decellularized by a chemical-enzymatic combined protocol that uses 1% Triton X-100 and a mixture of DNase, RNase and trypsin. Then, decellularized nerves were washed in PBS and subjected to chemical cross-linking using two concentrations of GP (0.1 and 0.25%). Non-cross-linked decellularized nerves were used as controls. The structure and extracellular matrix were evaluated by using H&E and MCOLL staining. Biomechanical properties of each sample were measured by tensile test using an Instron biomechanical analyzer.

The use of GP as cross-linker agent at a concentration of 0.1% or 0.25% did not result in evident changes in the histological pattern as compared to the control group. Interestingly, from the biomechanical perspective, both concentrations of GP resulted in a significant increase of values for the stress at fracture, strain at fracture and Young's Module biomechanical parameters as compared to the control group ($p<0.05$).

Crosslinking sciatic decellularized nerves with GP did not affect their histological pattern, but contributed to significantly improve biomechanical properties. However, further cell cytotoxicity and *in vivo* studies are needed to demonstrate the potential usefulness of these grafts in nerve reconstruction.

This study was Supported by Plan Nacional de Investigación Científica, Desarrollo e Innovación Tecnológica (I+D+I) from the Spanish Ministry of Economy and Competitiveness (Instituto de Salud Carlos III), grant FIS PI17/0393 (co-financed by ERDF-FEDER, EU).

[1] Philips C, et al. Ann Biomed Eng. 2018;46(11):1921-1937
[2] Philips C, et al. J Neural Eng. 2018;15(2):021003
[3] Campos F, et al. Biomed Mater. 2018;13(2):025021

Oral presentation: Session 2. Room D. Code: 5820

Histology and Histopathology
From Cell Biology to Tissue Engineering

Generation and in vitro characterization of elastic cartilage-derived chondrocyte microtissues

Sánchez-Porras D.[1], Durand-Herrera D.[1], García-García O.D.[1], Rodríguez M.A.[1,2], Ortiz-Arrabal O.[1], Munuera-Cabeza M.[1], Crespo P.V.[1] and Carriel V.[1]

[1]Tissue Engineering Group, Department of Histology, University of Granada and Instituto de Investigación Biosanitaria ibs, Granada, Spain, [2]Cátedra de Histología B, School of Dentistry, National University of Cordoba, Argentina

Elastic cartilage is a variety of cartilaginous tissue that forms part of several structures such as epiglottis, larynx, walls of external acoustic meatus and auricular pavilion. Microtia is one of the most common birth defects treated by plastic surgery being autologous costal cartilage transplant predominately performed for its treatment. The goal of cartilage tissue engineering is to produce a natural-like and functional cartilage substitute able to replace the damaged or undeveloped tissue. In this regard, reports demonstrated that cells with high biosynthetic activity are able to synthetize high amounts of extracellular matrix in culture and form stable 3D structures [1]. A recently described method based on cell self-assembly allowed us to generate biomimetic microtissues (MT) consisting in bioactive cell aggregates with potential usefulness in tissue engineering [2]. The aim of this study is to generate and characterize MT derived from human elastic chondrocytes.

To elaborate human elastic chondrocytes MT, 250,000 human elastic chondrocytes were isolated from human cartilage biopsies and seeded in agarose chips generated using tailor-made PDMS molds. MT were allowed to form and develop in culture using two different culture media (expansion and chondrogenic medium). Morphometric analysis was carried out by phase-contrast microscopy. Cell viability, proliferation and cell damage was determined by Live/Dead, WST-1 and DNA quantification tests, respectively, in each culture condition. As controls, chondrocyte cultures were used.

Microscopic images showed that chondrocytes cultured with expansion and chondrogenic media began to aggregate from day one of development, but times of stabilization of the MT are different depending on the culture medium. In the case of the expansion medium, MT were not stable until the fourth day of *ex vivo* development, whilst MT cultured with chondrogenic medium were stable from the second day. It should be noted that MT tended to lose peripheral cell cohesion with expansion medium, whereas chondrogenic medium allowed the maintenance of MT stability across the whole culture period. According to the viability assays, MT remained viable during the whole culture period, although MT with the chondrogenic medium showed a slightly lower percentage of cell death, which was consistent with results found in 2D culture controls. The WST-1 assay determined that cell metabolic activity levels were higher in expansion medium MT, with this activity being lower in MT when compared to the 2D controls with the same culture media.

Chondrocytes are able to form stable MT, remaining viable throughout the whole culture period. However, clear differences were found between both culture media in terms of viability and morphometric parameters. Nevertheless, further histological and molecular studies are still needed to determine the functionality and the synthesis of essential extracellular matrix molecules by these MT.

Supported by CS PI-0257-2017, Regional Ministry of Health, Junta de Andalucia, Spain.

[1] Jaimes-Parra BD, et al. Histol Histopathol. 2018;33(2):147-156
[2] Durand-Herrera D, et al. Histochem Cell Biol. 2018;150(4):379-393

Oral Presentations

Session 3

Friday, 16-18 hours

Oral presentation: Session 3. Room A. Code: 5914

Histology and Histopathology
From Cell Biology to Tissue Engineering

Student´s experience using a game-based response system (Kahoot) in histology

García-Caballero L.[1], Caneiro J.[1,2], Gándara M.[3] and Gallego R.[1]

[1]Área de Histología, Departamento de Ciencias Morfológicas, Facultad de Medicina y Odontología de la Universidad de Santiago de Compostela, [2]Servicio de Anatomía Patológica, Complejo Hospitalario Universitario de Santiago, Santiago de Compostela, España

Within the framework of the adaptation to the European Higher Education Area, one of the main objectives is to ensure that students develop a much more active role in teaching, and to achieve it there are some support tools that can favour the interaction between teachers and students, while fighting the apathy during lectures. Nowadays, to increase student´s motivation, technology is being increasingly integrated into teaching environments. In particular, game-based student response systems have been found to be beneficial for academic achievement, motivation and classroom dynamics improve. The aim of this study was to examine student´s experience using a game-based response system (Kahoot) in Medicine, within the subject Special Histology, searching for the advantages and disadvantages from student´s point of view.

Kahoot system was used in the four groups of first course of Medicine grade (Facultad de Medicina y Odontología, Universidad de Santiago de Compostela), who were enrolled in Human Special Histology (obligatory subject with 6 ECTS). After lectures, 5 questions related to the lecture subject were proposed using Kahoot, and students had to answer them using their mobile phones. Four answers were available for each question, but only one was the correct one. At the end, a survey was made. The aim of this survey was to evaluate their level of satisfaction with the Kahoot system.

The survey included 13 questions and the answers were rated from 1 to 5 (1 was strongly disagree and 5 totally agree). The mean for all answers was 3.52 (range between 2.52 and 4.45). Students thought that the system was very useful for self-evaluation (75.0% voted 4 or 5) and for stimulating their participation (71.1%). Kahoot improved their comprehension and retention of new concepts (66.7%), and increased their level of attention (65.5%). On the other hand, they felt that the system would be appropriate for lectures attendance evaluation (51.2%). However, they did not consider it appropriated for evaluating their academic performance (50.6% voted 1 or 2) and they also consider that the system did not motivate them to study before lectures (45,2% answered 1 or 2). Finally, they thought that the best moment to use Kahoot is after each lecture (56,55%).

Conclusions: 1) The students considered that the Kahoot system was very useful for stimulating their participation and for self-evaluation. It also increased their level of attention and improved their comprehension and retention of new concepts. 2) However, they felt that this system did not motivate them to study before lectures and that it was not appropriate to evaluate their academic performance. 3) The best moment to use Kahoot is after lectures.

Oral presentation: Session 3. Room A. Code: 4676

Histology and Histopathology
From Cell Biology to Tissue Engineering

Use of the virtual microscope as an active tool for autonomous learning

Sáez F.J., Gómez-Santos L. and Badiola I.

Department of Cell Biology and Histology, School of Medicine and Nursing, University of the Basque Country UPV/EHU, Bº Sarriena s/n, 48940 Leioa (Vizcaya), Spain

The implementation of the new degrees within the European Higher Education Area has enhanced autonomous learning through active methodologies. The University of the Basque Country UPV/EHU has strengthened the method of autonomous and cooperative learning (Ikaskuntza Kooperatibo eta Dinamikoa, IKD), which emphasizes that students are the owners of their learning. Following this model, the teachers of the subject Human Histology have implemented a teaching model in the laboratory practices based on the previous study using virtual microscopes.

The tissue slides corresponding to each practice session were scanned in a format that allowed their observation using the software Aperio ImageScope. The digital files were deposited in a digital repository. Before the face-to-face practical session, each student had to look in the sample for the objectives indicated in the practice sheet, capture the image and copy it in the practice sheet. Later, in the classroom session in the laboratory, the student worked on the sample with the real microscope. The teacher monitored each student's work.

At the end of the course, we conducted a survey among the students with the following items:

Observing the preparations with the virtual microscope has made it easier for me to study them in the laboratory.

Preparing the practices with a virtual microscope is a waste of time

Working with a virtual microscope is easy.

It is an advantage that the preparations of the virtual microscope are the same as those of the laboratory.

In general, I am satisfied with having worked with the virtual microscope.

Working in this way the laboratory practices has helped me to better understand the concepts worked on in other teaching modalities.

The student had to respond by indicating their degree of agreement on a scale of 0 (totally disagree) to 5 (completely agree).

The degree of agreement of the students, expressed in arithmetic mean, is shown in the table 1. The students agreed that the preparation of the laboratory practices by means of virtual microscopy facilitated the work in the laboratory (*observing the preparations with the virtual microscope has made it easier for me to study them in the laboratory*; 4.53). They also thought that it facilitates the study in other teaching modalities (*working in this way the laboratory practices has helped me to better understand the concepts worked on in the other teaching modalities*, 4.24). In addition, the students considered that they did not waste time (*preparing the practices with a virtual microscope is a waste of time*, 1.66) and they were satisfied with the work done (*in general, I am satisfied with having worked with the virtual microscope*; 4.05).

Table 1. Degree of agreemen with the assertions of the virtual microscopy survey

Item	Degree of agreement
1	4,53
2	1.66
3	3.68
4	4.30
5	4.05
6	4.24

The use of virtual microscopy for the autonomous work of the student seems a good method for the preparation of microscopy practices in histology.

Oral presentation: Session 3. Room A. Code: 5795

Histology and Histopathology
From Cell Biology to Tissue Engineering

That obscure object of histology images: do they have subliminal information? a graph-based and survey study

De Juan J.[1,2], Pérez-Cañaveras R.M.[3], Girela López J.L.[1,4], De Juan Pérez A.[5] and Peña-Amaro J.[6]

[1]Biotechnology Research Group, [2]IUIEG, [3]Department of Nursing, Faculty of Health Sciences, [3]Department of Biotechnology, Faculty of Sciences, University of Alicante, Spain, [5]University Hospital, San Juan, Alicante, Spain, [6]Department of Histology, Faculty of Medicine, University of Córdoba, Spain

Tissue concept is a useful tool for knowing the microscopic structure of the organism and its relationship with its composition, function and injuries. The histological images (HIs) from light microscope are its primary study source. The learning, identify, recall and diagnose of HIs is based on its repeated observation. However, this method is monotonous and very time-consuming. To improve student learning and to understand HIs, we have proposed a systematisation of the microscopic histological components or "Tissue Structures" (TS). TS were classified into three levels according to their complexity: TS1 (cells, fibres and ground substance), TS2 ('fundamental tissues'), and TS3 integrated by TS1 and TS2 adopting a spatial configuration (laminar, spherical and polygonal). Here, we will analyse only the HIs from TS2. This work aims to obtain: (1) morphometric data from HIs of TS2, (2) The opinion of students and teachers about HIs of TS2 and (3) To detect hypothetic gender differences.

Computer-Graph-Based analyses were applied to 15 HIs from several TS2. Over each HIs, a Voronoi analysis was applied to obtain several parameters: Nearest neighbourhood distance (NN), Nearest Neighbor Regularity Index (NNRI), Voronoi Domain Area (VDA), Voronoi Domain Regularity Index (VDRI), among others. The same 15 micrographs and a brief questionnaire; about the complexity, beauty, simplicity and difficulty to memorize HIs; were presented to 2 people groups: (a) 62 undergraduate students group of the first-year of two degrees, Biology and Marine Sciences, respectively. None of them had previously studied Histology and (b) 10 expert teachers in Histology. Questions were punctuated between 1-5. The 15 HIs of TS2 were divided into two groups: TS2-I (epithelia and nervous tissue) and TS2-II (others fundamental tissues).

The NN, NNRI, VDA and VDRI values are minor in TS2-I than in TS2-II. This data are congruent with a major cellular separation in TS2-II, due to the presence of fibres and extracellular matrix in them. According to students, 7 out of 15 HIs (46,66%) were considered 'complex or very complex', against 2 out of 15 HIs (13,33%) between teachers. The number of HIs considered 'simples and very simples' were: 6 out of 15 (40%) between students, 11 out of 15 (73%) between the teachers, 13 out of 15 (93,33%) between women, and 9 out of 15 (66,66%) between men. Regarding the HIs beauty, 9 out of 15 HIs (60%) were considered 'beauty and very beauty' by students, regarding only 5 out of 15 HIs (40%), for teachers. In both groups (students and teachers) women choose as 'beauty or very beauty' a major number of HIs: 9 out of 15 HIs (60%) and 12 out of 15 HIs (80%), respectively front only 4 out of 15 HIs (26,66%) in both male students and teachers. The other data were less consistent.

In conclusion: 1) The graph-based methodology seems to be a potent tool to analyse and classify the fundamental tissues. 2) The survey detects important differences, between students and teachers and between women and men, in HIs valuation.

Oral presentation: Session 3. Room A. Code: 5859

Histology and Histopathology
From Cell Biology to Tissue Engineering

Forms in nature applied to the cytological and histological teaching-learning process

Pérez F.A.[1], D'Ottavio A.E.[2] and Roma S.M.[1,2]

[1]Cátedra de Histología y Embriología, Facultad de Ciencias Médicas and [2] Consejo de Investigaciones, Universidad Nacional de Rosario, República Argentina

There exist innumerable forms in nature resulting from the elaboration of a set of basic patterns, whose designs are restricted by the curved space and by an austerity based on the scarce availability of resources and the minimum energy cost. Like the forms of human cells and tissues resemble those of nature, it becomes relevant in a morphological discipline as Histology not only to understand the form but also to associate the function with the simplest configuration and the lowest energy consumption. Taken it into account, some human cell and tissue designs similar to others found in the inanimate and organic world were chosen for applying them to the cytological and histological teaching-learning process. These designs were: (a) the sphere, observable in some cell nuclei and the adipocytes, storing and protecting; (b) the hexagon, existing in epidermis and hepatic lobules, covering and paving; (c) the spiral, detectable in DNA, packaging; (d) the helix, perceptible in the tropocollagen, binding, and (e) the fractals, visible in the neurons and blood vascular systems as well as in the respiratory tree, occupying space efficiently and minimizing the distance to the source.

In this context, the present communication reports a morphological-based model employed in 2017 and 2018 during the Assistant-Student Course of our Chair (n=40 students; 70% females). Through images and videos, the referred chosen forms were compared with natural examples in the different thematic units for illustrating the presence of structural coincidences between inert world and living matter with similar functions. The students subsequently filled an online form with a scale from 0 (disagreement) to 2 (total agreement) for evaluating their degree of satisfaction with this morphological proposal. In addition to their majority agreement with the applied approach, they perceived that it was quite motivational and that this way of managing forms during the teaching-learning process resulted also innovative for relating and integrating external and natural forms, familiar to them, with the more complex histological structures.

Oral presentation: Session 3. Room A. Code: 5912

Histology and Histopathology
From Cell Biology to Tissue Engineering

"Sketching" learning to think through histology

Valencia Villa G.[1,4], Padrón Posteraro R.[1,3,4], De la Hoz Herazo H.[1,2] and Herrera Bedoya M.J.[1,2,4]

[1]Universidad del Norte de Barranquilla, Barranquilla, Colombia, [2]Hospital de la Universidad del Norte, Colombia, Barranquilla, [3]CEDU (Centro de Excelencia Docente de la Universidad del Norte), Barranquilla, [4]ASCOM[4] (Asociación colombiana de Morfología), Colombia

Histology, due to the microscopic conditions of its study, produces radically different emotions in student, conditioned on the individual ability to associate images to functional tissue processes. Taking advantage of these characteristics and considering the premise that the brain thinks in images led us to consolidate several methodological strategies, carried out in class, through which we fostered the "learning to think through histology". We assumed this challenge and now we show you how it works and the results of that learning process.

This study was carried out with 152 third semester students of medicine, who were studying nervous system. Two class models were compared: traditional and innovative, using images from histological slides taken with a virtual microscope. Also, they were exposed to a theoretical-practical material on how to learn through schematic drawings or "sketches" in the previous semester. In the innovative classes, students needed to explain the requested questions using histological images or "sketches." Once in class, students' responses were presented and discussed with the whole class. A total of five images (1, 2, 4, 5, and 7) were studied under the innovative model in different classes. In the traditional model, there were no questions sent to students or there was no indication of how to work on them. However, the professor explained the class using histological images using the traditional settings. Later, students were requested to complete a survey (via google) to provide their opinion on the two class models as well as to participate in focus group discussions.

A relatively lower percentage of students (70%) perceived traditional classes as helpful when answering the situation analyses presented in the final exam compared to 92% of students who saw the innovative classes more helpful. In addition, there was an important difference in the students' performance in those items related to the topics reviewed under the innovative class model. Finally, students also found that complex images (e.g., inner ear) were more difficult to learn given the bigger challenge to connect them to pre-learned images.

Sketching and studying histological images facilitate not only the students' understanding of normal and altered functioning of the human body but also their analytical thinking skills development, which constitutes any health-related professional's basic ability.

Oral presentation: Session 3. Room B. Code: 5748

Histology and Histopathology
From Cell Biology to Tissue Engineering

TNFR1 antagonism delays axotomy-induced retinal ganglion cell death

Lucas-Ruiz F., Galindo-Romero C., Salinas-Navarro M., González-Riquelme M.J., Vidal-Sanz M. and Agudo-Barriuso M.
Experimental Ophthalmology, IMIB-Arrixaca, University of Murcia, Murcia, Spain

Axonal injuries to mammalian central nervous system neurons cause their death and an immediate and irreversible loss of functionality. Apoptosis plays a fundamental role in neuronal degeneration after optic nerve axotomy. Tumor Necrosis Factor Receptor 1 (TNFR1), activates the extrinsic pathway of apoptosis and is upregulated after optic nerve crush (ONC; Agudo, 2008). Therefore, blocking this receptor may be a key target for preventing or delaying ONC-induced retinal ganglion cell (RGC) death. Besides blocking pro-death pathways, it is feasible to promote survival pathways through the tyrosine kinase B (TrKB) receptors, activated by brain derived neurotrophic factor (BDNF), which block apoptosis at the mitochondrial level. The aim of this work is to analyze the level of neuroprotection by blocking TNFR1, as well as potentiating neuronal survival with BDNF treatment with cAMP adjuvant.

The left optic nerve of C57/BL6 was subjected to optic nerve crush. Animals were divided into: ONC+vehicle, ONC+intravitreal injection of BDNF, TNFR1 antagonist (R7050), and/or cAMP, ONC+intraperitoneal administration (TNFR1 antagonist). Analyses were carried out at 5 and 14 days post lesion and treatment. Intact retinas were used as controls. Retinas were fresh dissected for qPCR assessment of *caspase 3* and *4*, *transforming growth factor ß1* and *Tnfr1* expression levels. For anatomy, retinas were dissected as flat mounts, the whole population of RGCs was immunoidentified with Brn3a, automatically quantified and their topography plotted using neighbor maps.

After ONC there was an overexpression of the studied genes at 5 days post ONC. At day 9 only *Tnfrs1* levels were higher than in intact retinas. The TNFR1 antagonist, R7050 is not toxic for RGCs, as assessed after intravitreal injection into intact retinas- Intravitreal and intraperitoneal treatment with R7050 alone, promoted a significant RGC neuroprotection at 5 days post ONC. The combination of R7050 with BDNF and cAMP treatment produced a significant RGC neuroprotection at 14days post lesion.

Blocking the extrinsic signal of apoptosis by R7050 delays RGC death. Intraperitoneal treatment (systemic treatment) does not differ from intravitreal treatment, which is interesting because it can be used for other injuries of the central nervous system where access is not as simple as the retina.

Oral presentation: Session 3. Room B. Code: 5764

Histology and Histopathology
From Cell Biology to Tissue Engineering

Methylene blue prevents retinal damage caused by perinatal asphyxia in the rat

Rey-Funes M.[1,†], Fernández J.C.[1,2,†], Peláez R.[3,†], Soliño M.[1], Contartese D.S.[1], Dorfman V.B.[4], López-Costa J.J.[1], Larrayoz I.M.[3,¶], Loidl C.F.[1,¶] and Martínez A.[3,¶]

[1]Instituto de Biología Celular y Neurociencia "Prof. E. de Robertis", Facultad de Medicina, Universidad de Buenos Aires, Argentina, [2]Primera Cátedra de Farmacología, Facultad de Medicina, Universidad de Buenos Aires, Argentina, [3]Center for Biomedical Research of La Rioja (CIBIR), Logroño, Spain, [4]Centro de Estudios Biomédicos, Biotecnológicos, Ambientales y Diagnóstico (CEBBAD), Universidad Maimónides, Buenos Aires, Argentina

[†]These authors contributed equally to this study and should be considered co-first authors.

[¶]These authors contributed equally to this study and should be considered co-last authors.

Perinatal asphyxia (PA) is responsible for a large proportion of neonatal deaths and numerous neurological sequelae, including visual dysfunction and blindness. In PA, the retina is exposed to ischemia/reoxygenation, which results in nitric oxide overproduction and neurotoxicity. We hypothesized that methylene blue (MB), a guanylyl cyclase inhibitor and free-radical scavenger currently used in the clinic, may block this pathway and prevent PA-induced retinal degeneration.

Male rat pups were subjected to an experimental model of PA. Four groups were studied: normally delivered (CTL), normally delivered treated with 2 mg Kg^{-1} MB (MB), exposed to PA for 20 min at 37ºC (PA), and exposed to PA and, then, treated with MB (PA-MB). Forty five days after birth rats were subjected to electroretinography, sacrificed, and the eyes were studied by histology, TUNEL assay, and gene expression analysis.

Electroretinography showed that PA animals had significant defects in the a- and b-waves and oscillatory potentials. The same animals presented a significant increase in the thickness of the inner retina and a large number of TUNEL-positive cells. All these physiological and morphological parameters were significantly prevented by the treatment with MB. Gene expression analysis demonstrated significant increases in iNOS, MMP9, and VEGF in the eyes of PA animals, which were prevented by MB treatment.

MB regulates key players of inflammation, matrix remodeling, gliosis, and angiogenesis in the eye and could be used as a treatment to prevent the deleterious visual consequences of PA. Given its safety profile and low cost, MB may be used clinically in places where alternative treatments may be unavailable.

Oral presentation: Session 3. Room B. Code: 5769

Histology and Histopathology
From Cell Biology to Tissue Engineering

Hypothermia applied during or after perinatal asphyxia prevents retinal damage in rats

Rey-Funes M.[1], Contartese D.S.[1], Soliño M.[1], Fernández J.C.[1], Peláez R.[2], López-Costa J.J.[1], Larráyoz I.M.[2], Dorfman V.B.[3], Martínez A.[2] and Loidl C.F.[1]

[1]Laboratorio de Neuropatología Experimental, Instituto de Biología Celular y Neurociencia "Prof. E. De Robertis" (IBCN), Facultad de Medicina, Universidad de Buenos Aires, CONICET, Buenos Aires, Argentina, [2]Angiogenesis Study Group, Center for Biomedical Research of La Rioja (CIBIR), Logroño, Spain, [3]Centro de Estudios Biomédicos, Biotecnológicos, Ambientales y Diagnóstico (CEBBAD), Universidad Maimónides, Buenos Aires, Argentina

Perinatal asphyxia (PA) can be the cause of different degrees of retinopathy, which in severe cases can lead to blindness. Clinical studies reveal that obstetric complications and in particular PA develop ischemic retinopathy (IR). In a rat model of PA, we have shown neurodegeneration, gliosis, and neurovascularization compatible with IR. In this model, a protective effect of hypothermia was demonstrated when applied during PA. In the present work we want to show that hypothermia has a protective effect both when applied during and immediately after PA. Since CIRP (Cold-inducible RNA-binding protein) and RBM3 (RNA binding motif protein-3) are proteins inducible by cold that could mediate the beneficial effects of hypothermia, we also investigated the molecular response of these proteins in the retina when exposed to cold.

Rats exposed to PA were subjected to hypothermia during or after PA using a well-tested experimental model. In order to evaluate the integrity of the visual pathway, animals were subjected to electroretinography at 60 days of age. Molecular and histological techniques were applied to the eyes of all experimental groups collected at 6, 12, 24 and 48 h, and 6 days after birth.

A significant increase in the nucleotide and protein expression of CIRP and RBM3 was observed from 12 h in both controls and asphyctic animals exposed to hypothermia. At 24 h, a significant decrease in the expression of CIRP and RBM3 was observed, by Western blotting, in the animals treated with hypothermia when compared to the PA animals. The expression of CIRP and RBM3 was located in ganglionic neurons and cells of the inner nuclear layer by immunohistochemistry and confocal microscopy. A significant decrease in TUNEL positive cells was observed in the experimental groups treated with hypothermia when compared with the PA groups under normothermia conditions. Furthermore, PA resulted in a significant reduction in the amplitude of the a and b wave and oscillatory potentials of the electroretinograms whereas animals treated with hypothermia had a significant correction of these values.

Hypothermia can be used as a useful and affordable method to prevent asphyxia-related vision losses. This work opens new perspectives to understand the cold-inducible molecular mechanisms that may be involved in the neuroprotection triggered by the treatment with a hypothermic shock.

Oral presentation: Session 3. Room B. Code: 5772

Histology and Histopathology
From Cell Biology to Tissue Engineering

Topographical distribution of retinal cone-photoreceptors in the yellow-legged gull, *Larus michahellis* (Naumann, 1840)

Victory Fiol N., García Irles M., Navarro-Sempere A. and Segovia Huertas Y.
Department of Biotechnology, University of Alicante

The retina of most birds contains a type of long-wavelenght-sensitive (LWS) double cone and four different types of cone maximally sensitive to long, medium (MWS), short (SWS) and either violet (VS) or ultraviolet (UVS) wavelength (Hart, 2001). Thus, many bird species are tetrachromatic. Moreover, the colour vision in birds is more complex by the presence of coloured oil droplets in the outermost part of the internal segments that are implied in guiding the light arrival to the outer segments. The oil droplets in the principal and accessory members of the LWS double cones and the UV/UVS, SWS, MWS and LWS cones are designated as: P (principal), Ac (accessory), T (transparent), C (colourless), Y (yellow) and R (red), respectively. Cone photoreceptor complement varies both across the retina and between species, and many of these variations reflect differences in visual ecology. In this study we describe the type of cone-photoreceptors and their density and distribution in the retina of yellow-legged gulls (*Larus michahellis*) and the possible implication in its visual ecology.

Retinas of 4 adult specimens of *L. michahellis* were studied. As tissue processing for light microscopy destroys the oil droplet colour, retinas were studied in fresh. Retinas were placed on the slide with the photoreceptors at the top, coverslipped and rapidly examined under the microscope. Different retinal regions were microphotographed at x100 magnification and differences in oil droplet densities and percentages among the retinal regions were analysed using two-way ANOVA and a T-test.

In *L. michahellis* five distinct cones were found: four types of single cones and a type of double cone. Topographic maps show that the density of the different photoreceptors varied across the retina, so that the cones are present in specific pattern. Cones are concentrated more in the dorsal than ventral quadrant, and they are more abundant in the central retina than the periphery. A high density of red and yellow oil droplets are found in the dorsal quadrant of the retina, extending nearly to the central retina and the fovea. On the other hand, transparent oil droplets are the least abundant in the retina and colourless oil droplets are abundant in the nasal quadrant. Finally, unlike single cones, double cones have fewer differences between the central and peripheral retina.

The relative abundance of the different cone types across the retina may reflect different colour discrimination capabilities. Thus, ventro-nasal quadrant with abundant colourless oil droplet is an ideal position for viewing the sky and perceives very gradients of short spectral wavelengths which could be used in aerial navigation. The dorso-temporal quadrants are suitable for viewing the sea and would help enhance contrast between fishes and the sea.

Oral presentation: Session 3. Room B. Code: 5773

Histology and Histopathology
From Cell Biology to Tissue Engineering

Retinal specializations in the retina of yellow-legged gull, *Larus michahellis* (Naumann, 1840): central area and foveae

Victory Fiol N., Segovia Huertas Y., Navarro-Sempere A and García Irles M.
Department of Biotechnology, University of Alicante

Improved visual acuity in birds may be correlated with the presence within the retina of well-developed areae and foveae (often one or two) in which the density of the photoreceptors and associated visual cells are higher and contain a predominance of cones over rods. Areas can be circular (an area centralis) or elongated (a visual streak) thickenings of the retina. A depression or fovea is of variable depth and size, located within either a central o lateral area and represents a further adaptation for diurnal vision and greater visual acuity (Meyer, 1977). In the fovea, adjoining cells are centrifugally displaced in angle producing a pit that is filled by the vitreous humor allowing a sharper vision. According to the shape of the slopes of the foveal pit, they are classified in concaviclivate or convexiclivate fovea. The convexiclivate fovea is a funnel-shaped depression found in diurnal lizards and birds. The cocaviclivate fovea is shallower. Although as a rule, the deep fovea is situated about the center of the retina its location and depth vary among species. In the case that there is a second fovea, it can be so shallow that it can go unnoticed. Its location and depth can also vary. This study investigates the specific retinal layer thickness and foveal pit shape of the areae and foveae on the retina of *L. michahellis* in an attempt to correlate them with de visual function.

Four retinas of *L. michahellis* were fixed in 4% paraformaldehyde and 1.6% glutaraldehyde in phosphate buffer for 24h. Central region and foveae were located and processed for electron microscopy. Semithin sections containing the center of the fovea was identified as the section with the deepest foveal depth. Measurements of retinal layers were made with ImageJ and depth and width of foveae were calculated with FOVEA, a standardized software.

The retina of *L. michahellis* has a central area and two different foveae: the deep fovea in the central region and the shallow fovea in dorsal-nasal region. The central fovea is characterized by a remarkably deep and an excavated pit which is 234 μm in depth and 630 μm in width. The depth of the shallow fovea is 48 μm in profundity and 217 μm in width. In both foveae retinal layers do not disappear but undergo important modifications: 1) absence of rods, 2) increase in the number of cones which become thinner and longer that elsewhere in the retina, 3) increase in the number of bipolar and ganglion cells which are obliquely disposed, 4) stalks of muller cells are spanning the internal retina, forming a complex network in the most central part of the fovea.

The retina of *L. michahellis* has two foveae. Convexiclivated foveae are associated with diurnal birds and it is related to binocular vision, so it would fit with behaviour of this species: diurnal and predatory activity. The presence of a second shallow fovea in the dorsal/nasal region suggests a role in the lateral monocular vision.

Oral presentation: Session 3. Room B. Code: 5853

Histology and Histopathology
From Cell Biology to Tissue Engineering

Glial response in an animal model of retinal degeneration induced by taurine depletion and/or light-exposure

Martínez Vacas A., Di Pierdomenico J., Agudo Barriuso M., Vidal Sanz M., Villegas Pérez M.P. and García Ayuso D.

Departamento de Oftalmología experimental de la Universidad de Murcia and Instituto Murciano de Investigación Biosanitaria, Hospital Virgen de la Arrixaca (IMIB Arrixaca), Murcia, Spain

Taurine is considered a non-essential amino acid that is found in high concentration in several tissues, especially in excitable tissues such as the retina. Despite of being the most abundant amino acid in the retina its role still remains unclear. However, it has been documented that taurine depletion causes photoreceptor and retinal ganglion cell loss and increases light-induced retinal degeneration, suggesting that its role may be of great importance for neuronal survival in the retina. In this work, we have studied the course of photoreceptor degeneration and the macro and microglial reactivity in an animal model of induced taurine depletion alone or in combination with light exposure to decipher whether light exacerbates the noxoius effect of taurine depletion.

Albino Sprague-Dawley rats (n=20) were divided into two groups: the experimental group (n=10) received β-alanine (3%) in the drinking water to induce taurine depletion, while the control group (n=10) received regular water. One month later, half of the animals in each group were exposed to white light (3000 lux) continuously for 48 hours. All the animals were processed 2 months after the beginning of the experiment. Eyes were cryostated and immunoreacted with antibodies against L/M- and S- opsin, rhodopsin, anti-Iba 1 and anti-GFAP and counterstained with DAPI.

Taurine depletion caused photoreceptor degeneration, that was characterized by morphological changes and a decrease of the outer nuclear layer thickness, microglial cell activation and migration from the inner to the outer retinal layers, and GFAP over-expression. The combination of taurine depletion and light-exposure increased photoreceptor degeneration as well as microglial activation and migration, and GFAP expression.

Taurine is essential for photoreceptor survival and taurine depletion increases retinal susceptibility to light damage. Retinal glia may be involved in retinal degeneration under taurine depletion.

Oral presentation: Session 3. Room B. Code: 5885

Histology and Histopathology
From Cell Biology to Tissue Engineering

New technique to study the functional integrity of the retinal pigment epithelium in rodents

Valiente-Soriano F.J., Salinas-Navarro M., Di Pierdomenico J., García-Ayuso D., Villegas-Pérez M.P., Vidal-Sanz M. and Agudo-Barriuso M.

Departamento de Oftalmología, Facultad de Medicina, Universidad de Murcia and Instituto Murciano de Investigación Biosanitaria-Virgen de la Arrixaca (IMIB-Arrixaca) Murcia, Spain

Retinal pigment epithelium (RPE) is a pigmented cell layer located between the neurosensory retina and the choroid. The main functions of the RPE are to transport nutrients to the photoreceptors, to compose the blood–retinal barrier, to phagocyte the membrane of the photoreceptor outer segments for their renewal, and to absorb light to prevent photooxidation. To study the integrity, morphology and functionality of this layer is crucial to understand the pathogenesis of retinal degenerations.

Adult female albino Sprague-Dawley rats (SD; 60 days old) were used in this experiment. To label the RPE, under general anaesthesia, 1.5 µl of 3% Fluorogold (FG, Fluorochrome Inc., Engelwood, CO, USA) diluted in saline were intraviterally administered (IVA). Rats were analysed 15 minutes or 24 hours after IVA and their eyes were prepared as cross-sections and immunoreacted against RBPMs, PKC-α, Parvalbumin and C-Arrestin to identify RGCs, rod-bipolar cells, amacrines cells and cones, respectively.

In cross sections of retinas analyzed 15 minutes after the intravitreal injection of FG retinal ganglion cells axonal fibers, the somas of neurons in all the retinal layers, as well as the RPE were labelled with FG. The somas of retinal ganglion cells (RGCs), rod-bipolar cells, amacrines cells and cones were labelled with FG. Furthermore, photoreceptor outer and inner segments were well defined by FG accumulation. At twenty-four hours, the RPE was more strongly labelled while the rest of neurons remained the same with the exception of photoreceptors. Indeed, 24 hours after FG administration, few of photoreceptor nuclei were labeled and their outer and inner segments were devoid of FG. Interestingly, retinal glial cells (Müller cells, microglia and astrocytes) were not labelled with FG. Thus, we can hypothesize that FG labelling after intravitreal administration accumulates in neurons by a transneuronal mechanism that goes from RGCs to photoreceptor cells. In the interaction between photoreceptors and the RPE, the RPE cells phagocytoses the tracer from the photoreceptor cells and accumulates it inside their somas.

Intraocular injection of FG is a reliable technique to label functional RPE in rats.

Oral presentation: Session 3. Room C. Code: 5758

Histology and Histopathology
From Cell Biology to Tissue Engineering

Course of microglial activation after optic nerve crush in the injured and contralateral un-injured retinas

González-Riquelme M.J., Vidal-Sanz M., Galindo-Romero C. and Agudo-Barriuso M.
Departamento de Oftalmología, Facultad de Medicina, Universidad de Murcia, Murcia, Spain and Grupo de Oftalmología Experimental, Instituto Murciano de Investigación Biosanitaria Virgen de La Arrixaca (IMIB-Arrixaca), Murcia, Spain

Microglia cells respond to injury and infection, and act in the first line to defense tissue and promote the destruction of invading pathogens. To this end, M1 microglial cells release pro-inflammatory factors and various neurotoxic mediators that if cronified, may cause neuronal death. Inflammation is resolved by M2 microglial cells, with an antiinflammatory phenotype that leads to wound healing and brings back tissue homeostasis. The main purpose of this work is to analyze the temporal course of microglial activation and M2 appearance in the mouse retina after optic nerve crush (ONC), a well characterized model of neuronal degeneration. In this model, retinal ganglion cell (RGC) death occurs in two phases, a quick one where RGC loss is first significant at day 3 and proceeds lineally until day 9. During this quick phase 50% of RGC have died at day 5, and 85% at day 9. Thereafter the second phase of RGC death commences, and they die slowly but continuously and by 45 days post lesion, only 2% of them survive.

ONC was performed in the left optic nerve of adult female C57/BL6 mice. Both retinas of each animal were dissected as flat mounts at 3, 5, 9 and 45 days after the axotomy (n= 4-6 retinas/time point). As control, intact retinas were analyzed in parallel. Flat mounts were subjected to double Immunodetection of Iba1 (microglial cells) and CD2016 (M2 state), photographed and the total number of M2 cells quantified and plotted to assess their topographical distribution.

In the injured retinas, there is a significant increase of $CD206^+$ cells at 5 and 9 days post-lesion. At 45 days, however, their number has decreased below the number found intact retinas. In the contralateral uninjured retinas, the number of M2 cells decreases significantly compared to intact ones at all time points of analyses. In intact and contralateral retinas M2 cells are few, and they are found scattered across the retina. After injury, they increase around the optic nerve disk, and the retinal periphery.

Optic nerve axotomy induces an increase of M2 microglial cells in the injured retina that reflects the course of RGC loss, peaking during the quick phase of RGC death. Interestingly, M2 microglial cells decrease in the contralateral uninjured retina.

Oral presentation: Session 3. Room C. Code: 5765

Histology and Histopathology
From Cell Biology to Tissue Engineering

Amniotic membrane for the treatment of diabetic foot ulcers

Rodríguez Valiente M.[1], García Hernández A.M.[2], Blanquer M.[2], Almansa Saura S.[1], Bernabé García A[3]., Liarte Lastra S.D.[3], Algueró M.C.[2], Fuente Mora C.[4], Alcaraz P.J.[1], Moraleda J.M.[2], Castellanos Escrig G.[1] and Nicolás Villaescusa F.J.[3]

[1]Department of General Surgery, Hospital Clínico Universitario Virgen de la Arrixaca, Biomedical Research Institute of Murcia (Instituto Murciano de Investigación Biosanitaria, IMIB-Arrixaca), El Palmar, Spain, [2]Cell Therapy Unitat Hospital Clínico Universitario Virgen de la Arrixaca, Biomedical Research Institute of Murcia (Instituto Murciano de Investigación Biosanitaria, IMIB-Arrixaca), El Palmar, Spain, [3]Molecular Oncology and TGFß, Research Unit at Hospital Clínico Universitario Virgen de la Arrixaca, Biomedical Research Institute of Murcia (Instituto Murciano de Investigación Biosanitaria, IMIB-Arrixaca), El Palmar, Spain, [4]FFIS de la Región de Murcia, Support Research Unit at Hospital Clínico Universitario Virgen de la Arrixaca, Biomedical Research Institute of Murcia (Instituto Murciano de Investigación Biosanitaria, IMIB-Arrixaca), El Palmar, Spain.

The diabetic foot is an important complication of diabetes mellitus that requires a multidisciplinary approach to avoid amputations of the lower limbs. In the wound and diabetic Foot Unit of the Virgen de la Arrixaca University Clinical Hospital (HCUVA), we treat patients with complex ulcers using cryopreserved human allogeneic Amniotic Membrane (AM). AM therapy is considered an advanced therapy according to the Directive 2009/120/CE, as it contains cells that do not have the same function in the donor and the recipient. AM have analgesic, antimicrobial and anti-inflammatory properties related to its ability to synthesize and release substances that include cytokines and signaling molecules. It is an easy to collect and apply tissue, that does not induce rejection and with ideal characteristics to treat these ulcers. Our objective was to determine the safety and efficacy in healing-epithelialization by applying AM in the treatment of chronic diabetic foot ulcers.

AM was obtained from healthy donors with scheduled cesarean sections due to obstetric causes and negative serology for infectious diseases. The AM was fragmented and cryopreserved in the cell therapy Unit under sterile conditions. From May 2014 to November 2017, we treated 18 patients with diabetic macro and microangiopathy, polyneuropathy and deformations in the feet that have complex diabetic foot ulcers with more than 8 weeks of evolution. AM was applied weekly on the wound bed. Biopsies of the wound were performed before and after the application of AM in two patients. Sections were stained in paraffin blocks with Hematoxylin and Eosin were observed by light microscopy. Patients with clinical signs of infection or an active neoplastic process were excluded. All patients signed the informed consent. The hospital ethics committee approved the protocol. The Spanish Agency of Medicines gave the authorization as compassionate use in all patients.

The median age of the patients was 62 years (16 to 82 years old). The mean time of treatment prior to the application of AM was 24 months and a half. The average area of the wounds was 10.56 cm2 (0.52-42.5). 17 out of 18 patients (94%), achieved a complete resolution of the wound with entire epithelization, and in one patient, the area of the wound was reduced by 75%. The mean time of epithelialization with AM was 5 months (1.5-13) with a mean of 11.22 membranes applied (4-40). The biopsies showed a normal structure of the skin and a correct healing. There were no signs of infections in 17 patients, during the treatment. One patient underwent excision of a bone fragment of the fifth metatarsal due to osteomyelitis. No patient developed any tumor during the treatment.

Our results show that treatment with cryopreserved human MA is a safe and effective treatment in patients with uninfected complex ulcers of the diabetic foot, where conventional treatments have failed.

Oral presentation: Session 3. Room C. Code: 5799

Histology and Histopathology
From Cell Biology to Tissue Engineering

Reconstruction of muscle volumetric loss: histological and ecographic analysis

Leiva-Cepas F.[1,2,3*], Benito-Ysamat A.[4], Ruz-Caracuel I.[1,2**], Gil-Belmonte M.J.[1], Jimena I.[1,2,3], Agüera-Vega A.[1,2], Villalba-Montoro R.[5] and Peña-Amaro J.[1,2,3]

[1]Research Group in Muscle Regeneration, University of Córdoba, Spain, [2]Department Morphological Sciences, Section of Histology, Faculty of Medicine and Nursing. University of Córdoba. Spain, [3]Maimónides Institute for Biomedical Research IMIBIC, Reina Sofia University Hospital, University of Cordoba, Spain [4]Section of Musculoskeletal Radiology, Reina Sofia University Hospital, Córdoba, Spain

Present address:

* Department of Pathology. Reina Sofia University Hospital, Cordoba, Spain.

** Department of Pathology. La Paz University Hospital, IDIPAZ. Madrid, Spain.

Skeletal muscle has a great regenerative capacity against the injury. However, in the case of serious injuries such as muscle volumetric loss (MVL), regeneration fails and the muscle evolves towards fibrosis. The importance of using acellular scaffolds that promote the regenerative capacity of the muscle itself has recently been highlighted. In the present study, we compared the histological and ultrasound characteristics of skeletal muscles after implantation of different types of materials in an experimentally induced VLM.

A cylindrical fragment (6 mm x and 5 mm fragment Ø) was extracted from the medial portion of the *tibialis anterior* rat muscle. Animals were divided into groups of 4 rats according to the product implanted in the VLM: autologous adipose tissue (AAT), decellularized matrix (DM), osteovit® (OST), fibrin-agarose (FA) and hemostatic paper (PH). Two groups were used as normal control and control in which the normal degenerative-regenerative process had been caused by the injection of a myotoxic agent. The rats were sacrificed 60 days post-implantation and the muscles were processed for histological, histochemical and immunohistochemical analysis. The histomorphometric study was carried out on cross sections in which five areas were microphotographed in each of which were analyzed: number of fibers, transversal area and smaller diameter of the muscle fibers, as well as the percentages of fibers with internal nuclei, disoriented fibers and of area occupied by fibrosis. Before the sacrifice an ultrasound study was performed.

In all the experimental groups, the lesion was identified ultrasonographically, with well-defined borders, but of variable morphology (rounded, angulated or patched). The echogenicity was also increased in all groups. However, the echo-structure showed a slight distortion in the AAT group and important in the OST and DM groups. In all groups, color and power ultrasound Doppler sonography did not show significant changes in the vascularization of the implantation area.

The materials and / or tissues used generated skeletal muscle/fibrosis in the MVL: AAT (80/20%), OST (69/31%), DM (32/68%) and PH (25/75%). In FA group, a response to foreign material was generated (0/100%). The highest percentage of fibers with internal nuclei was reached by the AAT group (62%), while the lowest corresponded to PH (39.6%). The disorientation of fibers was greater when using DM (39%), AAT (24%), OST (20%) and PH (3%). Although in no group did the mean size reached by the newly formed fibers reach a normal size, it was in the OST group (536 ± 103.1) that the fibers showed significant atrophy with respect to all the experimental groups (AAT: 2385±241; DM: 1536.8±159.8, PH: 1505.7±207.4), control (3400.6±184.4) and regenerative (3514.8±153.8).

Our study shows that, unlike other materials, it was the implantation of AAT in the MVL that allowed us to generate a new muscle with better but not reaching the complete histological and ultrasound maturation.

Oral presentation: Session 3. Room C. Code: 5810

Histology and Histopathology
From Cell Biology to Tissue Engineering

Generation of novel substitutes of the human oral mucosa with improved in vivo angiogenic potential

Blanco-Elices C.[1], Morales-Álvarez C.[1], Chato-Astrain J.[1], Martín-Piedra M.A.[1], Oruezabal R.I.[2], Sánchez-Quevedo M.C.[1], Fernández-Valadés R.[1,3] and Garzón I.[1]

[1]Tissue Engineering Group, Department of Histology, University of Granada and Instituto de Investigación Biosanitaria ibs, Granada, Spain, [2]Andalusian Initiative in Advanced Therapies (IATA), Seville, Spain, [3]Division of Pediatric Surgery, University Hospital Virgen de las Nieves, Granada, Spain

Oral mucosa (OM) is a bilayered structure playing a crucial role as a defensive barrier of the oral cavity. Tissue engineering allowed the successful generation of different artificial oral mucosa (AOM) models [1]. However, the complete construction of an AOM is often challenging due to the limitations associated to in vivo biointegration of bioengineered tissues, which are typically avascular. The purpose of our research is to generate a novel model of human AOM preconditioned with a pre-vascular cell type in order to increase its biointegration properties.

Four types of fibrin-agarose AOM were generated by tissue engineering: 1) Control AOM containing 700,000 human oral mucosa fibroblast (HFOM) in the stromal layer as previously generated by the research group [2]; 2) AOM containing 350,000 HFOM and 350,000 human endothelial cells (HUVEC); 3) AOM with 350,000 native human dental pulp stem cells (DPSC) and 350,000 HFOM; 4) AOM with 350,000 DPSC differentiated to the endothelial lineage using a conditioning medium and 350,000 HFOM. In vivo evaluation was carried out by grafting the four types of AOM in the dorsal skin of athymic Nude- Foxn1^{nu} mice. Histological analyses were carried out after 4 and 8 days post-implantation using Von Willebrand factor (VW-F) immunofluorescence.

Gross analysis revealed the development of an initial scar in all experimental groups. Histologically, pre-implanted tissues consisted of a cell-enriched stroma with an epithelial layer on top. After *in vivo* grafting, a borderline newly-formed tissue (interphase area) was found below the implanted AOM. This area showed a strongly positive VW-F reaction. The extension of the interphase area was different among the experimental groups, and tended to be moderate in groups 2 and 3 and intense in groups 1 and 4. Immunofluorescence analysis revealed a positive reaction in groups 2 and 4.

Our results support the potential usefulness of the novel AOM pre-conditioned with differentiated DPSC. Generation of these bioartificial tissues could increase the formation of small-size blood vessels at the interphase between the host and the grafted tissue, which may improve biointegration of the artificial tissue. This study suggests that differentiated endothelial-like mesenchymal stem cells could be a good strategy for improving angiogenesis. Future *in vivo* experiments should be performed to characterize these preliminary results.

Supported by the Spanish Plan Nacional de Investigación Científica, Desarrollo e Innovación Tecnológica (I+D+i) from the Spanish Ministry of Economy and Competitiveness (Instituto de Salud Carlos III), Grants FIS PI18/0331 and PI18/0332 (cofinanced by FEDER funds, European Union).

[1] Garzón I, et al. Int J Artif Organs. 2009;32(10):711-9
[2] Martín-Piedra MA, et al. Histochem Cell Biol. 2017;147(3):377-388

Oral presentation: Session 3. Room C. Code: 5812

Histology and Histopathology
From Cell Biology to Tissue Engineering

Histological quality control of human bioengineered skin used for the treatment of severely-burnt patients

Chato-Astrain J.[1], Martín-Piedra M.A.[1], Garzón I.[1], Carmona G.[2], Martínez-Vílchez A.[1], Rodríguez I.A.[1,3], Campos A.[1] and Alaminos M.[1]

[1]Tissue Engineering Group, Department of Histology, University of Granada and Instituto de Investigación Biosanitaria ibs, Granada, Spain, [2]Andalusian Initative in Advanced Therapies, Seville, Spain, [3]Cátedra de Histología B, School of Dentistry, National University of Cordoba, Argentina

Treatment of severely-burnt patients is a medical challenge. The development of bioartificial human skin substitutes by tissue engineering offers a treatment alternative for these patients [1]. In this regard, our research group previously designed and generated a model of human bioengineered skin (UGRSKIN) that showed promising results in laboratory animals [2] and is currently used for the treatment of patients with extensive and deep skin burns. Although this skin model was histologically evaluated in preclinical testing, a histological analysis of the bioartificial skin grafted in burnt patients is still in need. The objective of the present work is to carry out a preliminar histological analysis of the skin implanted in severely-burnt patients to determine the suitability of this skin model for the treatment of these patients.

Human skin biopsies were obtained from patients treated with the autologous UGRSKIN model due to extensive and deep skin burns. These biopsies were obtained after 1, 2 and 3 months of the grafting procedure and fixed in formalin for histological analysis. In each sample, we analyzed cell proliferation by the immunohistochemical detection of Ki67, keratinocyte differentiation by the analysis of involucrin expression and immunogenicity by the detection of type-I HLA molecules. Native human skin was used as control.

Histological analysis of the bioengineered skin grafted in patients revealed the presence of an epithelial layer on top of a dermal substitute that closely resemble the human native skin. After 1 month of the grafting procedure, the epithelial layer was positive for involucrin, a marker of late epithelial differentiation found in control skin, on spinosum and granulosum strata. This expression remained constant in 2 and 3 month-samples. Similarly, expression of Ki67 was found at the basal epithelial stratum from the first month and during the 3 months of the analysis, and was comparable to the native tissue. Finally, we found that type-I HLA was mildly positive in keratinocytes of basal and spinosum strata of control skin, but its expression was decreased in the grafted skin.

The clinical use of the UGRASKIN model of artificial skin allowed the development of a regenerative skin in the patient with the presence of an epidermal layer that closely resembled native epidermis, not only in terms of morphology and structure, but also in terms of proliferative activity of the basal stratum and epithelial differentiation of suprabasal strata. These results support the clinical use of this model of autologous bioengineered skin for the treatment of severely-burnt patients from a histological standpoint.

This study was supported by Grant CS PE-0383-2018, FIBAO Foundation, Spain.

[1] Martín-Piedra MA, et al. Eur Cell Mater. 2019 Mar 29;37:233-249
[2] Carriel V, et al. Cells Tissues Organs. 2012;196(1):1-12

Oral presentation: Session 3. Room C. Code: 6179

Histology and Histopathology
From Cell Biology to Tissue Engineering

Study of the adnexal skin unit on thick sections

Poblet E.[1,2], Gil-Liñan A.I.[1,2], Ocaña-Castillo B.[1,2], Godoy-Alba C.[1,2], García-Molina F.[1,2], Martínez-García C.[1] and Hardman J.A.[3]

[1]School of Medicine, University of Murcia, Murcia, Spain, [2]Reina Sofía University General Hospital, University of Murcia, Murcia, Spain, [3]Department of Dermatological Sciences, Faculty of Biology, Medicine and Health, University of Manchester, UK

We have recently described the Adnexal Skin Unit (aSU) concept that propose that the different adnexal structures of the cutaneous tissue - the hair follicle, the sebaceous glands, the arrector pili muscle, the appocrine glands and the eccrine glands- constitute a morphological and functional closely related unit.

On this study we reconstruct the human skin structure using thick vertical and transversal sections focusing on skin adnexa.

Human scalp skin was obtained from autopsy scalp tissue. Immunoflorescence of 60 µm thick sections was performed with the monoclonal mouse anti-human cytokeratin antibody (clones AE1-AE3, Agilent-Dako, Denmark) using the Alexafluor 488 (Thermo Fisher Scientific) as a fluorochrome. Panoramic confocal laser microscopy was performed with the Pannoramic Confocal 3DHISTECH facilities (Budapest, Hungary). We also used conventional histochemical stainings performed on vertical and transversal thick tissue sections of skin to demonstrate its adnexal composition. A computer assisted methodology was used to reconstruct the 3D skin structure.

Computer assisted 3D reconstruction of transversal immunohistochemically stained sections with a pan-keratin antibody confirmed previous observations of the adnexal skin unit structure and permitted a more precise visualization of the hair follicle and eccrine sweat glands interrelation. Eccrine ducts were directed to an area just below the sebaceous glands were they formed the secretory coils. The acinar portion of the eccrine sweat glands appeared integrated into the follicular units, with prolongations into the spaces that appeared between hair follicles of the same follicular unit. Direct observation of vertically oriented thick sections using histochemical stainings permitted a direct evaluation of adnexal skin structure that corroborate the intricate and integrated morphology of skin adnexa, as demonstrated with the 3D computer assisted methodology.

In this study we have confirmed an anatomical close proximity of the different skin adnexa of the human scalp skin. Presence of hair follicles, sebaceous glands, arrector pili muscle and the secretory portion of eccrine glands forming closely related structures is a common finding at the scalp. This anatomical structure of closely related structures establishs a new model that prompt to search skin physio-pathology with a broader perspective, in which every element may cooperate or influence the others during regeneration and skin diseases. The aSU structure represents the identification of an easily accessible source of highly privileged multi-lineage cells with differentiation potential.

Oral presentation: Session 3. Room D. Code: 5692

Histology and Histopathology
From Cell Biology to Tissue Engineering

Histological features of the wasting disease affecting commercial exploitations of *Pleurotus ostreatus*. First steps towards the identification and characterization of the pathogen

Vilariño M.[1,2], Tello-Martín M.[2,3], Pérez M.[2,3] and Martínez A.[1,2].

[1]Centro de Investigación Biomédica de La Rioja (CIBIR), Logroño, La Rioja, Spain, [2]European Mushroom Working Group, EMushWG, [3] Centro Tecnológico de Investigación del Champiñón de La Rioja (CTICH), Autol, La Rioja, Spain

The commercial cultivation of edible mushrooms is one of most important agricultural economic sectors in La Rioja, providing employment and subsistence for a large number of people. In the last few years, the crops of the oyster mushroom (*Pleurotus ostreatus*) have been seriously affected by a wasting disease of unknown origin, which is responsible for important economic losses. This study was designed to better understand the morphological changes experienced by the carpophores and try to pinpoint the nature of the potential pathogen responsible for the disease.

Several specimens of *P. ostreatus* were collected in local mushroom farms. Some of them were healthy (n=10) whereas others were affected by the disease (n=10). Small fragments were fixed in FEA (5% formaldehyde, 45% ethanol, 5% acetic acid) for 24 h, dehydrated, and paraffin embedded. Sections (4 µm-thick) were stained with hematoxylin-eosin. Additional fragments were fixed in 2% glutaraldehyde in cacodylate buffer for 5 h, incubated in 5% sucrose in cacodylate buffer, contrasted with osmium tetroxide, dehydrated, and embedded in plastic resin. Semithin (1 µm-thick) sections were stained with methylene blue and examined with a light microscope. Ultrathin (60 nm-thick) sections were stained with uranyl acetate and lead hydroxide, and examined with an electron microscope (Jeol, JEM 10-10).

The histological structure of mushroom carpophores is based on the close relations among hyphae, providing a palisade-like structure in the periphery which acts as a barrier with the outside (functionally similar to the epidermis in plants) whereas the interior is spongier (similar to the plant´s parenchyma). Diseased mushrooms had a compromised hyphal architecture, losing in some cases the external palisade, allowing some bacteria to colonize the mushroom body. This only happened in the most affected specimens, but most diseased mushrooms did not have any bacteria inside their fruiting bodies, thus indicating that the disease is most likely not caused by a bacterial infection. Interestingly, diseased hyphae were more basophilic than the healthy ones, suggesting a metabolic acidification due to the disease. Semithin sections provided additional information on the morphology of the diseased hyphae that were characterized by a darker and denser cytoplasm. The number of affected hyphae correlated with the severity of the disease. Electron microscopy showed that diseased hyphae presented a retracted cytoplasm, a large thickening of the cell wall, and a number of small vesicles in the cytoplasm (30-60 nm in diameter) that are consistent with a viral infection.

Morphological characterization of the diseased specimens of *P. ostreatus* suggests that the wasting disease responsible for important economic losses in commercial growths is not due to bacterial or fungal infections but to the presence of viral particles of unknown origin. We are now in the process of identifying the viral specie(s) responsible for the disease and designing preventative measures to be applied in the commercial mushroom factories.

Oral presentation: Session 3. Room D. Code: 5700

Histology and Histopathology
From Cell Biology to Tissue Engineering

About human embryonic hematopoiesis: a morphological approach

Pereda J. and Valencia B.
Laboratorio de Embriología Humana, Escuela de Medicina, Facultad de Ciencias Médicas, Universidad de Santiago de Chile, Chile

To produce terminally differentiated erythrocytes, embryonic hematopoiesis is segregated into two generational waves that occur at different times and in different anatomical sites. In humans, the first wave occurs in the yolk sac (YS) and is initiated on day 17 post-fertilization (pf), generating a transient population of primitive erythroblasts (PE), which are nucleated blood cells critical for oxygen transport and for embryo survival, and macrophages that assist in tissue remodeling and immune defense. Concerning the anatomical site where the second wave of hematopoiesis takes place, it is a matter of controversy; for some authors this wave commences in the YS, as occurs in the mouse, with the production of definitive erythroblasts and a transient pool of erythromyeloid progenitors. For others, the second wave is produced within the embryo. In the absence of morphological information, the site where it is initiated is a matter that remains unknown. The aim of this work was to investigate, using a morphological approach, whether the YS is involved in the initiation of the second hematopoietic wave that invades the embryo's body during week 5 pf. For that, the yolk stalk, the only link between the YS and the embryo, was investigated as an indicator of blood cell transit.

Six normal human embryos including their YS were studied by light and scanning electron microscopy using conventional procedures. The ages of the specimens were: 4 (2), 5 (2) and 6 (2) weeks pf. The samples were selected from the embryo-fetal collection of the Universidad de Santiago de Chile.

In humans the transport of PE from the capillary plexus of the YS to the embryo occurs via the vitelline vein that runs along the yolk stalk, from week 4 until the end of week 5 pf. In the yolk stalk, between weeks 4 and 5 pf, PE were observed within the vitelline vein of the yolk stalk. At the end of week 5 pf, the amount of blood cells was drastically reduced. On week 6 pf the yolk stalk collapses. At the end of week 6 pf the involution of the YS begins, ending its functional activity on week 7 pf. In the embryo's body, at the end of week 5 pf, both the liver sinusoidal bed and the central vein of the immature liver was invaded by a large amount of PE. On week 7 pf, hematopoiesis is initiated in the liver and definitive erythrocytes start being seen in circulation.

The scarce number of PE observed within the vitelline vein of the yolk stalk at the end of week 5 pf could not explain the huge amount of PE observed within the embryo as derived from the YS. Therefore, we concluded that the second hematopoietic wave in humans should be initiated in the embryo's body rather than in the YS, as occurs in the mice. We postulated that the PE observed in the embryo between weeks 5 and 6 pf are probably generated from a different hematopoietic focus within the embryo.

Funding by DICYT project 02-1601PT

Oral presentation: Session 3. Room D. Code: 5717

Histology and Histopathology
From Cell Biology to Tissue Engineering

Histological and morphometric study of the components of the sinus and atrioventricular nodes in horses and dogs

Gómez-Torres F.A.[1,2], Ballesteros-Acuña L.E[2] and Ruíz-Sauri A[3,4]

[1]Doctorate Student in Medicine, Department of Pathology, Faculty of Medicine, Universitat de Valencia, Valencia, Spain, [2]Department of Basic Sciences, Medicine School, Universidad Industrial de Santander, Bucaramanga, Colombia., [3]Department of Pathology, Faculty of Medicine, Universitat de Valencia, Valencia, Spain, [4]INCLIVA Biomedical Research Institute, Valencia, Spain

The first descriptions of the cardiac conduction system were performed on the hearts of sheep, dogs and cattle; since then, the histology of the conduction pathway has been described in numerous studies, but little research has been done to date regarding the morphometric study of these structures, both in humans or animals. The cardiac nodes are the source of the electrical impulse that is transmitted to the heart. The aim of this work is study the histological and morphometric characteristics of the different components of the sinus and atrioventricular nodes in horses and dogs that help to know the physiopathology of these nodes.

A group of ten horse hearts and five dog hearts were used. The region of the sinus and atrioventricular nodes was sectioned serially, and the block of tissue removed for study. All samples were fixed in 5% formaldehyde solution, and embedded in paraffin. Histological sections were acquired with a microtome and underwent staining with hematoxylin-eosin and Masson's trichrome. For the acquisition of the images light microscopy was used (Leica DMD108 optic microscope) and the samples were assessed using a morphometric analysis with the Image-Pro Plus 7.1 software.

The shape of the horse's sinus node is oblong and in dogs, it varies from rounded to oblong. The P cells of the node in both species are large and pale and their T cells are small, pale and elongated. The area of P and T cells in horses (976 μm^2 and 1,090.8 μm^2 respectively) are significantly higher than in dogs (106 μm^2 and 604.6 μm^2 respectively) ($p=0.001$ for P cells and $p=0.039$ for T cells). The horse's atrioventricular node presented an oblong shape and in dogs, presents a spindle shape. The P and T cells are pale in the horse, while in the dog they are dark, similar in color to the myocardiocytes. In this node the area (618.2 μm^2 in horses, 353.8 μm^2 in dogs) and the maximum diameter (32.2 µm in horses, 24.3 µm in dogs) of the P cells in horses were greater than those found in dogs ($p=0.004$ for area and $p=0.006$ for maximum diameter). Likewise, in T cells, the area (438.6 μm^2 in horses, 204.9 μm^2 in dogs) and the maximum diameter (47.4 µm in horses, 27 µm in dogs) were higher in horses than in dogs ($p=0.021$ for both values). The sinus and atrioventricular nodes are not surrounded by a capsule of irregular dense connective tissue, due to this characteristic only the morphology of the cells allows to identify the node.

The lower cell density in any of the cardiac nodes, especially in P cells of sinus node, can decrease electrical conduction within the nodes and in the internodal tracts, which would reflect the presence of cardiac arrhythmias derived from poor conduction, even in morphologically normal hearts.

Oral presentation: Session 3. Room D. Code: 5718

Histology and Histopathology
From Cell Biology to Tissue Engineering

Histological and morphometric structure of the sinus and atrioventricular nodes in humans and pigs

Gómez-Torres F.A.[1,2], Sebastian-Aguilar R.[3] and Ruíz-Sauri A[4,5]

[1]Doctorate Student in Medicine, Department of Pathology, Faculty of Medicine, Universitat de Valencia, Valencia, Spain, [2]Department of Basic Sciences, Medicine School, Universidad Industrial de Santander, Bucaramanga, Colombia, [3]Computational Multiscale Simulation Lab, Universitat de Valencia, Valencia, Spain, [4]Department of Pathology, Faculty of Medicine, Universitat de Valencia, Valencia, Spain, [5]INCLIVA Biomedical Research Institute, Valencia, Spain

Increased interest in disorders of the function of cardiac conduction system have allowed to develop the knowledge of its anatomy, histology and its vascularization. This research is focused on describing the morphometry of sinus and atrioventricular nodes of humans and pigs, to determine the similarities and recommend the use of this animal species as a model in clinical experimentation.

We analyzed 10 hearts of adult human males and 10 pig's hearts males. The samples were assessed using an optic microscope Leica DMD108 and the computerized morphometric study was carried out by software Image-Pro Plus 7.1. With the morphometric study we have determined the number of cells and different parameters of shape and size of the sinus and atrioventricular nodes: area; roundness; maximum, minimum and mean diameter. Next, we have included these data in a SPSS statistical program. In order to obtain a morphometric profile, for each parameter data were expressed as the interval where the 66% of the whole population is included and the average of this interval. See Table.

The sinus node in humans and pigs has an oblong shape. The area of this node and its cells in humans was 1584.8 mm^2 and 8.9 mm^2 respectively. In pigs, its area was 1525 mm^2 and its cells was 13.4 mm^2. In humans and pigs, the atrioventricular node has an oblong shape. The area of this node and its cells in humans was 1617.3 mm^2 and 20.3 mm^2 respectively. In pigs, its area was 1541.8 mm^2 and its cells was 0.9 mm^2, this indicates a high presence of connective tissue inside both nodes. According to the morphometric profile, the parameters of the cells of the nodes of humans and pigs allow to identify them clearly, finding statistically significant differences in the area of the P cells (p=0.004) and in the maximum diameter (p=0.011) of the T cells of the sinus node; similarly, these differences were observed in the area and the maximum diameter of the P cells of the atrioventricular node (p=0.001), being higher in humans in the sinus node and higher in pigs in the atrioventricular node.

We have reported through a morphometric profile that the structure of sinus and atrioventricular nodes of humans and pigs show few differences, so we conclude that this type of animals can be used as models for hemodynamic applications and experimental studies that include atrial electrical conduction and in this way prevent the presentation of arrhythmias that can generate sudden deaths in both.

	Sinus node (μm)			AV node (μm)		
	P	T	Myoc.	P	T	Myoc.
Humans						
Maximum diameter	32-39 (35)	57-75 (66)	22-28 (25)	18-25 (21)	45-69 (57)	19-25 (22)
Minimum diameter	20-23 (21)	11-14 (12)	16-19 (17)	13-15 (14)	9-11 (10)	12-17 (14)
Roundness	1.10-1.19 (1.14)	2.35-3.13 (2.74)	1.09-1.13 (1.11)	1.09-1.17 (1.13)	2.11-3.10 (2.60)	1.08-1.15 (1.11)
Pigs						
Maximum diameter	22-32 (27)	37-53 (45)	19-22 (20)	38-50 (44)	49-69 (59)	22-29 (25)
Minimum diameter	16-21 (18)	7-12 (10)	12-16 (14)	22-28 (25)	11-14 (12)	15-19 (17)
Roundness	1.08-1.12 (1.1)	1.91-2.44 (2.17)	1.08-1.13 (1.10)	1.16-1.27 (1.21)	1.90-2.84 (2.37)	1.09-1.16 (1.12)

Oral presentation: Session 3. Room D. Code: 5721

Histology and Histopathology
From Cell Biology to Tissue Engineering

Redistribution of arylsulfatase a on the human sperm membrane after capacitation *in vitro*

Huerta-Retamal N.[1], Sáez-Espinosa P[1], Robles-Gómez L.[1], Romero A.[1], Avilés M.[2] and Gómez-Torres M.J.[1,3]

[1]Departamento de Biotecnología, Universidad de Alicante, Alicante, España, [2]Departamento de Biología Celular e Histología, Universidad de Murcia e IMIB, Murcia, España, [3]Cátedra Human Fertility, Universidad de Alicante, Alicante, España

The Arylsulfatase A (ARSA) is part of a molecular complex containing also HSPA2 and SPAM1. Previous work has revealed that a lack of ARSA protein expression causes failure for the spermatozoa to adhere the oocyte zona pellucida. The objective of this study was to know the immunolocalization of ARSA receptor in spermatozoa before and after different times of in vitro capacitation and analyze the changes on its location.

The samples were obtained from five normozoospermic donors. The capacitation was carried out by swim-up for one and four hours. Assessment of the ARSA receptor location was performed by indirect immunofluorescence using anti-ARSA antibody. In each physiological condition, a minimum of 200 cells were observed by confocal microscopy and the data were analyzed using Student t distribution ($P<0.05$).

Before capacitation, we only detected a 8.61% of positive spermatozoa for ARSA while after capacitation the percentage of positive cells significantly increased to 61.86%, and 55.55% after one and four hour respectively. Furthermore, we described ARSA receptor distribution patterns (Figure 1). Moreover, we noticed that in labelled incapacitated spermatozoa, the most abundant pattern was P2 (2.89%). The percentage of cells with this pattern significantly increased after in vitro capacitation (12.72% and 8.9% after one and four hours respectively). Similarly, ARSA was slightly distributed over the acrosomal region (P3) of 2.86% of cells before capacitation. The presence of this pattern significantly increased after capacitation, when it was observed in 12.89% one hour capacitated cells and in 5.67% four hour capacitated sperm cells. However, after capacitation, the significantly most representative pattern was P4 (27.20% and 28.20% both in one and four hours in capacitated sperm), increasing significantly from 2.86% cells showing P4 before capacitation. Interestingly, after capacitation we observed ARSA distributed intensely over the periacrosomal region accompanied with a slightly labelling throughout the acrosome (P5). This ARSA location was not observed in sperm prior to capacitation. However, this pattern showed a correlation with capacitation time being P5 represented in 9.13% and 12.78% cells after one and four hours capacitation respectively.

Our data suggest that ARSA receptor is modified according to in vitro capacitation. As capacitation time increases, we observed a higher sperm population showing ARSA in the acrosomal and periacrosomal area, the region of greater interaction with the oocyte. Therefore, by increasing capacitation time we can improve sperm selection.

Support: VIGROB-186 and Human Fertility Chair of the University of Alicante

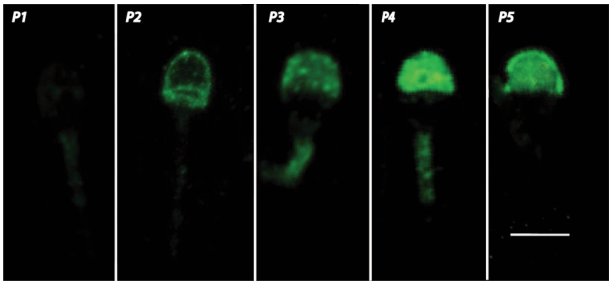

Figure 1: pattern 1 (P1) without labelling; pattern 2 (P2), fluorescence on the equatorial band and the periacrosomal region; pattern 3 (P3) slightly labelling in the acrosome; pattern 4 (P4), intense fluorescence in the acrosomal region; pattern 5 (P5) weak fluorescence among the acrosomal region accompanied by an intense labelling at the periacrosomal region. Scale bar 10 um.

Oral presentation: Session 3. Room D. Code: 5934

Histology and Histopathology
From Cell Biology to Tissue Engineering

Proliferation, apoptosis and number of Sertoli cells in photoinhibited Syrian hamster testes (*Mesocricetus auratus*) owing to a short photoperiod

Martínez-Hernández J., Seco-Rovira V., Beltrán-Frutos E., Serrano-Sánchez M.I., Ferrer C. and Pastor L.M.

Department of Cell Biology and Histology, School of Medicine, IMIB-Arrixaca, Regional Campus of International Excellence, Campus Mare Nostrum, University of Murcia, Murcia, Spain

In photoinhibited Syrian hamster testes, the Sertoli cells (Sc) apoptosis index (AI) has been described in regression owing to short photoperiod (Seco-rovira et al., 2015) but the proliferative activity and its effect on the population of Sc during recrudescence remains unknown. This study aims to determine the proliferation index (PI) and of total Sertoli cells number in both fully photoinhibited and non-photoinhibited testes (Control).

For this, a total of 14 hamsters were used (9 treated (TR) and 5 controls (CT). The treated animals were subjected to an 8:16 light-dark photoperiod, while the control animals were subjected to a 12:12 light-dark photoperiod. Nine treated animals plus five from the control group were sacrificed at 12 week of exposure to short photoperiod when the testes was fully regressed. Testes were fixed in methacarn and embedded in paraffin. The degree of testicular regression was checked according to histological criteria as previously is described (Seco-Rovira et al., 2015). Histological sections of testes were observed in confocal (PCNA and vimentin immunohistochemistry) and light microscopy (H&E). PI of the Sertoli cells was calculated as the number of PCNA+/Vimentina+ Sertoli cells / Total number of Sertoli cell (Sertoli cells PCNA+/Vimentina+) + Sertoli cells PCNA-/Vimentina+) x100. The total number of Sertoli cells was calculated using a point-counting method in H&E sections. Using the AI index previously obtained (Seco-rovira et al., 2015), the total number of proliferative Sertoli cells (TpSc) and apoptotic Sc (TaSc) was calculated.

The existence of PCNA+ and vimentine+ cells in both groups, which corresponded to Sertoli cells in proliferation, were demonstrated. The PI of Sc was significantly higher in TR than CT ($P < 0.05$). As regards the total number of Sc per testis, a significant decrease was observed in the TR with respect to CT ($P<0.05$). No significant differences were found both groups as regards the TpSc and AI. Finally, the TaSc was higher in CT than TR group ($P<0.05$). Conclusions: a) The number of Sertoli cells decreased in photoinhibited hamster testes indicating great loss in the Sertoli cell population by apoptosis throughout the regression; b) PI increase in fully regressed testes as well as an similar AI to the control would allow the rapid recovery of the Sertoli cell population at the beginning of the recrudescence and would give support of new spermatogenesis.

Funded by GERM 19892/15 from Fundación Seneca CARM).

Seco-Rovira, V., Beltrán-Frutos, E., Ferrer, C., Saez, F. J., Madrid, J. F., Canteras, M. and Pastor, L. M. (2015). Testicular histomorphometry and the proliferative and apoptotic activities of the semin-iferous epithelium in Syrian hamster (*Mesocricetus auratus*) during regression owing to short photoperiod. Andrology 3, 598–610.

Oral presentation: Session 3. Room D. Code: 5921

Histology and Histopathology
From Cell Biology to Tissue Engineering

Qualitative and quantitative histological analysis of the effect of melatonin administration in ischemia/reperfusion gastric model in rats

Peña-Mercado E.[1], García-Lorenzana M.[2] and Beltran N.E.[3]

[1]Posgrado en Ciencias Naturales e Ingeniería, Universidad Autónoma Metropolitana-Cuajimalpa, [2]Departamento de Biología de la Reproducción, Universidad Autónoma Metropolitana-Iztapalapa, [3]Departamento de Procesos y Tecnología, Universidad Autónoma Metropolitana-Cuajimalpa, Ciudad de México, México

Ischemia/reperfusion injury (I/R) is defined as the paradoxical exacerbation of dysfunction and cell death, after restauration of blood flow to ischemic tissues. This type of injury can induce multiple organ failure. In gastric ulceration models, the administration of melatonin has presented gastroprotective effects attributed to its antioxidant capacities, in addition to the activity increase of antioxidant enzymes, stimulates the production of prostaglandins, decreases the infiltration and function of neutrophils, and also decreases the number of apoptotic cells in the epithelium of the gastric mucosa. The aim of this work was to evaluate the effect of melatonin administration in the gastric mucosal damage induced by an I/R model for 24 hours.

Adult male Wistar rats with controlled photoperiod and feeding were used. Three groups were formed: Control, I/R without treatment and I/R with treatment (Tx). Ischemia was produced by clamping the celiac artery during 60 min, followed by a reperfusion period of 24 hours. Administration of melatonin (5 mg/kg i.p.) was performed 5 min before blood flow restoring.

In the Control group, no apparent injury was observed. In the I/R without Tx group, erosion of the gastric mucosa and interstitial edema were identified. In the I/R with Tx group, edema cells were found and some in a necrotic process; however, the glandular architecture was found conserved. At the lamina propria level, acute inflammatory process was found. The quantitative analysis showed a significant increase ($p<0.001$) in the injury score in I/R without Tx group (5.4±0.12) with respect to the Control group (0.47±0.12); whereas in the I/R with Tx group a reduction in the score (3.8±0.10) was identified with respect to the I/R without Tx group ($p<0.001$), indicating a decrease in the severity of gastric mucosa damage.

The administration of melatonin decreased the gastric mucosa damage in an I/R model for 24 hours.

Oral presentation: Session 3. Room D. Code: 6177

Histology and Histopathology
From Cell Biology to Tissue Engineering

Cytoskeleton changes are crucial in the selective cytotoxic effect of CT4, a flavonoid from *Chromolaena tacotana*

Castellanos-Sánchez C.[1,2], Ovelleiro D.[1], Hernández R.[1], Peinado M.A.[1] and Siles E.[1]

[1]Departamento de Biología Experimental, Universidad de Jaén, España, [2]Facultad de Ciencias, Universidad de Ciencias Aplicadas y Ambientales, Bogotá, Colombia

Colorectal cancer is a leading type of cancer ranked as the second and third top in terms of mortality and incidence, respectively. Although currently its treatment has been considerably improved, it is urgent to find new selective anticancer agents with better safety and efficacy. *Chromolaena tacotana* is a shrub from the Andean region traditionally used against infections and some type of cancers. Given that this specie is rich in a variety of flavonoids potentially bioactive, the aim of this is study was to analyze the antitumoral effect of the particular flavonoid 5,7,3´,4´-tetrahydroxy-3-methoxyflavone (CT4) isolated from the leaves of *C. tacotana* on the colon tumor cell line RKO.

Cultured RKO colorectal adenocarcinoma cells and normal CCD18-colon cells were treated for different times ranging from 12 to 48h, with different concentrations of CT4, being its cytotoxic effect evaluated by MTT assay. Intracellular generation of reactive oxygen species (ROS) was analysed using 2',7'-dichlorofluorescin diacetate. The percentage of cells in each phase of the cell cycle was assessed by flow cytometry with the Vindelow's reagent. The induction of apoptosis in the cell culture was evaluated by flow cytometry using the Annexin-V–FITC apoptosis detection kit (Immunostep). Changes in protein profiles were evaluated using label free relative protein quantification by nanoscale liquid chromatography coupled to tandem mass spectrometry (NanoLC-MS/MS Analysis). Deregulated proteins were studied using the Encyclopedia of Genes and Genomes (KEGG). The effect of CT4 on microtubules was determined by immunofluorescence (Leica TCS SP5 II) with a monoclonal antibody to α-tubulin (Sigma, St. Louis, MO, USA). Finally, the morphological changes after CT4 treatment were evaluated by sequentially analyzing cell cultures with phase-contrast microscopy.

The results indicate that, after 48h of treatment, the bioactive compound CT4 exerts a cytotoxic effect on the colon adenocarcinoma cells RKO (IC_{50}= 38,48 μM), but not on normal colon cells (CCD18-co). This cytotoxic effect is accompanied by a sharp increase in the intracellular generation of ROS, also detected at lower concentrations of CT4 (eg. 20 μM), by the accumulation of cells in the G2/M phase of the cell cycle and, finally, by a significant increase in late-apoptotic cells. The proteomic analysis reveals that 932 proteins are differentially expressed in CT4-treated RKO cells. KEGG analysis shows that two of the top enriched canonical pathways are remodeling of epithelial adherens junctions (p=4.69 10^{-8}) and actin nucleation by ARP-WASP (p=4.11 10^{-3}). A time course study with confocal and phase-contrast microscopy corroborates that cytoskeletal changes are concomitant to morphological changes in the cells and to the induction of cell death.

Our results reinforce the crucial role of the cytoskeleton on the cytotoxic effect of CT4.

CT4 was kindly provided by Dr. Torrenegra from the Universidad de Ciencias Aplicadas y Ambientales (Colombia).

Poster Presentations

Poster Presentations

Session 1

Thursday

Topics:

Tissue Biology
Histology of Organs and Systems
Histopathology
Teaching
Tissue Engineering

Poster presentation: Session 1. Topic: Tissue Biology. Code: 5095

Histology and Histopathology
From Cell Biology to Tissue Engineering

Changes in the tissue concentration of lipofuscin in the musculature of fish species *Astyanax altiparanae* after acute exposure to LAS (linear alkylbenzene sulfonate)

Ciamarro C.M.[1], Pitol D.L.[2], Pereira B.F.[3] and Caetano F.H.[1]

[1]Estadual University of São Paulo, Campus of Rio Claro, SP, Brazil, [2]University of São Paulo, FORP, Ribeirão Preto, SP, Brazil, [3]Federal University of São Paulo, Campus of Diadema, SP, Brazil

There are several problems in the characterization of skeletal muscle aging, considering that it has fibers that give the tissue a heterogenic characteristic and that its physiological state can be modified very seasonally, besides having to consider its trophic regimen in addition to the influence of other systems, as the nervous and the endocrine. One of the age-related changes in skeletal muscle is the mass decrease and reduced exercise capacity. Lipofuscin has been shown, in both invertebrate and vertebrate models, as a good marker of cell aging, since after its formation either by natural aging or by environmental influences, it remains in the cell until its death, considering that indicates the decline in lysosomal activity.

For this experiment, 40 individuals of the species Astyanax altiparanae of the same age were used, which were kept in 2 boxes of polyethylene, with capacity for 500 liters each. These were divided into 2 groups of 20 individuals each, being one the control and the Treatment 1: water containing LAS (linear alkylbenzene sulfonate), base of the biodegradable detergents. Acute exposure to the component (7 days) was performed, after which 10 individuals from each group were collected, and the pectoral and caudal muscles (red and white) were sampled. For the analysis of lipofuscin, 5 7µm sections were analyzed with the aid of a fluorescence microscope, under the light filter of 450 - 490nm, without any staining reaction, in view of the autofluorescence of this compound. The total area occupied by lipofuscin in the tissue was quantified using the ImageJ software, which obtains this data by quantifying the number of fluorescent spots in the tissue. The data were submitted to the Shapiro-Wilk test to verify the normality of the groups and later to the ANOVA/Tukey test for parametric data and Kruskal-Wallis/Dunn for non-parametric data to determine the significance of the results. All the experiment was duplicated.

The only fibers that presented significant difference were those of the red caudal musculature, in which a significant difference ($p<0.05$) was obtained between the treatments.

Caudal musculature was affected by the pollutant, even in a short period of exposure, generating an “early aging” that can affect the swimming and consequently all it’s ecological behavior.

Poster presentation: Session 1. Topic: Tissue Biology. Code: 5697

Histology and Histopathology
From Cell Biology to Tissue Engineering

Histological tissue distribution of DLK1 and DLK2 during E16.5 mouse embryo organs: similarities and differences

Garcia-Gallastegi P.[1], Crende O.[1], Ruiz-García A.[2], Ibarretxe G.[1], Rivero-Hinojosa S.[3], González-Siccha A.D.[4], Laborda J.[5], García-Ramírez J.J.[2] and Unda F.[1]

[1]Department of Cell Biology and Histology, Faculty of Medicine and Nursery, University of the Basque Country, UPV/EHU, Leioa, Bizkaia, Spain, [2]Department of Inorganic and Organic Chemistry and Biochemistry, Medical School, Regional Center for Biomedical Research, Unidad Asociada de Biomedicina (UCLM-CSIC), University of Castilla-La Mancha, Albacete, Spain, [3]Center for Cancer and Immunology Research, Children's Research Institute, National Health System, Washington, USA, [4]Departamento de Bioquímica, Facultad de Farmacia y Bioquímica, Universidad Nacional de Trujillo, Trujillo, Perú, [5]Department of Inorganic and Organic Chemistry and Biochemistry, Pharmacy School, Regional Center for Biomedical Research, Unidad Asociada de Biomedicina (UCLM-CSIC), University of Castilla-La Mancha, Albacete, Spain

DLK1 and DLK2 are transmembrane proteins belonging to the EGF-like repeat-containing family that function as non-canonical NOTCH inhibitory ligands. DLK1 is usually downregulated after embryo development and its distribution in some adult and embryonic tissues has been described. However, the expression and role of DLK2 in embryo and adult tissues remains unclear.

To better understand the relevance of both proteins during embryo development, we analyzed the expression pattern of DLK1 and DLK2 in 16.5-day-old mouse embryos (E16.5) and evaluated the possible relationship between these two proteins in embryo tissues and cell types.

We found that DLK1 and DLK2 proteins exhibited a broad distribution pattern, which was positively detected in mouse developing organs, such as brain, vertebral column, cartilage, skeletal muscle, salivary glands, liver, lung, intestine, thymus, kidney and adrenal gland. Indeed, in the salivary gland, vertebral column and lung, DLK1 and DLK2 show an opposite expression pattern indicating that both proteins could play a synergistic role during cell differentiation.

This study provides additional information for understanding temporal and site-specific effects of DLK1 and DLK2 during mouse embryo morphogenesis and cell differentiation.

Poster presentation: Session 1. Topic: Tissue Biology. Code: 5699

Histology and Histopathology
From Cell Biology to Tissue Engineering

Potential neuroprotective role of apolipoprotein D in a cellular model of multiple sclerosis induced by cuprizone

Martínez-Pinilla E., Rubio N., del Valle E., Tolivia J. and Navarro A.

Department of Morphology and Cell Biology, University of Oviedo, Asturias, Spain, Instituto de Neurociencias del Principado de Asturias (INEUROPA), Asturias, Spain, Instituto de Salud del Principado de Asturias (ISPA), Asturias, Spain

Apolipoprotein D (Apo D) is a multifunctional lipocalin able to bind and transport small hydrophobic ligands. In the central nervous system, Apo D is increased during aging and in some neurodegenerative diseases like Multiple Sclerosis (MS). However, little is known about the mechanisms of action of Apo D in this pathology. The aim of this work was to study the Apo D function in a cuprizone cellular model of MS in human neuroblastoma (SH-SY5Y) and human oligodendrocyte (HOG) cell lines, and in neuron-oligodendrocyte co- cultures.

We addressed the study of the neuroprotective role of Apo D by two different strategies i.e. by using an antipsychotic drug, as a possible inductor of Apo D expression, and by using the human Apo D (hApo D) itself, purified from human breast gross cystic disease fluid. For this purpose, we treated SH-SY5Y cells, HOG cells, and co-cultures with different concentrations of hApo D or antipsychotic drug prior to the addition of cuprizone. Once the treatments were concluded, we analyzed the effects on cellular viability by a MTT viability assay and, if necessary, we quantified Apo D immunosignal in these experimental conditions.

Our results demonstrated that antipsychotic drug was able to prevent the loss of cell viability caused by treatment with cuprizone in the HOG cells while increasing the expression of Apo D. In contrast, the neuroprotective effect of antipsychotic drug in the SH-SY5Y cells was independent of the Apo D expression. With regard to the hApo D, we found that it was able to directly revert the loss of cell viability caused by treatment with cuprizone in our MS cellular model in the two cell lines and in the neuron-oligodendrocyte co- cultures.

Apo D exerts a neuroprotective effect in the cuprizone cellular model, both in the case in which it is added exogenously as when we increase its levels by treatment with an antipsychotic drug. This could be due to its role as an antioxidant molecule in the arachidonic acid metabolism, therefore being part of the cellular oxidative damage protection mechanism.

Moreover, all this highlights that the cuprizone cellular model of MS is a useful approach for the study of Apo D function and opens new avenues for investigate its implication in the pathophysiology of MS.

This work was supported by FISS Instituto de Salud Carlos III and FEDER (Fondo Europeo de Desarrollo Regional) (PI15/00601) grant.

Poster presentation: Session 1. Topic: Tissue Biology. Code: 5870

Histology and Histopathology
From Cell Biology to Tissue Engineering

"Focus stacking" photographic technical for analysis of cnidocytes in sea anemones

Márquez-Ramos J.A., Hernández-Calderas I., Cordero-Ramos D.I., Matadamas-Guzmán F.M., Jerónimo-Juárez J.R., Valdez-Peralta H.I. and Guzmán-García X.

Laboratorio de Ecotoxicología, Histología, Departamento de Hidrobiología, División de Ciencias Biológicas y de la Salud, Universidad Autónoma Metropolitana Unidad Iztapalapa, Ciudad de México, México.
xochitlguga@gmail.com

The histological study requires specialized techniques that allow an adequate processing in addition to microscopic technology for the analysis of biological samples. The "Focus stacking" is a digital technique that uses the combination in a single image of photographs with different depths of field to obtain greater clarity. One of the advantages offered by this technique is that the sharpness of the image covers more space which is useful when analyzing large tissue structures. This technique requires a paid software like Zerene Stacker or free software like ImageJ. In the tissue study of sea anemones, the characterization of the form and type of cnidocytes (specialized cells of this group) is essential for their taxonomic identification, however, these cells have a length of 21.6 µm and in a common microscope are incomplete. The aim was to recognize sea anemone cnidocytes by means of the "Focus stacking" technique in order to help the analysis of these cells.

A digital camera, Canon model Powershot G10, mounted on a Carl Zeiss microscope, was used to make the microphotographs. 10 microphotographs of cnidocytes were taken at a different focal point in the same field. In each capture, the focus distance of the observed field was gradually increased. The number of photos varied depending on the size of the object observed from one pair to dozens (for deep scenes). The focus was adjusted by means of the microscope and the diaphragm aperture, ISO sensitivity, shooting speed and camera focus were considered. Subsequently, the images obtained with the Zerene Stacker 1.04 program for the analysis of anemone cnidocytes were processed and the AxioVision 4.8 program was measured in length and width.

20 fields of 10 slides (100X) were analyzed and 100 photomicrographs were obtained, and 12 stacks were generated. In these combinations the target cells were observed totally focused. The stacking of photographs allows us to distinguish the tissue morphology with greater clarity and depth of visual field. Using this technique, in a sea anemone collected in Tecolutla, Veracruz México, four types of cnidocytes were differentiated: Spirocysts (cells in spiral form), Basitrics that are narrow and elongated, Mastigoforos and Holigrotricos (narrow and slightly twisted cells whose difference between them is the size) The length of the cells was 21.9 µm (spirocytes), 20.9 µm (Basitricos), 16.33 µm (Mastigoforos) and 24.32 µm for Holigotricos. The average width of the cnidocytes was 2 µm

In microphotographic analysis of image compositions allowed to identify cells more accurately. The advantages it can give us when processing images of this type, is a three-dimensional perspective of cellular structures. In sea anemone, the correct characterization of these cells allows an approach to their taxonomic identity. This technique is accessible for those laboratories that do not have powerful software and specialized and low-cost photographic equipment.

Poster presentation: Session 1. Topic: Tissue Biology. Code: 5871

Histology and Histopathology
From Cell Biology to Tissue Engineering

Cellular response after injury in sea anemone *Bunodosoma sp.* of Tecolutla, Veracruz

Matadamas-Guzmán F.M.[1], Calderas-Hernández I.[1], Márquez-Ramos J.A.[1], Valdez-Peralta H.I.[1], Cordero-Ramos D.I.[1], Guerrero-Legarreta I.[2], Segoviano-Ramírez J.C.[3], García-Barrientos R.[4] and Guzmán-García X.[1]

[1]Laboratorio de Ecotoxicología, Departamento de Hidrobiología, División de Ciencias Biológicas y de la Salud, Universidad Autónoma Metropolitana Unidad Iztapalapa, Ciudad de México, México, [2]Laboratorio de Macromoléculas, Departamento de Biotecnología, División de Ciencias Biológicas y de la Salud, Universidad Autónoma Metropolitana Unidad Iztapalapa, Ciudad de México, México, [3]Unidad de Bioimagen, Centro de Investigación y Desarrollo en Ciencias de la Salud, Universidad Autónoma de Nuevo León, Monterrey, Nuevo León México, [4]Universidad Politécnica de Tlaxcala, Tlaxcala. México.
xochitlguga@gmail.com

During the recovery of any damaged tissue after an injury, the ability of each organism to turn lost tissue to normality is involved. Laboratory animals are used as a model to investigate and understand the causes, diagnosis and treatment of diseases that affect humans and animals. Marine organisms are subject to unique conditions, which causes them to synthesize molecules that have no equivalence with their terrestrial counterparts. Cnidarians have an important phylogenetic position to understand muscle evolution, because they are the first organisms that developed muscle cells. Sea anemones have five cell types: myoepithelial, interstitial, glandular, cnidocyte and nerve cells. The capacity of tissue repair of these organisms is crucial for their survival in different situations, such as predator's action and environmental changes. Recommendations for experimental animal treatments suggest that a minimum number of animals should be used. In order to carry out studies in anemones, a method is required which does not include the sacrifice of the organisms and ensures their survival for future studies.

The bioassay consisted of collecting 10 sea anemones from Tecolutla, Veracruz. They were separated into five groups, two organisms each, in order to analyze injury differences with respect to time (8, 24, 48, 72 and 624 h). 2 mm diameter circular biopsy in the middle area of the column with a dermatological punch was performed. Biopsies were fixed with 10% formaldehyde solution in PBS 1 mM, pH7.4. 5 µm sections were obtained and stained with hematoxylin-eosin, Masson trichrome and Mallory trichrome.

Ciliated cylindrical pseudostratified epithelial tissue alternating with granular cells, in the apical zone and muscular tissue in the basal zone of the skin, from all anemones biopsies, were observed. The granulated ones are secretory type cells and the transparent ones with the cilia are of the gastrodermic type. Into the biopsies taken at different times the mesoglea region showed clusters of polyhedral cells, indicating a possible proliferation, just one stratum of simple cubic epithelial tissue, a possible cell migration into stratified epithelial tissue and appearance of germinal follicles.

The taking of the biopsies allowed implementing the histological study of the sea anemones column. A tissue organization in the injury zone after 624 hours was generated showing complete repair and normal histological aspect like those from healthy non-injured skin. The tissue results indicate the presence of different cells whose function and differentiation results of interest in different processes. The use of anemones as a study model organism is of significant economic expense, involving collection, maintenance and special care. Therefore, sacrifice of these organisms should be the last option.

Poster presentation: Session 1. Topic: Tissue Biology. Code: 5883

Histology and Histopathology
From Cell Biology to Tissue Engineering

Peripheral nerve regeneration is regulated by the activation of the small rac GTPase: preliminary results

Gayoso M.J.[1,2], Gayoso S.[1,2], Caloca M.J.[3] and Garrosa M.[1,2]

[1]Department of Cell Biology, Histology and Pharmacology, Faculty of Medicine, University of Valladolid, Valladolid, Spain, [2]Institute of Neurosciences of Castile and Leon (INCYL), University of Valladolid, Spain, [3]IBGM, CSIC, University of Valladolid, Valladolid, Spain

Rac is a main regulator of the actin cytoskeleton dynamics. Due to this function, Rac has important roles during nervous system development. Alterations in Rac signaling are the cause of a great number of human neurodegenerative diseases such as Parkinson and Alzheimer diseases. In the mouse brain, Rac is widely distributed with the highest expression in cerebellar nuclei and subcortical structures. Rac is also expressed in the mouse peripheral nerves and activated by injuries. Our objective is to determine the possible effect of Rac activation in an experimental model of sciatic nerve crush.

A knock-out mouse model that lacks a negative regulator of Rac was used. In this model, we measured the length of nerve regeneration after a double-crossed sciatic crush and compared to that of control mice. We are interested in the first steps of nerve regeneration and therefore we determined the length of regenerated fibers past one week of the lesion. The whole sciatic nerve piece was embedded in epoxy-resin and thick (300 µm) and semithin serial sections were performed. Then samples were stained with toluidine blue. Finally, the samples visualized under light microscopy. Myelinated fibers have been used as the marker of regeneration since unmyelinated fibers are difficult to detect with this technique.

In these preliminary results, the knock-out mice reached a length of regenerated nerve longer than that of control mice.

These results suggest that the activation of Rac has a positive effect in peripheral nerve regeneration.

Supported by Grants of Junta de Castilla y León for Regenerative Medicine Network and of the University of Valladolid for Neurobiology GIR (2018-19).

Poster presentation: Session 1. Topic: Tissue Biology. Code: 5941

Histology and Histopathology
From Cell Biology to Tissue Engineering

Caloric restriction alters the hormonal profile and testicular metabolome resulting in sperm head defects in Wistar rats

Martins A.D.[1,2], Jarak I.[1,2], Morais T.[3,4], Carvalho R.A.[5], Oliveira P.F.[1,2,6,7], Monteiro M.P.[3,4] and Alves M.G.[1,2]

[1]Department of Microscopy, Laboratory of Cell Biology, Abel Salazar Institute of Biomedical Sciences (ICBAS), University of Porto, Porto, Portugal, [2]Unit for Multidisciplinary Research in Biomedicine, Institute of Biomedical Sciences Abel Salazar (UMIB-ICBAS), University of Porto, Porto, Portugal, [3]Department of Anatomy, Institute of Biomedical Sciences Abel Salazar (ICBAS), University of Porto, Porto, Portugal. [4]Obesity and Bariatric Services and Centre for Obesity Research, University College of London Hospitals, UCL, London, U.K. [5]Department of Life Sciences, University of Coimbra, Coimbra, Portugal, [6]Department of Genetics, Faculty of Medicine, University of Porto, Porto, Portugal, [7]i3S - Instituto de Investigação e Inovação em Saúde, Universidade do Porto, Porto, Portugal
alvesmarc@gmail.com

There is a worldwide increasing concern with food habits. The worrying prevalence of obesity and metabolic diseases are the main reason for this concern. However, we overlook a new dietary trend in modern societies that is associated with caloric restriction (CR), not only to lose weight, but mostly due to the confidence that it has many health effects. Indeed, caloric restriction (CR) is reported to increase life span and delay age-related problems. However, some negative effects were described, but male fertility implications are still to be elucidated. This study aims to assess sperm quality, seminiferous tubules status, as well as testicular metabolism in Wistar rats subjected to CR during 28 days, when compared with control rats fed *ad libitum*.

Male Wistar rats (6-week old) were randomly distributed in two groups: one control fed *ad libitum* (n=6) and one group of rats subjected to CR (fed with 30% less calories) (n=6) during 28 days. The 28 days were chosen based on the duration of the seminiferous epithelial cycle, which is approximately 13 days, thus allowing 2 cycles. After that period, the testes were extracted from the rats, fixed in 4% of paraformaldehyde and then sliced in 5 micrometres sections. The slices were stained with haematoxylin-eosin and 25 diameters of seminiferous tubules of each animal tubules were measured. The plasmatic hormonal profile was determined using commercial kits. Sperm parameters (concentration, morphology and viability) were analysed using sperm form the corpus of the epididymis. The metabolites were extracted from the testes using a polar and nonpolar approach. The 1H-NMR spectra from the extracts were recorded using a Varian Inova 600 MHz. Differentially expressed metabolites were used to identify the most relevant metabolic pathways affected using MetabAnalyst.

In the end of the experiment the rats subjected to CR presented lower body weight (298.0±2.6 g compared with 347.1±6.5 g) though no alterations were detected in seminiferous tubules diameters (283.9±4.7 mm), when compared to control rats (289.8±2.7 mm). The hormonal levels of ghrelin (1.0±0.2 ng/mL compared with 0.4±0.1 ng/mL) and glucagon like peptide-1 (44.5±3.5 pM compared with 24.2±3.9 pM) were higher, whereas leptin levels (1.8±0.4 ng/mL compared with 6.9±0.7 ng/mL) were lower in rats subjected to CR. Interestingly, the analysis of testicular metabolomics revealed a distinct metabolic profile between rats subjected to CR or fed *ad libitum*. A further bioinformatic analysis revealed that glutamate and glutamine pathways were particularly affected in the testis after CR. Concerning sperm quality, no differences were found in concentration or viability of sperm. However, a higher number of head defects (8.7±1.7%) was detected in the sperm of rats subjected to CR, when compared to sperm from rats fed *ad* libitum (3.1±1.0%).

This study shows that CR affects plasmatic hormonal profile and testicular metabolism, which is correlated with increasing sperm head defects. These results provide evidence that CR can compromise male fertility.

Poster presentation: Session 1. Topic: Tissue Biology. Code: 5942

Histology and Histopathology
From Cell Biology to Tissue Engineering

MCT1-knockout mice present morphological alterations in the testis, sex hormones dysregulation and arrested spermatogenesis

Bernardino R.L.[1], D'Souza W.N.[2], Rato L.[3], Rothstein J.L.[2], Dias T.R.[1,3,4], Chui D.[2], Wannberg S.[2], Alves M.G.[1] and Oliveira P.F.[1,5,6]

[1]Department of Microscopy, Laboratory of Cell Biology, Institute of Biomedical Sciences Abel Salazar (ICBAS) and Multidisciplinary Unit for Biomedical Research (UMIB), University of Porto, Portugal, [2]Amgen Inc., Thousand Oaks, CA, USA, [3]University of Beira Interior, Covilhã, Portugal, [4]LAQV/REQUIMTE - Laboratory of Bromatology and Hydrology, Faculty of Pharmacy, University of Porto, Portugal, [5]Department of Genetics, Faculty of Medicine, University of Porto, Portugal, [6]i3S-Instituto de Investigação e Inovação em Saúde, Universidade do Porto, Portugal
pfobox@gmail.com

Monocarboxylate transporters (MCTs) are important lactate transporters expressed in mammalian cells. In testis, the lactate is produced by the Sertoli cells and transported to germline cells. It has been teported that MCTs play a pivotal role in testis energy metabolism, essentially MCT4, but nothing is known about the role of MCT1 in testis and male fertility. The principal metabolic substract of germline cell is lactate. MCT1 is the main responsible for the lactate uptake by germ cells. The main purpose of this study was to explore the role of MCT1 in male reproduction.

Conditional Knockout MCT1 (cKO) mice were used for study of testicular morphology, morphometric data evaluation and analysis of sperm parameters by stained with hematoxylin and eosin and visualization in the optical microscope. Steroid hormones measurement, namely testosterone and 17β-estradiol levels were determined using ELISA commercial kits.

cKO animals show a decrease in gonadosomatic index, testis weight and seminiferous tubular diameters. Deletion of MCT1 causes morphological changes in seminiferous tubules and Sertoli cells, as well as failure in spermatogenesis with depletion of germ cells and absence of spermatozoa. cKO mice also present dysregulation in sex hormones, with a decrease in serum 17β-estradiol levels.

MCT1 is essential for the normal occurrence of spermatogenesis and for testicular morphology. cKO mice presented spermatogenesis arrest and compromised fertility. This study demonstrates the crucial role of MCT1 for spermatogenesis in a first attempt to report some of the molecular mechanisms that may mediate these effects. Nevertheless, further studies are needed to unveil the relevance of MCT1 in male reproduction.

Poster presentation: Session 1. Topic: Tissue Biology. Code: 5943

Histology and Histopathology
From Cell Biology to Tissue Engineering

Aquaglyceroporins expression and glycerol permeability are modulated by estradiol in mouse sertoli cells

Bernardino R.L.[1*], Carrageta D.C.[1*], Silva A.M.[1], Alves M.G.[1], Soveral G.[2,3] and Oliveira P.F.[1,4,5]

[1]Department of Microscopy, Laboratory of Cell Biology, Institute of Biomedical Sciences Abel Salazar (ICBAS) and Unit for Multidisciplinary Research in Biomedicine (UMIB), University of Porto, Porto, Portugal, [2]Research Institute for Medicines (iMed.ULisboa), Faculty of Pharmacy, Universidade de Lisboa, Lisboa, Portugal, [3]Department of Bioquímica e Biologia Humana, Faculty of Pharmacy, Universidade de Lisboa, Lisboa, Portugal, [4]Department of Genetics, Faculty of Medicine, University of Porto, Porto, Portugal, [5]Instituto de Investigação e Inovação em Saúde (i3S), Universidade do Porto, 4200-135 Porto, Portugal

*These authors contributed equally.

pfobox@gmail.com

Metabolic diseases are related with severe fertility problems, partly due to increased aromatization of androgens to estrogens. Elevated levels of 17β-Estradiol (E2) are known to cause alterations on normal development of germ cells, compromising spermatogenesis. Spermatogenesis is dependent on Sertoli cells (SCs) function, since these cells ensure an adequate environment inside the seminiferous tubule. Herein, we determined the impact of elevated levels of E2 on aquaglyceroporins (AQPs) expression and glycerol permeability in mouse SCs (mSCs, TM4 cell line).

The expression of AQP3, AQP7, AQP9, and AQP11 were identified by RT-PCR and immunofluorescence techniques. Then, the expression was evaluated by qRT- PCR. Glycerol permeability was evaluated by stopped flow light-scattering.

We were able to identify for the first time the expression of AQP3, AQP9 and AQP11 in mouse testis and mSCs. AQP9 was about six times more expressed than AQP3 and sixty-four times more expressed than AQP11 in these cells. High E2 levels caused a decrease of AQP9 mRNA levels and had no influence on AQP3 expression. On the other hand, high E2 levels led to an increase in AQP11 mRNA levels. AQPs are the main transporters of glycerol in physiological conditions, where AQP9 and AQP3 are responsible for transmembrane transport and AQP11 for endoplasmic reticulum and lipid droplets transport. In addition to downregulating the expression of AQP9, E2 also decreased cellular glycerol permeability.

E2 is a regulator of mSCs physiology by modulating AQP9 expression and the permeability to glycerol, which has been referred as crucial player for the homeodynamics of these testicular cells and for spermatogenesis. Thus, as glycerol is essential for spermatogenesis by controling the blood-testis barrier permeability, it's evident that alterations caused by E2 in glycerol permeability can be related to infertility problems.

Poster presentation: Session 1. Topic: Tissue Biology. Code: 5944

Histology and Histopathology
From Cell Biology to Tissue Engineering

CFTR modulates aquaporin-mediated glycerol permeability in mouse sertoli cells

Carrageta D.F.[1*], Bernardino R.L.[1*], Alves M.G.[1], Soveral G.[2,3] and Oliveira P.F.[1,4,5]

[1]Department of Microscopy, Laboratory of Cell Biology, Institute of Biomedical Sciences Abel Salazar (ICBAS) and Unit for Multidisciplinary Research in Biomedicine (UMIB), University of Porto, Porto, Portugal, [2]Research Institute for Medicines (iMed.ULisboa), Faculty of Pharmacy, Universidade de Lisboa, Lisboa, Portugal, [3]Department of Bioquímica e Biologia Humana, Faculty of Pharmacy, Universidade de Lisboa, Lisboa, Portugal, [4]Department of Genetics, Faculty of Medicine, University of Porto, Porto, Portugal, [5]Instituto de Investigação e Inovação em Saúde (i3S), Universidade do Porto, Porto, Portugal

*These authors contributed equally.

pfobox@gmail.com

The cystic fibrosis transmembrane conductance regulator (CFTR) is an anion channel mainly responsible for the direct transport of HCO_3^- and Cl^-, which is crucial for pH regulation and fluid homeodynamics among the male reproductive tract. The absence or malfunction of CFTR results in cystic fibrosis, the most common lethal disease among Caucasians. Due to the wide expression and importance of CFTR, the male reproductive tract is highly affected by cystic fibrosis, resulting in a dysfunctional fluid homeodynamics and consequently in male infertility. Although CFTR is not permeable to water and glycerol, this channel acts as a molecular partner of aquaporins (AQPs) and directly regulates its function. Herein, we determined the role of CFTR on AQPs-mediated glycerol permeability in mouse Sertoli cells (mSCs).

The expression of CFTR in mSCs (TM4 cell line) was identified by Western Blot and Immunofluorescence techniques. Then, mSCs were treated with CFTR-inh172, a specific CFTR inhibitor, and glycerol permeability of mSCs was evaluated by stopped flow light-scattering technique.

We were able to identify the expression of CFTR in the plasma membrane of mSCs. Then, we observed that the inhibition of CFTR by its specific inhibitor, CFTR-inh172, decreased glycerol permeability in mSCs by 29.5% when compared with the control group.

CFTR is able to modulate AQP-mediated glycerol permeability in mSCs. As glycerol is essential for the control of blood-testis barrier and its accumulation results in the disruption of spermatogenesis, it is suggested that the malfunction of CFTR and the consequent decrease in glycerol permeability is a potential link between male infertility and cystic fibrosis.

Poster presentation: Session 1. Topic: Tissue Biology. Code: 5945

Histology and Histopathology
From Cell Biology to Tissue Engineering

Deletion of insulin-degrading enzyme impairs testicular morphology in mice

Meneses M.J.[1,2,3], Borges D.O.[1], Dias T.R.[2,4], Martins F.O.[1], Oliveira P.F.[2,5,6], Macedo M.P.[1,7,8] and Alves M.G.[2]

[1]CEDOC – Chronic Diseases Research Center, NOVA Medical School/Faculdade de Ciências Médicas, Universidade Nova de Lisboa, Lisboa, Portugal, [2]Department of Microscopy, Laboratory of Cell Biology and Unit for Multidisciplinary Research in Biomedicine (UMIB), Institute of Biomedical Sciences Abel Salazar (ICBAS), University of Porto, Porto, Portugal, [3]ProRegeM PhD Programme, NOVA Medical School/Faculdade de Ciências Médicas, Universidade Nova de Lisboa, Lisboa, Portugal, [4]Universidade da Beira Interior, Covilhã, Portugal, [5]I3S - Instituto de Investigação e Inovação em Saúde, University of Porto, Porto, Portugal, [6]Department of Genetics, Faculty of Medicine, University of Porto, Portugal, [7]Portuguese Diabetes Association - Education and Research Center (APDP-ERC), Lisbon, Portugal, [8]Department of Medical Sciences, University of Aveiro, Portugal

alvesmarc@gmail.com

Insulin-degrading enzyme (IDE), also known as insulysin, is a zinc metalloprotease responsible for insulin degradation. Therefore, *Ide* knockout (KO) mice present increased insulin levels. It is known that insulin dysregulation has a major impact in male fertility. Yet, the specific role of IDE in male reproductive function remains to be unveiled. Hence, we proposed to study the possible role of IDE in the male reproductive potential. Taking in consideration that insulin mediates key events for spermatogenesis, we hypothesized that IDE is associated with sperm quality.

Eighteen C57BL/6N mice were distributed in three groups according to the genotype: wild type (WT), heterozygous and KO male mice for *Ide*. Spermatozoa were collected from the cauda of epididymis and sperm parameters (concentration, viability, morphology and motility) were evaluated. Sperm viability was analyzed with eosin-nigrosin staining and sperm morphology was evaluated with Papanicolaou staining. Sperm concentration was assessed through a Neubauer chamber. Overall testicular morphology and the seminiferous tubules diameter were evaluated through hematoxylin and eosin staining. Gonadosomatic index, that indicates the gonad mass as a proportion of the total body mass, was also calculated.

Heterozygous and *Ide* KO mice presented normal sperm motility and concentration but decreased sperm viability. Interestingly, *Ide* KO mice presented an increase in sperm with abnormal morphology while heterozygous mice presented a decrease when compared to both WT and *Ide* KO mice. We also observed a decrease in the gonadosomatic index of *Ide* KO mice when compared to both WT and heterozygous mice, which was consistent with a decrease in seminiferous tubules diameter.

These results demonstrate that *Ide* KO mice have impaired sperm quality related with morphological changes in the testes. Overall, our data provide evidence that IDE plays an important role in determining male reproductive potential.

This work was funded by FEDER funds POCI - COMPETE 2020 – Programa Operacional para a Competitividade e Internacionalização no Eixo 1 (Project POCI-01-0145-FEDER-007491) and by "Fundação para a Ciência e a Tecnologia" – FCT to MJM (PD/BD/114256/2016); TRD (SFRH/BD/109284/2015); PFO (PTDC/BBB-BQB/1368/2014 and IFCT2015); MPM (PTDC/DTP-EPI/0207/2012 and PTDC/BIM-MET/2115/2014); MGA (PTDC/BIM-MET/4712/2014 and IFCT2015); iNOVA4Health (UID/Multi/04462/2013); and UMIB (PEst-OE/SAU/UI0215/2014).

Poster presentation: Session 1. Topic: Tissue Biology. Code: 5946

Histology and Histopathology
From Cell Biology to Tissue Engineering

Assessment of the expression of obesity-related genes in human sertoli cells and spermatozoa

Pereira S.C.[1,2,3], Martins A.D.[2,3], Moreira B.P.[2,3], Bernardino R.L.[2,3], Barros A.[4,5,6], Paiva S.[7], Sousa M.[2,3,6], Oliveira P.F.[2,3,4,5] and Alves M.G.[2,3]

[1]School of Sciences, University of Minho, Braga, Portugal, [2]Unity of Multidisciplinary Research in Biomedicine, Institute of the Biomedical Sciences Abel Salazar, University of Porto, Portuga, [3]Department of Microscopy, Laboratory of Cell Biology, Institute of the Biomedical Sciences Abel Salazar-University of Porto, Portugal, [4]i3S - Instituto de Inovação e Investigação em Saúde, University of Porto, Portugal, [5]Department of Genetics, Faculty of Medicine, University of Porto, Portugal, [6]Centre for Reproductive Genetics Professor Alberto Barros, Porto, Portugal, [7]Centre of Molecular and Environmental Biology, Department of Biology, University of Minho, Braga, Portugal
alvesmarc@gmail.com

Spermatogenesis is the process where the male gametes develop from germ cell to mature spermatozoa. This process is directly associated with Sertoli Cells (SCs) metabolism, since they provide the physical and metabolic support to developing germ cells. Metabolic disorders, such as obesity, are known to alter human SCs metabolism and, therefore, sperm quality. Obesity- related genes and epigenetic factors have been pointed out as causes for an overweight/obese phenotype, suggesting that children born from obese parents could have a genetic predisposition to develop metabolic disorders themselves. Herein we proposed to identify the expression of specific obesity-related genes in human SCs and human sperm cells through polymerase chain reaction (PCR) techniques. Furthermore, we hypothesized that the expression of obesity-related genes in human spermatozoa could respond to the body mass index (BMI) of the men. Moreover, we proposed that human spermatozoa and human Sertoli Cells could also express the proteins associated with these genes.

Human SCs were attained from human testicular biopsies from 6 men subjected to fertility treatment due to anejaculation. Sperm samples were attained from 100 men seeking for fertility treatment and with known BMI. Sperm parameters (morphology, viability and motility) were determined. The mRNA abundance of the melanocortin-4 receptor (MC4R), Glucosamine-6-phosphate deaminase 2 (GNPDA2), and Fat mass and Obesity (FTO) genes were evaluated by quantitative PCR (qPCR) in human SCs and spermatozoa. The protein expression of MC4R, GNPDA2, Transmembrane protein 18 (TMEM18) and FTO were identified by Western-Blot and Immunofluorescence techniques in human SCs and spermatozoa.

Our results showed that the expression of the studied obesity-related genes was not correlated with the BMI of men. Similarly, we could not identify a clear correlation between the rise of BMI values and a decreased sperm quality as revealed by analysis of the sperm parameters. However, we identify, for the first time, the presence of GNPDA2, MC4R, TMEM18, and FTO in human spermatozoa. We also identify, for the first time, the presence of MC4R and TMEM18 in human SCs. We further confirm that FTO is present in human SCs, as previously reported. Further correlations between obesity-related genes expression and fertility outcomes (i.e. biochemical pregnancy, fertility success) will be studied

Although it was not established a correlation between the expression of obesity-related genes and the BMI of the men in human spermatozoa, we cannot disregard that these genes interfere with several cellular functions. The presence of obesity-related genes in human spermatozoa and human SCs elicits a possible role in molecular mechanisms by which overweight/obesity promote infertility and subfertility in males.

Poster presentation: Session 1. Topic: Histology of Organs and Systems. Code: 5659

Histology and Histopathology
From Cell Biology to Tissue Engineering

Retinal differentiation in an altricial avian species, the zebra finch (*Taeniopygia guttata*): an immunohistochemical study

Álvarez-Hernán G.[1], Hernández-Núñez I.[1], Rico-Leo E.M.[2], Marzal A.[1], de Mera-Rodríguez J.A.[1], Rodríguez-León, J.[1], Martín-Partido G.[1] and Francisco-Morcillo, J.[1]

[1]Departamento de Anatomía, Biología Celular y Zoología, Facultad de Ciencias, Universidad de Extremadura, Badajoz, España, [2]Departamento de Bioquímica y Biología Molecular y Genética, Facultad de Ciencias, Universidad de Extremadura, Badajoz, España

Retinal development has been intensively studied in the chicken (*Gallus gallus,* a precocial bird species) as a model for investigating the mechanisms that coordinate the morphogenesis, histogenesis, and neuronal and glial differentiation. A previous study carried out in our laboratory (Álvarez-Hernán et al., 2018) has shown that some maturational features during visual system development occur at later stages in altricial bird species than in *G. gallus*. Furthermore, some features of immaturity, such as abundant mitotic activity, are observable in the retina of altricial hatchlings.

In the present study, a total of 28 zebra finch (*Taeniopygia guttata*) embryos from stage 24 (St24) (Murray et al., 2013) to St45 have been used. Immunohistochemical techniques have been carried out in retinal cryosections.

We have detected the first TUJ1-positive neuroblasts in the vitreal surface of the neuroblastic layer (NbL) at St24, coinciding chronotopographically with the appearance of the first PCNA-negative nuclei. The first Isl1-positive differentiating ganglion cells were located in the same region at St25. The onset of visinin-immunoreactivity was detected in the scleral region of the NbL at St28, coinciding temporo-spatially with the first PCNA-negative nuclei detected in this region. At St34, Prox-1-immunoreactive neuroblasts showing migratory morphology were firstly detected, suggesting that horizontal cell genesis started at this stage. All these maturational features were first detected in the central retina and, as development progressed, they spread to the rest of the retinal tissue following central-to-peripheral and vitreal-to-scleral gradients. At St45 abundant PCNA- and pHisH3-immunopositive elements were detected in the *T. guttata* retina, even in the regions where the layering was complete.

Retinal developmental features in *T. guttata* occurred later in development than in *G. gallus,* indicating faster development for precocial bird species. Furthermore, the *T. guttata* retina was not completely developed at hatching and abundant mitotically active precursor cells were found, suggesting that retinal neurogenesis was intense at perinatal stages. Therefore, *T. guttata* retina could be a powerful model system to study different aspects of neural development and regeneration in vertebrates.

This work was supported by grants from the Spanish Ministerio de Ciencia y Tecnología (BFU2007-67540), Ministerio de Economía y Competitividad (CGL2015-64650P) and Junta de Extremadura (PRI06A195, IB16121, GR18114; IB18113).

Poster presentation: Session 1. Topic: Histology of Organs and Systems. Code: 5677

Histology and Histopathology
From Cell Biology to Tissue Engineering

Effects of an anti-gonadotrophin releasing hormone vaccine on the morphology and structure of bull testes

Monleón E.[1,2,3], Noya A.[3,4], Garza M.C.[2], Ripoll G.[3,4] and Sanz A.[3,4]

[1]Dpartamento de Anatomía e Histología Humanas, Universidad de Zaragoza, Zaragoza, Spain, [2]Centro de Encefalopatías y Enfermedades Transmisibles Emergentes, Zaragoza, Spain, [3]Instituto Agroalimentario de Aragón, IA2 (CITA-Universidad de Zaragoza), Zaragoza, Spain, [4]Centro de Investigación y Tecnología Agroalimentaria (CITA) de Aragón, Zaragoza, Spain.

Vaccination against gonadotrophin-releasing hormone (GnRH) is used as an alternative to surgical castration for the purposes of reducing pain and distress in the animals. Currently, no anti-GnRH vaccine has been authorized for use in cattle in the European Union. The aim of the present study was to assess the effect of an anti-GnRH swine-specific vaccine (Improvac®, Zoetis, USA) on the morphology and structure of bull testes.

Sixteen calves were distributed into 2 equally sized groups depending on their LW at the beginning of study: light (172.9±30.00 kg) and heavy (323.8±37.79 kg). Half of the calves in each group were randomly selected to serve as the control (C) and vaccinated (VA) group. The calves were vaccinated at days 1, 21 and 104 of the experimental period. At slaughter (day 164), testes were weighed and measured, and then tissue samples were collected and fixed in formalin. Histological and immunohistochemical studies (anti-vimentin mAb and anti-human Ki-67 mAb, Dako Denmark A/S) were performed on the testes to measure the diameter of the seminiferous tubules and assess the testicular cell populations.

Hypoplasia of the testes was found to be associated with vaccination, since the weight, diameter and perimeter measurements, and volume of the testes were lower in VA calves than in C calves ($P<0.0001$). The C and HEAVY calves exhibited higher diameters of the seminiferous tubules than the VA and LIGHT calves ($P<0.001$ and $P<0.05$ respectively).

All C calves exhibited fully developed spermatogenesis. In contrast, the testes of all the VA calves except two exhibited a complete absence of spermatogenesis with a predominance of Sertoli cells in the seminiferous epithelium. Two of the VA calves (from the HEAVY group) exhibited normal microscopic features consistent with active spermatogenesis that was similar to that described in C calves. In the VA calves except the two from the HEAVY group, the seminiferous epithelium was immunolabelled with vimentin almost in its entirely, which indicated that it was largely composed of Sertoli cells. Only a few vimentin-negative cells, which corresponded to spermatogonia, were observed in the basal seminiferous epithelium; moreover, only a few of these spermatogonia were mitotically active, as indicated by Ki-67 immunolabelling. In C and the 2 VA calves from the HEAVY group, vimentin-positive Sertoli cells were evenly distributed between the spermatogenic cells, which comprised the majority of the cells. Ki-67 antigen staining revealed the presence of a large number of active spermatogonia and spermatocytes.

Our results demonstrate that immunization of male calves against GnRH with commercially available Improvac®, which was originally developed for use in boars, severely affects testicular morphology and structure. The effect of Improvac® is more pronounced and consistent in calves vaccinated at a low LW than at a heavy LW, which suggests that vaccination is more effective when calves are vaccinated prior to puberty.

Poster presentation: Session 1. Topic: Histology of Organs and Systems. Code: 5682

Histology and Histopathology
From Cell Biology to Tissue Engineering

Ultrastructural study of pig liver regeneration following ablation with irreversible electroporation

Iruzubieta P.[1], Gracia-LLanes J.[1], Monleón E.[1], Mejía E.[2], Castiella T.[2], Hernáez A.[3], Güemes A.[3], López-Alonso B.[4], Sarnago H.[4], Lucía O.[4], Burdío J.M.[4], Junquera C.[1]

[1]Departamento de Anatomía e Histología Humanas. [2]Departamento de Anatomía Patológica, Medicina Legal y Forense y Toxicología. Universidad de Zaragoza, Zaragoza, España, [3]Hospital Clínico Universitario Lozano Blesa, Zaragoza, España, [4]Departamento de Ingeniería Electrónica y Comunicaciones, Universidad de Zaragoza, España

Irreversible electroporation (IRE) provides an increase in cell membrane permeability following exposure to high-voltage that leads to cell death. IRE has emerged as a promising tool for treatment of multiple diseases including hepatic cancer. However, tissue regeneration mechanisms following IRE ablation have not been investigated yet. In a previous work, we analyzed pig liver tissue response following IRE ablation. Now we try to determine the cellular events that take place in the process of liver regeneration at ultrastructural level. Our findings suggest IRE ablation as a good model to study liver regeneration.

In this study, 4 pigs (40 kg) were treated using parallel-plate electrodes separated by the width of the liver (i.e. 1-1.5 cm) and applying 100 pulses of 100 μs, with a frequency of 0.5 Hz to avoid thermal damage, and 2000 V/cm electric field intensity. Post-operative biopsies were performed at 7 and 14 days after the stimulation. Samples were routinely processed for transmission electron microscopy visualization.

Seven days after electroporation, numerous activated hepatic stellate cells were positioned in the same direction within a collagen-rich extracellular matrix. These cells show long cytoplasmic projections, voluminous nuclei with peripheral heterochromatin and displaced nucleoli near the nuclear envelope. Cytoplasmic projections contact with neighbor cells originating a complex net. Abundant rough endoplasmic reticulum, polyribosomes and cortical actin filaments were found. Some of these cells show activated centrioles migrating from their usual perinuclear situation to cell membrane, where they form a primary cilium. Next to these cells, we found another, less frequent, cell population composed by rounded or oval cells with more electrondense cytoplasm and abundant polyribosomes. These cells show fine projections that contact with stellate cells.

Both types of cells stayed around of new-formed biliary ducts composed by cells with voluminous nuclei, numerous polyribosomes and small reticulum cisternae; cellular junctions begin to be established between these cells. Formation of small blood vessels is also observed. These new blood vessels are originated from cells with similar features that those forming biliary ducts. Hepatic lobules appeared later and hepatic cells showed some immature characteristics, like round scarce mitochondria, even fourteen days after IRE.

Hepatic stellate cells show primary cilia that may initiate cell differentiation through external signals. Hepatic regeneration following IRE ablation is sequential: biliary ducts and blood vessels are already formed at seven days while newborn hepatocytes appear later, around fourteen days after IRE.

Poster presentation: Session 1. Topic: Histology of Organs and Systems. Code: 5683

Histology and Histopathology
From Cell Biology to Tissue Engineering

Remodelling of liver tissue after irreversible electroporation in porcine

Monleón E.[1], Castiella T.[2], Mejía E.[2], Gracia-LLanes J.[1], Iruzubieta P.[1], Junquera C.[1], Hernáez A.[3], Güemes A.[3], López-Alonso B.[4], Sarnago H.[4], Burdío J.M.[4] and Lucía O.[4].

[1]Departamento de Anatomía e Histología Humanas, [2]Departamento de Anatomía Patológica, Medicina Legal y Forense y Toxicología, Universidad de Zaragoza, Zaragoza, España, [3]Hospital Clínico Universitario Lozano Blesa, Zaragoza, España, [3]Dpto. de Ingeniería Electrónica y Comunicaciones. Universidad de Zaragoza, Zaragoza, España

Irreversible electroporation (IRE) is an ablation technique that uses electric currents to cause cell death. This is a promising technique that is already being used to treat different tumors such as liver tumors. The aim of this study is to assess the tissue regeneration after ablation with IRE in normal porcine liver.

Three female pigs were included in the present study. IRE was performed under general anaesthesia, using electrodes and generator manufactured by the Group of Power Electronics and Microelectronics of the University of Zaragoza. The IRE treatment was composed of 100 pulses with 100-µs length, and 2000-kV/cm applied electric field. Liver samples were collected from the centre of the electroporated area 1, 7 and 14 days after IRE ablation. From each pig, liver samples from not ablated areas were used as control. Tissue samples were fixed in formalin and processed according to standard histopathological procedures. Results from histological examination has been previously described (Lopez-Alonso et al., 2019). In addition, tissue sections were stained with Masson`s trichrome and reticulin stains, and processed for immunohistochemistry using the following primary monoclonal antibodies: anti-human hepatocytes, anti-human cytokeratin 7 (CK 7) as a marker of bile ducts and anti-human smooth muscle actin (alpha-SMA) as a marker of hepatic stellate cells. All antibodies were obtained from Dako (Denmark).

One day after IRE, the characteristic hexagonal architecture of liver appeared preserved. Within the liver lobules, positive hepatocytes were arranged radially from the central vein, with collapsed hepatocytes in the centrilobular area. Reticulin network was also preserved and alpha-SMA positive cells with a dendritic configuration were quite evenly distributed within the lobules. Hepatic lobules were delimited by connective tissue septa where CK-7 positive biliary epithelial cells (with an anormal shape), alpha-SMA positive vascular muscle cells and a few alpha-SMA positive stromal cells were observed. Seven days after IRE, the characteristic liver architecture completely disappeared. Most of the IRE area was positive for alpha-SMA immunostaining but negative for hepatocytes. alpha-SMA linear immunostaining and connective tissue (revealed by Masson's Trichrome and reticulin staining) was surrounding irregular groups of cells forming ducts (Ck-7 positive) or linear structures. Fourteen days after IRE, the liver architecture and the immunostaining pattern were essentially similar to the control in all the IRE area, except the subscapular area. Generally, septa and portal tracts appeared slightly thickened with more connective tissue, alpha-SMA positive cells and CK-7 positive bile ducts. The subscapular area was similar to that describe for the liver 7 days after IRE.

In contrast to previous studies, our preliminary results show that in liver ablation by IRE the structure of the extracellular matrix (mainly the reticulin scaffold) is not conserved, but is produced during the regeneration process. However, there is a rapid hepatic tissue restoration as fourteen days after ablation the IRE zone was almost completely regenerated.

Lopez-Alonso et al. Histopathological and Ultrastructural Changes after Electroporation in Pig Liver Using Parallel-Plate Electrodes and High-Performance Generator. Sci Rep. 2019 25;9(1):2647

Poster presentation: Session 1. Topic: Histology of Organs and Systems. Code: 5743

Histology and Histopathology
From Cell Biology to Tissue Engineering

Normal human thyroid gland and primary cilium: morphometric analysis

Utrilla Alcolea J.C., González González A., Vázquez Román V., Fernández Santos J.M. and Martín Lacave I.

Department of Normal and Pathological Cytology and Histology, School of Medicine, University of Seville, Spain

Thyroid histopathology has been widely studied due to its medical importance and the striking morphological changes it undergoes. However, establishing the physiological substrate on which the pathological alterations develop can contribute for their better understanding. On this matter, the aim of this work is to carry out a detailed study of thyroid morphology at a physiological level, including a relatively novel aspect: the presence of primary cilia in thyrocytes.

Four human thyroid samples were used in the present research: 2 obtained from families with hereditary medullary thyroid carcinoma who underwent prophylactic thyroidectomy, and 2 normal thyroid samples adjacent to papillary thyroid carcinomas. The patients were two men (49 and 51 years old) and two women (25 and 61 years old). Consecutive 5 μm-thickness paraffin thyroid sections were obtained following the standard procedure. The double immunofluorescence staining was carried out according to the following procedure: a monoclonal anti-acetylated α-tubulin antibody that labels the axoneme was applied to visualize primary cilia, followed by Cy3-labeled donkey anti-mouse IgG secondary antibody (red), while epithelium was demonstrated with a polyclonal anti-E-cadherin antibody and subsequently with Cy2-labeled donkey anti-rabbit IgG antibody (green). Finally, DAPI was added for nuclei counterstaining. Corresponding controls of immunospecificity were performed.

Fifty thyroid follicles per sample were randomly selected and subjected to follicular perimeter, epithelial height, nuclei counting and primary cilia length and frequency measurements. These processes were performed via image analysis software: Image-Pro Plus 7.0 and ImageJ 1.8.0. Epithelial height was obtained by using the following mathematical formula:

In normal thyroid glands, we have found no linear relationship between the height of the follicular epithelium and the size of the thyroid follicle, having most thyroid follicles an epithelial height ranging from 2 to 4 μm, and a follicular perimeter ranging from 100 to 250 μm. We have analysed cilia frequency and length in relation to either epithelial height or follicular perimeter. The mean percentage of ciliated follicular cells in normal thyroid is 36.97±16.08%. No relationship of this variable with epithelial height or follicular perimeter is observed. The average cilia length is 1.4348±0.4284 μm. There is no relationship between the epithelial height of a follicle and the length of its primary cilia. On the other hand, there is a positive non-significant trend between follicular size and cilia length.

From our results, it can be concluded there is a great heterogeneity of thyroid follicles in normal thyroid glands, without existing a linear relationship between epithelial height and follicular perimeter. We have also observed that significant reduction in average epithelial height occurs with aging.

Moreover, we have found no correlation between frequency of ciliated follicular cells and follicular epithelial height or perimeter. Likewise, cilia length is not related to epithelial height. However, it seems to be a non-significant tendency for primary cilia to become longer as follicular size increases.

Poster presentation: Session 1. Topic: Histology of Organs and Systems. Code: 5744

Histology and Histopathology
From Cell Biology to Tissue Engineering

Primary cilium expression in pendred syndrom

Vázquez Román V.[1], Rubio Díaz A.[1], Utrilla Alcolea J.C.[1], Fernández Santos J.M.[1], Martín Lacave I.[1] and Cameselle Teijeiro J.M.[2]

[1]Department of Normal and Pathological Cytology and Histology, Faculty of Medicine, University of Seville, Spain, [2]Department of Pathology, Clinical University Hospital, Universidad de Santiago, Santiago de Compostela, Spain

The primary cilium is a highly specialized organelle which emerges from the apical surface of the vast majority of cell types in different mammals, follicular cells included. Because of its location, it plays a key role in normal development and function of the thyroid gland, which is notably affected by Pendred's syndrome. Pendred's syndrome is an autosomal recessive disorder defined by congenital deafness, goiter and a partial defect in iodine organification, caused by mutations in SLC26A4/PDS gene. Since a defect in the primary cilium lead to several diseases called ciliopathies, and primary cilia maybe essential for the thyroid function, the aim of this study is to know whether if Pendred's syndrome is also a ciliopathy. For this reason, we analyze different histopathologic patterns in Pendred's syndrome thyroid glands, studying both the frequency and length of the primary cilium, to understand how this organelle is expressed within this disorder.

Four human samples obtained from Pendred's syndrome thyroid gland biopsies were analyzed. The samples were fixed in 4% neutral buffered formalin, embedded in paraffin, sectioned at 4-5 mm and mounted on silane-coated glass slides. For the immunofluorescence (IF) study, an antigen retrieval step was performed. As primary antibody, a monoclonal anti-acetylated a-tubulin, which labels the axoneme, was used, followed by Cy3-labeled donkey anti-mouse IgG secondary antibody. When double IF was performed, the slides were then incubated with polyclonal rabbit anti-E-cadherin antibody and, subsequently, with Cy2-labeled microscope (Olympus, BX50). Primary cilia lengths were morphometrically assessed using the Image Pro-Plus 7.0 software (Infaimon).

Pendred's syndrome thyroid glands show different morphologic patterns. The most representative are areas of normal thyroid follicles, inflammatory zones with abundant stroma between follicles, and follicular adenoma areas with micro-follicular components. According to the morphometric analysis of the primary cilium, the mean length in normal thyroid follicles is 2.00±0.64 mm, with a 74±12% of ciliated thyrocytes. The stromal follicular pattern is 1.49±0.60 mm long, and a 74±10% of ciliary frequency. Finally, tumor mass areas show the shortest cilia, with a length of 1.03±0.30 mm and a proportion of ciliated cells of 64±11%.

In the present study, we demonstrate that despite the variety of follicular patterns that exist in Pendred's syndrome thyroid glands, the frequency of the primary cilium does not show significant differences between different histopathologic areas. However, we found significant differences in relation to the length of primary cilia among areas.

Acknowledgements. Consejería de Economía, Conocimiento, Empresas y Universidad. Junta de Andalucía (CTS 439/2017).

Poster presentation: Session 1. Topic: Histology of Organs and Systems. Code: 5745

Histology and Histopathology
From Cell Biology to Tissue Engineering

Study of primary cilia in rat exocrine glands

Vázquez Román V., Cimpean A., Fernández Santos J.M., Utrilla Alcolea J.C. and Martín Lacave I.

Department of Normal and Pathological Cytology and Histology Faculty of Medicine, University of Seville, Spain

The primary cilium is an organelle that projects from the surface of most mammal cells, with only a few micrometers in length and, generally, unique. It is a specialized cellular compartment that functions as a dual sensor, mechanoreceptor and chemoreceptor. In recent years, the primary cilium has emerged as a hot topic in research due to its great complexity and wide range of pathological phenotypes resulting from its deficiency or disturbance. The ciliopathies are related to diabetes, Alzheimer's disease or obesity, pathologies that are of great concern for public health. This study describes the location of the primary cilium by immunofluorescence in various organs and exocrine glands. In addition, the normal pattern of the primary cilium in the pancreas has been analyzed by morphometry, with the aim of relating its dynamic structure and sensory function.

The experimental study carried out consists in performing immunofluorescence histological techniques on rat samples of: pancreas, liver, trachea, esophagus, parotid, submandibular, sublingual glands and kidney samples as controls. We used the primary antibody anti-α acetylated tubulin (Sigma-Aldrich, Germany) coupled with the secondary antibody Cy3 (Jackson, UK) and the anti- E Cadherin (Santa Cruz Biotechnology, USA) primary antibody coupled with the secondary antibody Cy2 (Jackson, UK), as well as DAPI. The samples were observed through a fluorescence microscope (Olympus, BX-50). The analysis was carried out with the ImageJ 1.8.0 software, and the statistical significance was determined using the T student test.

Primary cilium has been located in the bile ducts and parenchyma of the liver; submucose cells of the trachea and esophagus; parenchyma and a few ducts of salivary glands. Moreover, after analyzing the primary cilium in pancreas tissue, we obtained the following mean values: intralobular pancreas ducts had a length of 0.8±0.3 μm; the lengths in interlobular ducts were 1.5±0.6 μm and, finally, the mean length of the primary cilium in Langerhans islets cells was 1.76±0.51 μm.

We found coincidence between our own findings with respect to the location of the primary cilium in different exocrine glands referred in literature. Furthermore, we found statistically significant differences in the mean cilium length among ducts of different sizes, as well as between ducts and Langerhans islets cells. However, to further corroborate the sensory function of the primary cilium more research is still needed.

Acknowledgements. Consejería de Economía, Conocimiento, Empresas y Universidad. Junta de Andalucía (CTS 439/2017)

Poster presentation: Session 1. Topic: Histology of Organs and Systems. Code: 5776

Histology and Histopathology
From Cell Biology to Tissue Engineering

Comparative histology of pacinian sensory receptors of the fingers and toes of older persons

Gómez-García A.[1], Valverde-Navarro A.A.[2], Salvador-Clavell R.[1], Mata M.[1,3], Sancho-Tello M.[1], Ruiz-Sauri A.[1], Oliver-Ferrándiz M.[1], Carda C.[1,4] and Martín de Llano J.J.[1]

[1]Department of Pathology and Health Research Institute of the Hospital Clínico (INCLIVA), Faculty of Medicine and Dentistry, University of Valencia, Valencia, Spain, [2]Department of Human Anatomy and Embryology, Faculty of Medicine and Dentistry, University of Valencia, Valencia, Spain, [3]Ciberes, Instituto de Salud Carlos III, Spain, [4]Ciber-BBN, Instituto de Salud Carlos III, Spain

Tactile perception is the ability to detect mechanical stimuli applied to the surface of the body. In glabrous skin of hands and feet there are three types of encapsulated mechanoreceptors: Vater-Pacini, Meissner and Ruffini corpuscles. Pacinian corpuscles (PC) are large ellipsoidal structures characterized by a central nerve fiber surrounded by concentrically arranged multilayered cellular lamellae. Human PC structure and distribution have been described for the hands and fingers. Physiological studies have characterized the sensitivity to vibration of hand PC. However, few data have been published about the structure, distribution and sensitivity of the PC of the feet. These data correspond mainly to PC of the plantar surface, and there is a lack of information on PC of the toes. Furthermore, changes of PC sensitivity with ageing have been described for PC of hands and feet, but to our knowledge a relationship of PC histological properties and sensitivity loss has not been established for PC of the toes. The aim of our pilot study was to analyze the number, size, distribution, and morphology of PC of fingers and toes of the same individual to verify if any of these parameters could be related to the loss of sensitivity of feet described with aging.

The distal phalange of the first and second fingers and toes of both hands and feet of two bodies (subject A, female 77 years old; subject B, male 60 years old) donated to science to the department of Human Anatomy and Embryology were investigated. Samples were fixed in neutral buffered formalin, dehydrated and embedded in methyl methacrylate. Polymerized samples were sawed using a diamond wheel, and serial longitudinal sections of the medial region of the phalanges were wet ground, polished, and stained with Stevenel's blue. Sections were observed with a bright field microscope and digital images were recorded. Morphometry analysis of 3 sections from each sample was performed.

A higher amount of PC (about 4 times) was found in the first finger when compared to the second finger. The same trend was observed for the first and second toes, but the ratio was lower (1.5 times). Furthermore, in both individuals the amount of PC was 3 times higher for the first finger when compared with the first toe, while there were not differences when comparing the second finger and toe. A high variability was observed between individuals. Thus, subject A had 4-5 times more PC than subject B when comparing each of the 4 groups of samples (first and second fingers and toes). Several PC of the toes showed an atypical structure characterized by an irregular distribution of the cellular components, just maintaining the concentrically arranged lamellae in some minor zones.

This pilot work shows that PC density and morphology differ in fingers and toes, and that there is a high variability between individuals. Thus, the histological study of the PC of the toes could clarify the involvement of this mechanoreceptor in the loss of sensitivity of feet described with aging.

Poster presentation: Session 1. Topic: Histology of Organs and Systems. Code: 5830

Histology and Histopathology
From Cell Biology to Tissue Engineering

Response of retinal ganglion cells after acute ocular hypertension

Gallego-Ortega A.[1], Valiente-Soriano F.J.[1,2] and Vidal-Sanz M.[1,2]

[1]Departamento of Oftalmología, Murcia University and IMIB-Arrixaca, Murcia, Spain, [2]OFTARED, ISCIIII, Spain

Glaucoma is one of the most ocular frequent pathologies that leads to blindness in the population. For this reason, numerous experimental models have been devised to better understand the physiopathology of the disease. In this study, we have induced an acute ocular hypertension (AOHT) for 90 minutes to study the effects of acute ocular hypertension on the adult albino rat retina, and to analyze retina ganglion cells (RGC) and their intra-retinal axons.

In anaesthetized albino rats, the anterior chamber of the left eye was cannulated with a hydrostatic pressure system, raising the intraocular pressure from 10 mmHG to 75 mmHg, for 90 minutes. We prepared a control group (n=5) and three experimental groups that were analyzed at 3 (n=5), 5 (n=7) or 7 (n=7) days after AOHT. Rats were sacrificed, perfused through the heart briefly with 0.9% NaCl and then with 4% paraformaldehyde in 0.1M PBS, their eyes enucleated and both retinas prepared as wholemounts. The retinas were immunostained with Br3a antibodies and with RT97 antibodies to identify RGCs and the phosphorylated heaviest subunit (200kDa) of the neurofilaments, respectively. Retinas were photographed on a fluorescence microscope, retinal photomontages were constructed, $Brn3a^+$RGCs were counted automatically and isodensity maps were prepared. $RT97^+$RGCs were counted manually and plotted into a retinal map.

There was a progressive loss of RGCs, and by day 7 approximately 66% of the original population had disappeared. RT97-immunoreactivity showed a progressive degeneration of the intra-retinal axons. By 3 days, RT97-immunoreactivity depicted intra-retinal axons, and the signal increased with time up to 7 days after AOHT. RT97-immunoreactivity depicted signs of axonal degeneration such as the presence of beads along the axons, or the presence of balls or maces in place of the RGC soma. Co-expression of RT97 and Brn3a was not found in the same RGCs, and at increasing survival intervals the numbers of $RT97^+$RGCs increased while the numbers of $Brn3a^+$RGCs decreased.

90 minutes of acute ocular hypertension results 7 days later in the loss of approximately 66% of the $Brn3a^+$RGC population. AOHT also causes an anomalous expression of RT97 staining in the axons and somas of the CGRs, which is localized after 3 days and increases, reaching its maximum after 7 days.

Poster presentation: Session 1. Topic: Histology of Organs and Systems. Code: 5872

Histology and Histopathology
From Cell Biology to Tissue Engineering

Morphological and tissue analysis of sea anemones of Tecolutla, Veracruz, Mexico

Valdez-Peralta H.I.[1], Hernández-Calderas I.[1], Cordero-Ramos D.I.[1], Márquez-Ramos J.A.[1], Matadamas-Guzmán F.M.[1], Guerrero-Legarreta I.[2], Segoviano-Ramírez J.C.[3], Del Río Portilla M.A.[4,5] and Guzmán-García X.[1]

[1]Laboratorio de Ecotoxicología, Departamento de Hidrobiología, División de Ciencias Biológicas y de la Salud, Universidad Autónoma Metropolitana Unidad Iztapalapa, Ciudad de México, México, [2]Laboratorio de Macromoléculas, Departamento de Biotecnología, División de Ciencias Biológicas y de la Salud, Universidad Autónoma Metropolitana Unidad Iztapalapa Ciudad de México, México, [3]Unidad de Bioimagen, Centro de Investigación y Desarrollo en Ciencias de la Salud, Universidad Autónoma de Nuevo León, Monterrey, Nuevo León, México, [4]Laboratorio de Genética y Producción Acuática, Departamento de Hidrobiología, División de Ciencias Biológicas y de la Salud, Universidad Autónoma Metropolitana Unidad Iztapalapa, Ciudad de México, México, [5]Laboratorio de Genética Acuícola, Departamento de Acuicultura, División de Oceanología, Centro de Investigación Científica y de Educación Superior de Ensenada, Baja California Norte, México
xochitlguga@gmail.com

Sea anemones are benthic and sessile invertebrates. Taxonomic identification of most sea anemones requires morphophysiological and histological studies for suitable interpretation of the observed characteristics Therefore, it is necessary to apply routine and special techniques that allow a detailed description. Sea anemones represent a unique animal model in biotechnological research, nevertheless there is scarce information on this species, making cumbersome the taxonomic identification. The microscopic anatomy, using histological tools, allows to determine structures that facilitate taxonomic identification, and showing the presence of biocompounds of biotechnological interest. Currently, in Mexico, less than 50 species of anemones from other different regions than Tecolutla, Veracruz have been reported. The aim of this work was to study the morphological structure and microscopic anatomy of the Tecolutla sea anemone, to characterize this species and its biotechnological potential.

Thirty-five organisms were collected in the Tecolutla´s region (Veracruz, Mexico). The organisms were anesthetized to avoid stress by cooling down at 1°C per 10 min period up to 4°C. Subsequently, morphometric parameters were obtained, and morphologically analyzed for its macroscopic characteristics. Tissue analysis was carried out in sections of the pedal disc, column, oral disc and tentacles. The sections were fixed in Bouin solution and stained with H-E, Masson's Trichrome and Mallory's Trichrome. Each preparation was analyzed using a brightfield microscope. The taxonomic species was obtained using the morphological description proposed by Muñoz-González (2013).

The Tecolutla sea anemone has cylindrical shape; the oral disc is composed by 92 tentacles and 90 columnar bands, with the presence of warts. Dimensions were: 22mm oral disc, 13 mm pedal disc and 17 mm column. The longitudinal, basilar and parietobasilar muscle fibers, including collagen and elastin fibers were extensively observed in the pedal disc. Different arrangements of longitudinal and parietobasilar muscle fibers alternated in the column were observed, were collagen and elastin fibers support the gastrovascular cavity, and the sphincter muscle. Cell groups, with characteristics like myoepithelial cells, were also observed. Longitudinal and retractor muscle fibers with collagen fibrils were also observed in the oral disc. Finally, tentacles contained specialized cells, such as spirocysts, holotrichs and basitrichs. According to the morphometric, histological and morphological characters, the collected organisms belong to the genus *Bunodosoma.*

This work evidenced the presence of muscle fibers and the abundance of structural fibers, such as collagen and elastin, in sea anemones from Tecolutla, Veracruz, Mexico. The description of the internal structure of the column and the pedal disc is determinant for the sea anemone taxonomic genus identification. The sea anemones studied presented morphometric, histological and morphological parameters that belong to the genus *Bunodosoma.*

Poster presentation: Session 1. Topic: Histology of Organs and Systems. Code: 5876

Histology and Histopathology
From Cell Biology to Tissue Engineering

Internal structure of the eye of *Macrobrachium sp*. (Linnaeus, 1758) river prawn Actopan, Veracruz, Mexico

Barradas-Barradas J.R.[1], Valero-Pacheco E.[2] and Hernandez-Aguilar M.E.[3]

[1]Veracruzana University, post-graduate program of the institute of Neuroethology, Veracruz, Mexico, [2]Veracruzana University, Hydrobiology Laboratory, Faculty of Biology, Veracruz, Mexico, [3]Veracruzana University, Laboratory of Neuroendocrinology, Brain Research Center, Veracruz, Mexico
barradasbarradas.ricardo@gmail.com

The genus *Macrobrachium sp*, in the Atlantic Ocean, is distributed from South Florida to southern Brazil, including the Gulf of Mexico and the Caribbean Sea. It lives in freshwater waters, has nocturnal habits and is benthic (except in the larval stage). Because of its behavior it requires a sensory system that allows better orientation and detection of physical changes in the environment. The eyes are in charge of vision may be of superposition type, usually present in nocturnal organisms.

The objective of the present study was to describe the internal structure of the eye of the prawn of the Actopan River in Veracruz, Mexico and to determine if the structure of the eye corresponds to the type of superposition.

For this, 20 organisms were captured, desensitized with ice to perform the extraction of the eyes and immediately fixed in Bouin. Then they processed by routine histological techniques and stained with Hematoxylin & Eosin.

As a result, it was obtained that the shrimp omatide is formed by four cellular layers: the cornea, the crystalline lens, the cone wire and the rhabdomoma delimited by a membrane.

In conclusion, the cellular structure of the compound eye that presents the river shrimp is of the superposition type. However, it differs from the ocular structure already described in other arthropods of different habitat, so other staining techniques are needed to determine more detail.

Poster presentation: Session 1. Topic: Histology of Organs and Systems. Code: 5930

Histology and Histopathology
From Cell Biology to Tissue Engineering

Population changes in myoid cells during spontaneous recrudescence after exposure to short photoperiod in Syrian hamster

Beltrán-Frutos E.[1], Martínez-Hernández J.[1], Seco-Rovira V.[1], Serrano-Sánchez M.[1], Salmerón D.[2], Ferrer C.[1] and Pastor L.M.[1]

[1]Department of Cell Biology and Histology and [2]Department of Health and Social Sciences, and CIBER in Epidemiology and Public Health (CIBERESP), Madrid, Spain, IMIB-Arrixaca, School of Medicine, Regional Campus of International Excellence "Mare Nostrum Campus", University of Murcia, Murcia, Spain

The Syrian hamster is a rodent with seasonal reproduction whose testis undergoes modifications after exposure to a short photoperiod. After this process, it undergoes a spontaneous recrudescence stage where an increase in tubular diameter and length takes place, but it is unknown whether the myoid cells that are part of the lamina propria of these tubules undergo changes during this period. Therefore, the aim of this work was to study the quantitative changes and proliferative activity that the population of myoid cells undergo during recrudescence.

We exposed twenty 6 month old animals to a short photoperiod of 8:16 h light–dark. At 16, 19 and 21 weeks, the males exposed to short photoperiod plus the corresponding controls were killed. Animals were distributed into 4 groups: Initial Recrudescence (IR), Advanced Recrudescence (AR), Total Recrudescence (TR) and Control. To detect cell proliferation, the immunohistochemical technique was used, using Proliferation Cell Nuclear Antigen (PCNA) as proliferation marker. Proliferation activity and total number of myoid cells were calculated using a morphometric technique. Appropriate statistical analyses were performed.

Positivity to PCNA in myoid cells was recorded. Significant differences were observed in the proliferation activity between the initial recrudescence group and the other groups, the latter showing lower activity ($p<0.05$). The population of myoid cells increased during the recrudescence, significant so in the TR group ($p<0.05$).

The increase in the proliferative activity of myoid cells at the beginning of the process greatly contributes to the recovery of their population during recrudescence, which would explain the significant increase in the tubular volume between IR and AR.

Funded by GERM 19892/15 from Fundación Séneca CARM.

Poster presentation: Session 1. Topic: Histology of Organs and Systems. Code: 5931

Histology and Histopathology
From Cell Biology to Tissue Engineering

Changes in the expression pattern of connexin-43 during testicular regression due to short photoperiod in the Syrian hámster (*Mesocricetus auratus*)

Seco-Rovira V., Beltrán-Frutos E., Martínez-Hernández J., Serrano-Sánchez M.I., Ferrer C. and Pastor L.M.

Department of Cell Biology and Histology, IMIB-Arrixaca, School of Medicine, Regional Campus of International Excellence "Mare Nostrum Campus", University of Murcia, Murcia. Spain

During testicular regression due to short photoperiod, the Syrian hamster suffers testicular atrophy that leads to spermatogenesis arrest and with the loss of a large number of germ and Leydig cells. In the seminiferous epithelium, connexin-43 is present among Sertoli cells at the Sertoli cell barrier/blood-testis barrier (BTB), among Sertoli and germinal cells as well as in Leydig cells, where it is critical for both spermatogenesis and steroidogenesis. The aim of the present work was to study the possible variation that may take place in the expression of Connexin-43 in both the seminiferous epithelium and in the testicular interstitium during the different phases of testicular regression.

Twelve animals subjected to short photoperiod of 8:16 DL belonging to 3 groups of testicular regression - medium (MR), strong (SR) and total (ST) - and 4 control animals subjected to a normal photoperiod of 12:12 DL were used. Immunohistochemistry was performed for the detection of Connexin-43 in 3 sections of each animal and 25 fields were studied in each of the sections. Each field was subjected to a morphometric study to determine the immunopositive area in both the seminiferous epithelium and the testicular interstitium. In addition, by means of western blot and densitometry, protein expression was determined in the study groups.

Per unit of volume, the expression of Connexin-43 increased significantly during testicular regression with respect to the Control group reaching the highest expression in the SR group. This variation in the expression of Connexin-43 was observed in the seminiferous epithelium, but not in the testicular interstitium. Regarding the expression of total Connexin-43 per testis, it was significantly higher in the MR group with respect to the Control group, decreasing to values significantly lower than the Control in the TR group. Per testicular compartment a significant increase in the MR and SR groups and a decrease in the TR group to values similar to the Control group were observed, in the seminiferous epithelium. On the other hand, in the testicular interstitium there was a significant decrease in the SR and TR groups with respect to the Control group. Using the western blot technique, Conexin-43 was overexpressed in the SR and TR groups with respect to the Control group.

The present study shows that there are changes in the expression of Connexin-43 throughout the process of testicular regression. These variations affect the seminiferous epithelium and the testicular interstitium differently. The seminiferous epithelium is the reason of the increase in total connexin 43 expression observed per unit volume during testicular regression.

Funded by: GERM 19892/15 from Fundación Séneca CARM.

Poster presentation: Session 1. Topic: Histology of Organs and Systems. Code: 5933

Histology and Histopathology
From Cell Biology to Tissue Engineering

Distribution of mucins in human endocervical glands during the endometrial secretory phase

García-Molina F.[1], Seco-Rovira V.[2], Martínez-Hernández J[2]., Beltrán-Frutos E.[2], Ferrer C.[2], Martínez-Díaz F.[2], Pastor-Quirante F[1]. and Pastor L.M.[2]

[1]Departamento de Anatomía Patológica, Hospital General Universitario Reina Sofía Murcia, [2]Department of Cell Biology and Histology, Medical School, IMIB, Regional Campus of International Excellence "Campus Mare Nostrum", University of Murcia, Spain

The nature of cervical mucus secretions is modified during the menstrual cycle, showing different biophysical and biochemical properties throughout the cycle. It is now accepted that cervical mucus is not a homogeneous but a heterogeneous entity, that contains different types of mucus which vary in its proportion throughout the cycle. It has been proposed that specific regions of the endocervical mucosa secrete each of the different mucus types, but it is unknown whether their biochemical composition differs. The present work analyses the secretion in the endocervical glands during the endometrial secretory phase by means of conventional mucin histochemical techniques, in order to determine whether there are differences between the different parts of the endocervical canal as regards the composition of sialomucins, sulfomucins and neutral mucins.

For this purpose, three longitudinal sections of the endocervical canal from the uterus of four women showing endometrium in secretory phase were used: anterior, posterior and middle. The study was carried out under the control of the ethical research committee and the Biobank of the General University Hospital of Elche. The paraffin sections were stained with Alcian Blue pH 2.5 and Alcian Blue pH 1 and Alcian Blue pH 2.5-PAS. The canal was differentiated into three regions for analysis purposes: proximal, middle and distal (endocervix). In each of them, 20 fields were visualized with a 20X objective, and the staining intensity and the percentage of glands for each slide were evaluated for each slide. Subsequently, an average semiquantitative value for each woman of the mucin content was calculated, considering both the percentage and the staining intensity.

The three endocervical zones showed abundant mucin secretion which showed a more acid than a neutral character. No significant staining differences were observed between zones. In the three endocervical zones the positivity of Alcian Blue pH 2.5–PAS was significantly higher than for the other staining methods.

During the secretory or progestinic phase, mucus with sulphate or carboxyl groups was demonstrated throughout the endocervical canal. Their distribution is homogeneous showing a similar proportion of sialomucins and sulfomucines from the proximal to the distal zone. This result differs from that observed during the endometrial proliferation phase in whcich the distal zone of the endocervical canal swhowed mainly sialomucins. This difference may be related to changes in the types of mucus and fluidity that occur during the progestinic compared with proliferation phase in endocervical mucosa.

Funded by: GERM 19892/15. Fundación Séneca, CARM.

Poster presentation: Session 1. Topic: Histology of Organs and Systems. Code: 5954

Histology and Histopathology
From Cell Biology to Tissue Engineering

Morphological evaluation of the liver in wistar rats inoculated with *Rhipicephalus sanguineus* (Latreille, 1806) (Acari: Ixodidae) salivary gland extracts

Abreu R.M.M.[1] and Camargo-Mathias M.I.[2]

[1]Center for Biological Sciences and Nature (CCBN), Ufac, Rio Branco, AC, Brazil, [2]Department of Biology, Institute of Biosciences, São Paulo State University-Unesp, Rio Claro, SP, Brazil

The *Rhipicephalus sanguineusis* considered a species of medical and veterinary importance. The feeding process of these animals occurs due to the combined action of their mouthparts and the saliva produced by the salivary glands, vital organs for the biological success of the ticks. In addition, these glands act as storage sites for the pathogens transmitted to the host through the inoculation of the saliva.

In this sense, the present study had the objective to analyze the behavior of male Wistar rat hepatic cells submitted to in vivo application of the salivary gland extract (SGE) obtained from *R. sanguineus* female ticks.

The study involved 5 groups (4 male adults each): CG (non-inoculated individuals); PBS1 (one phosphate buffer saline injection); PBS2 (two PBS injections); SGE1 (one injection of salivary gland extract at 0.04 µg/µL) and SGE2 (two injections of salivary gland extract at 0.04 µg/µL). After the exposures, the livers were removed and submitted to the following histological and histochemical stains: HE, toluidine blue, xylidine Ponceau, alcian blue/PAS and osmium-imidazole.

The results showed that both the PBS and the SGE caused hepatic moderate alterations, such as: a) emergence of lipid plaques among the hepatic cords; b) cytoplasmic vacuolation of the hepatic cells; c) hepatocytes showing pyknotic nuclei; d) presence of homogeneous or granular secretion in the cytoplasm of the hepatocytes.

Despite the slight morphological alterations observed in the hepatic cells and tissue, the latter did not show signs of disorganization after the exposure to the extracts.

Poster presentation: Session 1. Topic: Histopathology. Code: 5017

Histology and Histopathology
From Cell Biology to Tissue Engineering

Rosenthal fibres as a model of gain of function. Immunohistochemical study in an Adult onset Alexander disease

Cabrera-Galván J.J.[1,2], Martínez-Martín M.S.[1,2], Galán-García M.E.[2], Déniz-García D[1] and Araujo-Ruano E.[1]

[1]Departamento de Morfología, ULPGC, [2]Servicio de Anatomía Patológica. Complejo Hospitalario Insular-Materno Infantil de Las Palmas de Gran Canaria, España

A common, neuropathological feature, used as a histopathological, diagnostic hallmark of Alexander disease (AD), is the diffuse presence of Rosenthal fibres. When stained with eosin and studied by light microscopy, these intracytoplasmic aggregations within astrocytes and their processes appear as round or elongated hyaline bodies. They contain GFAP, the main intermediate filament of astrocytes, as well as cellular stress proteins such as hsp27, alpha B-crystallin, and ubiquitin. Nonetheless, they are not pathognomonic, as they can also appear in cerebral scars and pilocytic astrocytomas. However, Rosenthal fibres obviously participate, in association with fibrous astrocytes, in AD pathogenesis.

Following a macroscopic autopsy study, tissue from selected visceral areas was fixed in 10% buffered formaldehyde. All the material was included in paraffin, cut into 4 mm sections, and stained with haematoxylin and eosin (H&E), periodic acid-Schiff (PAS) stain, and Kluver-Barrera stain for myelin visualisation. Immunohistochemical techniques were carried out using the following primary antibodies: anti-GFAP (Dako; 1:100), anti-alpha B-crystallin, Gennova;1:100), anti-ubiquitin (Gennova; 1:50) and anti-hsp27 (Gennova Scientific, 1:200). Thereafter, the sections were incubated with the Chenmate Dako Envision Kit-DAB®.

By the light microscope Rosenthal fibers appear as round or elongated formations of varibly sized with a hyaline appearance, as eosinophilic deposits with cylindrical granular particles and glial filaments upon H&E staining. Immunohistochemical labelling revealed abundant GFAP protein and the heat shock proteins alpha B-crystallin, ubiquitin, and hsp27, all in a context of aggregation and signs of cell stress, probably due to protein misfolding, as described in AOAD and in murine models, with a evident protein gain of function. We have detected ubiquitin at sites with high Rosenthal fibre density and lumps at the periphery, which agrees with the literature stating that the ubiquitin proteosome participates in the accumulation of the cellular stress proteins alpha B-crystallin and hsp27. We observed intense alpha B-crystallin labelling in Rosenthal fibres, glia, cytoplasm of astrocytes and their extensions, while scarce clusters of hsp27 tended to form at the periphery, similar to ubiquitin.

We cannot provide a solid explanation for how to interpret this morphological phenomenon in Rosenthal fibre formation. However, we hypothesise that those fibres were already stable, in a final phase of aggregation, as they were detected in histological sections of the cerebellum. On the other hand, they may no longer have induced ubiquitination of the misfolded proteins at that stage, whereas alpha B-crystallin activity may still have continued. In experimental models, Rosenthal fibres formed upon overexpression of wild type GFAP with scarce hsp27 and a lack of alpha B-crystallin, but not in the presence of mutant GFAP. Our observations indicated high levels of alpha B-crystallin and ubiquitin and very low ones of hsp27.

Rosenthal fibres, are characteristic aggregates being key to a histopathological diagnosis, were detected in the cerebellum and brainstem, though only at autopsy. This mechanism of formation includes gain of function of intermediate filaments and sequestration of the protein chaperones, as well as, the activation of stress response that form cytoplasmic fibrillar aggregates.

Poster presentation: Session 1. Topic: Histopathology. Code: 5559

Histology and Histopathology
From Cell Biology to Tissue Engineering

Primary cilia and spherosomes biogenesis in low grade glioma

Iruzubieta P.[1], Castiella T.[2], Monzón M.[1], Monleon E.[1], Berga C.[1], Gracia-Llanes J.[1] and Junquera C.[1]

[1]Departamento de Anatomía e Histología Humanas, Universidad de Zaragoza, España, [2]Departamento de Anatomía Patológica, Medicina Legal y Forense y Toxicología, Universidad de Zaragoza, España.

Primary cilium is a microtubule-based subcellular structure that protrudes out of the cell and plays different roles in cellular processes, including cell cycle, cytoskeleton regulation, signaling pathways or autophagy (Malicki et al. 2016). Normal astrocytes show primary cilium and they have been related to cell proliferation and differentiation (Sterpka et al. 2018). Even more, primary cilia have been found in several tumours, included brain tumours such as glioblastoma and medulloblastoma (Moser et al. 2014, Han et al. 2009).

On the other hand, spherosomes represent a new type of production of extracellular vesicles that may play a fundamental role in tumorogenesis (Junquera et al. 2016). Here we described for the first time primary cilia and spherosomes in low grade glioma.

Histological, immunohistochemical, immunofluorescence and ultrastructural techniques were performed in a case of diagnosed low grade glioma provided by the Pathology Department of Hospital Clínico Lozano Blesa.

Conventional H&E study showed an increased number of fusiform cells with a predominant fibrillar component, few mitosis and important vascularization with normal endothelial cells. These findings support the diagnosis of low grade glioma (likely a diffuse astrocytoma, WHO grade II). GFAP staining confirms the astrocytic nature of tumoral tissue. Electron microscope showed abundant gliofilaments and aberrant accumulation, acquiring a characteristic concentric disposition. Primary cilia were found in low grade glioma using immunofluorescence and ultrastructural experiments. Furthermore, electron microscope analyses allow us to track the ciliogenesis process through tumoral cells. First of all, activation of one of the centrioles (the so-called mother centriole) occurs. Activation can be detected by the formation of subdistal appendages, cargo traffic into the centriole and Golgi-derived vesicles accumulating near the distal pole. These vesicles fuse in a big ciliary vesicle (which will form the ciliary membrane) anchored to the mother centriole by transition fibers. Then, 9+0 primary cilia axoneme starts to grow protruding in the ciliary vesicle. Finally, ciliary vesicle binds the plasma membrane and the full-length axoneme is exposed to the extracellular medium. Sometimes, aberrant cilia were found, showing alterations in structural components such as the ciliary pocket or the axonemal microtubules. Spherosomes were also detected in relation to tumoral cells. Thus, multivesicular spheres originating from evagination of cellular membrane were showed. These multivesicular spheres fill up with spherosomes and are released to the extracellular medium by strangling plasmatic membrane.

Our ultrastructural and immunofluorescence experiments show that low grade gliomas present primary cilia and secrete spherosomas. Regarding these results, an increased number of spherosomes have been detected in low grade GIST compared to high grade (Junquera et al. 2016), suggesting that this structure may play an important role in early steps of tumorogenesis.

Authors would like to acknowledge the use of Servicio General de Apoyo a la Investigación-SAI, University of Zaragoza. This research received financial support from Diputación General de Aragón (DGA, T23_17R).

Poster presentation: Session 1. Topic: Histopathology. Code: 5674

Histology and Histopathology
From Cell Biology to Tissue Engineering

Reactive macroglia provide living scaffolds for spontaneous axon regeneration in conditions of traumatic neuroma in the lizard optic nerve

Romero-Alemán M.M.
Instituto Universitario de Investigaciones Biomédicas y Sanitarias, Universidad de las Palmas de Gran Canaria, Spain

Reptiles are the only amniotic vertebrates known to be capable of spontaneous axon regeneration in the central nervous system. However, this has been shown only in few species as the lizard *Gallotia galloti*. In healthy conditions, astrocytes co-express the intermediate filaments vimentin and GFAP in the adult lizard optic nerve and chiasm which reflects local adaptations to mechanical forces probably related to eye movements. Long-term axon regeneration occurs despite persistent astrogliosis after unilateral optic nerve transection in this lizard species. Astrogliosis is defined by hypertrophy, with up-regulation of intermediate filaments, and hyperplasia of reactive astrocytes. The present study aims to show the regeneration response in special cases of traumatic neuroma in the experimental lizard optic nerve and atrophy of the optic tract after long surviving periods (12 months post-lesion). The traumatic neuromas are unusual after the surgical procedure described below and occurs when both nerve stumps are not aligned. This extreme situation explores the limits of the regeneration competence of this lizard species.

Adult lizards were anaesthetized by intraperitoneal injection with diazepam/ketamine. An incision in the supraocular plaque exposed the right optic nerve, which was transected using iridectomy scissors. Next, the osteodermal plaque was put back into place. After a surviving period of 12 months, lizards were anesthetized and perfused transcardially (Bouin's fixative). The dissected brains showing traumatic neuroma in the optic nerve and severe atrophy of the contralateral optic tract were processed for paraffin embedding. Double ABC-immunoperoxidase stainings and sequential detection of vimentin (mouse monoclonal, DSHB, USA), and proteolipid protein (PLP, mouse monoclonal, Serotec/Biorad, USA) consisted of revealing one of them in black/dark grey using DAB solution containing 1% ammonium nickel sulphate, whereas only DAB was used afterwards with the other one in brown. Single ABC-Immunoperoxidase and Hematoxylin nuclei counterstaining were also performed.

The caudal optic nerve and optic tract in the experimental side showed significant atrophy in comparison to the intact side. Unexpectedly, some PLP-positive cell bodies and few myelinated nerve fibers were observed in the experimental side. These cells were undetected in the intact side. Moreover, intensely vimentin-positive reactive astrocytes showed a network-like structure in the experimental optic nerve and chiasm suggesting a role in reinforcing the cell scaffold caudal to the traumatic neuroma. By contrast, they were round-shaped with abundant cytoplasmic granules in the experimental optic tract which may be linked to a role in detritus removal. These different phenotypes suggest different functions of reactive astrocytes. Accordingly, some authors have shown that the cytoskeleton can affect cell behavior through cell surface integrin receptors. Hematoxylin nuclei counterstaining revealed more abundant nuclei in the experimental side indicating the gliosis persistence.

1) Some surviving retinal ganglion cells are able of axon regrowth despite the traumatic neuroma in the optic nerve and caudal atrophy. 2) Reactive vimentin-positive astrocytes form cell structural networks which can support spontaneous axon regrowth in the optic nerve/chiasm and debris removal in the optic tract. 3) Reactive PLP-positive oligodendrocytes are involved in the remyelination process of some regenerating nerve fibers.

Poster presentation: Session 1. Topic: Histopathology. Code: 5678

Histology and Histopathology
From Cell Biology to Tissue Engineering

Study of vascular density in endocrine area of islets of langerhans in non-obese diabetic mice

Idoate-Bayon A. and Bodegas ME.

Department of Pathology, Anatomy and Physiology, University of Navarra, Pamplona, Spain
aidoate.10@alumni.unav.es; mbodegas@unav.es

The non-obese diabetic (NOD) is a murine strain that spontaneously develops a form of diabetes type 1 similar to humans. In NOD mice, there is an islet lymphoid infiltrate described as insulitis. The inflammatory microenvironment of infiltration reduces the vascular density in islets of Langerhans by a decrease of endothelial cells number. This vascular density is very important to keep beta cells survival and glucose homeostasis. The aim of this study was to investigate in which phase of the infiltration process takes place the greatest reduction in vascular density.

Pancreas of 10 NOD-scid (control) and 9 NOD mice aged 20 weeks were used. Endothelial cells were detected by immunohistochemistry with anti- CD31 antibody in a total of 57 samples (30 NOD-scid and 27 NOD). NOD mice islets were classified into 5 groups according to their percentage of lymphoid infiltration: G0 without insulitis, G1<25%, 25≤G2<50%, 50≤G3<75% and G4 ≥75%. The percentage of CD31 immunoreactive area in the endocrine area of islet of Langerhans was quantified by computerized image analysis using. Student´s t test was used to analyze the differences.

No statistically significant difference was detected in vascular density between control and G0 (p=0,835), whereas any increment in insulitis was associated with a highly significant decrease of vascular density (p<0,001). The vascular density decreased very significantly in G1 compared to G0 (p=0,014) and in G3 with respect to G2 (p=0,027). However, no significant change was found when comparing G1 and G2 (p=0,580) or G3 and G4 (p=0,458).

Conclusions: 1) Vascular density in islets of Langerhans of G0 NOD mice is indistinguishable from that of control animals. 2) Endothelial cells destruction takes place at the initial stage of insulitis and also when lymphoid reaches 50-75%.

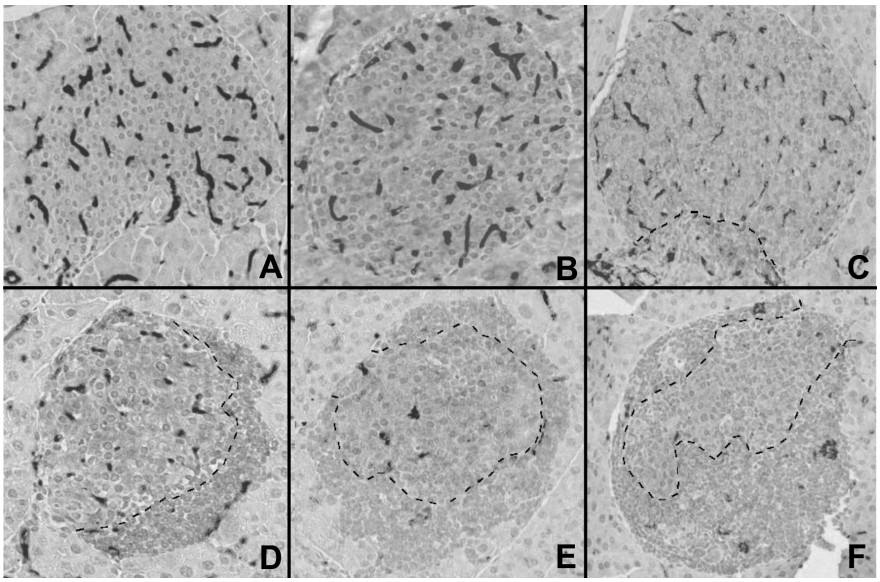

This study was funded by: “Ministerio de Sanidad y Consumo, Instituto de Salud Carlos III, Fondo de Investigación Sanitaria (FIS) (proyecto no P1050755) y Plan de Investigación de la Universidad de Navarra (PIUNA) (proyecto no 12028751)”.

Figure 1. Immunohistochemistry staining samples of representative islets (20x) from NOD-scid mice (A) and NOD mice with different degrees of insulitis (B: G0 no insulitis; C: G1; D: G2; E: G3; F: G4). Dashed line represents the limit of lymphoid infiltrate.

Poster presentation: Session 1. Topic: Histopathology. Code: 5679

Histology and Histopathology
From Cell Biology to Tissue Engineering

Study of vascular endothelial growth factor-A in endocrine area of islets of langerhans in non- obese diabetic mice

Idoate-Bayon A. and Bodegas M.E.
Department of Pathology, Anatomy and Physiology, University of Navarra, Pamplona, Spain
aiodate.10@alumni.unav.es; mbodegas@unav.es

The non-obese diabetic (NOD) is a murine strain that spontaneously develops a form of diabetes type 1 similar to humans. In NOD mice, there is an islet lymphoid infiltrate described as insulitis that decreases the vascular area in islets of Langerhans. The islet vasculature plays a crucial role to keep beta cells survival and function. Beta cells produce Vascular Endothelial Growth Factor-A (VEGF-A) that keep islet vasculature. Deletions of VEGF gene in beta cells reduce islet vascular density and increase glucose levels. The inflammatory environment can promote the production of VEGF-A. Also, the receptor of VEGF-A is overexpressed in endothelial cells of islets with insulitis. The aim of this study was to study the expression of VEGF-A in islets of Langerhans in NOD mice.

Pancreas of 10 NOD-scid (control) and 9 NOD mice aged 20 weeks were used. The VEGF-A was detected by immunochemistry with anti-VEGF-A antibody in a total of 57 samples (30 NOD-scid and 27 NOD). NOD mice islets were classified into 5 groups according to their percentage of lymphoid infiltration: G0 without insulitis, G1<25%, 25≤G2<50%, 50≤G3<75% and G4 ≥75%. The percentage of VEGF-A immunoreactive area in endocrine area of islet of Langerhans was quantified by computerized image analysis using. Student´s t test was used to analyze the differences.

Statistically very significantly decreased was detected in VEGF-A levels in G0 (p=0.028) and in G1 (p=0,010) compared to control, whereas any increment in insulitis was associated with a highly significant decrease of VEGF-A levels (p<0.001). However, no significant change was found when comparing G0 and G1 (p=0,249), G1 and G2 (p=0,145) or G2 and G3 (p=0.158). The decrease in VEGF-A levels was highly significant when comparing G4 and G3 (p<0.001).

Conclusions: 1) The expression of VEGF-A in NOD-scid mice is higher than in NOD mice. 2) VEGF-A levels do not decrease significantly as the infiltration progresses 3) VEGF-A levels decrease when insulitis reaches 75-100%.

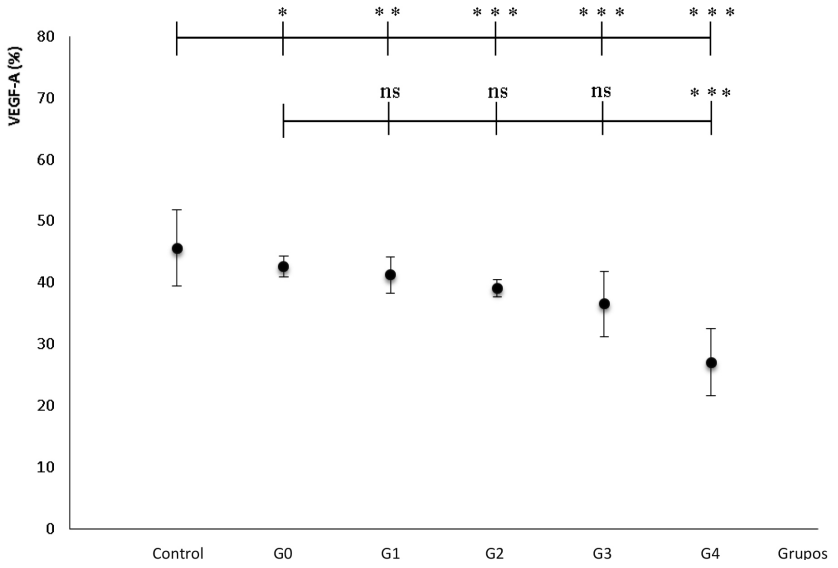

This study was funded by: “Ministerio de Sanidad y Consumo, Instituto de Salud Carlos III, Fondo de Investigación Sanitaria (FIS) (proyecto no P1050755) y Plan de Investigación de la Universidad de Navarra (PIUNA) (proyecto no 12028751)”.

Figure 1. Representation of means with a 95% confidence interval in all groups. The top horizontal bar represents the significance code between the control and all different groups. The bottom bar represents the significance code between the groups of insulitis and with it predecessor. Code: (ns; p>0,10), (*; p<0,05), (**; p<0,01) and (***; p<0,001).

Poster presentation: Session 1. Topic: Histopathology. Code: 5698

Histology and Histopathology
From Cell Biology to Tissue Engineering

Molecular and morphological analysis of the golgi apparatus of dopaminergic neurons in human substantia nigra: new citopathological findings in Parkinson's disease

Tomás M.[1], Martínez-Alonso E.[2], Martinez-Martinez N.[2] and Martínez-Menárguez J.A.[2]

[1]Department of Human Anatomy and Embriology, Medical School, Universitat de Valencia, Valencia, Spain, [2]Department of Cell Biology and Histology, Medical School, University of Murcia, Murcia, Spain

Parkinson's disease (PD) is the most common movement disorder and the second chronic progressive neurodegenerative disease after Alzheimer's disease. Fragmentation of the Golgi ribbon is a common feature of many neurodegenerative diseases, including PD. However little is known about the causes of this alteration. Most of the cytopathological findings of this disease have been obtained from cellular and animal experimental models but studies in human tissue are scarce. Our previous studies, using cellular models of Parkinson´s disease, demonstrate that fragmentation is an early event, previous to □-synuclein aggregation and cytoskeletal alterations, which is directly related to the alteration of the homeostasis of a limited number of Golgi regulatory proteins. The purpose of this study was to analyze the Golgi complex of dopaminergic neurons in the substantia nigra of PD necropsies using morphological and biochemical techniques.

Human nigra substantia pars compacta (SNpc) samples: The human postmortem control and PD samples used were obtained from the Neurological Brain Bank of Navarra, Banc de Teixits Neurològics (Serveis Cientificotècnics, Hospital Clínic, Universitat de Barcelona) and Fundación CIEN□□Instituto de Salud Carlos III). *Immunofluorescence:* 5 µm sections of paraffin-embedded, formalin-fixed susbtantia nigra samples were treated with 0.5% citrate buffer to maximize antibody penetration into the tissue before to the immunofluorescence tecnique. Autofluorescence was blocked with Sudan black. *Western blotting analysis:* Frozen samples of substantia nigra were lysated, resolved on NuPAGE gels, transferred onto PVDF membranes and immunolabelled. Proteins were detected by using ImageQuant LAS 4000. *Ultrastructural analisis:* Frozen and formalin-fixed samples were postfixed with glutarldehyde/osmium tetratoxide, dehydrated and embedded in Epon 812. For ultrastructural immunolocation samples were postfixed with 2% paraformaldehyde and 0.2% glutaraldehyde and processed for cryoimmunoelectron microscopy. *Statistical analysis:* Mann-Whitney U test was used to compare means between PD and control necropsies. P-values < 0.05 were considered significant.

At light microscopy, the Golgi apparatus of dopaminergic neurons from PD samples appeared fragmented and distributed throughout the cytoplasm. Electron microscopy demonstrated that the Golgi ribbon is altered but the typical stacked appearance of this organelle is not loss. The biochemical analysis showed a reduction of the levels of GTPase Rab 2 and Golgi structural protein GRASP65. In contrast, we found an increase of Rab1, the SNARE protein syntaxin 5 and regulatory protein golgin 84. The level of other proteins analyzed were not altered (tubulin, giantin, Rab8, GM130). We also observed main alterations in the distribution of Rab1 and the SNARE protein syntaxin 5, which is accumulated mainly out of the cell in extracellular inclusions.

We demonstrate for the first time that the expression of Golgi structural and transport regulatory proteins is altered in human samples of PD which may explain the fragmentation of this organelle. These alterations may disturb the trafficking of many proteins that are essential for neuronal function. New experiments in human samples will be need to give a complete view of the cytopathology of PD.

Poster presentation: Session 1. Topic: Histopathology. Code: 5713

Histology and Histopathology
From Cell Biology to Tissue Engineering

Microscopic study of the infarct-related coronary artery in a swine model of reperfused myocardial infarction

Ruiz-Sauri A.[1,2], Rios-Navarro C.[1], Ortega M.[1], Gavara J.[1], Marcos-Garces V.[3], Chorro F.J.[1,3,4,5] and Bodi V.[1,3,4,5]

[1]Institute of Health Research-INCLIVA, Valencia, Spain, [2]Pathology Department, Faculty of Medicine, University of Valencia, Valencia, Spain, [3]Cardiology Department. Hospital Clinico Universitario, Valencia, Spain, [4]Medicine Department, Faculty of Medicine, University of Valencia, Valencia, Spainm [5]Centro de Investigación Biomédica en Red – Cardiovascular (CIBER-CV), Madrid, Spain.

Coronary circulation provides oxygen and nutrients to the cardiac tissue. Following myocardial infarction (MI), the microscopic impairment of the microcirculation has been widely addressed, but few studies explored the consequences at epicardial level. Our objective was to evaluate the dynamics of the microscopic damage in the infarcted coronary artery post-MI in swine model of reperfused MI.

MI was induced in swine by transient 90-min coronary occlusion of the left anterior descending (LAD) coronary artery using angioplasty balloons. One control group and four MI groups were defined: 1) without reperfusion, and 2) 1-min, 3) 1-week, and 4) 1-month reperfusion (n=3, each). In each group, LAD (infarct-related artery) was isolated. Histological stainings (hematoxylin-eosin, Masson's trichromic, and orcein) and immunohistochemistry against CD31 (endothelial cells), a-smooth muscle cells, and CD45 (total leukocytes) were performed.

Abnormalities in the endothelial monolayer of the LAD artery started even before reperfusion (during ischemia). This damage dramatically increased after reperfusion, observing an almost absence of CD31+ cells in the tunica intima and some breaks in the internal elastic layer from the 1-min and 1-week reperfusion groups. No irregularities were found in the tunica media from the no reperfusion group, whereas an increased in its thickness was detected soon after reperfusion. In the 1-week reperfusion group, larger thickness, a desorganized muscular cells distribution, and edema were found. In the tunica adventitia, vasa vasorum density was reduced during the ischemic phase, remaining low in the 1-min and 1-week reperfusion group, while being restored after 1-month reperfusion. After coronary reperfusion, a higher leukocyte adhesion to the endothelium from the LAD artery was observed. The process evolves, resulting in a massive presence of CD45+ cells not only in the tunica intima, but also in the media and the adventitia monolayer isolated from the 1-week reperfusion group.

The microscopic structure of the infarct-related coronary artery was compromised after MI. This damage started during ischemia and boosted after reperfusion. Exploring these damages will be important for a better understanding of the pathophysiology of MI.

This study was funded by "Instituto de Salud Carlos III" and "Fondos Europeos de Desarrollo Regional FEDER" (PIE15/00013, PI17/01836, and CIBERCV16/11/00486 grants) and Generalitat Valenciana (GV/2018/116).

Poster presentation: Session 1. Topic: Histopathology. Code: 5719

Histology and Histopathology
From Cell Biology to Tissue Engineering

CD31 or CD34: which is the best marker for evaluating microvascular density in renal cell carcinoma?

Nuñez-Benito E.[1], Rios-Navarro C.[2], García-Bustos V.[3], Sales M.A.[4], Milian L.[2], Martín de Llano J.[1,2], LLombart-Bosch A.[1,2], Mata M.[1,2] and Ruiz-Saurí A.[1,2]

[1]Pathology Department, Faculty of Medicine, University of Valencia, Valencia, Spain, [2]Institute of Health Research-INCLIVA, Valencia, Spain, [3]Internal Medicine Service, University Hospital and Polytechnic La Fe, Valencia, Spain, [4]Pathological Anatomy Service, Hospital Clínico Universitario, Valencia, Spain

Angiogenesis is an essential process for tumor growth. Renal Cell Carcinoma (RCC) is characterized by rich neovascularization and often a prominent vascular network around tumor cells, but predicting response to anti-angiogenic therapy and evaluating the prognostic role of angiogenesis in RCC is difficult. Microvessel density (MVD), the most representative method for quantification of angiogenesis, remains controversial as an indicator of prognosis in RCC. The contradictory results are perhaps attributable to the use of heterogeneous markers to identify tumor blood vessels. CD31 and CD34 have been often used as endothelium specific markers and it has been proposed that they are expressed in different types of endothelial cells.

The main aim of this study was to analyze and compare in the same tissue section the MVD and other morphometric parameters in RCC blood vessels staining with CD31 and CD34.

Formalin-fixed and paraffin-embedded specimens were collected from 30 patients with RCC (10 clear cell, 10 papillary cell, and 10 chromophobe). All had been treated with radical nephrectomy. The MVD was evaluated by immunohistochemistry using anti-CD31 and anti-CD34 antibody. The four most vascularized areas (hot spot) were selected in two consecutive tissue sections. In each selected area, four 20X magnification microphotographs were taken and analyzed in order to obtain morphometric parameters. The same area was photographed to avoid discrepancies in the type and number of vessels in CD31 and CD34 tissue sections. Images were analyzed by ImagePro Plus 7.0 software to obtain microvascular area (MVA), MVD, and different morphometric parameters such as maximum diameter (Dm max), minimum diameter (Dm min), major axis, perimeter, radius ratio and roundness.

In all types of tumor, MVD was higher in CD31+ than CD34+ staining marks, but differences were only statistically significant in ccRCC ($p<0.05$) and pRCC ($p<0.01$). CD31+ MVA were smaller than CD34+, being statistically significant in pRCC ($p<0.05$) and ChrRCC ($p<0.05$). The mean values for the other morphometric parameters was higher in CD34+ vessels than CD31+ vessels. When we evaluated MVD using either CD31 or CD34 in each types of tumor, MVD was higher in ccRCC than pRCC ($p<0.001$) or than ChrRCC ($p<0.001$) but no differences were found between pRCC and ChrRCC. Moreover, the area of vessels, Dm max, Dm min, major axis and perimeter in ccRCC was smaller than other tumor types with statistically significant differences with ChrRCC.

In all three type of RCC, CD31+ vessels are more numerous and smaller than CD34+ vessel. The ccRCC samples display a higher MVD and smaller vessels than other types of tumor (pCCR and ChrCCR). Since we have observed different vascular pattern depending on the antibody used for microvasculature evaluation, a consensus might be achieved to determine which marker is better for define patient prognosis.

Poster presentation: Session 1. Topic: Histopathology. Code: 5725

Histology and Histopathology
From Cell Biology to Tissue Engineering

Outcome at 72 hours of brain injured newborn piglets after hypoxia-ischemia

Alvarez F.J.[1], Alvarez A.A.[2], Alonso-Alconada D.[2], Santaolalla F.[3] and Hilario E.[2]

[1]Biocruces-Bizkaia Health Research Institute, Cruces University Hospital, Barakaldo, Bizkaia, Spain, [2]Department of Cell Biology and Histology, School of Medicine, University of the Basque Country, Leioa, Bizkaia, Spain, [3]Department of Otolaryngology, School of Medicine, University of the Basque Country, Basurto University Hospital, Bizkaia, Spain.

Many newborn infants affected by hypoxic-ischemic (HI) brain injury could suffer handicaps. During HI event, brain cells suffer a primary energy failure resulting in a variable rate of cell damage; and this event is followed by a secondary phase with a failure of oxidative metabolism associated to excytotoxic edema, seizures, cerebral hyperperfusion. The improvement of the values of markers, as the amplitude-integrated electroencephalography (aEEG) and the near-infrared spectroscopy (NIRS), is correlated to a better prognosis at short and medium term. The aim of this study was to correlate values of these markers of brain activity with histological damage at short and medium term (6 or 72 hours after HI event).

Anesthetized piglets were randomly assigned to the Sham operated and HI groups (n=10 per group). Hypoxia-ischemia was induced by reversible clamping of both common carotid arteries and lowering the inspired oxygen (8-10%). The half of the piglets of both groups were sacrificed at 6 hours, and the other half were allowed to recover from experimental procedure, and sacrificed after 72 hours. Brain tissue oxygen index (TOI) was continuously monitored using NIRS. Brain activity was measured by aEEG. NIRS and aEEG were continuously recorded at 6 and 72 hours. Brains were fixed with formaldehyde, and paraffin sections processed and stained for Nissl, TUNEL and glial fibrillary acidic protein (GFAP) studies. Parietal cortex and hippocampus were studied, in accordance of stereotaxic atlas. Data are expressed as mean ± standard deviation. Mean values have been compared using the Kruskal-Wallis test for unpaired data and the Wilcoxon signed rank test for paired data.

During hypoxia-ischemia, a decrease in arterial pH (7.37±0.04 vs 7.18±0.08, $p<0.05$), PaO_2 mean values (108±7 vs 34±2 torr, $p<0.05$) and base excess (-0.7±2.1 vs. -12.9±4.8 mE/L) were observed in HI group in comparison to Sham. There was a decrease in TOI during HI insult, but mean values of TOI were recovered. aEEG remained stable during 72 hours in Sham group, but HI injury induced an 88% decrease. At 72 hours, the aEEG remained 57% lower than basal values ($p<0.05$). aEEG at 6 hours indicate the presence of seizures in all piglets. Nissl staining revealed a decrease in the number of neurons in cortex both at 6 and 72 hours, as well as an increase of the number of pyknotic cells (51.8 ± 3.5%). Also, in cortex of HI animals, the number of TUNEL positive cells was more than 6-fold higher than Sham group at 72 hours, although was not detectable at 6 hours. GFAP staining did not demonstrated differences between groups neither the number of astrocytes nor its morphology at 6 hours. However, at 72 hours the number of astrocytes in cortex had decreased, and the surviving astrocytes appeared swollen and smaller than in Sham animals.

Results suggest that although aEEG and NIRS are good markers of cerebral hypoxia in newborn piglet, the former marker gives a better outcome at 72 hours.

Poster presentation: Session 1. Topic: Histopathology. Code: 5726

Histology and Histopathology
From Cell Biology to Tissue Engineering

Early markers of cerebral hypoxia in newborn piglets

Alvarez A.A.[1], Alvarez F.J.[2], Alonso-Alconada D.[1], Blanco-Bruned J.L.[2] and Hilario E.[1]

[1]Department of Cell Biology and Histology, School of Medicine, University of the Basque Country, Leioa, Bizkaia, Spain, [2]Biocruces-Bizkaia Health Research Institute, Cruces University Hospital, Barakaldo, Bizkaia, Spain

Hypoxic-ischemic encephalopathy (HIE) of the newborn causes severe and long-term neurodevelopmental deficits. Brain cells suffer a profound or prolonged event of hypoxia-ischemia which, in many cases results in cell death. Thus, is necessary to find markers that properly identify the severity of the insult, in order to *early* determine the prognosis, prior to use any rescue treatment. Ideally, the optimal marker must be directly related to the neonatal brain damage (specificity), since the treatable babies would be clearly identified, providing useful data about the efficacy of the assayed treatment. Many studies have tried to correlate different markers with HIE, such as the amplitude-integrated electroencephalography (aEEG), the brain perfusion and oxygenation by near-infrared spectroscopy (NIRS), and other HI-related biomarkers. Unfortunately, the results have not been as positive as we might expect, and the optimal marker is not yet available. The aim was to study the association of hypoxia and early markers usually used in the clinical practice.

Anesthetized piglets (1 to 5-day old) were mechanically ventilated to maintain normoventilation Continuous three-lead electrocardiogram monitoring was used. Later, piglets were randomly assigned to the sham operated and hypoxic-ischemic (HI) groups. Hypoxia-ischemia was induced by reversible clamping of both common carotid arteries with vascular occluders and lowering the fraction of inspired oxygen of 0.08 to 0.10 over 20 min. Sham animals were similarly anesthetized and intubated but were kept in normoxia with their carotids unclamped. Three animals were used to assess the degree of HI insult by an intravenous perfusion of pimonidazole (hypoxic tissue marker), 30 min before the insult. Animals were immediately sacrificed after hypoxic-ischemic event. Brain tissue oxygen index (TOI) and variations in total hemoglobin index (THI) were continuously monitored using NIRS. Brain activity was measured by aEEG. Immunohistochemical sections of pimonidazole-marker cells were made for microscopical study. TNFalpha positive and pimonidazole-marker positive cells were evaluated by flow cytometry in different areas: cortexes (including occipital, frontal, temporal and parietal), thalamus, striatum, and hippocampus. Data are expressed as mean ± standard deviation (SD). Mean values have been compared using the Kruskal-Wallis test for unpaired data and the Wilcoxon signed rank test for paired data.

During hypoxia-ischemia, a decrease of PaO_2 mean values was observed in HI group (108±7 vs 34±2 torr). In HI animals, there was a acute decrease in TOI and in aEEG during hypoxic-ischemic insult as compared with Sham group. Pimonidazole staining of brain slices revealed an increase in the number of cells in all cerebral regions. The percentage of brain TNFα positive cells was more than 2-fold higher in HI group than in Sham one. The extension and the degree of hypoxia were wide and large as demonstrated by the percentage of pimonidazole positive cells (78±8% in cortexes; 79±12% in other brain areas).

Results suggest that aEEG and NIRS are good early markers of cerebral hypoxia in newborn piglet.

Poster presentation: Session 1. Topic: Histopathology. Code: 5730

Histology and Histopathology
From Cell Biology to Tissue Engineering

A histological approach to the neurogenic niche of the neonatal subventricular zone

Pacho M.[1], Pintor-Rial A.[1], Canduela M.J.[2], Álvarez A.[1], Hilario E.[1] and Alonso-Alconada D.[1]

[1]Department of Cell Biology and Histology, School of Medicine and Nursing, University of the Basque Country (UPV/EHU), Leioa, Bizkaia, Spain, [2]Department of Neurosciences, School of Medicine and Nursing, University of the Basque Country (UPV/EHU), Leioa, Bizkaia, Spain

There is still no definitive therapy for infants suffering from perinatal asphyxia, which leads to over 0,7 million neonatal deaths each year and 1,15 million newborns developing acute brain dysfunction known as neonatal encephalopathy. Time has come to focus efforts on therapies that could modulate the limited neurorestorative capacity of the brain. Following certain injuries, the subventricular zone (SVZ) can act as a persistent germinative zone generating neurons. This reactive neurogenesis may be more successful when tissue destruction and inflammation are minimized. The aim of the present work was i) to elucidate the response of the neonatal SVZ after hypoxia-ischemia (HI) and ii) to investigate the therapeutic potential of melatonin and 2-AG treatments in the SVZ of the immature rat.

HI was induced by the ligation of the right common carotid artery on 7-day-old (P7) anesthetized rat pups. After 3h of recovery, animals were placed in airtight jars and exposed for 2.5 hours to a humidified 92%nitrogen-8%oxygen mixture. After hypoxic exposure, pups were randomly assigned to 4 experimental groups and returned to their dams until euthanized per protocol. Sham-operated rat pups had neither artery ligation nor hypoxia (Sham). Melatonin-treated animals received three i.p. doses of melatonin (15 mg/kg, dissolved in normal saline:DMSO 95:5) at 5 min, 24h and 48h after HI (HI+MEL). 2-AG treated rats received a single i.p. injection of the endocannabinoid 2-AG (2mg/kg diluted in 2%DMSO, 1%Tween-80 in sterile 0.9%saline) immediately after the HI (2-AG). The HI-injured group (HI) received a corresponding volume of vehicle. At P14, animals were sacrificed and brains were perfusion-fixed and embedded in paraffin. Five-micrometer coronal sections were cut at the level of the anterior commissure, stained with HE and regional morphometry was evaluated. Ventricular and the SVZ dorsolateral tail areas were outlined and measured bilaterally. To analyze the incidence of HI across the dorsolateral SVZ, this was separated into three distinct regions: medial, mediolateral and lateral. For each region, the average cellularity was assessed by determining the number of cells per field.

In lesioned animals (HI group), we showed a significant (p=0,025) enlargement of the right (ipsilateral to damage) lateral ventricle when comparing to sham, reflecting adjacent striatal atrophy. This widening of the lateral ventricle was reverted with melatonin treatment (p=0.126 vs Sham) but not with 2-AG (p=0.013 vs Sham). We found no inter-regional differences in cell density, but a global decrease was observed in HI (764±32) and 2-AG (766±48) animals, reverted by melatonin (807±36; sham=808±45).

HI-induced lateral ventricle enlargement and decrease in SVZ cellularity was reduced by melatonin. Treatment modulation of neurogenic areas and precursors may account for neural restoration after neonatal brain injury.

Grants: UPV/EHU (GIU17/018).

Poster presentation: Session 1. Topic: Histopathology. Code: 5735

Histology and Histopathology
From Cell Biology to Tissue Engineering

Histology of rabbit liver (host models for ticks) exposed to castor oil acid esters

Camargo-Mathias M.I.[1], Sodelli L.F.[1], Furquim K.C.S.[1] and Oliveira S.R.[1]
[1]UNESP-Universidade Estadual Paulista, Biosciences Institute, Biology Department, SP, Brasil

The present study verified the effects of castor oil ricinoleic acid, a natural chemical acaricide, on the clinical blood and urine parameters and on the liver morphophysiology of female rabbits (used as a model of tick hosts) fed with commercial food enriched with castor oil esters.

To obtain the results, two bioassays were assembled: in the bioassay 1 the 03 rabbits received daily for 60 days, commercial feed without esters and in the 2 feed enriched with the esters (03 rabbits). The urine (analyte dosage) and blood (liver enzyme dosage) of the rabbits of both bioassays were analyzed. For histological analysis / histochemical liver fragments were fixed in paraformaldehyde and aquous Bouin. The material was stained with HE, PAS and bromphenol blue.

Bioassays 1 (commercial food + NaCl) and 2 (food + esters + NaCl) demonstrated that the clinical parameters of the hepatic enzyme alkaline phosphatase (FAT), gamma glutamyl transferase (GGT) and alanine aminotransferase (ALT) were not significantly altered, except for the hepatic enzyme aspartate aminotransferase (AST) of the rabbits belonging to Bioassay 2, which presented greater variability, indicating that the esters are hepatotoxic. The analyses of the urine samples for the parameters free hemoglobin, protein, bilirubin and urobilinogen demonstrated that the esters were not toxic to the female rabbits. The morphohistological and histochemical data showed that the rabbits fed with enriched food had the hepatic tissue altered, which was confirmed by the disorganization of the hepatic cords, enlargement of the intercellular space, presence of hepatocytes with little evident limits and irregular and pyknotic nuclei, mostly dislocated to the cell periphery due to the presence of vacuoles. Histochemically, the female rabbits of Bioassay 2 presented a decrease in the number of lipids and increased amount of glycogen. In addition, the hepatic cells of these rabbits showed activity of acid phosphatase, probably the result of the toxicity caused by the esters, with consequent disorganization of the liver cells and tissues.

Thus, the results provided by the present study signalize that the esters offered to the host rabbits under the experimental conditions described herein altered the morphophysiology of the hepatic tissue, important information regarding the exposure of tick hosts to this acaricide.

Poster presentation: Session 1. Topic: Histopathology. Code: 5737

Histology and Histopathology
From Cell Biology to Tissue Engineering

Expression of mitogen-activated protein kinase kinase 4 (MKK4) in histological lesions of human prostate

Durán E., Hortigüela C. and Arriazu R.
Department of Basic Medical Sciences, School of Medicine, CEU-San Pablo University, Madrid, Spain

Benign prostatic hyperplasia consists of non-malignant (non-carcinogenic) growth in the size of the prostate. The incidence of BPH increases with age. Prostate cancer (PCa) is the most common cancer and is the third leading cause of death in men in developed countries. Prostate cancer is very uncommon in men younger than 45 but becomes more common with advancing age. The average age at the time of diagnosis is 70. Mitogen-activated protein kinase kinase 4 (MKK4), a member of the mitogen-activated protein kinase (MAPK) family, is involved in the stress-activated protein kinase (SAPK) pathway and is phosphorylated and activated by mitogen-activated protein kinase kinase 1 (MKK1). Positional cloning coupled with *in vivo* metastasis assays suggested that MKK4 is a metastasis suppressor gene.The aim of this work was to study the expression of MKK4, for that, one hundred twenty samples with BPH and PCa were used.

Indirect Immunohistochemistry was realized in 90 samples of hyperplasia and prostate cancer. The primary antibody used was MKK4 (D-1:100 Epitomics, USA). Immunostaining percentage area of the markers was determined; these measurements were performed using a Leica DM6000 microscope and using ImageJ software. The mean ± standard error was calculated, and analysis of the data was done using t student. The level of significance was $p<0.05$. The software used was SPSS (IBM SPSS Statistics for Windows Armonk).

We compare the expression of MKK4 attending to the age of the patients (young patients have <70 years and old patients have ≥ 70 years) in relation to BPH and PCa groups. The level of MKK4 is lower in patients with PCa than patients who have BHP in both groups (young and old patients) ($p=0.004$) ($p=0.030$). Also, the expression of MKK4 is the lowest in young patients with PCa than the other groups ($p=0.038$). The metastasis process requires that tumor cells have the ability to adhere or separated from the stroma and extracellular matrix, if MKK4 inactivation plays a role in the development of metastasis, then the level of MKK4 expression in human prostate cancers should be decreased. For that reason, in our study the young patients who have PCa run less level of MKK4 than the old patients, in fact, BHP patients have more level of MKK4 than PCa too.

MKK4 play a role in metastasis cascade and his expression decreased with the age and the aggressiveness of the prostate disease.

Poster presentation: Session 1. Topic: Histopathology. Code: 5747

Histology and Histopathology
From Cell Biology to Tissue Engineering

Preliminar study of percutaneous needle electrolysis in a calcaneal tendinopathy mice model

Peñín A.[1], García Vidal J.A.[1], Escolar Reina P.[1], Martínez C.M.[1], Medina Mirapeix F.[1] and Pelegrín P.[1]

[1]Instituto Murciano de Investigación Biosanitaria IMIB-Arrixaca, Murcia, España

Percutaneous needle electrolysis (PNE) is an innovative physiotherapeutic technic that has been found to be more effective in the treatment of different types of tendinopathies than other techniques as dry puncture or acupuncture. The PNE is carried out with an ultrasound to guide the puncture place and then a non-thermal galvanic current is applied. This galvanic current produce ion instability that theoretically induce the formation of sodium hydroxide molecules, producing under the needle a pH modification and an oxygen pressure increase. However, the exact mechanism of PNE or the effects over the tissue morphology are not well understood, this study aimed to investigate tenocytes activation by determining tendon cellularity, and the inflammatory grade in the tissue.

In this study C57 BL/6 mice has been used. A tendinopathy was induced in the calcaneal tendon with the injection of 10 µg/µl of type A collagenase, 7 days after one calcaneal tendon was treated with ecoguided dry puncture, as a control for the puncture, and the other calcaneal tendon with ecoguided PNE. Also, mice without tendinopathy had been treated with dry puncture and PNE. The mice were sacrificed seven days after the treatments and the paws were processed for the histological studies. A decalcification, sizing, paraffin inclusion and microtome cuts were done. The cuts were stained with hematoxylin eosin staining and evaluated under the optic microscope at 20x and 40x. The paws were evaluated in a 0 to 3 scale, being 0 control (healthy tendon) conditions, 1 mild, 2 medium, and 3 severe, for inflammatory infiltrate and tendon cellularity grade. The median value of the values obtained for each of the paws of every group was expressed as the final value. There were some groups with intermediate values between stages qualified like 0/1, 1/2 and 2/3, expressing a grade intermediate between both.

Our results shown that in mice without lesion both dry puncture and PNE increased the inflammatory infiltrate grade, having a grade of 1. Also, both treatments were able to increase the tendon cellularity but in this case PNE presented a grade of 2 and the dry puncture a grade of 1/2. When the lesion was induced with the injection of collagenase a considerable increase of the inflammatory infiltrate and tendon cellularity was produced, having the inflammatory infiltrate a grade of 2 and the tendon cellularity a grade of 2/3. This increase was reduced in both studied parameters with PNE and dry puncture treatments. The reduction in inflammatory infiltrate grade produced by the dry puncture was a slightly higher than the one produced by the PNE, having the dry puncture a grade of 1 and the PNE a grade of 1/2. In the case of tendon cellularity the reduction produced with both treatments was the same, having a grade of 2.

In this work, we found that the dry puncture and PNE reduce the increase in inflammatory infiltrate and tendon cellularity grades in a tendinopathy induced by collagenase.

Poster presentation: Session 1. Topic: Histopathology. Code: 5751

Histology and Histopathology
From Cell Biology to Tissue Engineering

Apolipoprotein D expression in a mouse model of multiple sclerosis

Navarro A., del Valle E., Martínez-Pinilla E., Rubio N. and Tolivia J.
Department de Morphology and Cell Biology, Faculty of Medicine and Health Sciences, University of Oviedo, Instituto de Neurociencias del Principado de Asturias (INEUROPA), Instituto de Salud del Principado de Asturias (ISPA), Spain

The cumulative evidence has demonstrated that lipocalin Apolipoprotein D (Apo D) accumulates in areas of regeneration of damaged peripheral nerves and also in the cerebrospinal fluid of patients with neurodegenerative disorders, such as Alzheimer's disease, mainly in mature oligodendrocytes and reactive astrocytes. Therefore, the role of Apo D has been related to the processes of demyelination/remyelination. The cuprizone mouse model is commonly used in multiple sclerosis to study demyelination and remyelination in the corpus callosum and cerebellar peduncles consequence of the oligodendrocyte cell (OLGs) death caused by the administration of the toxic. The aim of this study was to know how the processes of demyelination and subsequent remyelination affected the expression of Apo D.

Eight weeks old C57BL/6 mice were caged individually and fed with standard grounded chow containing 0.2% w/w cuprizone for 3 and 6 weeks. The mice were weighted every two days and the water consumption was measured. Brains were obtained after intracardiac perfusion with 4% paraformaldehyde in phosphate buffer, removed from the skull and postfixed for about 12 to 18 hours. In transversal sections of 5 μm at +1.3 bregma level, a Luxol Fast Blue histochemical technique for myelin and a chromogenic immunohistochemistry for Apo D were performed. The Apo D labeling was quantified in a central area of the corpus callosum and the number of marked cells was counted.

The Apo D level decreases with cuprizone treatment from 3 to 6 weeks. When the treatment stops the Apo D level progressively recovers reaching the control values six weeks after. These data agree with those obtained on the myelination of the corpus callosum at the same level and in the same groups. When lowest is the myelination, less is Apo D density. When we count the number of Apo D marked cells, mainly oligodendrocytes, we can observe that the quantity of positive cells decreases with the time of cuprizone treatment, partially recovering the initial number when it is suspended. Northworthy, the Apo D labelling is higher than we expected according with number of OLGs recovered. It seems that Apo D protein appears in neuropile of remyelination area.

These data are in agreement with those found in the literature regarding the role of Apo D in myelination and remyelination processes. Thus, remyelination is accompanied by an increase in the expression of Apo D possibly due to a recovery of the amount of oligodendrocytes able to synthesizing this apolipoprotein and forming new myelin sheets.

This study has been funded by Instituto de Salud Carlos III though the project (PI15/00601) (Co-funded by European Regional Development Fund/European Social Fund "Investing in your future").

Poster presentation: Session 1. Topic: Histopathology. Code: 5759

Histology and Histopathology
From Cell Biology to Tissue Engineering

Hepatic alterations in *Mus musculus* rats after exposure to carvacrol acaricide

Barbosa Schiavolin M.[1,2], Rossini de Oliveira S.A.[2], Scopinho Furquim K.C.[1] and Camargo-Mathias M.I.[1]

[1]UNESP, Rio Claro, S.P., Brazil, [2]Faculdades Integradas Einstein de Limeira, Limeira, S.P., Brazil

Concerns regarding tick control have increased exponentially, stimulating the search for products at the same time more efficient and less harmful to nontarget organisms. Several studies address this issue in the literature, aimed at finding a new strategy to control these ectoparasites, i.e., focusing on chemicals extracted from plant extracts (natural) such as carvacrol, proven efficient against *Rhipicephalus sanguineus* s.l., *Amblyomma cajennense*, *R. microplus* and *Dermacentor nitens* ticks. Nevertheless, the literature lack information on the alterations that may be caused to nontarget organisms (including the hosts) when exposed to the chemical.

In this sense, the present study evaluated the liver of female *Mus musculus* rats exposed to carvacrol at the concentration of 20 µL/mL through morphohistological techniques.

The results showed that the exposed rats presented alterations in the liver, including cell and nuclear hypertrophy in the hepatocytes, decrease in the amount glycogen stored in the cytoplasm and tissue disorganization. These data allow us to infer that, despite being a natural compound and an efficient acaricide, carvacrol is toxic and modifies the morphophysiology of the liver of the exposed organisms.

Therefore, this bioactive cannot be considered safe to be used on large scale, once it is toxic both for the ticks (target organism) and for the host (nontarget organism).

Financial support: FAPESP

Poster presentation: Session 1. Topic: Histopathology. Code: 5762

Histology and Histopathology
From Cell Biology to Tissue Engineering

Platelet rich gel supernatants prevents structural damage of equine tendon explants challenged with lypolysaccharide

Bonilla-Gutiérrez A.F., Castillo-Franz C., López C. and Carmona J.U.
Grupo de Investigación Terapia Regenerativa, Universidad de Caldas, Manizales, Colombia

Currently, platelet-rich plasma (PRP) and its related hemoderivatives as platelet-rich gel supernatant (PRGS) are frequent treatment of horses with superficial digital flexor tendon (SDFT) tendinopathy. It is though these hemoderivatives have regenerative properties slowing or reverting the catabolic effects of the proinflammatory stimuli of mediators implicated in the catabolic damage of these musculoskeletal tissues.

The study included the evaluation of 5 experimental groups of equine SDFT explants challenged with lypolysaccharide (LPS) as follows: 1 SDFT group without addition of any PRGS and 4 SDFT groups cultured with leukocyte concentrate (Lc) –PRGS (Lc-PRGS) and leukocyte reduced (Lr) –PRGS (Lr-PRGS) of two different concentrations (25% and 50%). Furthermore, a control SDFT group without addition of LPS and any PRGS was included. All groups were cultured at 48 h and then the tendon explants were harvested for histopathological evaluation. Allogeneic venous blood from 6 clinically healthy horses was used. PRPs were obtained through a manual double centrifugation tube method and PRGS were obtained after PRP activation with calcium gluconate. SDFT explants were stained with either hematoxylin and eosin or Alcian blue. Tendon preparations were assessed for roundness of the nuclei of the fibroblasts, cell density, vascularization, the pattern of the collagen fibers and determine the deposition of ground substance.

Platelet counts were significantly ($P<0.01$) different between whole blood (x 1) and Lc-PRP (x 2.5) and similar between whole blood and Lr-PRP (x 1). WBC counts were also significantly ($P<0.01$) different between the hemoderivatives, with whole blood having the highest concentration (x1), followed by Lc-PRP (x 0.45), and Lr-PRP (x 0.015). The total histology score evaluation was similar for SDFTs of the control group without LPS and those cultured with both PRGSs at two concentrations. On the other hand, SDFTs of the control group plus LPS showed a significantly ($P<0.05$) worst total histology score in comparison with the rest of SDFTs groups. Fibroblasts, cellular density and vascularization histology score was no significantly different between all groups evaluated. SDFTs of the control group and those treated with both Lr-PRGS concentrations exhibited significantly ($P<0.05$) better (lesser) score for ground substance deposition and collagen pattern orientation compared to the SDFTs of the control group plus LPS and those explants cultured with both Lc-PRGS.

The results suggest that Lc-PRGS and Lr-PRGS could maintaining some histology characteristics in equine SDFT explants cultured over 48 h. The difference observed for collagen arrangement in the samples treated Lc-PRGS and Lr-PRGS could be associated with the anabolic effect of some growth factor contained in these hemoderivatives. However, the general histology score was apparently better in tendons cultured with both Lr-PRGS concentrations. These findings suggest that the Lr-PRGS could be more suitable for tendinopathy treatment. However, further molecular studies should be guaranteed to know the antiinflammatory effect of both PRGS and thus could stablish a rationale therapeutic approach in the treatment of horses with SDFT tendinopathy.

Poster presentation: Session 1. Topic: Histopathology. Code: 5770

Histology and Histopathology
From Cell Biology to Tissue Engineering

Proprotein convertase expression in wild type and globozoospermic mouse testis

Sáez F.J.[1], Velado A.[1], Gómez-Santos L.[1], García-Gallastegui P.[1], Crende O.[1], Madrid J.F. [2], Badiola I[1]. and Alonso E[1].

[1]Department of Cell Biology and Histology, School of Medicine and Nursing, University of the Basque Country UPV/EHU, Leioa (Vizcaya), Spain, [2]Department of Cell Biology and Histology, School of Medicine, Regional Campus of International Excellence "Campus Mare Nostrum", University of Murcia, IMIB-Arrixaca, Murcia, Spain

The proprotein convertase family plays a key role in posttranslational modifications of proteins in the secretory pathway of cells, and is responsible for the regulation of many processes both inside and outside the cell. The convertases that seem to be of major interest in testis are *pcsk3* or furin (expressed ubiquitously), *pcsk4* (expressed exclusively in testis) and *pcsk6* or PACE4 (never looked for in testis, but expressed in different hormone-producing cells). In fact, a lack of *pcsk4* expression has been linked to an infertile phenotype related to acrosomal function. The GOPC protein (Golgi-associated PDZ and coiled-coil motif-containing protein) takes part in the formation of the acrosome during spermiogenesis. GOPC knockout mice have globozoospermic sperm and are infertile. The study of this anomaly could help in the process of identifying and solving today's worldwide fertility problem or help in the development of male non-hormonal contraceptive methods.

The aim of this work was to analyze the expression of *pcsk3, pcsk4* and *pcsk6* in the testis of wild type and knockout Gopc$^{-/-}$ mice and its possible role in spermatogenesis.

We tested the expression of the *pcsk3*, *pcsk4* and *pcsk6* genes in C57 BL/6 and Gopc$^{-/-}$ mouse testis by means of RT-qPCR with RNA from testis included in paraffin blocks. To make sure the quality of the RNA was enough, we also carried out a multiplex preamplification. The housekeeping genes used as positive controls were *rpl13* and *rps15*. Three replicas were made for each individual analysis and negative controls were made for each primer to make sure there was no contamination.

Pcsk3, *pcsk 4* and *pcsk6* were expressed in mouse testis. For the first time we have shown that there is expression of *pcsk6* in the mouse testis. Furthermore, the expression of the three convertases analized increases in Gopc$^{-/-}$ mice. The expression of *pcsk6* was increased two fold in the knockout mice.

The results indicate that there is a relationship between the alteration of GOPC and the expression of proprotein convertases. Now it is necessary to know in which cells the studied convertases are expressed and what role these proteins play in spermatogenesis.

Poster presentation: Session 1. Topic: Histopathology. Code: 5778

Histology and Histopathology
From Cell Biology to Tissue Engineering

Determination of novel histological biomarkers for improved diagnosis and prognosis of human melanoma

Apraiz A.[1], Penas C.[1], Rasero J.[2], Asumendi A.[1], Arroyo-Berdugo Y.[1], Ezkurra P.A.[1], Morales M.C.[1], Cortés J.M.[2], Pérez-Yarza G.[1] and Boyano M.D.[1]

[1]Department of Cell Biology and Histology, UPV/EHU, Leioa, Spain, [2]Biocruces-Bizkaia Institute, Barakaldo, Spain

Early and accurate classification of patients is the cornerstone of precision medicine, intimately linked to the optimal management of cancer. This is especially relevant for melanoma, the most deadly type of skin cancer due to its high metastatic capacity and the limited therapeutic tools available to combat the spread of the disease. In fact, distant metastases are associated with median survival rates ranging from 6 to 15 months. Currently, differentiation among nevus (benign melanocytic lesion) and melanoma (malignant lesion) requires of an expert and the evaluation of several histo-morphological features including symmetry, border regularity, pigmentation pattern or lesion-size. Surgical removal of any suspicious lesion is followed by its histological analysis and staging, mainly based on the tumor thickness (Breslow thickness). Nevertheless, incorrect classification and particularly biological heterogeneity of primary melanomas lead to a very variable survival of early stage melanoma patients. This scenario supports the investment in the description of more precise tools for diagnosis and especially, for the prognosis of early stage patients.

Comparative proteomic analysis of melanoma cells lines and melanocytes was carried out by 2D-PAGE and LC-MS/MS. Differentially enriched proteins were validated at protein level (Western Blotting) or at mRNA level (RT-QPCR) in 10 melanomas and 4 normal melanocytic cells lines and most robust putative biomarkers selected for further analysis on human histological samples together with other proteins with functional relation. 32 nevi and 166 melanoma (AJCC stage I-II) formalin-fixed and paraffin-embedded biopsies were processed and stained for the selected proteins prior image scanning and classification as negative, low or high-expression samples for each of the target proteins. Samples were further re-classified as “negative” or “positive” for the most advanced statistical analysis by R 3.4.4.

PEBP1, PIR and ANXA5 levels revealed clear differences among normal melanocytes and melanoma cells and were selected, together with BCL2, BCL3 and MITF for the histological analysis. Strong and comparable staining pattern was observed for MITF and ANXA5 among nevi and melanoma samples. Moreover, we could not detect any particular pattern that could be useful to discriminate among early stage (I-II) melanoma patients with good (disease-free) and bad (metastasis) evolution. Therefore, MITF and ANXA5 were removed for further statistical analysis. According to data obtained in the cell line-based analysis, PIR and especially PEBP1 staining was stronger in nevi samples compared with melanoma samples. Fisher exact test corroborated the statistical significance of this finding. PIR nor PEBP1 were able to discriminate among early stage melanoma patients that remained disease-free and those that developed metastasis although a deepen analysis by histological melanoma subtypes pointed towards a differential expression of PIR among nodular melanoma patients with good and bad prognosis. Statistically different pattern was observed for BCL3 (but not BCL2) staining among stage I-II patients with good and bad evolution but also among stage I and stage II melanoma patients.

PEBP1 is a new and strong diagnostic biomarker for melanoma while PIR may represent a prognosis biomarker for certain melanoma subtypes.

Poster presentation: Session 1. Topic: Histopathology. Code: 5789

Histology and Histopathology
From Cell Biology to Tissue Engineering

Lung histopathological changes after dietary olive oil in a pristane-induced systemic-lupus erythematosus model

Utrilla J.C.[1], Castejón-Martínez L.[2], Fernández-Santos J.M.[1], Vázquez-Román V.[1], Martín-Lacave I.[1] and Alarcón de la Lastra C.[2]

[1]Department of Normal and Pathological Cytology and Histology, School of Medicine, University of Seville, Seville, Spain, [2] Department of Pharmacology, Faculty of Pharmacy, University of Seville, Seville, Spain

Systemic lupus erythematous (SLE) is a female predominant autoimmununе disease characterized by multiorgan disorders. Current therapy options include corticosteroids or immunosupressing drugs at the cost of considerable adverse effects and long-term morbidity. Therefore, there is a need for safer and more effective therapeutic strategies for SLE patients. In this sense, the interest of nutritional therapy is growing, such as the use of olive leaf extracts. Oleuropein (OL) is the most abundant of all the constituents of olive leaf extract and it have many beneficial properties. Pristane in BALB/c mice is an animal model of SLE widely used to test potential therapeutic agents that appears to mimic human idiopathic lupus more closely than the spontaneous strains. Even though pristane-SLE is a systemic disease, extrarenal, especially the pulmonary involvement, has not been well described. Therefore, the aim of the present study was to evaluate the use of OL and Peracetylated oleuropein (Per-OL) enriched-diets in a pristane-induced SLE model, specifically, in lung samples.

A total of 35 two-month-old female BALB/c mice were randomized in four experimental groups: (1) Sham group fed with standard diet (SD) (SD-sham group) (n=10); (2) pristane group received standard diet (SD-SLE group) (n=20); (3) pristane oleuropein group (OL) fed with standard diet supplement with OL (100 mg/kg diet) (n=15) and (4) pristane Per-OL group (Per-OL) fed with standard diet supplement with peracetilated oleuropein (100 mg/kg diet) (n=15). SLE was induced by intraperitoneal injection of 0.5 ml pristane (99% pure, Sigma). At the end of the experimental period (24 weeks), animals were euthanized and specimens were collected. Lungs were fixed in neutral buffered 4% formaldehyde, and embedded in paraffin. Five-µm sections were stained with hematoxylin-eosin and Masson trichrome stainings. Morphological changes were evaluated at the light microscopic level by two different observers. Results are expressed as percentages of cases exhibiting some of the histological characteristics.

In contrast with lung controls, we identified numerous oil droplets of different sizes in alveolar septa after pristane treatment (60%), that persisted after OL (40%) or PER-OL (60%) diets. Not perivascular or peribronchiolar infiltrates were observed in any of the treatment groups, however, inflammatory infiltrates was seen around oil droplets in pristane-treated mice (80%), and after OL diet (80%), and lightly increased in PER-OL fed animals (100%). Alveolar hemorrhage was also found in some extensive areas of the lung in all pristane-treated mice (100%), and was slightly reduced after OL (75%) and PER-OL (75%) diets. Thickened alveolar septa and some alveolar atrophy, with alveolar compensatory expansion and bulla formation were characteristics of pristane-treated mice (50%), and persisted after OL (50%) and PER-OL (70%) diets. Finally, no interstitial lung fibrosis was observed.

In relation to the variation of histological aspects among groups, OL and PER-OL diets reduced the extension of hemorrhage induced in lung after pristane, but have not effect in the frequency of oil droplets scattered along lung parenchyma. Furthermore, there is even an apparent increase in the inflammatory reaction developed around oil droplets in mice supplemented with PER-OL.

Poster presentation: Session 1. Topic: Histopathology. Code: 5790

Histology and Histopathology
From Cell Biology to Tissue Engineering

Magnetic stimulation treatment reduces atrophy and muscle injuries in an experimental model of multiple sclerosis

Peña-Toledo M.Á.[1,2], Ruz-Caracuel I.[1,3*], Leiva-Cepas F.[1,2,3**], Jimena I.[1,2,3], Peña-Amaro J.[1,2,3], Luque E.[2,3] and Túnez I.[2,4]

[1]Research Group in Muscle Regeneration, University of Córdoba, Spain, [2]Maimónides Institute for Biomedical Research IMIBIC, Reina Sofia University Hospital, University of Cordoba, Spain, [3]Department Morphological Sciences. Section of Histology, Faculty of Medicine and Nursing, University of Córdoba, Spain, [4]Department Biochemistry and Molecular Biology, Faculty of Medicine and Nursing, University of Córdoba, Spain

Present address:

* Department of Pathology. La Paz University Hospital, IDIPAZ. Madrid, Spain.

** Department of Pathology. Reina Sofia University Hospital. Cordoba, Spain.

The experimental model of Multiple Sclerosis, Experimental Autoimmune Encephalomyelitis (EAE) causes, in addition to the nervous system, changes in muscle histology indicative of a neurogenic lesion as target and core-targetoid lesions in muscle fibers. Magnetic stimulation (MS) has been tested in the EAE model showing neuroprotective effects at the clinical, biochemical and histological levels. In the present communication we analyze if the application of magnetic stimulation could counteract the muscular involvement in an experimental model of MS, decreasing the histological lesions and normalizing the biochemical parameters that appear in the skeletal muscle.

EAE was induced in Dark Agouti rats with MOG + Freund's adjuvant. Fourteen days after induction, when first disease signs appeared, MS treatment was started for 24 days. A clinical assessment of the motor capacity was made. After treatment completion, animals were sacrificed and soleus muscles were excised and processed by freezing for light microscopy. Histological and histochemical techniques were performed in cryosections and lesions were quantified. Image Pro Plus 6.0 and SigmaStat 3.1 were employed for morphometrical and statistical analysis, respectively. Lesions were counted per area and the following histomorphometrical parameters were calculated: cross-sectional area, minimum diameter and fiber typing.

The results reveal that treatment with MS exerted an improvement in symptoms as well as a reduction in the parameters of oxidative stress. At the histological level, a significant improvement was found ($p<0.05$) in muscle atrophy induced by EAE (type I fibers: 1362.90±192.71, type II fibers: 1052.49±194.33) compared to the EAE + MS group (type I fibers: 1737.35±352.04, type II fibers: 1634.09±334.41) and the number of cytoarchitectural lesions that decreased significantly ($p<0.05$), being 3.86±1.49 in the EAE group compared to 1.23±0.5 in the EAE + MS group. While in the EAE group the highest percentage (57.48) were core-targetoid lesions, in the MS treatment group were spot-type lesions the most numerous (25.95%), which is compatible with a structural recovery of the injured muscle fibers.

Treatment with MS improves the histological lesions of the skeletal muscle in experimental autoimmune encephalomyelitis. This myoprotective capacity, together with the neuroprotective, suggests that MS could be a very useful tool for MS.

Poster presentation: Session 1. Topic: Histopathology. Code: 5797

Histology and Histopathology
From Cell Biology to Tissue Engineering

Histological analysis of sarcopenia in Psoas muscle

Jiménez-Vílchez A.J.[1], Gil-Belmonte M.J.[2], Leiva-Cepas F.[2,3,4,*], Ruz-Caracuel I.[2,3,**], Peña-Toledo M.A.[3,4], López-Espejo M.E.[2], Gómez-Cabello I.[2] and Jimena I.[2,3,4]

[1]Department of Physical Medicine and Rehabilitation. Reina Sofia University Hospital, Córdoba, Spain, [2]Department Morphological Sciences, Section of Histology, Faculty of Medicine and Nursing, University of Córdoba, Spain, [3]Research Group in Muscle Regeneration, University of Córdoba, Spain, [4]Maimónides Institute for Biomedical Research, IMIBIC, Reina Sofia University Hospital, University of Cordoba, Spain

Present address:

*Department of Pathology. Reina Sofia University Hospital. Cordoba Spain

**Department of Pathology. La Paz University Hospital. IDIPAZ. Madrid. Spain

Sarcopenia is a condition consisting in retroplasia which affects skeletal muscle during ageing. It is characterized by a loss of muscle mass and a reduction in muscular strength. This leads to physical disability, a lower quality of life and a higher risk of mortality. Although the exact ethological factor remains unknown, factors such as an increased proteolysis, hormone disruption, a loss of motoneurons and a diminished vascularization are thought to affect skeletal muscle. *Psoas* has recently been proposed to be a sentinel muscle in the diagnosis of sarcopenia using imaging techniques. However, this muscle is not commonly biopsied in clinical practice due to its location.

The aim of this study is to examine the morphology of Psoas in sarcopenic patients by performing a histological analysis.

Postmortem samples from individuals aged 50 years old (middle age group) and individuals aged 80 (elderly people group) were obtained. Samples were examined by using histological and inmunohistochemical techniques. A morphometrical analysis was performed to determine the shape and size of muscle fibers, to show denervation-reinnervation processes, to establish satellite cell density and muscle vascularization.

A microscopy analysis evidenced a disruption in muscle components, including muscle fibers, satellite cells, connective tissue, innervation and vascularization in the group of elder people. A reduction in the number of muscle fibers as well as atrophy in both types of muscle fibers appeared to be evident. Fiber type grouping was observed in the 80-year-old group while it did not appear in the younger age group. There were notable differences in vascularization regarding capillary density, which was lower in elder individuals. There was also a proliferation in adipose tissue and fibrosis in elderly people group that did not show in middle age group.

This study proves that there is an alteration in the morphology of skeletal muscle in older people with sarcopenia. Psoas muscle experimented characteristic features of the sarcopenia process which could be seen through the microscope. These changes were not observed in the middle age group. Further research with a higher number of samples is needed in order to assess the use of Psoas in the diagnosis of sarcopenia.

Poster presentation: Session 1. Topic: Histopathology. Code: 5825

Histology and Histopathology
From Cell Biology to Tissue Engineering

Can bone trabeculae be useful for the assesment of the femoral neck in hip fracture patients?

Crespo P.V.[1], Sánchez-Quevedo M.C.[1], Crespo-Lora V.[2], García J.M.[1], Cano J.R.[3], Cruz E.[3] and Guerado E.[3]

[1]Tissue Engineering Group, Department of Histology, University of Granada and Instituto de Investigación Biosanitaria ibs, Granada, Spain, [2]UCG Anatomía Patológica, Complejo Hospitalario de Jaén, Spain, [3]Division of traumatology and Orthopedic Surgery, Hospital Costa del Sol, Marbella, Spain

Hip fractures in old age pose a significant public health problem. Osteoporosis is usually cited as a necessary cause. However, other studies suggest that the main risk factor for hip fracture in the elderly is trauma -usually, an accidental fall- and not osteoporosis [1]. The objective of this work is to determine whether or not the osteoporotic hypothesis may be true as a cause of hip fractures. This hypothesis states that the bone density and mineral composition are impaired in patients with hip fractures as compared to patients without this condition, and this alteration may favor the incidence of the disease.

We studied 40 patients treated with arthroplasty: 20 of them had a neck fracture of the femur and 20 of them were treated due to coxarthrosis. All patients were managed following the same diagnostic protocol and received identical antibiotic, anesthetic, surgical and antithrombotic prophylaxis. Bone biopsies were taken from the femoral head extracted to each patient. For histological study, these samples were fixed in 4% buffered formaldehyde for 24 hours followed by demineralization by immersion with continuous gentle agitation in EDTA, for 7 days, until the total disappearance of the hydroxyapatite. After washing, samples were embedded in paraffin before dehydration in a decreasing solution of ethanol and xylene, and 5µm sections were obtained and stained with hematoxylin and aqueous eosin. Three different images of each sample were taken using a Nikon Eclipse i90 light microscope at 4 different magnifications, and analyzed using ImageJ 1.51w software.

No statistically significant differences between both diagnostic groups were observed for the number, area, width and inter-trabecular distance. Significant differences were obtained for the length of the trabeculae, which was higher in the group of patients with coxarthrosis, but not when the groups were compared by gender. When compared by age, higher intertrabecular distance was observed in patients older than 75 years (middle age range) but not for the rest of the parameters analyzed here.

In previous studies using analytical electron microscopy, we observed non-significant differences in calcium, phosphorus and Ca / P levels between both groups [2]. However, in this histological study, we found significant differences for the length of the trabeculae and the intertrabecular distance. These data could explain the epidemiology of hip fracture in older patients, which may have larger distances among bone trabeculae, and shorter length and width of each trabecula, which could be associated to the most severe fracture patterns.

Supported by CTS-115 (Tissue Engineering Group).

[1] Guerado E, et al. Injury. 2016;47:S21-4
[2] Crespo PV, et al. Histology and Histopathology: cellular and molecular biology. 2017;32:(1)134

Poster presentation: Session 1. Topic: Histopathology. Code: 5837

Histology and Histopathology
From Cell Biology to Tissue Engineering

Histopathological characterization of ovine pulmonary adenomatosis in the municipal slaughterhouse of La Unión Huánuco

Chuquiyauri M.[1] and Aliaga B.[2]

[1]Faculty of veterinary medicine and zootechnics, National University Hermilio Valdizán de Huánuco, Perú, [2]Private practice

Sheep production in the world is very widespread, with 1164,000,000 sheep worldwide and 87,000,000 in South America. In our country there are approximately 12'184,000 sheep that generate 31,758 tons of carcass and 12,938 tons of wool, producing economic income for more than 1'250,000 families in the Peruvian highlands. These animals can present many diseases that are important socioeconomically and/or health for the country, it is also a susceptible species to suffer neoplasms such as ovine pulmonary adenocarcinoma (APO) or Jaagsiekte disease, viral contagious neoplasia of sheep, being rare in Goats.

The objective of this study was to determine the presence of the disease through the histopathological characteristics of the lungs of sheep affected with the Jaagsiekte virus.

508 lungs of sheep were observed in the municipal slaughterhouse of La Union for a period of two months between October and November, collecting 14 samples of lungs with nodular lesions in 10% formaldehyde. It was analyzed for definitive confirmation in the Histopathology Laboratory of the Faculty of Veterinary Medicine and Zootechnics of the National Hermilio Valdizán University.

It was observed that in 12 sheep lungs, histopathological characteristics such as the proliferation in adenomatous form at the level of the alveoli, type II pneumocytes and at the level of the respiratory bronchiole to Clara cells, macrophages were observed in the same way, flooding the pulmonary alveoli and lymphocytic infiltration at the level of the pulmonary parenchyma, also finding in two cases inflammation and thickening of the alveolar septa with deposit of fibrous tissue and hyperplasia of alveolar smooth muscle tissue with lymphocyte infiltration.

The histopathological characteristics found in the lungs of sheep are compatible with the disease of Ovine Pulmonary Adenomatosis, being in two cases associated with the disease of Progressive Ovine Pneumonia or Maedi-Visna, being a precedent the presence of the disease virus in the mountains of the Huánuco region.

Poster presentation: Session 1. Topic: Histopathology. Code: 5838

Histology and Histopathology
From Cell Biology to Tissue Engineering

Effects of sub-lethal doses of the polybrominated BDE-47 on the histopathology of digestive gland of *Mytilus galloprovinicialis*

Esteban M.A.[1], Espinosa Ruiz C.[2], Morghese M.[2], Renda G.[2], Santulli A.[2,3] and Messina C.M.[2]

[1]Fish Innate Immune System Group, Department of Cell Biology and Histology, College of Biology, University of Murcia, Mare Nostrum Campus. Spain, [2]University of Palermo, Department of Earth and Sea Science, Laboratory of Marine biochemistry and ecotoxicology, Trapani, Italy, [3]Consorzio Universitario della Provincia di Trapani, Marine BiologyInstitute, Trapani, Italy
esteban@um.es

Polybrominated diphenyl ethers (PBDEs) belong to the class of the flame retardants and are persistent and toxic pollutants, responsible of several negative effects on marine organisms. Marine bivalves, due to its feeding habits, can be exposed to a large quantity of pollutants, that can be bio-transformed in the digestive gland, the main organ involved on detoxification.

In this experiment, specimens of *Mytilus galloprovincialis,* allowed in experimental aquaria, were fed on microalgae contaminated with different sub-lethal concentrations of PBDE-47. The treatment with the compound was maintained for 15 days, followed by 15 days of detoxification. Samples of digestive glands were collected and prepared for light microscopic examination after 0 (T0), 15 (T15) and 30 (T30) days and cell structure and activity were evaluated.

The present results demonstrated that the exposure to different doses of BDE-47 was able to produce significant signs of inflammation in digestive gland from mussel. The presence of edema in digestive tubule, as well as a significant increase in the digestive tubule thickness was observed in mussels exposed to the contaminant. Furthermore, after 15 days of detoxification (T30), the analyses still showed evident signs of inflammation in mussels exposed to BDE-47, suggesting the total recovery is not happening.

The pollutant BDE-47, when tested at environmentally realistic levels, may induce a chronic status of inflammation that can compromise not only the functionality of the digestive gland and its detoxification capacity, but also can represent the basis for the impairment of the whole animal welfare and body homeostasis.

This work was supported by the project CISAS “Centro Internazionale di Studi Avanzati su Ambiente, ecosistema e Salute umana”, funded by CIPE –MIUR- CUP B62F15001070005 and Fundación Seneca de la Región de Murcia (Grupo de Excelencia grant no. 19883/GERM/15).

Poster presentation: Session 1. Topic: Histopathology. Code: 5845

Histology and Histopathology
From Cell Biology to Tissue Engineering

Biocompatibility and tissue inflammatory reactions of four commercial bleaching products

García-Bernal D.[1], Oñate-Sánchez R.E.[2], Martínez C.M.[3], Moraleda J.M.[1] and Rodríguez-Lozano F.J.[1,2]

[1]Cellular Therapy and Hematopoietic Transplant Unit, Hematology Department, Virgen de la Arrixaca Clinical University Hospital, IMIB-Arrixaca, University of Murcia, Spain, [2]School of Dentistry, University of Murcia, Spain, [3]Experimental Pathology Unit, IMIB-Arrixaca, University of Murcia, Spain.

Multiple side effects related to bleaching have been found to occur in the dental pulp tissue, including decreased cell metabolism and viability. In this work we evaluated the *in vitro* diffusion capacity, cytotoxicity and biocompatibility of four commercial bleaching products on human dental pulp stem cells (*h*DPSCs).

Two commercial bleaching gels hydrogen peroxide-based (HP), Norblanc Office 37.5% (Nor-HP) and Opalescence Boost 40% (Opal-HP) were applied for 30 min to enamel/dentine discs. Other two gels from the same manufacturers, 16% carbamide peroxide-based (CP), Norblanc Home (Nor-CP) and Opalescence CP 16% (Opal-CP), were applied for 90 min. The diffusion of HP was analysed by fluorometry. Cytotoxicity was determined using the MTT assays, determination of apoptosis, immunofluorescence assays and intracellular reactive oxygen species (ROS) level. Tissue inflammatory reactions were evaluated histopathologically in rats. Statistical differences were analyzed by one-way ANOVA and Bonferroni post-test ($\alpha<0.05$).

Normon products showed lower cytotoxicity, diffusion capacity compared to Ultradent products. A high intracellular ROS level was measured in *h*DPSCs after exposure to Opal-HP. Finally, a severe necrosis both coronal and radicular pulp was observed in Opal-HP.

Similar concentrations of carbamide peroxide and hydrogen peroxide in a variety of bleaching products exhibited different responses on cells and dental pulp tissue, suggesting that bleaching products contain unknown agents in that could influence in their toxicity.

Poster presentation: Session 1. Topic: Histopathology. Code: 5855

Histology and Histopathology
From Cell Biology to Tissue Engineering

PEDF elevation in relation to the process of calcification in placentas of women with gestacional venous insufficiency

Ortega M.A.[1], Romero B.[1], Asúnsolo Á.[2], Sainz F.[3], Bravo C.[2,4], Martínez-Vivero C.[1], Fraile O.[1], Álvarez-Rocha M.J.[1], De León-Luis J.[5], Álvarez-Mon M.[1,6], Buján J.[1] and García-Honduvilla N.[1]

[1]Department of Medicine and Medical Specialties, Faculty of Medicine and Health Sciences, University of Alcalá, Alcalá de Henares, Networking Biomedical Research Center on Bioengineering, Biomaterials and Nanomedicine (CIBER-BBN), Ramón y Cajal Institute of Sanitary Research (IRYCIS), Madrid, Spain, [2]Department of Surgery, Medical and Social Sciences, Faculty of Medicine and Health Sciences, University of Alcalá. Ramón y Cajal Institute of Sanitary Research (IRYCIS), Madrid, Spain, [3]Angiology and Vascular Surgery Unit, Central University Hospital of Defense-UAH, Madrid, Spain, [4]Service of Gynecology and Obstetrics, Central University Hospital of Defense-UAH, Madrid, Spain, [5]Service of Gynecology and Obstetrics, Section of Fetal Maternal Medicine, University Hospital Gregorio Marañón, Madrid, Spain, [6]Immune System Diseases-Rheumatology and Oncology Service, University Hospital Príncipe de Asturias, Alcalá de Henares, Madrid, Spain

Pregnancy is a period in a woman's life in which the possibility of developing disorders of the venous system increases, such as venous insufficiency of the lower limb (VI). At present, some studies show the existence of an association between pregnancy and damage to the placenta (hypoxia and apoptosis) in relation to VI. The aim of this study was to investigate the possible existence of an increase in calcification and molecules involved in placentas of women with VI in relation to this placental damage.

62 women with VI associated with pregnancy and 52 healthy control women (C) were studied. Histological techniques (Von-Kossa) revealed the presence of calcifications, as well as the classification of them. Immunohistochemistry (IHC) was used to study the protein expression of PEDF.

The presence of calcifications was higher in placentas of women with VI compared with the control population (72.72% VI vs. 52.9% C). The calcification found was classified according to the pattern that was presented. The type of calcification found in placentas of women with VI was of a dystrophic and metastatic pattern. Large accumulations of calcic formations were appreciated both in the decidual basal and at the level of the terminal villi. The study of gene expression of PEDF was performed by RT-qPCR. The levels of gene expression of PEDF were significantly higher in women with VI (25,643 AU ± 0.178 AU VI vs. 24,486 AU ± 0.195 AU C, $p<0.0001$). Accordingly, an increase in the protein expression of PEDF is observed in the placental villi of women VI.

Our results continued as the VI affects the normal functioning of the placental villi, causing a process of calcification.

This work was supported by grants from the National Institute of Health Carlos III (FIS-PI18/00846) and B2017/BMD-3804 MITIC-CM.

Poster presentation: Session 1. Topic: Histopathology. Code: 5866

Histology and Histopathology
From Cell Biology to Tissue Engineering

Exploring melanoma heterogeneity using imaging mass spectrometry

Garate J.[1], Fernandez R.[1], Ochoa B.[2], Martí-Laborda R.[3], Martin-Saiz L.[1], Asumendi A.[4,8], Lage S.[4], Velasco V.[5,8], Artola J.L.[6,8], Zabalza I.[7,8], Fernandez J.A.[1] and Boyano M.D.[4,8]

[1]Department of Physical Chemistry, UPV/EHU, Leioa, Spain, [2]Department of Physiology, UPV/EHU, Leioa, Spain, [3]Hospital Universitari Arnau de Vilanova, Lleida, Spain, [4]Department of Cell Biology and Histology, UPV/EHU, Leioa, Spain, [5]Department of Pathology. Cruces University Hospital. Barakaldo, Spain, [6]Department of Dermatology. Galdakao-Usansolo University Hospital. Galdakao, Spain,[7]Department of Pathology. Galdakao-Usansolo University Hospital. Galdakao, Spain, [8]Biocruces-Bizkaia Institute, Barakaldo, Spain

It is well known that tumor heterogeneity is responsible in part for the malignant progression and the resistance to therapies. Such heterogeneity has a molecular origin and it is not easily identified by traditional histology, which is the gold standard in melanoma diagnosis and prognosis. In this context, new technologies are emerging which enable tissue characterization as molecular level. Among them, imaging mass spectrometry (IMS) is experiencing a fast development due to its intrinsic ability to map hundreds or thousands of molecular species in a tissue section without previous labelling. In some sense, IMS is a new type of digital histology, where the different types of cells, or even different populations of the same type of cells, are identified based on their molecular signature. Here, we present a preliminary study of the application of this technique to nevus and melanoma, to highlight their cellular heterogeneity.

Frozen sections (15 µm) from nevi and primary melanoma were covered with 1,5-diaminonaphtalene (DAN) using a glass sublimator and were scanned using a LTQ-Orbitrap XL (Thermo Scientific) working at 60.000 mass resolution and 25 µm of spatial resolution (oversampling) in negative-ion mode. Data handling and analysis were carried out using MatLAB^{TM} and Orange Biolab.

The images created using IMS faithfully reproduce the histology of the tissue, highlighting that some heterogeneity exist, even in nevus, which is not easily identified using traditional histology. The images from melanoma demonstrate that the technique is able to distinguish between dermis, epidermis, tumor cells and cells from the immune system. Furthermore, the images demonstrate that the lipid fingerprint of different nodules is not identical, pointing to the existence of several subpopulations of tumor cells.

Imaging mass spectrometry allows us to study tumor cell heterogeneity and tissue microenvironment features in order to understand the malignant progression of melanoma.

Poster presentation: Session 1. Topic: Histopathology. Code: 5888

Histology and Histopathology
From Cell Biology to Tissue Engineering

Angiogenesis-lymphangiogenesis and vascular endothelial growth factor distribution in primary human pterygium

Martín-López J.[1], Pérez-Rico C.[2,3], García-Honduvilla N.[1,4], Buján J.[1,4] and Pascual G.[1,4].

[1]Department of Medicine and Medical Specialties, Faculty of Medicine and Health Sciences, University of Alcalá, Alcalá de Henares, Madrid, Spain, [2]Department of Surgery, Medical and Social Sciences, Faculty of Medicine and Health Sciences, University of Alcalá, Alcalá de Henares, Madrid, Spain, [3]Department of Ophthalmology, University Hospital Principe de Asturias, Alcala de Henares, Madrid, Spain, [4]Networking Biomedical Research Centre on Bioengineering, Biomaterials and Nanomedicine (CIBER-BBN) and Ramón y Cajal Health Research Institute (IRYCIS), Madrid, Spain

Pterygium is a common invasive ocular disease in which a fleshy fibrovascular tissue from the bulbar conjunctiva encroaches onto the cornea. The pathogenesis of pterygium involves several factors such as the presence of active angiogenic factors. Expansion of the lymphatic microvasculature has also been hypothesized. This study examines the activity of the angiogenic/lymphangiogenic factor VEGF and the expression of vascular and lymphatic endothelial proteins in pterygia and normal conjunctival tissues.

Primary grade 2 pterygium (n=20) and normal conjunctiva (n=20) biopsies were obtained during surgery after written informed consent. mRNA expression for CD31, podoplanin, and VEGF (isoforms VEGF-A and VEGF-165) were determined by qRT-PCR. Tissue samples were also processed for immunohistochemical techniques to examine the lymphatic and vascular endothelium (anti-D2-40, anti-CD31 respectively) and VEGF-A and VEGF-C levels and distribution.

VEGF-A gene expression levels failed to differ between the healthy and pterygium tissues. However, expression of its more angiogenic isoform, VEGF-165, was significantly higher in the pterygia. Immunohistochemistry revealed the greater presence of VEGF-A, compared to VEGF-C, in pterygium than conjunctiva, both in blood vessels and extracellular matrix. In addition, pterygia showed higher expression levels of the endothelial junction protein CD31. Lymphatic marker D2-40 expression was slightly augmented in this pathological tissue. The ratio between blood and lymphatic vessel counts was 1.05 in the normal conjunctiva and 3-fold this value in pterygium.

In pterygium, while both lymphangiogenesis and angiogenesis take place, the formation of new blood vessels is the most relevant event, correlating with the increased expression of vascular endothelial CD31 and an elevated blood/lymphatic vessel ratio. The presence of high levels of VEGF-A in both vessel networks and extracellular matrix in human pterygium tissue may have a major impact on angiogenesis in this pathological tissue.

Poster presentation: Session 1. Topic: Histopathology. Code: 5900

Histology and Histopathology
From Cell Biology to Tissue Engineering

Histological effects of the oral administration of microcystin-LR extract in *Ambystoma mexicanum* larvae

Benítez Flores J.C., González Valle M.R. and Chávez Ríos A.
Histology Laboratory, Morphology and Function Unit, FES Iztacala, UNAM, Mexico

Ambystoma mexicanum is a neotenic amphibian, endemic from Mexico, actually accord of the International Union for the Natural Conservation (IUNC), his conservation state is defined as in dangerous risk; one of the factor has contributed to this situation is the eutrophization of the acuatic environment in wich he lives. This situation is favorable for the massive reproduction of some cianobacterias belonging to the *Microcystis* genera, wich are associated with mortality of acuatic organisms. In many acuatic enviroments in which this ajolote lives, some investigators are detected many species that produces microcistines. In this work we evaluate the histologic changes produced in different organs for the oral administration of microcystin-LR to 8 months age larvae.

We used 14 healthy larvae of *Ambystoma mexicanum* of 8 months age, which were separated in two groups: experimental and control. The larvae of the control group were feed only with commercial pellets. The individuals of the experimental groups were feed daily during 30 days with pellets containing 20 micrograms of microcystin-LR. At the end of the experiment the larvae were sacrified. Blood smears were stained with Geimsa and samples were obtained from: skin from diferent regions, stomach, intestine, colon, liver, heart, gills, lungs, kidney and spleen. The samples were fixed with 10% formaldehide and were embedded with paraffin for the conventional method. The sections were stained with H-E and were analized for determine the histologic changes.

The histologic analysis allowed us determinate that the organs with most severe alterations were the liver, kidney, the intestine and the blood; the gills had moderate changes and the rest of organs did not have pathologic changes. In the liver the changes were moderate steatosis, accompanied of multifocal necrosis, also appearance and hipertrofia of melano-macrophage centers. In adition were observed diffuse severe atrophy of the subcapsular hematopoietic component. To kidney level the microscopic lesion consists of severe diffuse necrosis of both types convoluted tubules. In the blood smears the erithrocytes showed changes in accord with hypocromic anemia associated with changes in the leucocyte proportions.

The microcystin-LR produces in *Ambystoma mexicanum* severe non-reversible damage in organs with a high metabolism that involves life, wich are compatible with behavioural changes such as lethargy, decreased appetite and mild emaciation. The microcystin-LR can be considered as a factor that compromises the survival of this specie in nature

Poster presentation: Session 1. Topic: Histopathology. Code: 5908

Histology and Histopathology
From Cell Biology to Tissue Engineering

Evaluation of mandibular bone in an osteoporosis rat model

Trejo-Iriarte C.G.[1], Estrada-Hernández M.G.[1], García-Honduvilla N.[2,3], Gómez-Clavel J.F.[4], Garrido Fariña G.[5], Valdez-Martínez J.I.[1] and Buján Varela J.[2]

[1]Laboratorio de Investigación en Odontología Almaraz, FES-Iztacala, Universidad Nacional Autónoma de México, México, [2]Departamento de Medicina y Especialidades Médicas, Facultad de Medicina y Ciencias de la Salud, Universidad de Alcalá, Instituto Ramón y Cajal de Investigación Sanitaria (IRYCIS), Centros de Investigación Biomédica en Red de Bioingeniería, Biomateriales y Nanomedicina (CIBER-BBN), Madrid, España, [3]Centro Universitario de la Defensa de Madrid, Madrid, España, [4]Carrera de Cirujano Dentista, Laboratorio de Investigación y Educación en Odontología, FES-Iztacala, Universidad Nacional Autónoma de México, México, [5]Laboratorio de apoyo a Histología y Biología, FES-Cuautitlán, Universidad Nacional Autónoma de México, Estado de México, México
cynthia.belegii@gmail.com

Osteoporosis is a systemic polynergic, chronic and progressive disease, characterized by low bone density and micro-architectural deterioration of bone tissue. For that reason, leading to bone fragility and increased fracture risk. The evidence of mandible bone loss in women with osteoporosis has been little studied. The mandible bone has a particular pattern resorption and their lost have important repercussions, not just for loss of teeth, but also, in aesthetic, functional and phonetic form.

To evaluate new strategies in regenerative medicine through as tissue engineering, animal models offers advantages such as: higher replicability, efficiency, low cost, etc.. In this way, our objective was to evaluate if the rat osteoporosis model exhibit changes in the mandibular bone and is useful for testing new strategies in bone regeneration.

We used 20 female Wistar rats (200±50g). Randomly, in half of the specimens (n=10) were induced osteoporosis by bilateral ovariectomy (group: ovx), the remaining specimens (n=10) (sham OLD group) were kept in the process of aging at the same time. The rats were weighed and, each month after the third month, radiographic images were taken of femur and mandible bones, and the level of urine calcium was determined to verify that the ovx group had developed the disease. The osteoporosis was diagnosed at 8 months; then, in all specimens were made a defect in the right cortical mandibular (4mm long x 3 mm wide and 1 mm deep); the left side remained as the control side. After 30 days, the mandibles were obtained for routine histological evaluation. This study was approved by the Iztacala Commissions: Ethics (1268), and Biosecurity (089).

We observed significant differences in weight, since the ovx group increased its weight to twice the OLD group. Radiographically, the visual differences were evident only in the femur. However, histologically in the mandibular bone we observed an increase in the trabecular space, as well as evident narrowing of the trabeculae in the ovx group, with respect to the sham OLD group. When we performed the defects, we observed that in the ovx group the size of the bone defect was maintained, while in the sham OLD group the size decreased and in part we observed osteoid tissue filling.

In the model of OVX, after 8 months of ovariectomy, it was possible to diagnose osteoporosis and we found important histological differences between the mandibular bone of the sham OLD group and the ovx group, as well as a delay in the repair and bone regeneration, consequently, the evaluated animal model will be useful to us to prove new therapies of bone regeneration.

Poster presentation: Session 1. Topic: Histopathology. Code: 5915

Histology and Histopathology
From Cell Biology to Tissue Engineering

Is there correlation between the HER2 amplification level and the response to neoadjuvant treatment with trastuzumab and chemotherapy?

García-Caballero L.[1], Vázquez-Boquete A.[3], Santiago M.P.[2], Reboredo C.[2], Molina A.[2], Mosquera J.[2], Gallego R.[1], García-Caballero T.[1,3], Concha A.[2] and Antolín S.[2]

[1]Facultad de Medicina y Odontología, Universidad de Santiago, [2]Complejo Hospitalario Universitario de A Coruña, [3]Complejo Hospitalario Universitario de Santiago, Santiago de Compostela, España

Breast cancer is the most frequent malignant tumor in women (one in eight will suffer throughout its life) and in Spain it is still the first cause of cancer death in women (in countries like the United States it was surpassed in recent years by lung cancer). Survival has markedly improved in recent decades, mainly due to significant advances in early diagnosis and treatment. However, a significant percentage of patients (around 25%) have recurrences and finally die of metastatic disease. In addition to classical prognostic factors (size, histological type, grade or nodal status), the immunohistochemical subtype determines evolution to a large extent. Luminal subtypes (with positive hormonal receptors) have a good prognosis in general, triple negative (negativity for estrogen receptor, progesterone receptors and HER2) remains of poor prognosis, and HER2 positive significantly improved its prognosis after 1998 thanks to the therapy anti-HER2. To prescribe anti-HER2 therapy, the determination of HER2 status is usually carried out by immunohistochemistry, followed by in situ hybridization in equivocal cases (2+). There are contradictory data in the literature regarding correlation between the results of HER2 determined by FISH and the evolution. Thus, some authors find no correlation (Dowsett et al., 2009, Perez et al., 2010), while others did (Denkert et al., 2013, Fuchs et al., 2014, Press et al., 2016). The aim of this work was to correlate the results of FISH (ratio HER2/CEN17 and number of HER2 signals/nucleus) with the grade of response (Miller-Payne grading system) to neoadjuvant treatment with trastuzumab and chemotherapy.

We analyzed 100 consecutive cases of brest carcinoma treated with trastuzumab and chemotherapy in neoadjuvancy in the Complejo Hospitalario Universitario de A Coruña between 2005 and 2016. In the Complejo Hospitalario Universitario de Santiago, 4 tissue microarrays were prepared and the IQFISH (Dako-Agilent) technique was performed using 3.5 micrometers thick sections. For quantification, specific filters for Texas red and Fluorescein were used. Following the ASCO-CAP guidelines (Wolff et al., 2018), cases were considered positive if HER2/CEN17 ≥2.0 and HER2/nucleus ≥4 or HER2/CEN17 <2.0 and HER2/nucleus ≥6 (co-amplification).

Amplification for HER2 was found in 92 of the 100 cases studied. In these 92 cases, the mean of HER2/CEN17 ratios was 7.4±3.8 (range: 1.3-19.9) and the mean of HER2 signals/nucleus was 18.1±7.1 (range: 4.0-31.4). Coamplification was shown in 4 cases. Pathological Complete Response (pCR), grade 5 of Miller-Payne grading system (Ogston et al., 2003) was obtained in 58% of the patients whose tumors showed amplification. Of the 4 cases with coamplification, two obtained pCR and the other two, partial responses (grades 3 and 4 of Miller-Payne). No pCR was obtained in the 8 patients with tumors negative for FISH (not amplified). The analysis of the quantitative results demonstrated a statistical significant direct correlation between pCR and both HER2/CEN17 ratios and HER2 gene copies/nucleus (p=0.02 and p=0.04, respectively).

Conclusions: 1) The rate of pCR obtained after neoadjuvant treatment was 58% in HER2 positive cases (amplified cases). 2) No pCR was obtained in negative cases (not amplified). 3) There is a positive correlation between the HER2 amplification level and the rate of pCR obtained after neoadjuvant therapy with trastuzumab and chemotherapy.

Dowsett M, Procter M, McCaskill-Stevens W, de Azambuja E, Dafni U, Rueschoff J, Jordan B, Dolci S, Abramovitz M, Stoss O, Viale G, Gelber RD, Piccart-Gebhart M, Leyland-Jones B. Disease-free survival according to degree of HER2 amplification for patients treated with adjuvant chemotherapy with or without 1 year of trastuzumab: the HERA Trial. J Clin Oncol. 2009; 27(18):2962-9.

Perez EA, Reinholz MM, Hillman DW, Tenner KS, Schroeder MJ, Davidson NE, Martino S, Sledge GW, Harris LN, Gralow JR, Dueck AC, Ketterling RP, Ingle JN, Lingle WL, Kaufman PA, Visscher DW, Jenkins RB. HER2 and chromosome 17 effect on patient outcome in the N9831 adjuvant trastuzumab trial. J Clin Oncol 2010; 28(28):4307-15.

Denkert C, Huober J, Loibl S, Prinzler J, Kronenwett R, Darb-Esfahani S, Brase JC, Solbach C, Mehta K, Fasching PA, Sinn BV, Engels K, Reinisch M, Hansmann ML, Tesch H, von Minckwitz G, Untch M. HER2 and ESR1 mRNA expression levels and response to neoadjuvant trastuzumab plus chemotherapy in patients with primary breast cancer. Breast Cancer Res. 2013; 15(1):R11.

Fuchs EM, Kostler WJ, Horvat R, Hudelist G, Kubista E, Attems J, Zielinski CC, Singer CF. High-level ERBB2 gene amplification is associated with a particularly short time-to-metastasis, but results in a high rate of complete response once trastuzumab-based therapy is offered in the metastatic setting. Int J Cancer. 2014; 135(1):224-31.

Press MF, Sauter G, Buyse M, Fourmanoir H, Quinaux E, Tsao-Wei DD, Eiermann W, Robert N, Pienkowski T, Crown J, Martin M, Valero V, Mackey JR, Bee V, Ma Y, Villalobos I, Campeau A, Mirlacher M, Lindsay MA, Slamon DJ. HER2 Gene Amplification Testing by Fluorescent In Situ Hybridization (FISH): Comparison of the ASCO-College of American Pathologists Guidelines With FISH Scores Used for Enrollment in Breast Cancer International Research Group Clinical Trials. J Clin Oncol. 2016; 34(29):3518-28.

Wolff AC, Hammond MEH, Allison KH, Harvey BE, Mangu PB, Bartlett JMS, Bilous M, Ellis IO, Fitzgibbons P, Hanna W, Jenkins RB, Press MF, Spears PA, Vance GH, Viale G, McShane LM, Dowsett M. Human Epidermal Growth Factor Receptor 2 Testing in Breast Cancer: American Society of Clinical Oncology/College of American Pathologists Clinical Practice Guideline Focused Update. J Clin Oncol. 2018; 36(20):2105-22.

Ogston KN, Miller D, Payne S, Hutcheon AW, Sarkar TK, Smith I, Schofield A, Heys SD. A new histological grading system to assess response of breast cancers to primary chemotherapy: prognostic significance and survival. Breast. 2003; 12(5):320-7.

Poster presentation: Session 1. Topic: Teaching. Code: 5887

Histology and Histopathology
From Cell Biology to Tissue Engineering

Implementation of a new method of continuous evaluation that favor the development of the practical microscopic human organography competences in the degree in medicine

Pascual G.[1,2], Pérez-Köhler B.[1,2], García-Honduvilla N.[1,2], Buján J.[1,2] and González-Santander M.[1]

[1]Department of Medicine and Medical Specialities, Faculty of Medicine and Health Sciences, University of Alcalá, Alcalá de Henares, Madrid, Spain, [2]Networking Biomedical Research Centre on Bioengineering, Biomaterials and Nanomedicine (CIBER-BBN) and Ramón y Cajal Health Research Institute (IRYCIS), Madrid, Spain

Practical teaching is considered essential in the training of the medical student and must be carried out through the active participation of the student. The practical classes are the teaching method that strengthens the understanding of the concepts explained in the theoretical lessons, read in textbooks or exposed in seminars. It implies the development of skills, allowing to consolidate in an easier way those more theoretical concepts.

The main objective has been to develop a continuous evaluation system that allows a greater development of the practical competences in the subject of Human Organography in the Degree in Medicine at the University of Alcalá.

In order that students can optimally take advantage of the practical sessions, they were organized in small groups of 25 to 30 students. The practical sessions were dedicated to the study, observation and recognition of different tissues and organs under the optical microscope. In these practical sessions, the teacher will provide the student with a series of histologic specimens related to the tissue or organ involved, will explain the objectives of the practice and will guide the student's observations, clarifying any doubts that may arise about the identity of the histological structures. The main innovation of the new implemented method is that twenty minutes before reaching the end of each practical session the student will have to perform a test of recognition of tissue structures in relation to the practice performed. This test was based on different images, obtained from the histologic specimens used, which will be projected in large format to perform the histological diagnosis and associated structures identification.

Using the new method, a more active student participation was observed throughout the practice. The test at the end of each practical session allowed an immediate verification of the achievement of the considered competences, the development of the observation capacity along the practice session as well as the decision making, which allowed the student to confront theory and reality and develops self-confidence. Only 11.85% of the students did not develop the practical competences of the subject. The adequate coordination between the theoretical classes and the practices favored that they complement and potentiate each other effectively, contributing to an integral formation.

The proposed new methodological strategy favors the acquisition of the practical competences of the subject and promotes a more active participation of the student.

Poster presentation: Session 1. Topic: Tissue Engineering. Code: 5865

Histology and Histopathology
From Cell Biology to Tissue Engineering

Polylactic acid scaffolds, an optimal auxiliary in mandibular bone regeneration

Trejo-Iriarte C.G.[1], Rodríguez-Cortés C.A.[1], Álvarez-Pérez M.A[2]., Aguilar-Trujillo M.A.[1], Medina L.[3,4], García-Honduvilla N.[5,6], Estrada-Hernández M.G.[1], García-Muñoz A.[1] and Buján J.[5]

[1]Laboratorio de Investigación en Odontología Almaraz, FES-Iztacala, Universidad Nacional Autónoma de México, México, [2]Laboratorio de Ingeniería de Tejidos, Facultad de Odontología, División de Estudios de Posgrado e Investigación, Universidad Nacional Autónoma de México, México, [3]Instituto de Física, Universidad Nacional Autónoma de México, México, [4]Unidad de Investigación Biomédica en Cáncer INCan/UNAM, Instituto Nacional de Cancerología, México, [5]Departamentos de Medicina y Especialidades Médicas, Facultad de Medicina y Ciencias de la Salud, Universidad de Alcalá, Instituto Ramón y Cajal de Investigación Sanitaria (IRYCIS), Centros de Investigación Biomédica en Red de Bioingeniería, Biomateriales y Nanomedicina (CIBER-BBN) Madrid, España, [6]Centro Universitario de la Defensa de Madrid, Madrid, España
cynthia.belegii@gmail.com

Bone loss in the mandibular bone causes functional and aesthetic alterations. Current solutions to this problem are autologous grafts. They are considered the gold standard; however, they have some disadvantages that limit their use, due to the need for a second surgery, availability of competent sites and the limited amount of tissue that can be obtained from donor. Several strategies have been proposed to improve osteogenesis and osteogenic efficiency. The tissue engineering techniques allows the use of biomaterials as scaffolds, for achieving an optimal goal. Different biomaterials have been used as scaffolds with physical-chemical properties that resemble the tissue to be repaired. The Polylactic acid (PLA), shows interesting characteristics such as simple processing, low cost, high versatility (designs can be made according to the tissue where it will be implanted), biocompatibility, and biodegradability. When we use PLA than extracellular matrix scaffold, this biomaterial promoted cell adhesion, cell differentiation, and a new bone matrix creation.

The aim of the work is to evaluate the bone regeneration potential of a PLA-10% scaffold to improve mandibular bone regeneration.

We use PLA-10% biomaterials manufactured by electrospinning as filling material for mandibular bone defects. In vivo, we used 18 male Wistar rats (200 ± 50g) to create defects in the right mandibular cortex: 4mm long x 3 mm wide x 1mm deep. Two different strategies were used: Group PLA-10%, (the PLA membrane as a filling biomaterial) n=10; and SHAM group (without filling) n=8, where the defect damaged but not filled. After 30 days post-surgery, the jaws were removed for histological evaluation. This study was endorsed by the Commissions: Ethics (folios 1074, 1211 and 1227), and Biosecurity (folios 0036, 0071 and 0079) of the FES Iztacala.

In both groups, no inflammation was observed at 30 days post-surgery time. There was apposition of connective tissue observed around of the defects. In the PLA-10% group, the filling material was integrated and acted as scaffold, which allowed the host cells to migrate to the defect site to begin the process of bone remodeling. In the sham group, only about 50% filling was found by connective tissue, compared with the PLA10% group that presented the biomaterial, integrated and with evident areas of bone regeneration.

The PLA-10%, used as scaffold, showed good behavior as a bone filler, allowing colonization of the surrounding tissue with incipient bone regeneration. This is a good one indicative of a repairing process. Therefore, we consider that this used biomaterial can be an ideal candidate for bone tissue engineering.

Poster presentation: Session 1. Topic: Tissue Engineering. Code: 5909

Histology and Histopathology
From Cell Biology to Tissue Engineering

The histological behaviour and kinetics of calcification were evaluated during the spontaneous repair of a critical mandible defect in rat

Trejo-Iriarte C.G.[1], Alberto-Medina L.[2,3], Serrano-Bello J.[4], Mercado Márquez C.[5], Gutiérrez-Escalona R.[1], Bujan-Varela J.[6] and García-Honduvilla N.[6,7],

[1]Grupo de Investigación en Células Troncales e Ingeniería de Tejidos (GICTIT), Laboratorio de Investigación en Odontología Almaraz, FES-Iztacala, Universidad Nacional Autónoma de México, México, [2]Instituto de Física, Universidad Nacional Autónoma de México, México, [3]Unidad de Investigación Biomédica en Cáncer INCan/UNAM, Instituto Nacional de Cancerología, México, [4]Facultad de Odontología, División de Estudios de Posgrado e Investigación, Universidad Nacional Autónoma de México, México, [5]Departamentos de Medicina y Especialidades Médicas, Facultad de Medicina y Ciencias de la Salud, Universidad de Alcalá, Instituto Ramón y Cajal de Investigación Sanitaria (IRYCIS), Centros de Investigación Biomédica en Red de Bioingeniería, Biomateriales y Nanomedicina (CIBER-BBN) Madrid 28805, España, [6]Centro Universitario de la Defensa de Madrid, Madrid, 28047, España

In the constant research for new therapies for bone regeneration for mandibular bone loss, there is not much information about the size of defect and its capability for remodelling. The aim of this study was focused on a critical size defect model in mandible of rat. The histological behaviour and kinetics of calcification were evaluated during the spontaneous repair process.

Male Wistar rats (200±50g), were used to perform a mandible critical defect. Two different sites were chosen. One of them, Anterior defect, was made below mental foramen in the right hemimandible (Ad group). The other one, Posterior defect (Pd group) this defect was made forward and down the oblique line on mandible in the left side. The defect consisted of a rectangle (4 mm height x 3 mm length x 1 mm depth) made using a carbide ball end mill at 800 rpm. Both Ad and Pd groups were used for histological studies at 7, 14, 30 and 60 days after surgery (n=5 each group and time). The imaging data was acquired *in vivo*, using Albira micro-PET small animal imaging system, resulting in a: 558x558x516 image matrix with a voxel size of 125 μm. The scans where made at 7 days intervals up to 60 days after surgery. The evaluation of tissue regeneration was accomplished by manually drawing a Region of interest (ROI) in order to calculate it´s area, and then comparing it with the 7 days ROI. Hydroxyapatite concentration was calculated as a function of the difference between the density values from the defect area and the ones from a hydroxyapatite phantom of known composition, the comparison was normalized using the adjacent healthy tissue density values. This study was approve by the Iztacala Commissions: Ethics (folios 1074), and Biosecurity (folios 036).

No animals died during or after surgery, and complete reepithelialization of wounds was observed after 60 days in all specimens. At 7 days the hole defects were colonized by granulation tissue with inflammatory cells and macrophages. At 14 days bone repair is observed in both locations (anterior and posterior) from native bone edges. Remodelling signs with osteoid substance and small islands among the active connective tissue, with vascular supply. At 30 days we can observe the presence of a dense fibrous connective tissue and osteoid substance and new bone formed areas. Finally, at 60 days the defect was not complete restored, even there was neobone formed. Little differences were observed in bone tissue remodellation between anterior and posterior defects. Homogeneous bone tissue in the anterior defect and irregular deposit for osteoid substance and hypertrophic vascularization y the posterior defect remodellation. MicroCt images showed complementary dates on histology results. Blurring of the sharp contours of initial created defect at seven days, to observe new bone increasing at 14, 21 days. However, any sign of tissue repair stopped after 21 days with no changes in hydroxyapatite concentration between the 21 day data and the 60 day data, in both regions of the mandible, a non-linear analysis of the data shows a rate constant (k) of 0.03 to 0.05 per day, and a plateau value of 85% at 60 days indicates that full bone regeneration not be possible spontaneously.

We conclude that the proposed model of a critical size defect in both locations (anterior and posterior) shows properties to critical defect because showed incomplete regeneration to 60 days; that during the life of the animal, the tendency is that the defect does not close. Our model is valid to maxillofacial and dentistry bone tissue regeneration therapy protocols, its procedure very reproducible with a measurable constant of regeneration by day in a reliable way.

Poster Presentations

Session 2

Friday

Topics:

Teaching
Comparative Histology
Plant Histology
Tissue Engineering
Techniques
Tissue Biology

Poster presentation: Session 2. Topic: Teaching. Code: 5545

Histology and Histopathology
From Cell Biology to Tissue Engineering

Elaboration of a manual of practical histology classes: an integrated collaboration between students and teachers

Pereira B.F.[1], Caperuto L.C.[1], Carvalho J.E.[1] and Pitol D.L.[2]

[1]Federal University of São Paulo - Campus of Diadema - SP – Brazil, [2]University of São Paulo - FORP - Ribeirão Preto - SP - Brazil

The teaching of histology is in a constant process of modification and updating before the introduction of new technologies to which both teachers and students have access. The use of electronic media, such as digital atlases, has been gaining strength in several educational institutions. The problem that this type of material entails is the visualization only of general and/or amplified visions of materials that were highly selected and often treated by image programs, generating discomfort to the students when they are submitted to the analysis of slides that were elaborated by them or come from specialized companies. This is due to the artifacts that they may contain, such as folds, bubbles, metachromasia, discoloration, etc. This requires an approach that is inclusive of technological development as well as the methodologies used previously. With this, the objective of this work was to identify the difficulties of the students in learning histology and to elaborate together with them a practical lesson manual that allows the understanding of slides in an easy way.

For the preparation of this didactic material, 1000 students from the Medicine, Nutrition, Pharmacy and Biology courses were interviewed; and they were questioned about the following aspects: What information would be needed in a didactic material to facilitate the understanding and execution of the practical classes; Does drawing make a difference in learning? If yes, what would be the ideal layout for this activity; Is the inclusion of activities with an atlas is important for learning? If so, how this activity should be like? After the application of the questionnaire, the information was compiled for the elaboration of a manual of practical classes and evaluated by the students for possible improvements.

As a final result, two volumes of the manual of practical classes were elaborated, the first one containing the epithelial, connective (and its derivations), muscular and nervous tissues; the second containing the remaining organs and systems. As to the content, as an indication of the students, an introduction was included at the beginning of each chapter, containing only the theoretical information necessary for the visualization and understanding of the material. The inclusion of drawings was considered positive, and the layout of the ideal page was the one that presented a space for the inclusion of the identification of the slides as well as additional information, such as the technique used and a circular space, similar to the vision of the microscope for elaboration the drawing. In the section of the atlas were added photos as close as possible to the slides observed in class, indicating specific structures for identification and asked for the student to make a legend for the figure, containing the identification of the material as well as the technique used. In the end, two sections of questions were included, one referring to practical classes and one to theory.

The combination of virtual elements such as images, as well as drawings and questionnaires proved to be effective and a valid tool for the learning and application of histology, aiding in other disciplines such as pathology and physiology, for example, besides facilitating student's performance in research in the area and in the labor market.

Poster presentation: Session 2. Topic: Teaching. Code: 5671

Histology and Histopathology
From Cell Biology to Tissue Engineering

Students satisfaction with teaching of histology before and after the adaptation to the european higher education area in the ULPGC

Romero-Alemán M.M.[1,2]

[1]Departamento de Morfología, Facultad de Ciencias de la Salud, [2]Instituto Universitario de Investigaciones Biomédicas y Sanitarias, Universidad de las Palmas de Gran Canaria, Las Palmas de Gran Canaria, Spain

The guidelines of the European Higher Education Area (EHEA) have produced relevant changes in the teaching culture which require evaluation according to the European standards for quality. The *Agencia* Nacional de Evaluación de la Calidad y Acreditación (ANECA) in collaboration with the local agencies are the official organizations involved in the evaluation of the quality of individual lecturers and researchers for the continuous improvement and adaptation to the EHEA. Most of the Spanish Universities present an evaluation procedure validated by the mentioned official organizations. In the Universidad de Las Palmas de Gran Canaria (ULPGC) the evaluation programme so-called Docentia-*ULPGC* is in effect since 2008 and the student satisfaction surveys are key tools in this programme. However, the ULPGC had conducted student satisfaction surveys on the lecturer´s teaching activity since the nineties. The present study aims to compare the students´ satisfaction before (1999-2007) and nearly after the introduction of the EHEA (2011-2017) regarding the same lecturer in equivalent subjects (mainly of the Medical Degree) belonging to the same area of knowledge (Histology/Cell Biology).

We used institutional data on the student satisfaction surveys regarding the same lecturer of histology-related subjects which were available for the academic staff at the ULPGC website. These data consisted on 408 surveys obtained during the adaptation to the EHEA (academic years 2011-12, 2012-13, 2013-14, 2014-15 and 2016-17) and 362 surveys collected during the pre-EHEA period (academic years 1999-00, 2001-02, 2002-03, 2004-05 and 2005-06). First and second year medical students and first year physiotherapy students participated in the surveys on the last day of class and before the ordinary examination sessions. Summary statistics (sample size, average and standard deviation) regarding four teaching-related factors were evaluated by the students: 1) teaching methods, 2) lecturer´s attitude, 3) evaluation process and 4) lecturer´s global score (all factors included). These four factors were compared between both periods using the T-Student test for paired samples and equal variances or the Welch´s T-test for paired samples and unequal variances. F-Snedecor test determined the equality of two samples variances. The statistical significance was set at <0.05.

The students´ satisfaction was acceptable before and after the introduction of the EHEA since the average scores for all mentioned factors ranged between 3.55 and 4.13 on a 5-points scale. The evaluation of the teaching methods was significantly better ($p=0,02$) during the EHEA period whereas the lecturer´s attitude ($p<0.0001$), the evaluation process ($p<0.0001$) and the lecturer´s global score ($p=0.0003$) were better during the pre-EHEA period.

In general, there was a good level of students´ satisfaction during both periods indicating a suitable teaching activity with independence of the educational model. The improvement of the teaching methods during the EHEA period may be related to the accumulated teaching experience and updating. However, strategies and resources related to the lecturer´s attitude and evaluation methods are necessary for a more effective adaptation to the EHEA model and to improve the student´s satisfaction in the future.

Poster presentation: Session 2. Topic: Teaching. Code: 5696

Histology and Histopathology
From Cell Biology to Tissue Engineering

Exploring new virtual educational methodologies applicate to cell and tissue biology

Márquez J. and Crende O.
Department of Cell Biology and Histology, Faculty of Pharmacy, University of Basque Country (UPV/EHU), 01006 Vitoria-Gasteiz, Spain.

The Degrees in Pharmacy and Human Nutrition and Dietetics of the UPV-EHU have during the first four-month period of their first course the basic subject of Cell and Tissue Biology. This subject represents a first contact about the knowledge of the structure and function of cells and tissues in the living organisms. In this way, one of the competences that students have to achieve is to learn the basic methods for the study of the cell and the human tissues. To develop this competence, traditionally in the teaching method of laboratory practices, students had to identify and draw different objectives previously explained by the teacher in a series of histological preparations using a conventional light microscope. However, nowadays a virtual microscopy is an alternative or effective complementary methodological resource to classical classroom practices.

A virtual microscopy is a technological tool that allows the visualization of high-resolution microscopic digital images through a computer, imitating the functionality of a traditional light microscope. In this case, a database of digital images was created (virtual repository) and supply to the students with a free software, which permits the simulation of the optical microscopy. Once the students have all the material, they had to identify and paste on a notebook the required objectives by using the virtual repository and the virtual microscopy in the non-attending hours of class. This work acted as additional material to the traditionally attending laboratory practices. Finally, to evaluate the students' experience in the use of virtual microscopy an electronic survey was designed through eGela platform.

The results of the student opinion survey showed that the combined methodology of the light microscope in the laboratory and the virtual microscope on non-attending hours has resulted in a very useful tool to better interpretation, understanding and integration of the histological concepts.

This methodology allowed to develop the transversal competence of autonomous work and enables the flipped classroom method, focusing the class on the resolution of problems and possible doubts in the attending hours.

Poster presentation: Session 2. Topic: Teaching. Code: 5788

Histology and Histopathology
From Cell Biology to Tissue Engineering

Pathology trainees perception towards histology

Ruz-Caracuel I.[1,2,*], Leiva-Cepas F.[1,2,3,**], Gil-Belmonte M.J.[2], López-Espejo M.E.[2], Osuna Soto J.[2], Jimena I.[1,2,3] and Peña J.[1,2,3]

[1]Research Group in Muscle Regeneration, University of Córdoba, Spain, [2]Department of Morphological Sciences, Section of Histology, Faculty of Medicine and Nursing, University of Córdoba, Spain, [3]Maimónides Institute for Biomedical Research IMIBIC, Reina Sofia University Hospital, University of Córdoba, Spain
Present address:
* Department of Pathology. La Paz University Hospital, IDIPAZ. Madrid, Spain
** Department of Pathology. Reina Sofia University Hospital. Córdoba, Spain

Human Histology and Pathology are two close related areas. Histology is focused on the description of the normal architecture of human tissues and its changes within physiological processes. Meanwhile, Pathology studies changes in organs and systems caused by diseases. Both disciplines share the same tools and techniques. However, in Spain Medical Histology falls inside Histology area of knowledge at the university whereas Pathology is a medical specialty. That makes two worlds of what we considered two very close fields of knowledge. Our objective is to know Spanish Pathology trainees perception towards their knowledge about Histology and the role of this subject.

A survey consisting of ten items valued using a Likert 0-5 scale and five demographic questions was elaborated using Google Forms. This survey was delivered among Spanish Pathology trainees through social media applications (WhatsApp & Twitter).

A total of 81 pathology trainees answered the survey with the following distribution: 42% were “Licenciado en Medicina” (former curriculum), 39.5% were “Grado en Medicina” (current curriculum) and 18.5% had studied Medicine out of Spain. All training levels were present: 28.4% postgraduate year 1 (PGY1), 22.2% PGY2, 17.3% PGY3 and 32.1% PGY4.

The trainees valued the usefulness of knowing Histology at the beginning of the residency program with a 4.56±0.81 (mean ±standard deviation out of 5). They considered their Histology training during the Degree with a 3.22±1.07 and their training using the microscope with a 2.60±1.18. Moreover, they valued their level of knowledge of Histology with a 3.68±0.76, the level of their attending pathologists with a 4.11±0.79 and their level of knowledge of Histological techniques with a 3.21±0.96. In the teaching area, they valued with a 4.44±0.74 that Histology and Pathology should share the same Department at Universities and their capability to teach Histology with a 3.23±0.99. In a general scope, they valued with a 3.72±1.06 the usefulness of Histology for Medicine practice out of Pathology and they scored 1.89±0.92 the level of Histology of non-pathology trainees. It was remarkable participants from the former curriculum valued higher their Histology training during the Degree than participants from the current curriculum (3.41±1.58 vs 2.97±1.00, respectively)

There is a high agreement among Pathology trainees that Histology knowledge is important for their training. A warning should be raised because trainees from the current medical curriculum valued their Histology training lower that their mates from the former curriculum. Noteworthy, the item with the highest score is that Histology and Pathology should share the same Department at Universities.

Poster presentation: Session 2. Topic: Teaching. Code: 5798

Histology and Histopathology
From Cell Biology to Tissue Engineering

Assessment of histology teaching in physiotherapy degree

Ruz-Caracuel I.[1,2,**], Leiva-Cepas F.[1,2,3,*], Gil-Belmonte M.J.[2], Gómez-Cabello I.[2], Agüera-Vega A.[1,2], Peña-Toledo M.A.[1,3] and Jimena I.[1,2,3]

[1]Research Group in Muscle Regeneration, University of Córdoba, Spain, [2]Department Morphological Sciences, Section of Histology, Faculty of Medicine and Nursing, University of Córdoba, Spain, [3]Maimónides Institute for Biomedical Research, IMIBIC, Reina Sofia University Hospital, University of Córdoba, Spain
Present address:
* Department of Pathology. Reina Sofia University Hospital. Córdoba. Spain
** Department of Pathology. La Paz University Hospital. IDIPAZ. Madrid. Spain

We regard the knowledge of Histology as an essential part of Physiotherapy students' training. However, this subject is not always included in Physiotherapy studies of many other Spanish Universities. The study *curricula* for the Degree in Physiotherapy at the University of Córdoba includes a course named Tissue Basis in Physiotherapy which was established in our Faculty during the academic year 2016-2017. This subject is taught during the second year, it has 5 ECTS and includes theoretical as well as practical classes.

The aim of this study is to know the students' perception regarding a Histology course in the degree of Physiotherapy based on the assessment of some specific items.

We conducted an anonymous survey amongst students who had taken the course of Tissue Basis in Physiotherapy during two academic years (2016-2017 and 2017-2018). A total number of 77 individuals participated in this survey, which corresponded to 100% of students. Students were asked about some items focused on objectives, assessment systems, and academic activities concerning the teacher. Each item was evaluated by the student using a Likert scale ranging from 1 to 5. They were also asked about their perception of the subject, whether they considered it to be interesting or difficult. Some questions regarding attendance to theoretical and practice lessons were posed.

Briefly, the scores (mean ± standard deviation) related to the objectives were 4.58±0.65 (2016-2017) and 4.47±0.65 (2017-2018), assessment system was 4.54±0,66 (2016-2017) and 4.42±0.76 (2017-2018), and academic activities were 4.85±0.44, (2017-2018) and 4.54±0.61, (2018-2019). It was remarkable that 90% of students usually attended lessons, 92% stated to be really interested in the subject, although a 92,5% considered it to be a subject of high difficulty.

It seems that students know what the aims of this course are. They also stated to understand the assessment criteria that will be used as well as the activities that need to be done in order to achieve it. Notably, the results evidenced a high attendance rate and great interest towards the subject. Consequently, we think that the format and design of this course is adequate for the learning of transverse key skills.

Poster presentation: Session 2. Topic: Teaching. Code: 5826

Histology and Histopathology
From Cell Biology to Tissue Engineering

Evaluation of perceptions on tissue engineering as advanced therapy by postgraduate medical doctors. a conceptual, procedural and attitudinal study

Sola M.[1], Campos F.[2], Chato-Astrain J.[2], Ruyffelaert A.[3], Sánchez-Quevedo M.C.[2], Carriel V.[2], Garzón I.[2] and Campos A.[2]

[1]Family Medicine Unit, School of Medicine, University of Granada, Spain, [1]Tissue Engineering Group, Department of Histology, University of Granada and Instituto de Investigación Biosanitaria ibs, Granada, Spain, [3]Department of French Philology, University of Granada, Spain

Artificial tissues generated by Tissue Engineering are important therapeutic tools that are considered by the European Medicines Agency as medical products. However, most medical and pharmacy schools do not include specific formation on this topic in their curricula. A proper knowledge on this field would be important, since professionals of the pharmaceutic and medical areas are the responsible for the generation and use of these novel medical products and are also the main agents involved in health education during their medical activity. The present study is focused on the analysis of conceptual, procedural and attitudinal components perceived by postgraduate medicine residents toward these novel therapeutic tools.

To evaluate the perception of medical residents, we used a specific questionnaire including items related to 3 components (conceptual, procedural and attitudinal) divided in 13 topics. Each question was rated by each resident from 1 to 5 using a Likert-like scale. Statistical analysis were carried out by using the ANOVA test for pair-wise comparisons. Average values and standard deviations were calculated for each item, for each topic and for each component for male and female residents separately and for the entire sample together. To identify statistically significant differences between groups, we used ANOVA.

First, we found that the highest scores were assigned by the residents to the procedural component, followed by the attitudinal component, with the lowest values corresponding to the conceptual component. Differences among the three components were statistically significant ($p<0.05$). Average scores were statistically higher for males than for females for the conceptual and procedural components. Analysis of the topics included in the conceptual component revealed that the highest scores were found for the “Cell and tissue basis of the human body” topic, whereas the lowest values were found for “Regulatory frame”, with statistically significant differences among all topics ($p<0.001$). For the procedural component, the highest values were found for the “Biofabrication components for advanced therapies”, whilst the lowest were found for the “Centers for biofabrication and storage of advanced therapies”, with statistical differences among all topics ($p<0.001$) except for “Application and use of advanced therapies” vs. “Biofabrication components for advanced therapies”. For the attitudinal component, the highest scores corresponded to “Valuation of treatment with advanced therapies” and the lowest scores were found for the “Valuation of centers for advanced therapies” topic, with $p<0.001$ for all comparisons. In general, these results imply that medical postgraduates perceived that procedures about the implementation of advanced therapies are well established, especially in their application, although their knowledge of fields like the regulatory frame are limited. They perceived to be aware of the risks of these therapies and would prefer hospitals for their application and research centers for their fabrication.

Our analysis suggests that the background and expectatives of postgraduate medical doctors includes key aspects related to the novel advanced therapies, but future training programs and health policies should reinforce specific formative programs in these fields.

Supported by CTS-115 (Tissue Engineering Group of the University of Granada).

Poster presentation: Session 2. Topic: Teaching. Code: 5827

Histology and Histopathology
From Cell Biology to Tissue Engineering

Identification of cognitive threshold concepts in histology

Martín-Piedra M.A.[1], Saavedra-Casado S.[2], Campos F.[1], Ruyffelaert A.[3], Sánchez-Porras D.[1], Durand-Herrera D.[1], Irastorza-Lorenzo A.[1] and Campos A.[1]

[1]Tissue Engineering Group, Department of Histology, University of Granada and Instituto de Investigación Biosanitaria ibs, Granada, Spain, [2]Hospital Comarcal de Melilla, Spain, [3]Department of French Philology, University of Granada, Spain

Threshold concepts [1,2] are cognitive notions whose understanding implies a significant and irreversible learning for the discipline to which the concepts belong. Theoretically, understanding a threshold concept is transformative for learning, resulting in an integrative reinforcement effect with other related disciplines. Therefore, learning threshold concepts requires a relevant effort, but once understood, they are hardly forgotten. The identification of the threshold concepts of Histology is a didactic strategy for the optimization of teaching and the reinforcement of Histology as a transversal discipline for the integration of the rest of the disciplines of Medicine curricula.

64 first year students of the degree in Dentistry were enrolled in this study. The study was carried out once the students had finished their compulsory studies in Histology. Previously, relevant information about threshold concepts as a teaching strategy was provided by an expert histologist. Then, students were asked to rate 6 basic threshold concepts previously selected by the teachers using a 5-point Likert scale to determine whether or not these concepts were threshold concepts according to the students' perception.

All concepts were rated by students with high values (higher than 3), meaning that these notions previously selected as key terms by the teachers were also considered by students as concepts whose comprehension is crucial for learning Histology. The concepts of morphology (4.34±0.84) and its relation with structure and function (4.28±0.87) were considered as the most relevant terms. It is possible that this interaction be perceived as a highly integrative notion. The concept of paradigm was rated 3.67±1.02. Teachers selected this item as a threshold concept due to the relevance of histology in a paradigm shift for clinical therapy, together with the development of tissue engineering. It is possible that students are not as aware as teachers of the relevance of Histology in the near future.

Identification of threshold concepts by the students could contribute to determine which concepts are the most problematic, integrative and transforming for the students, allowing a more significant comprehension of Histology concepts and terms. In general, our analysis of students' perception regarding threshold concepts provided relevant information that could be used for the design of teaching programs that should modulate the way and time in which Histology is taught in the future with the objective of achieving a more integrative understanding.

Supported by CTS-115 (Tissue Engineering Group of the University of Granada).

[1] Bhat T, et al. Med Educ. 2018;52(6):620-631
[2] Neve H, et al. Med Teach. 2016;38(8):850-3

Poster presentation: Session 2. Topic: Teaching. Code: 5828

Histology and Histopathology
From Cell Biology to Tissue Engineering

Perception of the students enrolled in a participative teaching program in tissue engineering at the University of Granada

Garzón I.[1], Chato-Astrain J.[1], Sánchez-Porras D.[1], Durand-Herrera D.[1], García-García O.D.[1], Fernández-Valadés R.[1,2], Oyonarte S.[1,3] and Martín-Piedra M.A.[1]

[1]Tissue Engineering Group, Department of Histology, University of Granada and Instituto de Investigación Biosanitaria ibs, Granada, Spain, [2]Division of Pediatric Surgery, University Hospital Virgen de las Nieves, Granada, Spain, [3]Cell and Tissue Bank of Granada-Almería, Spain

Tissue engineering is a well-stablished experimental science in which engineering and biological principles are used to develop bioengineered tissues that could restore the structure and function of damaged tissues. The usefulness and effectiveness of these techniques allowed the generation of several types of artificial tissues that were successfully translated to the clinical setting, and a number of novel medicines will be generated in the future by tissue engineering [1]. One of the objectives of the curricula in Medicine and related areas should be the progressive incorporation of this discipline in the different formative programs. In this context, the University of Granada has recently implemented the studies of Tissue Engineering as an elective subject for students of the degree in Biotechnology, while this subject was previously incorporated to the Medicine curriculum. In both cases, a participative teaching program is used.

The purpose of this study is to analyse the level of satisfaction of the Tissue Engineering students enrolled in both University degrees.

A Tissue Engineering teaching program integrating classical lecture-based teaching was implemented with a complete laboratory formation approach. This laboratory formation consists of 5 practical modules: cell culture, cell viability, scaffolds design, decellularization and quality controls. Each module has its own set of learning objectives. To evaluate the perception of the students regarding this participative learning program and their satisfaction with the teaching system, a specific questionnaire was used. Each student was asked to score each question of the questionnaire using a Likert-like score ranging from 1 to 5.

Both groups of students (medical and biotechnology students) showed high global levels of satisfaction with the course (average 4.67 in medical students and 4.31 in biotechnology students). Perception related to the teaching method combining classical lectures with a strong laboratory formation was scored 4.67 by medical students and 4.42 by biotechnology students. Finally, the evaluation system used in this subject was rated by the medicine and biotechnology students 4.50 and 4.19, respectively.

These results show the highly positive perception of the students enrolled in the Tissue Engineering subject. The fact that the student participates actively in the formation process and the strength of the practical modules were very well valuated by the students. In addition, our results suggest that the participative learning model approach is better valuated by medical students as compared to biotechnology students, probably due to the fact that biotechnology students are more used to basic laboratory teaching approaches than medical students. In summary, this combined learning system could be a good approach for teaching Tissue Engineering and may be implemented in other related subjects.

Supported by CTS-115 (Tissue Engineering Group)

[1] Sola M, et al. PLoS One. 2019;14(4):e0214950

Poster presentation: Session 2. Topic: Teaching. Code: 5829

Histology and Histopathology
From Cell Biology to Tissue Engineering

Influence of the type of evaluation on the final performance of students of medical cytology

Chato-Astrain J., Martín-Piedra M.A., Sánchez-Porras D., Irastorza-Lorenzo A., García-García O.D., Carriel V., Alaminos M. and García J.M.

Tissue Engineering Group, Department of Histology, University of Granada and Instituto de Investigación Biosanitaria ibs, Granada, Spain

Different types of exams are routinely used to evaluate performance of the students enrolled in the subjects of cytology and histology. However, several reports suggest that the type of exam may significantly influence performance of Medicine and Health Sciences students [1]. In fact, the learning strategies used by the students may vary according to the type of exam, ranging from metacognitive to repetition strategies. In addition, it has been suggested that medical students may have difficulty performing and interpreting certain types of information that is provided to them during the evaluation process [2].

The present work is focused on the analysis of different types of exam questions that are presented to a group of medical students in order to determine their performance and success rate in each type of question.

The subject *Cytology, Inheritance and Development* is taught during the first year of the degree in Medicine of the University of Granada, and a final exam is done at the end of the subject to evaluate each student's knowledge and skills. In this work, we analyzed all questions related to human cytology of this final exam. These questions are presented to the students in different forms: 1) a set of 20 multiple-answer test questions, 2) a long question to develop in one page, 3) 2 short questions to answer in brief, 4) 2 drawings and cytology images that the student should identify and interpret, 5) 2 structures that the student must draw, 6) a problem that the student must solve using the previously-acquired cytological knowledge. 231 students took the final exam and were included in the study. For each type of question, averages and standard deviation scores were obtained. Differences between two specific types of questions were assessed using the ANOVA test, and correlations were analyzed by the Kendall tau test.

Analysis of the different types of questions revealed that the highest scores corresponded to the images that the student must interpret (7.62±1.91), whereas the lowest scores were found for the problem-based questions (3.53±2.41). Differences among the different question types were statistically significant for all comparison except for long questions vs. drawings to do and drawings to do vs. problems (ANOVA $p<0.05$). No differences among genders were found for any of the types of questions (ANOVA $p>0.05$), but a significant correlation among all exam types was detected ($p<0.05$ for the Kendall tau test).

These results suggest that students feel more comfortable and perform better when they are asked to interpret a cytological image or to choose among different pre-set questions in a test. In contrast, they find difficulties to correlate different concepts that are necessary to solve a problem. Although these results should be confirmed in the future, we may hypothesize that the learning strategies that medical students use to apply are rather based on visual memorization of concepts and images instead of a real significant knowledge correlating and integrating all the acquired knowledge. Therefore, an integrative teaching approach should be implemented.

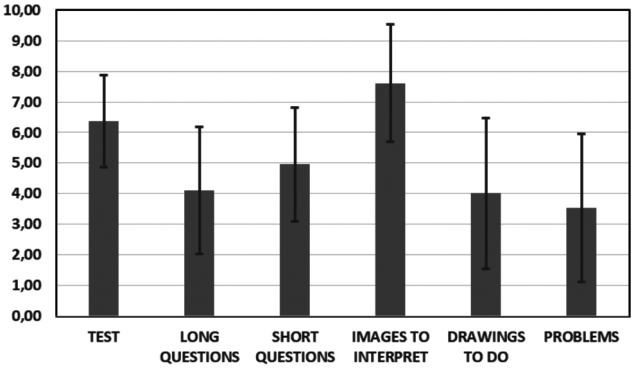

Fig. 1. Average and standard deviation scores assigned by the students to each type of question.

Supported by CTS-115 (Tissue Engineering Group).

[1] Bloom TJ, et al. Curr Pharm Teach Learn. 2018;10(2):235-242

[2] Stansfield RB, et al. BMC Med Educ. 2016;16(1):268

Poster presentation: Session 2. Topic: Teaching. Code: 5836

Histology and Histopathology
From Cell Biology to Tissue Engineering

Gamification and mobile devices: use of kahoot! as a tool for test practice in the cell biology and histology subject

del Valle E., Martínez-Pinilla E., Tolivia J. and Navarro A.

Department de Morphology and Cell Biology, Faculty of Medicine and Health Sciences, University of Oviedo, Spain. Instituto de Neurociencias del Principado de Asturias (INEUROPA), Spain. Instituto de Salud del Principado de Asturias (ISPA), Spain

The development of the Information Technologies and Communication Technologies (ICTs) opens a new world of possibilities in Higher Education, among them to try to increase students' motivation. With this premise we have incorporated the use of mobile devices in the Cell Biology and Histology subject together with the free platform Kahoot! due to the small problem that we observed in the students of the first year of the Degree in Biology, in which the subject of Cell Biology and Histology is located. The theoretical knowledge of the students is evaluated through a multiple choice type test, being for the majority of them the first time they face this type of exam. We think, it would be useful when preparing the test that the students could have a prior training with some extra motivation, which led us to choose Kahoot!, since this tool not only allows us to create questionnaires but offers real time results, establishing a ranking in which students can see their position. Therefore, we are at the same time training, reviewing and playing.

The teacher creates a series of multiple choice tests with questions similar to those of the evaluation exam. During the Classroom Practice the students answer the questions on their own devices, while games are displayed on a shared screen to unite the lesson. At the end on the test, results are discussed and those questions with the less number of hits are reviewed and explained by the students who have succeeded.

The use of Kahoot! has increased the motivation of students with a percentage of class attendance of 79.8%. The students valuate the experience as very positive as playing Kahoot! gives them a taste of what the real exam could be as well as information about what parts of the subject they need to revised. There were also differences between the results obtained in the Kahoot! test and those of the official evaluation with most of the students having higher marks in the last one.

Kahoot! is a suitable tool for multiple choice test practice, increases student's motivation and gives them information about their particular level of knowledge about the different topics of the subject.

Poster presentation: Session 2. Topic: Teaching. Code: 5928

Histology and Histopathology
From Cell Biology to Tissue Engineering

Evaluation of the teaching of the contents of histology in the degrees of nursing, physiotherapy and pharmacy

Madrid J.F.[1] and Sáez F.J.[2]

[1]Department of Cell Biology and Histology, School of Medicine, University of Murcia, [2]Department of Cell Biology and Histology, School of Medicine and Nursing, University of the Basque Country UPV EHU, Leioa, Vizcaya, Spain

The Royal Decree 1393/2007 establishes the ordering of university teaching in Spain. In its preamble some objectives are the harmonization of European university systems, and the stimulation of the flexibility and capacity of innovation of the universities, among others. In the same communication, the universities are given autonomy for the design of study program, but they will be verified by the accreditation agencies that created the national and regional authorities. On the other hand, the degrees that qualify for professional practice related to health should respond to certain criteria established by national authorities (RD 967/2014). To what extent does this regulation, which on the one hand unifies, but on the other hand make flexible, affect the homogeneity of the teaching of Histology contents in the different Degrees, specifically those of Nursing, Physiotherapy and Pharmacy?

Histology has four blocks of teaching: Cytology or Cell Biology, General Histology, Special Histology, and General Embryology. The teaching activity can be developed through lectures, laboratory practices, seminars, etc. Surveys were taken to the members of the Spanish Society of Histology and Tissue Engineering to obtain information on the number of theoretical hours, practices, seminars, etc. in which the Cell Biology, General Histology, Special Histology and General Embryology are imparted, in the degrees of Nursing, Physiotherapy and Pharmacy. In the case of universities in which no information was obtained by the surveys, we tried to find it in the corresponding web pages.

The results are very varied among the three degrees analyzed. But within the same degree they also differ greatly from one University to another, being the teaching of Histology in many of them absent. And in the cases in which there is a subject that contains the teaching of Histology its content is very varied in terms of the extension dedicated to the four blocks. The block of General Embryology is practically nonexistent.

The Universities have exercised their autonomy in the design of the study programs, with a maximum flexibility. The accrediting agencies have not exercised a homogenizing role that, while tolerating university flexibility and autonomy, ensures a certain degree of similarity in the teaching of the same degree in the different Universities. These differences make it difficult for students to move, since the credits taken at one University would not be recognized at the destination university.

The accrediting agencies should play a role that guarantees a certain measure of similarity in the teaching of the same degree in the different Universities, at least in the degrees that qualify for the exercise of a profession. The Scientific Societies can help in this work.

Poster presentation: Session 2. Topic: Comparative Histology. Code: 4641

Histology and Histopathology
From Cell Biology to Tissue Engineering

Prenatal histomorphological development of the rumen in *Dama dama*

Redondo E.[1], Gázquez A.[1], Ortega C.[2], Peña F.J.[2] and Masot A.J.[1]

[1]Histology and Pathology and [2]Laboratory of Equine Reproduction and Spermatology, Department of Animal Medicine, Faculty of Veterinary Science, University of Extremadura, Cáceres, Spain

Histological studies on ruminal mucosa have been carried out in both domestic (García et al. 2012) and wild-type ruminants (Franco et al. 2017). Comparative análisis of the forestomach mucosa in red deer during prenatal development (Masot et al., 2007) confirm that prenatal development of the red deer rumen is similar to that reported in goat (García et al. 2012), but somewhat slower than that recorded for sheep (Franco el al., 2011) and cattle (Vivo et al.,1990). The aim of the present study was to describe the morphology of the fallow deer rumen during prenatal development, using structural, histomorphometric and immunohistochemical methods.

A total of 25 fallow deer embryos were used, from the first stage of prenatal life until birth. Tissues for histological examination were fixed in 4% buffered formaldehyde, routinely processed and stained with Hematoxylin-Eosin, Masson`s Trichrome and Gomori's reticulin. Samples for morphometric analysis were viewed through a microscope equipped with a digital video camera; digital images were analyzed using the Nis-Element 2.30 software package. The UltraVision One HRP polymer system was performed on tissue from forestomach for immunohistochemistry. Samples were incubated with the following primary antibodies: 1:10 mouse monoclonal anti-Synaptophysin; ready-to-use rabbit polyclonal anti-Glial Fibrillary Acidic Protein; ready-to-use mouse monoclonal anti-Vimentin; 1:50 rabbit polyclonal anti-Neuropeptide Y; and 1:50 rabbit polyclonal anti-Vasoactive Intestinal. For scanning electron microscopy samples were fixed in 2.5% buffered, dehydrated through graded ethanol and amyl acetate, and dried in a critical-point dryer. Sections were covered with coating materials including gold and examined at a magnification of 10 to 800x.

The appearance of the rumen from the primitive gastric tube was observed at 51 days of prenatal 21% gestation). By 57 days (24% gestation) the ruminal wall comprised three layers: an internal epithelial layer, a middle layer of pluripotential blastemic tissue and an external layer or serosa. Ruminal pillars were visible at 72 days (30% gestation), and by 85 days (35% gestation) ruminal papillae were starting to appear. Synaptophysin cells were detected at 85 days (35% gestation) in the lamina propria, submucosa, tunica muscularis and myenteric plexus; while glial fibrillary acidic cells, and vimentin cells, were found at 108 days (45% gestation) and 63 days (26% gestation), respectively, in lamina propria, submucosa, tunica muscularis and serosa. Neuropeptide Y and vasoactive intestinal polypeptide were detected immunohistochemically at 180 days (75% gestation) and 192 days (80% gestation) respectively, in both the lamina propria and submucosa. Under scanning electron microscopy, by 80 days (33% gestation) small ruminal papillae were observed protruding from the surface.

In comparison to other wild and domestic-type ruminants, histomorphogenesis of the rumen in *Dama dama* was similar to that reported in red deer and goats, but rather slower than that observed for sheep or cattle.

Poster presentation: Session 2. Topic: Comparative Histology. Code: 4642

Histology and Histopathology
From Cell Biology to Tissue Engineering

Prenatal histomorphological development of the reticulum in *Dama dama*

Redondo E.[1], Gázquez A.[1], Ortega C.[2], Peña F.J.[2] and Masot A.J.[1]

[1]Histology and Pathology and [2]Laboratory of Equine Reproduction and Spermatology, Department of Animal Medicine, Faculty of Veterinary Science, University of Extremadura, Cáceres, Spain

Several studies have addressed the prenatal development of stomach compartments in domestic and wild ruminants, but few have dealt specifically with the reticulum (García et al., 2013a). Moreover, the ontogenesis of the reticulum in *Dama dama* had not previously been charted. The aims of the present study were as follows: to describe the morphological changes occurring in the *Dama dama* reticulum during prenatal development, using scanning electron microscopic, histomorphometric and immunohistochemical techniques.

A total of 25 fallow deer embryos were used, from the first stage of prenatal life until birth. Tissues for histological examination were fixed in 4% buffered formaldehyde, routinely processed and stained with Hematoxylin-Eosin, Masson's Trichrome and Gomori's reticulin. Samples for morphometric analysis were viewed through a microscope equipped with a digital video camera; digital images were analyzed using the Nis-Element 2.30 software package. The UltraVision One HRP polymer system was performed on tissue from forestomach for immunohistochemistry. Samples were incubated with the following primary antibodies: 1:100 mouse monoclonal to Cytokeratin; 1:10 mouse monoclonal anti-Synaptophysin; ready-to-use rabbit polyclonal anti-Glial Fibrillary Acidic Protein; ready-to-use mouse monoclonal anti-Vimentin; 1:50 rabbit polyclonal anti-Neuropeptide Y; and 1:50 rabbit polyclonal anti-Vasoactive Intestinal. For scanning electron microscopy samples were fixed in 2.5% buffered, dehydrated through graded ethanol and amyl acetate, and dried in a critical-point dryer. Sections were covered with coating materials including gold and examined at a magnification of 10 to 800x.

Differentiation of the reticulum of the primitive gastric tube was observed at 55 days of prenatal life (23% gestation). By 60 days (25% gestation) the reticular wall comprised three layers: an internal epithelial layer, a middle layer of pluripotential blastemic tissue and an external layer or serosa. The primary reticular crests were visible at 91 days (38% gestation) as evaginations of the epithelial stratum basale. Secondary reticular crests were observed at 146 days (61% gestation). Epithelial cytokeratin immunopositive cells were observed at 85 days (35% gestation) in the stratum basale of epithelium. The synaptophysin cells were stained at 85 days (35% gestation), in the lamina propria, submucosa, tunica muscularis and serosa. The vimentin and glial fibrillary acidic cells, were observed at 60 days (25% gestation) and 103 days (43% gestation), respectively, in myenteric and submucosal plexuses, and scattered throughout the lamina propria, submucosa, tunica muscularis and serosa. The neuropeptide Y, and vasoactive intestinal polypeptide cells were detected at 180 days (75% gestation) and 190 days (80% gestation), respectively, in the lamina propria, submucosa, muscular mucosae, tunica muscularis, serosa and myenteric plexuses.

Prenatal development of the reticulum appears to take place somewhat earlier in *Dama dama* than in sheep or cattle, but at a similar stage to that reported in goats and red deer.

Poster presentation: Session 2. Topic: Comparative Histology. Code: 4643

Histology and Histopathology
From Cell Biology to Tissue Engineering

Prenatal histomorphological development of the omasum in *Dama dama*

Redondo E.[1], Gázquez A.[1], Ortega C.[2], Peña F.J.[2] and Masot A.J.[1]

[1]Histology and Pathology and [2]Laboratory of Equine Reproduction and Spermatology, Department of Animal Medicine, Faculty of Veterinary Science, University of Extremadura, Cáceres, Spain

During prenatal life, the stomach of ruminant animals suffers some morphological changes to suit its function in postnatal life. In the omasum, the morphological changes are the growth and development of the omasal laminae covered with conical papillae in order to play a role in the digestive process. This work studies the morphological changes taking place in the *Dama dama* omasum during prenatal development using histomorphometrics, scanning electron microscopic and immunohistochemistry analysis as well as carrying out a comparative analysis of this species with other wild (red deer) and domestic-type ruminants.

A total of 25 fallow deer embryos were used, from the first stage of prenatal life until birth. Tissues for histological examination were fixed in 4% buffered formaldehyde, routinely processed and stained with Hematoxylin-Eosin, Masson's Trichrome and Gomori's reticulin. Samples for morphometric analysis were viewed through a microscope equipped with a digital video camera; digital images were analyzed using the Nis-Element 2.30 software package. The UltraVision One HRP polymer system was performed on tissue from forestomach for immunohistochemistry. Samples were incubated with the following primary antibodies: 1:10 mouse monoclonal anti-Synaptophysin; ready-to-use rabbit polyclonal anti-Glial Fibrillary Acidic Protein; ready-to-use mouse monoclonal anti-Vimentin; 1:50 rabbit polyclonal anti-Neuropeptide Y; and 1:50 rabbit polyclonal anti-Vasoactive Intestinal. For scanning electron microscopy samples were fixed in 2.5% buffered, dehydrated through graded ethanol and amyl acetate, and dried in a critical-point dryer. Sections were covered with coating materials including gold and examined at a magnification of 10 to 800x.

Differentiation of the omasum as a separate compartment of the primitive gastric tube was observed at 35 days of prenatal life (23% gestation). By 38 days (25% gestation) the omasal wall comprised three layers: an internal epithelial layer, a middle layer of pluripotential blastemic tissue and an external layer or serosa. Omasal laminae appeared in the following order: primary at 38 days (25% gestation), secondary at 50 days (33% gestation), tertiary at 59 days (39% gestation) and quaternary at 64 days (43% gestation). Neuroendocrine cells were detected by synaptophysin at 52 days (35% gestation), in the lamina propria, submucosa, tunica muscularis and myenteric plexus; while glial cell markers (glial fibrillary acidic protein, and vimentin) were observed at 64 days (43% gestation) and 38 days (25% gestation), respectively, in myenteric and submucosal plexuses, and scattered throughout the lamina propria-submucosa and tunica muscularis. Sympathetic and parasympathetic nerve fibers and nerve bodies were detected via neuropeptide Y and vasoactive intestinal polypeptide at 95 days (63% gestation) in the lamina propria and submucosa, tunica muscularis and serosa.

Prenatal development of the omasum appears to take place somewhat earlier in *Dama dama* than in sheep or cattle, but at a similar stage to that reported in goats and red deer.

Poster presentation: Session 2. Topic: Comparative Histology. Code: 5777

Histology and Histopathology
From Cell Biology to Tissue Engineering

The structural and ultrastructural anatomy of the whale eye, with special interest in the structures that control eye pressure

Vecino E., Zulueta A., Pereiro X. and Ruzafa N.

Experimental Ophthalmo-Biology Group, Department of Cell Biology and Histology, Faculty of Medicine, University of the Basque Country UPV/EHU, Vizcaya, Spain

The eye of the second largest mammal of the world, the fin whale *(Balaenoptera physalus),* was studied 24h post-mortem (after its beaching), comparing its structure to that of the human eye. To understand the capacity of this very large mammal (20 tons) to adapt its eye to very variable pressures, from those at sea level to a depth of 300 mts, the anatomy, structure and ultrastructure of the eye was studied. Glaucoma is the leading cause of blindness in humans, mainly provoked by an increase in eye pressure. Analysing the mechanisms used by other mammals to stabilize eye pressure could provide clues to understand these alterations and their possible solutions in humans.

The structure and ultrastructure of the fin whale's very large eye ball (1 Kg) was first studied macroscopically and then, by HE and trichromic staining of paraffin sections, before carrying out an ultrastructural analysis by scanning and transmission electron microscopy. Special attention was paid to the corneo-esclera angle, as well as to the retina and ciliary body. A tissue specific to this animal found at the back of the eye caught our attention and was therefore studied in more detail.

Macroscopically, the fin whale eye has a very thick sclera (4 cm) that protects the retina from the back of the eye. There was no corneal epithelium and the collagen fibres of which were thinner than those in the sclera. Clots were found in diverse eye structures, like the iris and retina, forming very regular structures like a hive. Moreover, the retinal vasculature was comprised of very large radial blood vessels that are situated quite superficially, occupying the retinal ganglion cell layer, inner plexiform layer and part of the inner nuclear layer. A cavernous tissue was detected at the back of the eye, surrounding the optic nerve, and it is composed of blood vessels of different sizes surrounded by a very dense network of elastic fibres.

We propose that the thick sclera of the fin whale eye is an adaptation to the deep sea habitat, serving to protect the retina from the pressures to which it is exposed in the depths of the ocean. The cornea occupies a limited space at the front of the eye ball is protected by large eyelids. The retraction of the eye in deep sea and its extrusion at the surface is aided by a cavernous tissue, which is thought to represent a physiological adaptation to the changes of pressure at different sea depths.

Supported by Retos Mineco FEDER (RTC-2016-48231), PUE 2018-4, UPV/EHU PPGA 18/18

Poster presentation: Session 2. Topic: Comparative Histology. Code: 5800

Histology and Histopathology
From Cell Biology to Tissue Engineering

Histological effects of two brewery by-products-based diets in mullet (*Chelon labrosus*) liver

Piñera-Moreno R.[1], Vílchez-Gómez L.[1], Ceballos-Francisco D.[1], Guardiola F.A.[1,2] and Esteban M.A.[1]

[1]Department of Cellular Biology and Histology, Faculty of Biology, University of Murcia, Campus of International Excellence, *Campus Mare Nostrum,* Murcia, Spain, [2]*Centro Interdisciplinar de Investigação Marinha e Ambiental* (CIIMAR), University of Porto, Porto, Portugal
faguardiola@um.es, aesteban@um.es

The importance for Mugilidae in aquaculture is based on their worldwide presence and the natural ability to take advantage in their nutrition of single-cell proteins (microalgae, bacteria, marine fungus and yeasts) or detritus (Cardona, 2015). However, there are few published works that evaluate the morphology of the hepatic tissue of these species fed diets supplemented with by-products or waste from the food industry. Therefore, the aim of this study was to evaluate the effects of the two brewery by-products formulated diets in the liver of *Chelon labrosus*.

Raw materials from the waste of a brewing industry were used to prepare both diets. The diets were isolipidic, isoprotein and isoenergetic, while two different fatty acid profiles were considered. Diet A had a marine profile of fatty acid (fish oil) whilst the Diet B had a terrestrial profile of fatty acid (extra virgin olive oil). Both diets included 62.5% of spent brewer's yeast of the wet weight. The diets were tested in fish maintained at two different salinity concentrations (1 and 36 ppm). Eight tanks with twenty fish each one were used. The fish were fed daily at a rate of 1.5% body weight for 60 days. At the end, five fish of each tank were sacrificed. The livers were dissected and fixed (10% neutral buffered formalin, 24 h). After serial dehydration steps in alcohol, the samples were embedded in paraffin, sectioned (5 µm), mounted and stained with haematoxylin-eosin. Slides were analysed by a light microscope (Leica DM750) and images were acquired with a Leica MC170 digital camera for analysis using ImageJ. These parameters were evaluated: *i)* total lipidic area, *ii)* nuclei numbers and *iii)* mean area of hepatocytes.

The results showed that the level of the total lipidic area and the nuclei numbers in the liver of fish fed Diet A at 36 ppm was higher compared to group fed Diet B at both salinities. Finally, the mean area of hepatocytes increased in the liver of fish fed Diet A compared to fish fed Diet B at the same salinity (1 ppm). These results confirm that the liver is a good sensitive organ for determining the nutritional effects of experimental diets.

This research was funded by the *Fundación Biodiversidad* (Convocatoria-Pleamar, FEMP 2017/2424) and the *Fundación Séneca de la Región de Murcia* (grant number 19883/GERM/15, *Grupo de Excelencia*).

Cardona, L. 2015. Food and Feeding of Mugilidae. In: *Biology, Ecology and Culture of Grey Mullets (Mugilidae)*. CRC Press, Boca-Raton; London; New York: pp. 165–195.

Poster presentation: Session 2. Topic: Comparative Histology. Code: 5927

Histology and Histopathology
From Cell Biology to Tissue Engineering

Immunohistochemical study of hypoxia markers in porcine oviducts during the estrous cycle

Párraga Ros E.[1], López Albors O.[1], Aparicio González M.[1], Boronat Belda T.[2], Candanosa Aranda E.[3] and Latorre Reviriego R.[1]

[1]Department of Anatomy and Comparative Pathology, Campus of Excellence Mare Nostrum, Veterinary Faculty, Murcia, Spain, [2]Unit of Cell Physiology and Nutrition, Miguel Hernández University, Elche, Alicante, Spain, [3]Veterinary Pathology, Faculty of Veterinary Medicine, National Autonomous University of México

Oxygen (O_2) rates in the oviduct are essential during the implantation and embryonic development in both human and animal reproduction. In this sense, hypoxia inducible factors (HIFs) are considered the main regulators of O_2 homeostasis. The HIF complex activates target genes involved in several processes such as the suppression of oxidative phosphorylation and the promotion of glycolysis by the expression of glycolytic enzymes and the glucose transporters (GLUT1 and GLUT3). HIFs are also involved in the energy metabolism through pH control by the action of the carbonic anhydrase (CA), a family of enzymes that regulate bicarbonate concentration in hypoxic situation, especially CAIX. Research works showed the oviductal expression of hypoxia markers in rodent models. However, in other models such as pigs no previous studies have been reported. Therefore, the objective was to characterize the expression of HIF-2α, GLUT1 and CAIX in porcine oviducts throughout the estrous cycle.

Oviducts of adult sows (n=15) were collected at a local slaughterhouse immediately post-mortem. Ovarian morphology was used to establish the estrous cycle phase. The middle portion of the ampulla and isthmus were removed and fixed in paraformaldehyde at 4ºC for histological and immunohistochemical analysis. The primary rabbit polyclonal antibodies HIF-2α, GLUT1 and CAIX (1:100, Abcam Inc.®) and secondary goat anti-rabbit IgG antibody (1:200) were used. Histological sections of ureter, kidney and uterus were the positive controls by the high expression of HIF-2α, GLUT1 and CAIX in these organs respectively. The negative controls were sections that were not added to the primary antibody. The immunohistochemical staining was quantified with a Leica QWin® work station from a series of 10 digital pictures randomly taken from each stained section, considering for each antibody separately the histological layer (epithelium, lamina propria and muscularis), the oviduct portion (ampulla and isthmus), and the functional stage (Follicular, F; Early luteal, EL; Late luteal, LL). Data of % immunopositively area were used for a descriptive analysis (SPSS, IBM Statistics Inc., Chicago, IL, USA) and the differences among the estrous cycle analyzed with the non-parametric Mann-Whitney test for $p<0.05$ of significance.

All the three markers showed a ubiquitous expression in the oviduct, especially in the epithelium. Significantly lower expression of HIF-2α was found in the luteal phases (EL and LL), especially in the isthmus. GLUT1 expression did not change throughout the estrous cycle, but differences were found between the ampulla and isthmus at F and EL phases. CAIX showed higher levels in the isthmus but only by cycle differences between the F and EL phases in ampulla.

The ubiquitous expression of hypoxia markers enhances the relevance of O_2 in the porcine oviduct physiology. The differential expression of HIF-2α, GLUT1 and CAIX throughout the estrous cycle and the portion of the oviduct, might have functional implications related to pre-implantation in the embryonic development or the conservation of the spermatozoon and oocytes during the fertilization. These precedent demand further studies aimed at determining the factual O_2 tension levels under physiological conditions.

Poster presentation: Session 2. Topic: Plant Histology. Code: 5791

Histology and Histopathology
From Cell Biology to Tissue Engineering

Seed anatomy of six *mimosa* species (Leguminosae-Mimosoideae) distributed in Mexico

Montaño-Arias S.A.[1], Zavaleta-Mancera H.A.[2], Grether R.[3], Montaño N.M.[3], Camargo-Ricalde S.L.[3] and Pacheco L.[3]

[1]Colegio de Postgraduados en Ciencias Agrícolas, [2]Posgrado de Ciencias Agrícolas, Unidad de Microscopía Electrónica, Departamento de Botánica, Estado de México, México, [3]Universidad Metropolitana de México, Campus Iztapalapa, Departamento de Biología, Ciudad de México, Mexico
arias_susan@hotmail.com

The morphology of the seeds of some species of the subfamily Mimosoideae has been studied in order to contribute to the taxonomy of *Mimosa*. However, the seed anatomy of many of these species has yet to be described, and therefore their taxonomic and ecological implications are unknown. Thus, in this work, the anatomy of the seed coat of six *Mimosa* taxa distributed in Mexico was described and analyzed.

Eight individuals per species were selected, with similar height and coverage. All of the mature fruits from each individual were collected and the seeds were extracted immediately thereafter. From only healthy, mature seeds, those of similar size and weight were selected. They were then processed for light microscopy (LM) and scanning electron microscopy (SEM). The LM seeds were softened in distilled water for 2-3 h. The seed coat and the cotyledons were separated and fixed in FAA. The tissues were processed for paraffin. For SEM, the dry tissues were coated with gold and were observed with a JEM 6390 SEM, at 10 kV.

The seed coats showed one or two layers of sclereids: one layer of macrosclereids and another of osteosclereids. Likewise, all of the species exhibit the lucid line which is located in the apical or medial portion of the macrosclereids. All the seeds of the species have a prominent external cuticle and a vitreous endosperm. These characters prevent initial germination and increase the longevity of the seed, and are the likely cause of its impermeability.

Poster presentation: Session 2. Topic: Plant Histology. Code: 5794

Histology and Histopathology
From Cell Biology to Tissue Engineering

Influence of altitude on the wood anatomy of *Mimosa luisana*, a species endemic to Mexico

Montaño-Arias S.A.[1], Chicharo-Alonso P.S.[2], Camargo-Ricalde S.L.[2], Grether R.[2], Montaño N.M.[2] and Pacheco L.[2]

[1]Colegio de Postgraduados en Ciencias Agrícolas, Departamento de Botánica, Estado de México, México, [2]Universidad Metropolitana de México, Campus Iztapalapa, Departamento de Biología, Ciudad de México, México
arias_susan@hotmail.com

Mimosa luisana Brandegee (Leguminosae-Mimosoideae) is biologically, ecologically, and culturally important in the Tehuacán-Cuicatlán Valley. The results of biological, ecological, and physiological studies show that *M. luisana* is potentially valuable for the ecological restoration of semi-arid environments; however, studies that might validate this proposal are needed. Thus, the objective of this work was to determine the anatomical characters that are influenced by altitude.

Three sites with different altitudes were selected: *i*) Site one (S1), 881 masl; *ii*) Site two (S2), 993 masl, and *iii*) Site three (S3), 1,653 masl. At each site, three individuals of similar height and coverage were selected. In the laboratory, blocks were prepared for the macroscopic study. For the microscopic description, cubes of 1x1 cm were prepared in order to obtain transverse, tangential, and radial sections (20 µm), which were then stained with safranin-fast green and mounted in synthetic resin.

Regardless of altitude, the wood showed diffuse porosity, and the vessels are round and oval; the diameter of the vessels varies between sites: at S1, the vessels are of the largest diameter and are thick-walled, while at S3, the vessels are of the least diameter and are thin-walled. Length does not depend on altitude, since the vessel elements are short in all three cases. The rays are homogenous with procumbent cells, but the wood from S1 exhibits mainly triseriate and rarely biseriate rays, while the wood from S2 and S3 shows biseriate and rarely uniseriate rays. The shortest fibers are those of S3.

The results indicate that the characters influenced by altitude are vessel diameter and wall thickness, the number of ray series, and fiber length, which is consistent with the results of other studies of other plant taxa.

Poster presentation: Session 2. Topic: Plant Histology. Code: 5802

Histology and Histopathology
From Cell Biology to Tissue Engineering

Petiole and rachis histology of eight species of the genus *Diplazium* (Athyriaceae-Polypodiopsida)

Pacheco L.[1], Montaño Arias S.A.[1,2] and Guzmán-Cornejo L.[1]

[1]Área de Botánica, Departamento de De Biología, Universidad Autónoma Metropolitana-Iztapalapa, Ciudad de México, México, [2]Colegio de Posgraduados Campus Montecillo, Estado de México. Mexico
pacheco@xanum.uam.mx

Diplazium is a worldwide genus of almost 350 species in primary wet montane forests; with about 100 species that are in the Neotropics. The morphology of the sporophyte is very variable and there are too few studies regarding the phylogeny of the genus. The histological characteristics are not generally taken into account for the segregation of the species in groups and subgroups. The histology of the petiole and rachis of *D. aberrans, D. atirrense, D. ceratolepis, D. chimborazense, D. lellingeri, D. pactile, D. pinnatifidum y D. rivale* was studied as a contribution to the knowledge of the genus and looking for additional characteristics that could help to separate the species in groups.

The material was collected in different locations of Costa Rica and Ecuador. The backup material is found in the Metropolitan Herbarium (UAMIZ). The petioles and rachis were preserved in Formalin-Acetic acid-Alcohol (FAA), after many dehydration stages with gradual alcohols; the material was included in wax to be cut afterwards with an American Optical 820 Spencer microtome. Other sections of the same material were processed in a freezing microtome and others were hand cut. The sections were dyed with fast green safranin and were placed in synthetic resin. Other cuts were dyed in lugol, toluidine blue, acid fluoroglucine and sudan III, to detect cellular contents. Drawings and pictures were taken in a clear camera using a Carl Zeiss microscope.

The petiole of the studied leaves has two vascular bundles, formed by the xylem exarch, with hookliked-curved apex inwards, the phloem surrounds the xylem; the bundles stay separated upto the rachis where they join in its abaxial apex. In *D. aberrans* this union occurs in the base of the lamina and forms a U-like bundle. Every bundle is surrounded by one or two layers of rectangular cells of the pericycle and by a layer of the cells of the endodermis thickening in a U-like form or in the radial walls. The parenchyma cells are found in between the cells of the xylem. These parenchyma cells have vacuoles with unidentified cellular content, and in between these, we can find a mucilage cavity. The external cortex is a continuous layer of sclerenchyma, while the inner one and the pith have cells of the parenchyma with abundant excentric and concentric starch bodies. Abundant cavities of mucilage are found in the pith and in the cortex, except in *D. aberrans, D. pinnatifidum* and *D. rivale*. The pneumatophores are found in both sides of the petiole. The mucilage of these species is proper of a polysaccharide.

The presence of secretory tissues of polysaccharides can be a characteristic that help us separate in groups the species of *Diplazium*, because these can be found in the cortex and in the pith, associated to the parenchyma of the xylem as in *Diplazium asperum* or not found at all. However, due to the number of the species that has the genus more studies are needed.

Poster presentation: Session 2. Topic: Plant Histology. Code: 5803

Histology and Histopathology
From Cell Biology to Tissue Engineering

Leaf epidermis morphology of 15 species of the genus *Diplazium* (Athyriaceae-Polypodiopsida)

Pacheco L.[1], Montaño Arias S.A.[1,2] and Guzmán-Cornejo L.[1]

[1]Área de Botánica, Departamento De Biología, Universidad Autónoma Metropolitana-Iztapalapa, Ciudad de México, México, [2]Colegio de Posgraduados Campus Montecillo, Estado de México, México
pacheco@xanum.uam.mx, arias_susan@hotmail.com

Diplazium has over 350 species all around the world, from which, nearly 100 are neotropical. Morphologically, we can distinguish the genus by the back to back sori, the stalk of the sporangia with two or three cell rows, the annulus that comes back to its original position after its dehiscence, its basic chromosome number x=41, and by the spores with their perisporium wingliked. The leaf epidermis morphology of *D. aberrans, D. andinum, D. atirrense, D. ceratolepis, D. chimborazense, D. chocoense, D. godmanii, D. lellingeri, D. macrodictyon, D. pactile, D. pinnatifidum, D. ribae, D. rivale, D. sanderi*, and *D. stolzei* was studied as a contribution to the knowledge of the genus and looking for additional characters that could help us separate the species in taxonomic groups.

Leaf fragments were collected from the Metropolitan Herbarium (UAMIZ). Leaf segments of 1 cm^2 were discolored from an aqueous 6% solution of KOH during many days to observe the stoma type and the shape of the epidermis cells. Afterwards, it was dyed with watery safranin at 1% to facilitate its observation. The stoma index, the frequency of the stomata by mm^2, the size of guard cells, adjacent cells, abaxial and adaxial ordinary epidermal cells, were determined by taking 25 random measures of each species. To obtain the frequency of the stomata, the number of the stomata was counted with a 16X objective with Optovar 2 in a Carl Zeiss microscope. Drawings were made in a clear camera and pictures were taken in a Carl Zeiss microscope. The adult stomata were described according to van Cotthem (1970).

The abaxial and adaxial epidermis have a single compact layer of cells with walls slightly thickened. The epidermal cells are elongated with winding edges as in the majority of the species or almost isodiametric and with right edges as in *D. andinum, D. lellingeri* y *D. atirrense*. The stoma are hypostomatic of polocytic type and parietocytic subtype; the smallest guard cells correspond to *D. lellingeri* (36-60x12-20 mm) and the biggest to *D. pactile* (68-88x12-16 mm) and *D. aberrans* (64-84x16-20 mm). The subsidiary cells surround almost completely the guard cells, the shape of the subsidiary cells can be almost isodiametric with curved walls as in *D. atirrense* and *D. lellingeri* or cells with winding edges as in the majority of other species.

The size of the guard cells in *D. pactile* and *D. aberrans*, suggest that both species are polyploids. Because of the morphology of epidermis and subsidiary cells, two groups of species can be recognized, those with isodiametric cells as in *D. andinum, D. lellingeri* and *D. atirrense* and those with winding edges as in the rest of the taxa. However, due to the number of the species that has the genus, more studies are needed.

Poster presentation: Session 2. Topic: Plant Histology. Code: 5891

Histology and Histopathology
From Cell Biology to Tissue Engineering

Leaf epidermis morphology of six species of the genus *Anemia* (Anemiaceae-Polypodiopsida)

Delgadillo Rojas C.[1], Guzmán-Cornejo L.[2] and Pacheco L.[2]

[1]Licenciatura en Biología, Universidad Autónoma Metropolitana-Iztapalapa, Ciudad de México. México, [2]Área de Botánica, Departamento de Biología, Universidad Autónoma Metropolitana-Iztapalapa. Ciudad de México. México
cdelgadillo800@gmail.com, pacheco@xanum.uam.mx

The species of the genus *Anemia* are terrestrial, they live primary in the New World, but few live in Africa, India, and islands in Indian Ocean. There are about 115 species. The leaf epidermis morphology of *Anemia adiantifolia, A. hirsuta, A. jaliscana, A. karwinskiana, A. phyllitidis* and *A. speciosa*, was studied as a contribution to the knowledge of the genus and looking for additional characters that could help us separate the species.

The material was collected in different locations of Chiapas, Jalisco, and Veracruz, Mexico, additional fragments were collected from UAMIZ. The backup material is found in the Metropolitan Herbarium (UAMIZ). Leaf segments of 1 cm^2 were discolored from an aqueous 6% solution of KOH during many days to observe the stoma type and the shape of the epidermis cells. Afterwards, it was dyed with watery safranin at 1% to facilitate its observation. The stoma index, the frequency of the stomata by mm^2, the size of guard cells, adjacent cells, abaxial and adaxial ordinary epidermal cells, were determined by taking 25 random measures of each species. The adult stomata were described according to van Cotthem (1970).

The epidermis in *A adiantifolia* is pilosa, with stiff white hairs, *A. hirsuta* and *A. karwinskyana* have laminas hirsute, *A. jaliscana* has epidermis short hairly adaxially, *A. phyllitidis* is hirsute only on costae, *A. speciosa* is glabrate beneath. The stomata in *A. adiantifolia, A. phyllitidis* and *A. speciosa* are found on the abaxial surface, in *A. karwinskyana, A. hirsuta* and *A. jaliscana* are found on adaxial and abaxial surface. Four species have pericytic stomatal type; only *A. adiantifolia* and *A. karwinskiana* have polocytic stomatal type. The smallest guard cells correspond to *A. adiantifolia* and the biggest to *A. jaliscana; A. hirsuta* has small and big guard cells; the epidermal cells are elongated with winding edges as in the majority of the species only *A. speciosa* has amorphous epidermal cells. The subsidiary cells are ovate with winding edges in the majority of the species, but in *A. speciosa* and A. hirsute are orbicular with winding edges and *A. jaliscana* has its subsidiary cells elongated with winding edges.

There is much variation in the pattern of the epidermal cells. On the same plant the cells of the abaxial epidermis are generally more convoluted or more winding edges than are those of the adaxial epidermis. The size of the guard cells in *A. jaliscana* suggests that this species is polyploid. The different size of the guard cells in *A. hirsuta* suggests hybrid origin. The epidermis of these species is the first time to describe, but we need study additional taxa before we have an adequate understanding of the epidermis of *Anemia.*

Poster presentation: Session 2. Topic: Tissue Engineering. Code: 5688

Histology and Histopathology
From Cell Biology to Tissue Engineering

Human adipose derived stem cells (hASCs) as a therapeutic tool for oligodendrocytes oxidative stress damage

Garrido-Pascual P., Burón M., Palomares T. and Alonso-Varona A.
Faculty of Medicine and Nursing, University of the Basque Country UPV/EHU, Bizkaia, Spain

Oligodendrocytes, the myelin producing cells of the central nervous system (CNS), are remarkably vulnerable to oxidative stress due to their high metabolic rate and their low concentration of antioxidant enzyme glutathione. In a state of oxidative stress, oligodendrocytes may undergo irreversible damage of lipids, proteins and DNA, cell degeneration and death. In the field of regenerative medicine, it has been pointed out the relevance of human mesenchymal stem cells (hMSCs) for cell therapy. Among the different types of MSCs, human adipose-derived mesenchymal stem cells (hASCs) present several advantages. They can be easily obtained, display a greater proliferation capacity and low immunogenicity and secrete soluble factors that could regulate neuroinflammation and oxidative stress.Herein, we develop an *in vitro* model of oligodendrocytes exposed to oxidative stress microenvironment, in order to evaluate the therapeutic role of hASCs.

In this study, we differentiated human oligodendroglioma cell line (HOG) to oligodendrocytes (HOGd). For their differentiation, HOG cell line was cultured in high glucose (4.5 g/l) DMEM with N2 supplement, 30 nM triiodothyronine (T3) and 0.05% fetal bovine serum for 8 days. Differentiation was assessed by quantifying MOG, MBP and CNPase expression by western blot. Then, we cultured HOGd with 0.25 mM H_2O_2 for 1 hour. After the oxidation, damaged HOGd were cultured with: *i*, hASCs conditioned media (CM), *ii,* hASCs, and *iii,* hASCs subjected to oxidative stress. To analyze the neuroprotective effect of hASCs, at 0, 24 and 48h HOGd proliferation rate (Hoechst 33342), intracellular ROS levels (H2-DFC-DA probe) and mitochondrial membrane potential (MMP, MitoTracker®Red CMXRos probe) were measured.

Firstly, we confirmed the differentiation level of HOG cell line towards oligodendrocytes. The HOGd cells showed a higher expression of MOG, MBP and CNPase than HOG. When exposed to 0.25 Mm H_2O_2, HOGd reduced their proliferation rate, exhibited a higher intracellular ROS levels and higher MMP compared to control. Damaged HOGd cultured with hASCs CM showed a higher proliferation rate respect to control, whereas no change in ROS or MMP was observed. In the case of damaged HOGd cultured with hASCs, or hASCs subjected to oxidative stress, there were no differences regarding proliferation, however a significant decrease in ROS and MMP was detected when compared to control.

This *in vitro* model had proved to be adequate to evaluate the therapeutic potential of hASCs. Besides, it showed that hASCs subjected or no to oxidative stress ameliorated H_2O_2-induced toxicity in HOGd, being much more efficient than hASCs CM.

1.Liessem-Schmitz, A. et al. J. Mol. Neurosci. 66, 229–237 (2018).
2.Brand, A. et al. Neurochem. 105, 1325–1335 (2008).
3.Ni, J. et al. Cell. Physiol. Biochem. 48, 1710–1722 (2018).
4.Parimisetty, A. et al. J. Neuroinflammation 13, 67 (2016).

Poster presentation: Session 2. Topic: Tissue Engineering. Code: 5707

Histology and Histopathology
From Cell Biology to Tissue Engineering

Adipose-derived mesenchymal stem cells conditioned medium atenuated ultraviolet B-induced aging on human dermal fibroblasts

Burón Aizpiri M.[1], Garrido-Pascual P.[2], Alonso-Varona A.[1] and Palomares Casado T.[2]

[1]Department of Cell Biology and Histology, [2]Department of Surgery, Radiology and Physical Medicine and Nursey, Faculty of Medicine UPV/EHU, Leioa, Vizcaya, Spain

Ultraviolet B (UVB) irradiation is responsible for a variety of skin pathologies, ranging from sunburn or skin aging to cancer development [Schuch et al. 2014]. Epidemiological, clinical and biological studies indicate that solar UV radiation is the major etiological agent of skin cancers [Liu et al. 2013]; for these reasons, photoprotection has become a topic of increasing interest. Human adipose-derived stem cells (ADSCs) have been used for skin regeneration with promising results. However, recent studies have revealed that implanted cells do not survive for long; this limitation could be overcome by the use of ADSCs paracrine factors delivered to medium, instead of administering living cells. In fact, it has been indicated that conditioned media of ADSCs (ADSCs-CM) show therapeutic effects similar to those which can be achieved by the ADSCs themselves [Vizoso et al. 2017].

In this study, we investigated the effects of ADSCs-CM in UVB-irradiated human dermal fibroblasts (HFFs) as therapeutic potential in skin aging.

ADSCs were cultured in DMEM supplemented with Glutamax (1%), sodium pyruvate (1mM) and penicillin-streptomycin (100U/ml), and ADSCs-CM was collected at 48 hours. HFFs were cultured in DMEM, without phenol red, supplemented with 10% FBS, L-glutamine (4mM), sodium pyruvate (1mM) and penicillin-streptomycin (100U/ml). HFFs were treated with ADSCs-CM for 24 hours before UVB irradiation (5-37 mJ/cm^2). The *in vitro* effect of treatment was evaluated by determining: i) cell iability (colorimetric *Presto Blue* assay), ii) cell morphology (phalloidin-iFluor 488 staining), iii) senescence phenotype (activity of β-galactosidase, SA-β-gal), iv) cell migration (wound-healing model based on a two-well culture insert).

Pretreatment with ADSCs-CM for 24 hours had a stimulatory effect on the proliferation or irradiated HFFs compared to non-treated group. Furthermore, ADSCs-CM reduced the percentage of senescent SA-β-gal-positive cells and preserved the fibroblastic cell shape compared to untreated group. In addition, ADSCs-CM also promoted cell migration. Thus, at low irradiation doses, treated HFFs migrated 1.5 times higher than untreated cells.

ADSCs-CM increase proliferation and migration, and reduce senescence in UVB- irradiated HFFs. These results suggest that pretreatment with ADSCs-CM could have a photoprotective effect on cell photoaging caused by UV-B.

Liu Q. et al. Biotechnol Left. 2013; 35(10):1707-1714.
Schuch AP. Environ Sci Technol. 2014; 7;48(19):11584-11590.
Vizoso FJ. Int Mol Sci. 2017; 25;18(9).

Poster presentation: Session 2. Topic: Tissue Engineering. Code: 5731

Histology and Histopathology
From Cell Biology to Tissue Engineering

Biological characterization of electrospun webs for the adhesion and growth of human dental pulp and periodontal ligament stem cells

Salvador-Clavell R.[1], Pascual C.[2], Mata M.[1,3], Sancho-Tello M.[1], Milián L.[1], Carda C.[1,4], Blanes M.[2] and Martín de Llano J.J.[1]

[1]Department of Pathology and Health Research Institute of the Hospital Clínico (INCLIVA), Faculty of Medicine and Dentistry, University of Valencia, Valencia, Spain, [2]Research Group of Technical Finishing, Biomedicine and Health of the Technical Research Center AITEX, Alcoy, Spain, [3]Ciberes, Instituto de Salud Carlos III, Spain, [4]Ciber-BBN, Instituto de Salud Carlos III, Spain

Periodontal diseases are pathological conditions that affect the periodontal supporting structures of the teeth. The progression of the disease causes loss of periodontal ligament, cementum and alveolar bone and, eventually, loss of teeth. Several treatment approaches have been developed but complete periodontal regeneration cannot be predictably achieved. Electrospun webs are thin scaffolds composed of polymer fibers on which human cells can adhere, proliferate and, under some conditions differentiate. During the electrospinning process additives can be loaded that influence the characteristics of the web or will modify the properties of the cells grown on them. The results that we present correspond to the initial biological characterization of webs that we are using for the development of a double-sided web for the treatment of periodontal disease. Human dental pulp stem cells (hDPSC) and human periodontal ligament stem cells (hPDLSC) can differentiate, among other cell types, into osteoblasts and cementoblasts, respectively. The double-sided web will facilitate, on one side, the regeneration of the alveolar bone (cells differentiated from hDPSCs) and, on the other, the regeneration of the cementum, as well as the periodontal ligament connecting both structures (cells differentiated from hPDLSC).

Poly lactic-*co*-glycolic acid (PLGA), poly ε-caprolactone (PCL) and polyvinylpyrrolidone (PVP) webs were produced by electrospinning, treated with plasma and sterilized. hDPSC and hPDLSC stem cells were cultured following standard procedures. Culture media conditioned with web fragments for 1, 3, 7, and 30 days at 37 °C were tested to determine their cytotoxicity by means of the MTS cell viability test. Cell adhesion and proliferation on the webs were studied by clamping web sections on Millicell EZ slides and culturing cells on them. After eosin and DAPI staining, samples were observed by fluorescence microscopy. Finally, the properties of PLGA webs containing hydroxyapatite nanoparticles were studied.

PVP webs showed unwanted properties in cell culture media and its use was discarded. Media conditioned with PLGA and PCL webs for 1, 3 and 7 days were not cytotoxic for hDPSC and hPDLSC cells. When media conditioned in extreme conditions (i.e., 30 days conditioning) were used a slight decrease in cell viability was observed. The structure of PCL webs changed when cells were cultured on them for 1 to 7 days, likely because of the immersion in the cell culture media, avoiding the histological study of the cells. Both hDPSC and hPDLSC cells adhered and proliferated on PLGA webs. The structure of the PLGA webs was maintained and the webs could be handled for histological characterization. The addition of hydroxyapatite nanoparticles did not greatly modify the PLGA web physical properties when used for the culture of hDPSC but altered the cell distribution on the web.

PVP and PCL webs cannot be used in the experimental design that we have developed, as the webs show undesirable physical changes under these conditions. PLGA webs are not cytotoxic and allow one to culture hDPSC and hPDLSC on them. Hydroxyapatite nanoparticles alter the hDPSC distribution on PLGA webs and could promote osteoblast differentiation.

Poster presentation: Session 2. Topic: Tissue Engineering. Code: 5732

Histology and Histopathology
From Cell Biology to Tissue Engineering

Morphological analysis of an acellular nervous scaffold for its potential use in peripheral nerve injury reconstruction

Tamez-Mata Y.A.[1], Pedroza-Montoya F.E.[2], Martínez-Rodríguez H.G.[2], Ríos-Cantú A.A.[3], García-Pérez M.M.[3], Soto-Domínguez A.[4], Montes-de-Oca-Luna R.[4], Peña-Martínez V.M.[1] and Vílchez-Cavazos F.[1]

[1]Universidad Autónoma de Nuevo León, "Dr. Jose Eleuterio Gonzalez" University Hospital, Orthopedics and Traumatology Department and Bone and Tissue Bank, Nueva León, México, [2]Universidad Autónonoma de Nuevo León, School of Medicine, Biochemistry Department, Cell Therapy Laboratory, Nueva León, México, [3]Universidad Autónoma de Nuevo León, "Dr. Jose Eleuterio Gonzalez" University Hospital, Plastic Surgery Department, Nueva León, México, [4]Universidad Autónoma de Nuevo León, School of Medicine, Histology Department, Nueva León, México

Peripheral nerve injuries (PNI) are one of the most frequent causes of sensorimotor deficit and disability in adults. The surgical gold standard treatment for extensive lesions is autografts. However, these have certain disadvantages such as: limited availability, donor site morbidity and neuroma formation. For this reason, acellular nerve allografts (ANA) are an alternative option. The objective of this study was to compare the morphological characteristics of the fast decellularization method (FDM) in peripheral nerve (PI) versus freeze-thaw decellularization (FTD) and stored fresh (SF) nerve method, for its potential use in PNI reconstructions.

Lamb's (PI) were procured and processed by three different methods (FDM, FTD, SFN) over a period of five days. The FDM consisted on frequent changes of: sulfobetaines (SB-10 and SB-16), phosphate buffer (PB), phosphate buffered saline (PBS) and ABC chondroitinase; meanwhile FTD method, the nerves were freezed at -80°C and thawed at room temperature for 12 h; the nerves treated by SF method, were refrigerated at 4°C. Subsequently, the samples were fixed and processed by conventional histological technique. Histological stains with: Hematoxylin and Eosin (H&E) was performed for general evaluation, and Masson's Trichrome (MTC), to prove connective tissue nerve components. In addition, histochemistry with: Klüver-Barrier (KB), Periodic Acid of Schiff (PAS) and Marsland-Glees-Erikson (MGE) silver impregnation stains were executed; they selectively identify myelin, external lamina (EL) and axons, respectively.

Morphological analysis revealed that FDM efficiently removed (90%) cellular elements, cytoplasm and myelin in the nervous scaffold, compared with the FTD and SFN methods whose efficiency was 50 and 10%, respectively. Moreover, it was observed that with the FDM the connective tissue, the EL, and the axons were successfully preserved in the acellular scaffold.

Decellularization of peripheral nerve based on FDM was the most effective technique for cellular and myelin removal, with a successful preservation of extracelular matrix (ECM) and axons. The ECM components (collagen fibers and EL) are necessary elements for nerve recellularization. It is intended that with the FDM, several ANA could be developed and applied *in vivo* lambs and afterwards in clinical-medical area to reconstruct PNI in humans.

Histology and Histopathology
From Cell Biology to Tissue Engineering

Articular cartilage regeneration induced by scaffold implantation: *in vivo* and computational model

Márquez-Flórez K.[1,2,3], Garzón-Alvarado D.[1,2], Milián L.[3,4], Forriol Brocal F.[5], Carda C.[3,4,6] and Sancho-Tello M.[3,4]

[1]Department of Mechanical and Mechatronic Engineering, Universidad Nacional de Colombia, Bogotá, Colombia, [2]Numerical Methods and Modeling Research Group (GNUM), Universidad Nacional de Colombia, Bogotá, Colombia, [3]Department of Pathology, Universitat de València, Valencia, Spain, [4]INCLIVA Biomedical Research Institute, Valencia, Spain, [5]Orthopaedic Surgery Department, Clínico-Malvarrosa Hospital, Valencia, Spain, [6]CIBER-BBN, Spain.

We evaluated the mechanism of *in vivo* long-term cartilage regeneration (from 1 week to 12 months), after implanting a cell-free biostable polymeric scaffolds into a rabbit's knee. Also, we developed a simulation tool to predict the results of implanting the scaffolds within the defect in the articular cartilage. The animal model allows us to characterize the neo-tissue, while the computational model provides insights into the mechanical conditions for cartilage regeneration.

Cell-free polymeric-biostable scaffolds were implanted in a knee articular cartilage defect of 2-month-old rabbits[1]. Animals were sacrificed at 1 and 2 weeks, and at 1, 3, and 12 months after implantation. The morphological characteristics of the new tissue were studied through histological procedures.

For the computational model, a plain strain axisymmetric 2D geometry was developed to represent a simplify cartilage/bone/scaffold structure (Figure 1). Subchondral compact bone, trabecular bone, and implant were modeled as poroelastic materials[2], whereas the cartilage was modeled as a poroelastic fibril reinforced material[3].

At one week, the scaffolds remained aligned with the native articular cartilage and delimited by a sharp bloody line. By the second week, a thin layer of amorphous tissue was observed on top of the scaffold. At one month, the native cartilage had proliferated around the defect. At three months, the

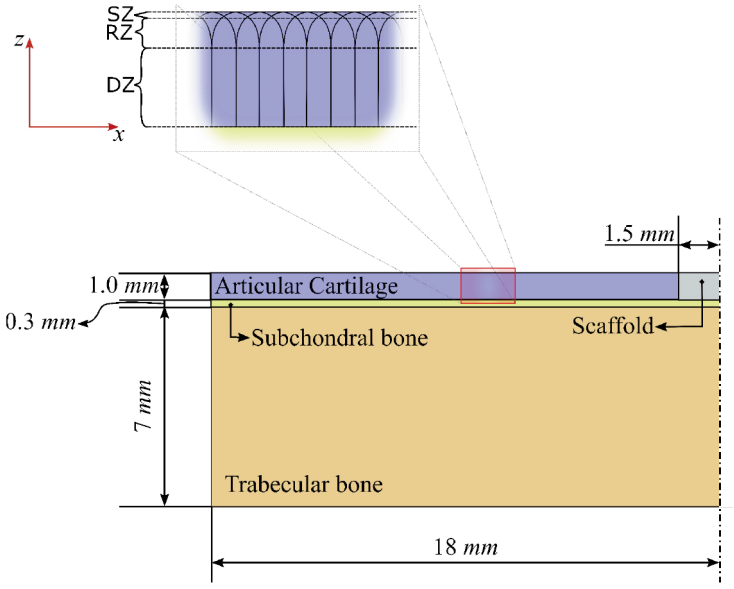

Figure 1. 2D finite element geometry with the collagen fibers (top) and scaffold implant (bottom). DZ: deep zone, RZ: radial zone, SZ: Superficial zone.

scaffolds were no longer aligned with the native articular surface and were covered by a neocartilage that was 125% (*a/a'*) thicker layer than the native one (Figure 2). At twelve months, the regenerated tissue was a hyaline-like cartilage, similar to the native tissue. The bottom of the scaffold ended at 1.755 *mm* (distance c') within the subchondral bone, whereas the thickness of the new cartilage was 95% (a/a') of the native cartilage (Figure 2).

From the computational model it was noticeable that the abnormal mechanical conditions that both bones, subchondral and trabecular, goes under might generate a bone remodeling process under the implant allowing it to move downwards inside the bone. Meanwhile, the scaffold gives support to the surrounding cartilage tissue generating ideal conditions for it to regenerate.

The superficial articular cartilage (hyaline-like) was regenerated, initially thicker than the native one and, after one year, it ended up with 5% thinner. Then, the scaffolding is important for the transmission of stress to the surrounding tissue. The computational simulation was able to explain the mechanical phenomenon that surrounds the regeneration of the articular cartilage, the regeneration times and tissues.

Supported by grant MAT2016-76039-C4-2-R from the Ministry of Science, Innovation and Universities (Spain). CIBER-BBN is funded by the VI National R&D&I Plan 2008-2011, Iniciativa Ingenio 2010, Consolider Program, CIBER Actions and with assistance from the European Regional Development Fund.

[1]Sancho-Tello, M. *et al. Int. J. Artif. Organs* 38, 210–223 (2015).
[2]Isaksson, H. *et al. J. Theor. Biol.* 252, 230–246 (2008).
[3]Wilson, W. *et al. J. Biomech.* 37, 357–366 (2004).

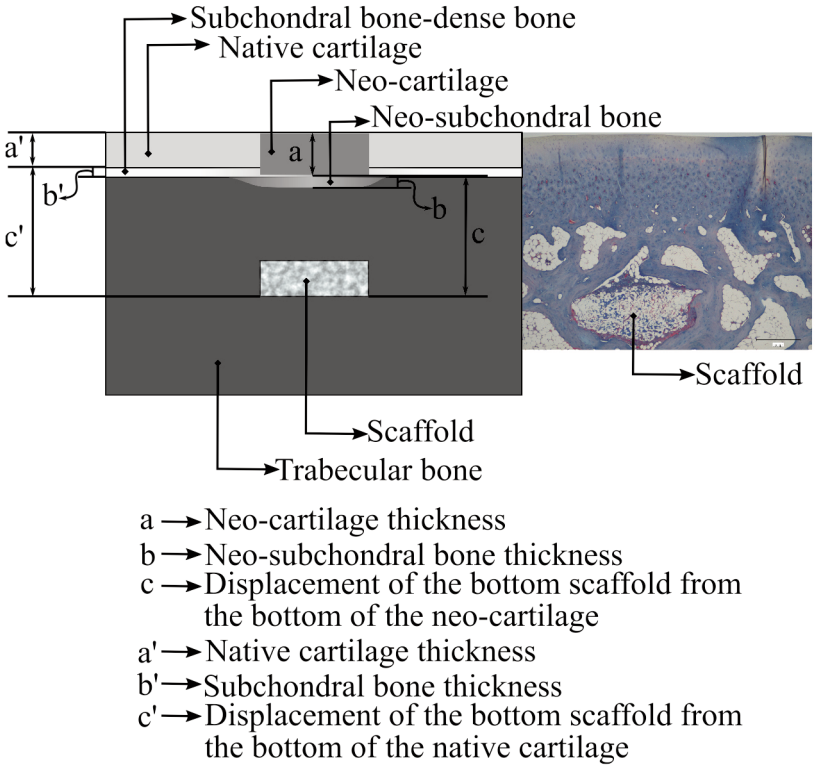

Figure 2. Measured distances in histological images.

Poster presentation: Session 2. Topic: Tissue Engineering. Code: 5766

Histology and Histopathology
From Cell Biology to Tissue Engineering

Identification of epithelial markers in bioartificial human corneas for clinical translation

Martín-Piedra M.A.[1], Garzón I.[1], González-Gallardo C.[2], Campos F.[1], Oyonarte S.[1,3], Martínez-Atienza J.[4], Rodríguez-Pozo J.A.[1] and Alaminos M.[1]

[1]Tissue Engineering Group, Department of Histology, University of Granada and Instituto de Investigación Biosanitaria ibs, Granada, Spain, [2]Division of Ophthalmology, University Hospital San Cecilio, Granada, Spain, [3]Cell and Tissue Bank of Granada-Almería, Spain, [4]Andalusian Initiative in Advanced Therapies (IATA), Seville, Spain

Fibrin-agarose bioartificial human corneas were previously designed and developed by the Tissue Engineering Group of the University of Granada [1], and these bioengineered organs are now used clinically in patients with severe corneal ulcers after approval of the Spanish Medicines Agency [2].

The objective of this work is to analyze the histological structure and function of human bioartificial corneas to determine their similarity to the human native cornea.

Fibrin-agarose biomaterials with a final agarose concentration of 0.1% were combined with primary cultures of human cornea keratocytes and cornea epithelial cells were subcultured on top of these stroma equivalents. After 28 days of culture, artificial corneas were subjected to plastic compression nanostructuration in order to increase their biomechanical properties and allow surgical handling and grafting.

These corneas were analyzed histologically to determine quality control parameters using hematoxylin-eosin staining and immunohistochemistry for the cornea epithelium marker cytokeratin 3/12 (KRT3/12).

Bioartificial corneas showed a stroma consisting of fibrin-agarose biomaterials combined with keratocyte cells immersed within and a stratified epithelium on top. Epithelial cells partially resembled the structure of control corneas, although their differentiation level was low. Very few differences were found between the most basal and the most apical cells, which tended to be round-shaped in the artificial cornea and flattened in control human cornea. However, expression of KRT3/12 was positive in all cell layers of both the artificial and the native human corneas.

Analysis of the epithelial layer of the bioartificial corneas showed that its level of differentiation was not complete, but the presence of a stratified epithelium partially resembled the native cornea. Expression of the specific marker KRT3/12 at the epithelial layer suggests that these epithelial cells could keep their cornea epithelial profile in the cornea substitute.

These results suggest that the bioartificial corneas generated in the laboratory fulfilled the requirements for clinical use.

Supported by the Spanish Plan Nacional de Investigación Científica, Desarrollo e Innovación Tecnológica (I+D+i) from the Spanish Ministry of Economy and Competitiveness (Instituto de Salud Carlos III), Grant FIS PI17/0391 (cofinanced by FEDER funds, European Union).

[1] Alaminos M, et al. Invest Ophthalmol Vis Sci. 2006;47(8):3311-7
[2] González-Andrades M, et al. BMJ Open. 2017;7(9):e016487

Poster presentation: Session 2. Topic: Tissue Engineering. Code: 5767

Histology and Histopathology
From Cell Biology to Tissue Engineering

Evaluation of the extracellular matrix and basement membrane in a human artificial cornea model generated by tissue engineering

Morales-Álvarez C.[1], Garzón I.[1], González-Gallardo C.[2], Martín-Piedra M.A.[1], Oyonarte S.[1,3], Ritoré-Hidalgo A.[4], Campos A.[1] and Alaminos M[1]

[1]Tissue Engineering Group, Department of Histology, University of Granada and Instituto de Investigación Biosanitaria ibs, Granada, Spain, [2]Division of Ophthalmology, University Hospital San Cecilio, Granada, Spain, [3]Cell and Tissue Bank of Granada-Almería, Spain, [4]Andalusian Initiative in Advanced Therapies (IATA), Seville, Spain

Tissue engineering biofabrication methods previously allowed the development of human artificial corneas, and the epithelial layer of these artificial organs were previously analyzed [1,2]. However, a proper functionality of these corneas is strictly dependent on a correct synthesis of key components of the cornea stroma and the basement layer. In this work, we analyzed these human artificial corneas to determine their suitability for future clinical use.

Cornea epithelial cells and stromal keratocytes were obtained from human scleral limbi. Both cell types were combined with biocompatible FA hydrogels to generate artificial human corneas. Differentiation of the epithelial layer was promoted by using air-liquid culture systems. These artificial corneas were evaluated ex vivo and grafted in vivo in the cornea of laboratory rabbits to determine their functionality as cornea substitutes. Qualitative and quantitative analysis of key components of the artificial corneal stroma and basement membrane were carried out by using histochemical and immunohistochemical methods.

First, histochemical methods allowed us to determine that the presence of elastic and reticular fibers was very rare in native and artificial corneas. Then, mature collagen fibers were very abundant in native corneas and in corneas grafted in animals, but very scanty in artificial corneas kept ex vivo in laboratory. The amount of proteoglycans as determined by alcian blue was high in controls and bioengineered corneas, especially after in vivo grafting. Immunohistochemistry for specific extracellular matrix components such as lumican and keratocan revealed no significant differences ($p>0.05$) between native controls and artificial corneas grafted in vivo. However, the basement membrane components analyzed here showed lower expression in artificial corneas as compared to controls.

In general, extracellular matrix components were comparable to native controls after in vivo grafting, with the exception of some specific basement membrane components. These findings suggest that the stromal layer of artificial corneas is very biomimetic and may have potential therapeutical usefulness.

Supported by the Spanish Plan Nacional de Investigación Científica, Desarrollo e Innovación Tecnológica (I+D+i) from the Spanish Ministry of Economy and Competitiveness (Instituto de Salud Carlos III), Grant FIS PI17/0391 (cofinanced by FEDER funds, European Union).

[1] Garzón I, et al. Investig. Ophthalmol Vis Sci. 2014; 55(7): 4073–4083
[2] Alaminos M, et al. Investig Ophthalmol Vis Sci. 2006; 47(8): 3311–3317

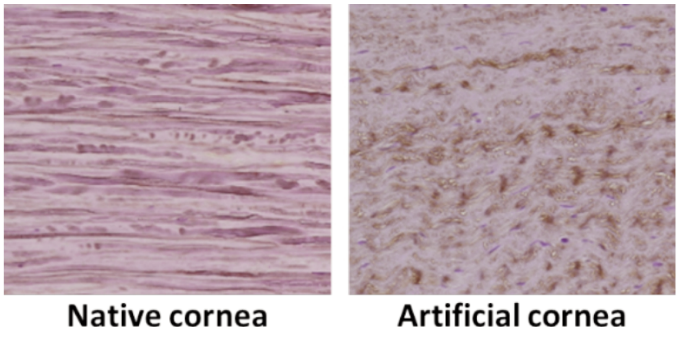

Figure 1: Lumican expression in native and artificial corneas.

Poster presentation: Session 2. Topic: Tissue Engineering. Code: 5768

Histology and Histopathology
From Cell Biology to Tissue Engineering

Development of a basement membrane in human orthotypical and heterotypical bioengineered corneas

Morales-Álvarez C.[1], Blanco-Elices C.[1], González-Gallardo C.[2], Oyonarte S.[1,3], Medialdea S.[4], Garzón I.[1], Martín-Piedra M.A.[1] and Alaminos M.[1]

[1]Tissue Engineering Group, Department of Histology, University of Granada and Instituto de Investigación Biosanitaria ibs. Granada, Spain, [2]Division of Ophthalmology, University Hospital San Cecilio, Granada, Spain, [3]Cell and Tissue Bank of Granada-Almería, Spain, [4]Division of Ophthalmology, University Hospital Virgen de las Nieves, Granada, Spain

Basement membrane provides structural support for cell growth and regulates cell migration, proliferation, cell polarity and differentiation by interactions with cell surface receptors and soluble growth factors. In the case of the human cornea, a specific layer called Bowman's layer connects the cornea stroma and the epithelium [1]. Due to its crucial role in epithelial cell attachment and physiology, bioengineered human corneas should have a fully functional and well-differentiated basement membrane. In the present work, we have analyzed the presence and development of a basement membrane in bioengineered human corneas generated from human cornea cells (orthotypical artificial corneas OAC) and from mesenchymal stem cells (heterotypical artificial corneas HAC) [2].

Corneal stromal substitutes were fabricated by immersing cultured human keratocytes in a nanostructured fibrin-agarose biomaterial. OAC were generated by seeding cornea epithelial cells obtained from sclera-corneal limbal rings on top of corneal stromal substitutes, whereas HAC were developed by seeding human umbilical cord Wharton's jelly stem cells on top of the stromal substitutes. These artificial corneas were kept ex vivo for 3 weeks. Then, both OAC and HAC models were grafted in the cornea of New Zealand rabbits and followed up for 3 months. The histological analysis of controls and bioingeenered corneas was carried out using periodic acid-Schiff (PAS) histochemical staining and immunohistochemistry for nidogen and perlecan as key molecules of the corneal basement membrane.

Bioartificial corneas kept in culture did not show a well-defined basement membrane as determined by PAS, and this correlated with the low signal found for nidogen and perlecan. However, after 3 months of in vivo development, a thin PAS-positive layer underlying the corneal epithelium was histologically observed, with positive immunoreactivity for nidogen and perlecan in both OAC and HAC models.

Our results suggest that the in vivo environment is necessary for a complete and terminal differentiation of the basement membrane component of human artificial corneas. In addition, the use of alternative cell sources for the generation of the cornea epithelial layer allowed us to obtain a cornea substitute whose basement membrane was able to mimic the differentiation process found in OAC. These results open the door to a future clinical use of HAC models generated by tissue engineering.

Supported by the Spanish Plan Nacional de Investigación Científica, Desarrollo e Innovación Tecnológica (I+D+i) from the Spanish Ministry of Economy and Competitiveness (Instituto de Salud Carlos III), Grant FIS PI17/0391 (cofinanced by FEDER funds, European Union).

[1] Alaminos M, et al. Invest Ophthalmol Vis Sci. 2006;47(8):3311-7
[2] Garzón I, et al. Invest Ophthalmol Vis Sci. 2014 Jun 6;55(7):4073-83

Poster presentation: Session 2. Topic: Tissue Engineering. Code: 5774

Histology and Histopathology
From Cell Biology to Tissue Engineering

Usefulness of poly(L-lactic acid) (PLLA) mats for human airway mucosa regeneration

Monleón I.[1], Martín S.[1], Milián L.[1,2], Mata M.[1,2,3], Armengot M.[2,4,5]; Monleón M.[6,7], Martinez C.[6,7] and Carda C.[1,2,7]

[1]Departamento de Patología. Facultad de Medicina y Odontología. Universidad de Valencia, Spain, [2]INCLIVA, Valencia, Spain, [3]CIBERES, ISCIII, Spain, [4]Departamento de Cirugía, Facultad de Medicina y Odontología, Universidad de Valencia, Spain, [5]Hospital Universitario La Fe, Valencia, Spain, [6]CBIT, Universidad Politécnica de Valencia, Valencia, Spain, [7]CIBER-bbn, ISCIII, Spain

Tracheal prosthesis represents the only therapeutic alternative for those patients affected of tracheal stenosis for whom surgery is limited because the extension of the defect. One of the disadvantages of tracheal prosthesis is the lack of a mucous layer containing ciliated cells, which leads to the accumulation of secretions affecting the pulmonary function of the patients. To study if nasal mucosa was a possible source of epithelial stem cells for airway mucosa regeneration and was to evaluate the usefulness of PLLA scaffolds to support airway mucosa growth.

Mats of PLLA were obtained with a home-made electrospinning equipment. A 10-mL syringe was loaded with PLLA solution. A syringe pump was used to feed the polymer solution at a rate of 4 mL/h. Twenty kilovolts was applied with a high-voltage power supply. The needle being in vertical position and the collector below in horizontal position. The scaffold properties were evaluated by SEM. Nasal cells were obtained by nasal biopsy while bronchial cells were obtained by bronchoscopy from the same donor. PLLA mats (in combination or not with collagen type I) epithelization was evaluated by fluorescence microscopy using rhodamine-phalloidin. E-cadherin expression was studied by immunofluorescence. Relative gene expression analysis of e-cadherin, MUC5AC, DIN1 and FOXJ1 were calculated by real time RT-PCR.

SEM analysis of PLLA showed and homogeneous distribution of PLLA fibers. The diameters of these fibers were of 0,1 μm. The distribution of the fibers was randomly and no aggregation was observed. Collagen coating of PLLA mats didn´t affect morphological to the fiber characteristics. Both mats (those associated or not with collagen type I) showed good adherence and improves cell attachment and proliferation. The epithelial cells seeded on the scaffolds generated a well cohesive epithelium with several cell contacts. MUC5AC, FOXJ1, DIN1 and E-cadherin expression was detected in the cells used in this study.

Results suggest the utility of nasal biopsies and PLLA mats for airway mucosa regeneration. No differences related to the collagen coating of PLLA mats was observed.

This work was supported by grants MAT2016-76039-C4-2-R (MST and CC) and PI16-01315 (MM) from the Ministry of Economy and Competitiveness of the Spanish Government and the Instituto de Salud Carlos III. CIBER-BBN and CIBERER are funded by the VI National R&D&I Plan 2008-2011, Iniciativa Ingenio 2010, Consolider Program, CIBER Actions and the Instituto de Salud Carlos III, with assistance from the European Regional Development Fund.

Poster presentation: Session 2. Topic: Tissue Engineering. Code: 5775

Histology and Histopathology
From Cell Biology to Tissue Engineering

Collagen related gene expression in human primary chondrocytes and dental pulp stem cells differentiated in alginate-agarose hidrogels

Oliver M.[1], Milián L.[1,2], Sancho-Tello M.[1,2], Martín de Llano J.[1,2], Mata M.[1,2,3] and Carda C.[1,2,4]

[1]Departamento de Patología, Facultad de Medicina y Odontología, Universidad de Valencia, Spain, [2]INCLIVA, Valencia, Spain, [3]CIBERES, ISCIII, Spain, [4]CIBER-bbn, ISCIII, Spain

Clinical management of large-size cartilage lesions is difficult due to the limited regenerative ability of the cartilage. We previously described the chondrogenic properties of alginate-agarose hydrogels in vitro. In this study, we explored the expression of the most important related cartilage differentiation genes in human primary chondrocytes and dental pulp stem cells (hDPSCs) cultured in a mixed alginate agarose scaffold.

Human articular chondrocytes and hDPSCs were isolated and cultured in proliferation medium containing DMEM high glucose, 50 µg/mL ascorbic acid, 10% FBS, non-essential aminoacids, and antibiotics. After three passages, the cells were cultured with chondral differentiation medium containing DMEM, 1% ITS, 1% FBS and 10 ng/ml TGF beta for up to 4 weeks. Chondrocytes differentiation expression markers were studied by immunofluorescence using antibodies against type I and II collagens and aggrecan through a confocal microscope. Morphology changes were evaluated by fluorescence microscopy using rhodamine-phalloidin. Total RNA was extracted from scaffolds and after preamplification, COL1A1, COL2A1, ACAN, COL10A, MMP1, MMP2, MMP3, MMP13, RUNX2, SOX5, SOX6, SPARC and TIMP expression were analyzed by real time RT-PCR.

Chondrocyte differentiation was significant in 3D scaffolds as it was demonstrated by the high expression of COL2 and ACAN as well by the low expression of COL1A1 of both cells studied. The cells cultured in alginate-agarose hydrogels formed spherical organoids of 20-30 cells in which the release of COLII and aggrecan becomes maximal. The cells cultured with differentiation medium exhibit a significant increase of COL2A1, ACAN, MMP3, SOX5 and SOX6 while COL10A, COL1A1 and MMP13 were significantly downregulated. No changes were observed in the rest of the genes analyzed.

Agarose-alginate hydrogels are a friendly environment for chondral differentiation becoming a realistic scaffold for cartilage regeneration.

This work was supported by grants MAT2016-76039-C4-2-R (MST and CC) and PI16-01315 (MM) from the Ministry of Economy and Competitiveness of the Spanish Government and the Instituto de Salud Carlos III. CIBER-BBN and CIBERER are funded by the VI National R&D&I Plan 2008-2011, Iniciativa Ingenio 2010, Consolider Program, CIBER Actions and the Instituto de Salud Carlos III, with assistance from the European Regional Development Fund.

Poster presentation: Session 2. Topic: Tissue Engineering. Code: 5782

Histology and Histopathology
From Cell Biology to Tissue Engineering

Osteoconductive properties of silica/chitosan/β-TCP sonogels designed for GBR in bone tissue engineering

Perez-Moreno A.[2], Reyes-Peces M.V.[2], Vilches-Perez J.I.[1], Piñero M.[2], Mesa Diaz M.M.[2], de la Orden E.[1], de la Rosa-Fox N.[2] and Salido M.[1]

[1]Departamento de Histología, SCIB, Facultad de Medicina, Universidad de Cádiz. España, [2]Departamento de Fisica de la Materia Condensada, Universidad de Cádiz, España

The success of bone tissue engineering rely on the capability of generating viable three dimensional structures with appropriate functional capabilities to restore bone tissue function capabilities. Silica-based biomaterials are known to play an important role in this field due to their osteoconductive and osteoinductive properties (1). Sonoaerogels are ultralight porous biomaterials designed trough an innovative methodology and we herein present an in vitro study in which normal human osteoblasts were grown in contact with Silica/Chitosan/β-TCP aerogels designed for bone tissue engineering in order to test osteoconductive properties of the material. These new three-dimensional scaffolds could be suitable to be used in bone tissue engineering (2).

Normal human HOB® osteoblasts were grown on sonogels designed in our labs and composed of TEOS + 8% chitosan and 10% β-TCP (SCh8T10), TEOS, TEOS + 10% TCP, TEOS + 8% chitosan, TEOS + 10% chitosan, TEOS + 8% chitosan + 20% TCP, 50%TEOS + 50% colagen, 38%TEOS + 50% colagen.

Bioactivity and degradation rates have tested prior to cellular assays. In order to identify osteoconductive properties in the sonogels, phenotypical changes, cell viability and proliferation, and initial cytoskeletal changes as markers of cell adhesion have been assessed. HOB® cells grown on a commercial hydroxyapatite composite (Bego Oss®) were used as positive control, and osteoblasts grown on coverslips were used as blank. Cells were immunolabelled with rhodamine phalloidine for cytoskeletal changes and DAPI for nuclear labelling. Cells were examined after 48 and 72 hours in culture. After 1 week in culture, the scaffolds were critical point dried and examined under a Quanta FEG 200 scanning electron microscope

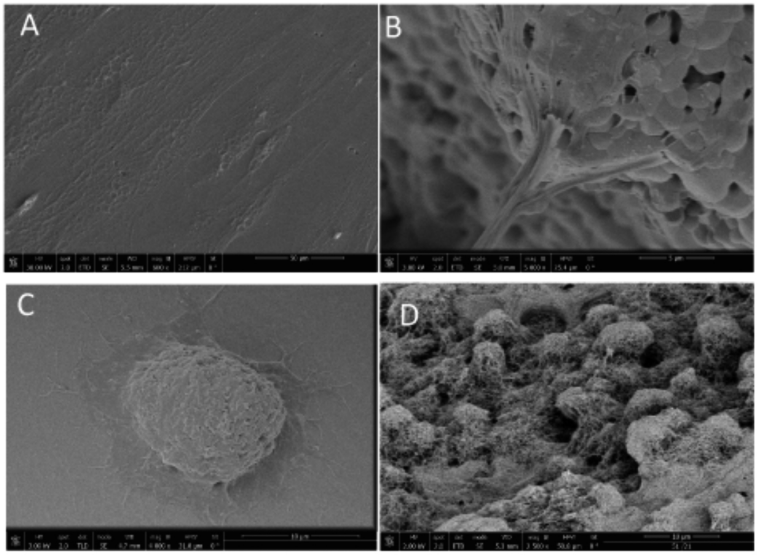

Figure 1: Representative images of preliminary results for HOB® cells grown on A: coverslip control group after 5 days in culture. Air drying for SEM.; B: HOB cells grown on Bego Oss after 5 days in culture, critical point drying for SEM; C: HOB cells grown on TEOS aerogel after 7 days in culture. Air drying for SEM; D: HOB cells grown in the presence of TEOS +12% chitosan+5% TCP after 7 days in culture, critical point drying for SEM

Sonogel response to cell culture medium demonstrated high variability, with changes in mechanical and chemical properties that have helped to redesign some of them. Osteoblastic response in the presence of aerogels above has been tested, and scaffolds were examined with SEM (Fig. 1) revealing scarce cellularity

Histology and Histopathology
From Cell Biology to Tissue Engineering

with no or little cell adhesion on the surface of the SCh8T10 and the BEGO OSS S®. Nevertheless, positive results can be described for TEOS/8% chitosan/10%TCP sonogel, where cell viability rised up to 98%. As shown in Figure 2, significative expression of stress fibers can be detected in HOB cells grown in TEOS/8% chitosan/10%TCP sonogel. Cell proliferation has been observed over time (Fig. 3).

Based in our preliminary results, aerogels containing organic polymers could promote the bone regeneration given the osteoblastic response obtained although improvements in the biomaterial must be carried out to optimize their osteoconductive property.

This work is 80% cofinanciated by Andalucia FEDER ITI 2014-2020 Grant for PI 013/017

1. Arcos D, Vallet-regí M. Acta Biomaterialia Acta Biomater [Internet]. 2010;6(8):2874–88. Ahttp://dx.doi.org/10.1016/j.actbio.2010.02.012
2. Goimil L, Braga MEM, Dias AMA, Gómez-amoza JL, Concheiro A, Alvarez-lorenzo C, et al. Biochem Pharmacol [Internet]. 2017;18:237–49. http: //dx.doi.org/ 10.1016/ j.jcou. 2017. 01.02

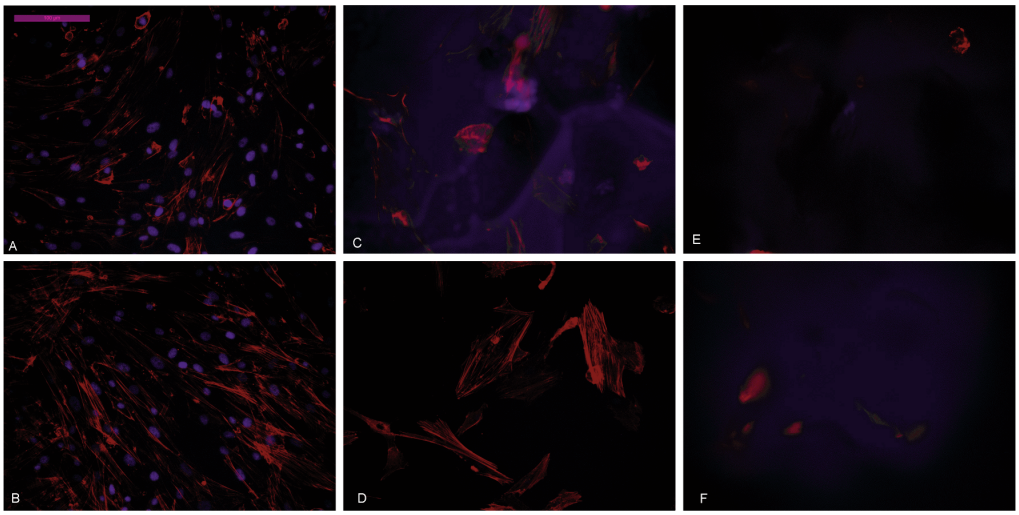

Figure 2: HOB® cells after 48 (upper line) or 72 h (lower line) in culture . In A;B: cells grown on glass coverslips, in C,D: cells grown on TEOS/8% chitosan/10%TCP, and E,F: cells grown on BegoOss® . Red immunolabelling with rhodamine phalloidin for actin cytoskeleton, Blue: DAPI labelling for nuclei.

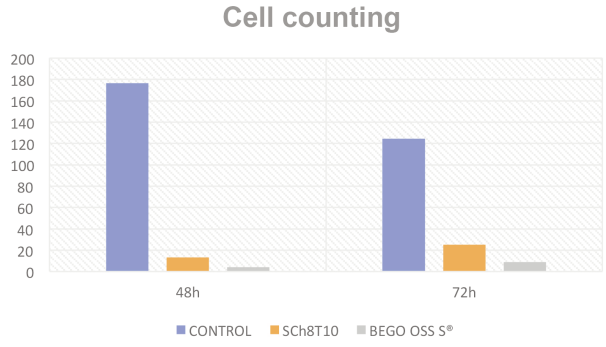

Figure 3: Cell counting of HOB® immunolabeled with DAPI (nuclei) seeded on the surface of particles of SCh8T10 aerogel, BEGO OSS S® and the control for the evaluation of cell viability at 48h and 72h.

Poster presentation: Session 2. Topic: Tissue Engineering. Code: 5783

Histology and Histopathology
From Cell Biology to Tissue Engineering

Osteoblastic response to bioactive silica/chitosan/β-TCP scaffolds in GBR. An *in vitro* pilot study

Perez-Moreno A.[2], Reyes-Peces M.V.[2], Vilches-Perez J.I.[1], López A.[1], Piñero M.[2], Mesa Diaz M.M.[2], Suffo M.[3], Diaz Ramos M.[1], de la Rosa-Fox N.[2] and Salido M.[1]

[1]Departamento de Histología, SCIB, Facultad de Medicina, Universidad de Cádiz, Españaa, [2] Departamento de Fisica de la Materia Condensada, Universidad de Cádiz, España, [3]Departamento Ingeniería Mecánica y Diseño Industrial, Universidad de Cádiz, España

The development of new biomaterials that promote bone tissue regeneration is experimenting great interest in recent years. Due to the aerogel's properties, these bioceramics could be promising candidates. They present a high specific surface, bioactivity, low density, an interconnected porous network and mesopores and can be easily modified through little adjustment in the sol-gel methodology and tailored according to the application needed. This technology allows the incorporation of organic polymers to the aerogel giving rise to the presence of molecules which are found in the native bone matrix (1). The present study is focused on the effects of bioactive Silica/Chitosan/β-TCP aerogels on human osteoblast HOB® for its application in guided bone regeneration.

Aerogels composed for TEOS + 8% Chitosan + 10% of β-TCP (SCh8T10) were tailored. Bioactivity, degradation rates and mechanical properties were tested prior to cellular assays. For in vitro assays, a coculture system was designed with inserts containing the particulated aerogel or the positive control BEGO OSS®, which allows HOB® osteoblasts to be seeded underlying, but not in direct contact with particulated material. Cells seeded on coverslip were used as blanks. Prior to cell seeding, particles were autoclaved. Cells were grown under standard conditions, changed every two days, and daily examined under contrast phase microscopy. After 48 h and 72 h in culture cells were immunolabeled with rhodamine/phalloidin and DAPI to study viability and actin cytoskeletal organization.

Aerogels were morphologically characterized by SEM (Fig. 1) . Cell viability assays**,** cell counts and growing curves determined an optimal seeding density (d=15.000 cells/cm^2) We found that the viability was higher than 98% in all the experimental groups and identified morphological changes in response to SCh8T10 particles. Direct examination with contrast phase microscopy revealed how the presence of aerogel induced phenotypical changes and cell proliferation (Figs. 2, 3) in a similar way to the commercial control. Immunolabelling with rhodamine phalloidine/DAPI (Fig. 2) confirmed the phenotypical changes, and also an increasing expression of stress fibers and focal adhesion points and cell proliferation both in SCh8T10 and in BEGO OSS S® groups in comparison with the

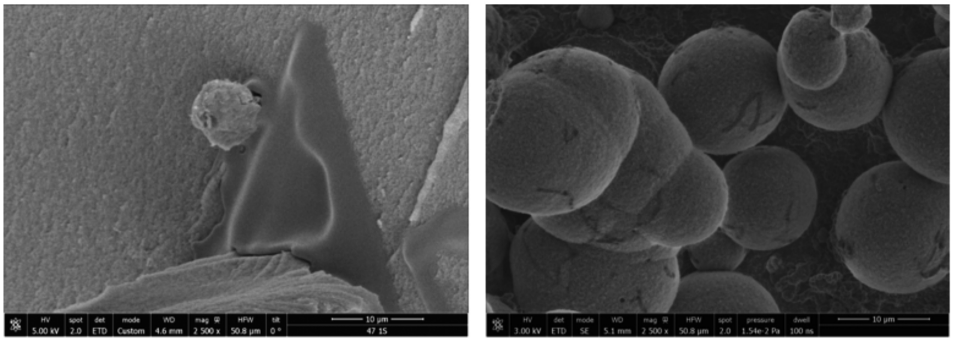

Figure 1. SEM micrographs of a Silica/Chitosan(8 wt%) aerogel fracture surface (A) as obtained by supercritical drying in CO_2 and (B) showing the growth of spherical hydroxyapatite crystals on the surface, after 4-weeks soaking in SBF

Histology and Histopathology
From Cell Biology to Tissue Engineering

control. Finally, some HOB® polarized only were observed in the SCh8T10 group, fact which is compatible with an osteoinductive role on HOB® cells.

We have developed an in vitro system that allows normal osteoblasts to grow in the presence, although not in contact, with silica/chitosan sonogels designed in our laboratories with the aim to valorate a possible osteoinductive role of the biomaterial. The results presented herein point to a positive effect on this sense with phenotypical differentiation of HOB® cells. The data obtained suggest that the SCh8T10 aerogel could be an interesting candidate for the GBR due to the morphological changes observed of HOB® in response to the particles of this biomaterial and further investigation to characterize its osteoinductive and osteoconductive properties could be carried out to study its potential in bone tissue engineering (2). Hopefully, mineralization studies should confirm the osteoinductive role of the designed biomaterial.

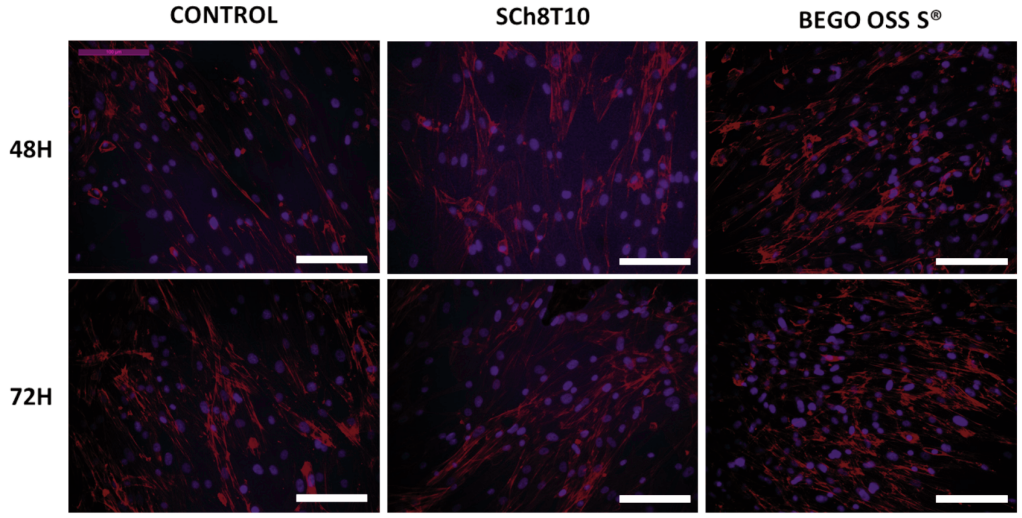

Figure 2: Fluorescence microscopy images of HOB® cultured in the presence of the particles of SCh8T10 aerogel, BEGO OSS S® and the control in coverslips for 48h and 72h. Red: Rhodamine/Phalloidin (actin) and blue: DAPI (nuclei). Scale bars: 100.

This work is 80% cofinanciated by Andalucia FEDER ITI 2014-2020 Grant for PI 013/017

1. Owens GJ, et al. Progress in Materials Science Sol – gel based materials for biomedical applications. 2016;77:1–79.
2. Terriza A, Vilches-pérez JI, et al. Osteoconductive Potential of Barrier NanoSiO 2 PLGA Membranes Functionalized by Plasma Enhanced Chemical Vapour Deposition. 2014;2014.

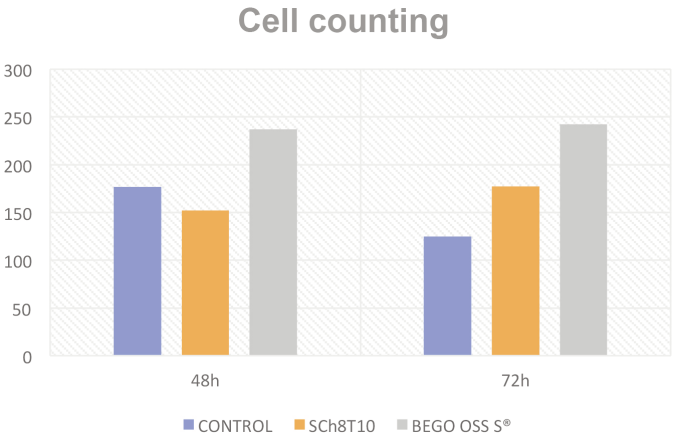

Figure 3 : Cell counting of HOB® immunolabeled with DAPI (nuclei) seeded in the presence of particles of SCh8T10 aerogel, BEGO OSS S® and the control for the evaluation of cell viability at 48h and 72h.

Poster presentation: Session 2. Topic: Tissue Engineering. Code: 5807

Histology and Histopathology
From Cell Biology to Tissue Engineering

Use of nanoformulated growth factors for the efficent culture of corneal epithelial cells

Irastorza-Lorenzo A.[1], Chato-Astrain J.[1], Larra E.[2], Villar-Vidal M.[3], Villullas S.[4], Ritoré-Hidalgo A.[5], Ponce-Polo A.[5] and Oruezabal R.I.[5]

[1]Tissue Engineering Group, Department of Histology, University of Granada and Instituto de Investigación Biosanitaria ibs. Granada, Spain, [2]AJL Ophthalmic SA, Vitoria-Gasteiz (Álava), Spain, [3]OSI Health XXI/Keralty Health, Vitoria-Gasteiz (Álava), Spain, [4]Biopraxis AIE/Biokeralty AIE, Miñano, Vitoria-Gasteiz (Álava), Spain, [5]Andalusian Initative in Advanced Therapies, Seville, Spain

Optimization of cell culture and tissue engineering protocols is a requirement for future scale-up and commercialization. In this regard, one of the limiting factors in cornea tissue engineering is culturing cornea epithelial cells, which tend to show limited proliferation rate in culture and often require the use of conditioning culture media [1]. The recent development of nanoformulated growth factors may contribute to increase metabolism and biological activity of cultured corneal epithelial cells and, therefore, to a more efficient culture process. In the present work, we have evaluated a novel nanoformulation of growth factors on corneal epithelial cells to determine its role as activator of the culturing process.

CCL-60 SIRC cells (Statens Serum Institut Rabbit Cornea) were kept in culture using a specific culture medium. Then, cells were trypsinized and subcultured on culture plates using the same culture medium supplemented with different factors: 1) control unsupplemented medium, 2) soluble growth factors, 3) control empty nanoformulations without growth factors, 4) nanoformulated growth factors, 5) 50% concentration of soluble factors and 50% concentration of nanoformulated growth factors, 6) 100% concentration of soluble factors and 100% concentration of nanoformulated growth factors. Cells were evaluated after 0 and 5 days using the Cell Proliferation Reagent WST-1 to determine the metabolic activity of cells cultured on each condition [2].

As expected, cells analyzed at day 0 showed no metabolic activity as determined by WST1. After 5 days of culture, the metabolic activity of the epithelial cornea cells varied among the different study groups, with the highest activity corresponding to groups 2, and 4, and the lowest activity found in groups 6 and 1.

The use of growth factors has showed its capability to increase cornea cell proliferation and biological activity. These factors demonstrated to be efficient when used in a soluble formulation as well as nanoformulated, as compared to control medium with no growth factors. Interestingly, the use of a doble dosage of growth factors was negative for the cells and reduced cell activity. These results support the use of these kind of growth factors for the generation of cornea epithelial cell cultures for use in tissue engineering by reducing the manufacturing times.

Supported by the Spanish Plan Nacional de Investigación Científica, Desarrollo e Innovación Tecnológica (I+D+i) from the Spanish Ministerio de Ciencia, Innovación y Universidades (Instituto de Salud Carlos III), Grant FIS PI17/0391 (cofinanced by FEDER funds, European Union) and the Spanish State Bureau of Investigation (Agencia Estatal de Investigación), and by FEDER funds, within the project RTC-2017-6696-1.

[1] Alaminos M, et al. Invest Ophthalmol Vis Sci. 2006;47(8):3311-7
[2] Martín-Piedra MA, et al. Cytotherapy. 2014;16(2):266-77

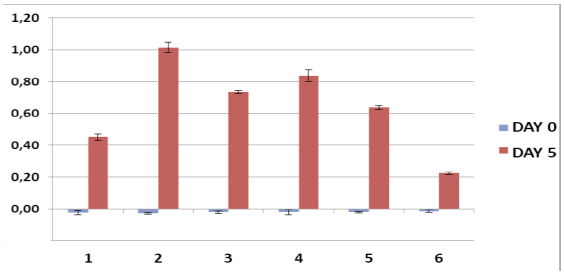

Figure 1. Cell proliferation and metabolic activity of SYRC cells cultured in different culture media (1 to 6).

Poster presentation: Session 2. Topic: Tissue Engineering. Code: 5808

Histology and Histopathology
From Cell Biology to Tissue Engineering

Design of novel biomaterials with definite anisotropic behaviour for use in tissue engineering

Ponce-Polo A.[1], Oruezabal R.I.[1], Carmona G.[1], Larra E.[2], Villar-Vidal M.[3], Villullas S.[4], López-López M.T.[1] and Alaminos M.[1]

[1]Andalusian Initative in Advanced Therapies, Seville, Spain, [2]AJL Ophthalmic SA, Vitoria-Gasteiz (Álava), Spain, [3]OSI Health XXI/Keralty Health, Vitoria-Gasteiz (Álava), Spain, [4]Biopraxis AIE/Biokeralty AIE, Miñano, Vitoria-Gasteiz (Álava), Spain, [5]Tissue Engineering Group, Department of Histology, University of Granada and Instituto de Investigación Biosanitaria ibs, Granada, Spain

Human tissues are typically anisotropic and show well-defined hierarchical, structures oriented in specific directions [1]. This definite 3D orientation is associated to tissue functions such as cell proliferation, migration and differentiation and are the responsible of the differential biomechanical properties shown by native tissues subjected to different types of mechanical stimuli. However, most currently available biomaterials, especially in the case of hydrogels, consist of a random three-dimensional network of fibers and particles swollen by water acting as isotropic materials. The recent use of magnetic nanoparticles allows the generation of hydrogel biomaterials that could be shaped and tuned in specific spatial directions in order to generate well-oriented structured inside the materials. The objective of this work is to design, generate and evaluate novel biomaterials containing biomagnetic particles to determine their potential use for the generation of anisotropic artificial tissues.

Fibrin-agarose hydrogels were generated by combining DMEM culture medium with human plasma, tranexamic acid (as anti-fibrinolytic agent), melted type VII agarose (at a final concentration of 0.1%) and calcium chloride (as inductor of the jellification process). MagP-OH magnetic nanoparticles consisting of a spherical core of magnetite coated by a layer of polymer were added to the mixture immediately before inducing the polymerization reaction. Then, a vertical magnetic field of 48 kA m^{-1} was applied for 5 minutes to induce particle orientation, and samples were allowed to completely jellify at 37ºC. Control artificial tissues were generated with the same materials but the magnetic field was not applied. Both tissue types were evaluated at the histological and biomechanical levels.

Histological analysis showed that both types of artificial tissues were compatible with a dense extracellular matrix structure similar to that of other types of tissues generated by the research group. Bioartificial tissues subjected to magnetic fields showed an anisotropic structure containing parallel thick strips of nanoparticles and fibers that were properly aligned in the direction of the magnetic field, whereas control tissues showed a randomly distributed structure. Biomechanical analyses demonstrated that the mechanical properties of tissues subjected to magnetic fields were higher than those of controls for the rigidity modulus, shear stress, shear strain and other biomechanical properties.

The use of novel nanoparticles able to respond to magnetic fields offers new possibilities for the generation of anisotropic human tissue substitutes with aligned internal structures able to response to specific strains. These results open the door to the future generation of tissues with strict biomechanical anisotropic requirements such as the human cornea, oral mucosa and palate.

Supported by the Spanish Plan Nacional de Investigación Científica, Desarrollo e Innovación Tecnológica (I+D+i) from the Spanish Ministerio de Ciencia, Innovación y Universidades (Instituto de Salud Carlos III), Grant FIS PI17/0391 (cofinanced by FEDER funds, European Union) and the Spanish State Bureau of Investigation (Agencia Estatal de Investigación), and by FEDER funds, within the project RTC-2017-6696-1.

[1] Fox AJS, et al. Sports Health. 2009;1:461–468
[2] Lopez-Lopez MT, et al. PLoS One. 2015;10(7):e0133878

Poster presentation: Session 2. Topic: Tissue Engineering. Code: 5809

Histology and Histopathology
From Cell Biology to Tissue Engineering

Cell-based strategies to promote *in vivo* vascularization in tissue engineered bioartificial constructs

Rodríguez-Hidalgo M., Zapater A., Blanco-Elices C., González-González A.L., Durand-Herrera D., Chato-Astrain J., Sánchez-Quevedo M.C. and Garzón I.

Tissue Engineering Group, Department of Histology, University of Granada and Instituto de Investigación Biosanitaria ibs, Granada, Spain

Vascularization is one of the main unsolved challenges in tissue engineering research. In this context, several vascularization strategies have been explored up to date, but some limitations still exist with respect to the cells used to generate prevascularized artificial tissues [1, 2].

In this work, we have compared the vascular potential of the following cell types used in human bioengineered tissues: mesenchymal stem cells (MSC) differentiated to the endothelial lineage, human umbilical vein endothelial cells (HUVEC) and human neonatal dermis microvascular endothelial cells (HMVECnd).

Human mesenchymal stem cells obtained from tissue biopsies and differentiated into endothelial-like cells using M199 conditioning media supplemented with 6ml of endothelial growth factor during 21 days. As controls, HUVEC and HMVECnd were cultured using enriched M199 media. 10,000 cells/cm^2 cells were cultured in chamber slides and fixed using 70% ethanol. After fixation, immunofluorescence was performed for CD31, CD45, Von Willebrand Factor (VWf) and VEGF markers to determine the endothelial profile and vascularization potential of each cell type. Flow cytometry characterization was carried out by identifying CD90, CD73, CD105 and CD45 markers.

Our results revealed that HUVEC and HMVECnd control groups showed mild expression of CD45, VWf, VEGF and CD31. In addition, MSC differentiated to endothelial-like cells tended to express high levels of CD45 and mild expression of VWf, VEGF and CD31. Flow cytometry showed high expression of CD90, and CD73 and low expression of CD105.

Vascularization of tissue constructs through the use of endothelial-like cells derived from MSC may offer advantages compared with the use of endothelial cells that are not easy to keep in culture. In this work, MSC showed endothelial differentiation potential, suggesting that these cells could be used for tissue prevascularization of large tissues developed by tissue engineering.

Supported by the Spanish Plan Nacional de Investigación Científica, Desarrollo e Innovación Tecnológica (I+D+i) from the Spanish Ministry of Economy and Competitiveness (Instituto de Salud Carlos III), Grant FIS PI18/0331 (cofinanced by FEDER funds, European Union).

[1] Esser TU, et al. Expert Opin Biol Ther. 2018 Dec 20. doi: 10.1080/14712598.2019.1561855. [Epub ahead of print]
[2] Frueh FS, et al. J Invest Dermatol. 2017;137(1):217-227

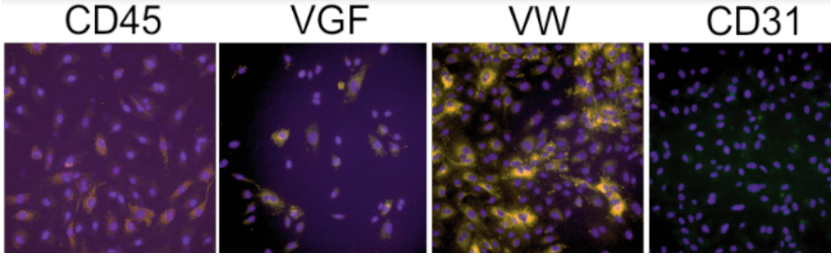

Figure 1: Detection of endothelial markers CD45, VEGF, VWf, and CD31 by immunofluorescence on Human MSC.

Poster presentation: Session 2. Topic: Tissue Engineering. Code: 5811

Histology and Histopathology
From Cell Biology to Tissue Engineering

Angiogenesis proteome analysis of preconditioned mesenchymal stem cells for use in oral mucosa substitutes

Blanco-Elices C.[1], Morales-Álvarez C.[1], Chato-Astrain J.[1], Martín-Piedra M.A.[1], Miranda-Fernández C.[1], Fernández-Valadés R.[1,2], Sánchez-Quevedo M.C.[1] and Garzón I.[1]

[1]Tissue Engineering Group, Department of Histology, University of Granada and Instituto de Investigación Biosanitaria ibs, Granada, Spain, [2]Division of Pediatric Surgery, University Hospital Virgen de las Nieves, Granada, Spain

Tissue engineering has shown promising results in generating tridimensional human oral mucosa (OM) substitutes [1]. However, vascularization is still one of the main challenges as bioengineered oral mucosa survival depends mainly on the rapid host blood supply. In this context, artificial OM stroma enriched in vascular progenitors could promote neovascularization. To evaluate the angiogenic potential of predifferentiated cells, we performed a proteome analysis of bone marrow mesenchymal stem cells (BMSC) differentiated to the vascular cell lineage.

BMSC were cultured using basal medium (control BMSC) and conditioning medium (differentiated BMSC). Conditioning medium consisted on 199 medium supplemented with endothelial factors for 21 days [2]. Human umbilical vein endothelial cells (HUVEC) were used as control. Once cultured, total proteins were extracted using MCL1 mammalian cell lysis kit. Then, the angiogenic profile of each cell type was identified using a human angiogenesis antibody array. Resulting data analysis was performed by pixel density with Image J software.

A differential protein expression profile was detected among the samples analyzed here, with a wide range of proangiogenic and antiangiogenic factors associated to each cell phenotype. Differentiated BMSC showed high expression of DPPIV, which plays a key role as proangiogenic factor by remodeling the extracellular matrix and promoting endothelial cell migration and tube formation. Interestingly, the angiogenic inhibitor SERPF1 was down-regulated in HUVEC and in differentiated BMSC. However, protein expression of certain proteins that are highly present in HUVEC cells such as agiopoietin-2 and endoglin was not detected at the same levels in differentiated BMSC.

Our *in vitro* study demonstrates that the use of angiogenic preconditioning media is able to induce the endothelial differentiation of human BSMC in culture. However, the low expression of certain types of proteis that are associated to the vascular phenotype suggests that bidimensional culture systems are not completely efficient, and further studies should determine the efficiency of 3D differentiation systems based on tissue engineering strategies.

Supported by the Spanish Plan Nacional de Investigación Científica, Desarrollo e Innovación Tecnológica (I+D+i) from the Spanish Ministry of Economy and Competitiveness (Instituto de Salud Carlos III), Grants FIS PI18/331 and PI18/332 (cofinanced by FEDER funds, European Union).

[1] Fernández-Valadés-Gámez R, et al. Biomed Mater. 2016;11(1):015015
[2] Vico M, et al. Histol Histopathol. 2015;30(11):1333-40

Poster presentation: Session 2. Topic: Tissue Engineering. Code: 5814

Histology and Histopathology
From Cell Biology to Tissue Engineering

EGF lipid nanoparticles for improving human skin keratinocytes proliferation

Irastorza-Lorenzo A.[1], Chato-Astrain J.[1], Vairo C.[2], Villullas S.[2], Gainza G.[2], Herran E.[2], Gainza E.[2] and Alaminos M.[1]

[1]Tissue Engineering Group, Department of Histology, University of Granada and Instituto de Investigación Biosanitaria ibs, Granada, Spain, [2]Biopraxis AIE/Biokeralty AIE, Miñano, Vitoria-Gasteiz (Álava), Spain

A rapid and efficient generation of primary cell cultures of human skin keratinocytes is one of the crucial steps in skin tissue engineering, and one of the unsolved problems in the field. In order to increase cell growth and proliferation, different growth factors and hormones are used in the culture medium, but new protocols, able to stimulate cell proliferation, are still in need. In this regard, encapsulation of bioactive factors in nanoparticles may contribute to increase their biological activity by providing controlled drug delivery [1]. In the present work, we evaluated the *ex vivo* effect of novel nanoparticles containing human recombinant epithelial growth factor (rhEGF) on the efficiency of keratinocyte cell cultures generated from human skin explants.

Human skin biopsies were obtained from healthy donors subjected to elective surgery. Biopsies were fragmented in small 1x1x1mm explants, which were explanted on tissue culture flasks. Three different culture media were used: 1) routine keratinocyte culture medium (KM) containing 10% FBS and growth factors, 2) KM supplemented with rhEGF encapsulated in lipid NP generated by BioPraxis Research [2], 3) KM supplemented with empty -mock- lipid NP. Cultured were evaluated after 11 days of *ex vivo* development to determine the number of keratinocyte colonies generated from each explant and the existence of fibroblast cells contaminating the cultures.

The phase-contrast microscopic evaluation showed that 27.7% of the explants cultured with KM-rhEGF-NP succeeded in generating pure keratinocyte cultures, whereas KM resulted in 16.6% colonies and KM-mock-NP in 5.5%. Cultured keratinocytes were morphologically normal and viability was preserved. Regarding contaminating fibroblasts, 5.5% of explants cultured with KM enriched with either rhEGF-NP or mock-NP and 11.1% of explants cultured with KM resulted in mixed fibrobast-keratinocyte cultures.

These preliminary results suggest that the use of rhEGF-NP could contribute to increase the efficiency of the explant technique and to reduce the number of cultures contaminated with dermal fibroblasts. Although results should be confirmed in the future, these results suggest that rhEGF-NP could increase the biological function or biodisponibility of rhEGF, resulting in a more efficient induction of cell growth in skin explants.

Supported by award no. AC17/00013 (NanoGSkin) by ISCIII thorough AES 2017 and within the EuroNanoMed framework.

[1] Tarhini M, et al. Int J Pharm. 2017;522(1-2):172-197
[2] Gainza G, et al. J Control Release. 2014;185:51-61

Poster presentation: Session 2. Topic: Tissue Engineering. Code: 5815

Histology and Histopathology
From Cell Biology to Tissue Engineering

Tissue engineering of the human vagina mucosa

Campos F.[1], Chato-Astrain J.[1], Irastorza-Lorenzo A.[1], Durand-Herrera D.[1], Sánchez-Porras D.[1], Godoy-Guzmán C.[2], Martínez-Gómez C.[3] and Garzón I.[1]

[1]Tissue Engineering Group, Department of Histology, University of Granada and Instituto de Investigación Biosanitaria ibs, Granada, Spain, [2]University of Santiago de Chile (USACH), Santiago, Chile, [3]Institut Universitaire du Cancer de Toulouse (IUCT), France

Vaginal defects can result as consequence of traumatic injuries, infectious diseases, cancer and other conditions [1]. Vagina structural defects are often repaired by using autologous tissue graft obtained from intestine and other organs and tissues, with variable results [2]. In this regard, tissue engineering could provide bioartificial tissues potentially useful for vaginal repair that may be free from the side effects and complications associated to the use of these extra-vaginal tissues. In addition, recent evidence [3] demonstrated that human mesenchymal stem cells (MSC) have important differentiation potential to different cell lineages and could be used for the generation of oral mucosa and skin epithelia without the need of obtaining tissue-specific biopsies.

The aim of this study is to describe a novel model of human vagina mucosa substitute generated by tissue engineering and to evaluate this tissue substitute at the in vitro level for its future clinical translation.

Artificial human vagina mucosa substitutes were bio-fabricated by using orthotypical and heterotypical cell cultures using fibrin-agarose three-dimensional scaffolds. The orthotypical model consisted on human vagina epithelial cells and fibroblasts cultured in 3D systems for 7 and 28 days of ex vivo development. Heterotypical vagina tissues were fabricated using the same 3D system with human vagina fibroblasts immersed in biomaterials, but the epithelial layer consisted of human umbilical cord Wharton's jelly mesenchymal stem cells (WJMSC) inducted to epithelial vagina differentiation by epithelial-mesenchymal interaction [3]. For histological analysis, all samples were fixed and embedded in paraffin and histological sections were stained with hematoxylin and eosin.

The histological analysis showed that bio-fabricated human artificial vagina mucosa appropriately supported the generation of an epithelial layer with 2-3 cell layers in both models, the orthotypical and the heterotypical. However, heterotypical models showed a higher stratification of the epithelial-like layer as compared to the orthotypical models. The structure of both epithelial strata were compatible with a normal tissue, although the differentiation level found in native vagina was not reached by the artificial organs.

This study suggests that a bioengineered substitute of the human vagina mucosa can be generated in the laboratory. WJMSC showed differentiation potential towards the vagina mucosa epithelium and could be used for the fabrication of vagina substitutes by tissue engineering. These bioartificial substitutes could have putative clinical usefulness in the future.

Supported by CTS-115 (Tissue Engineering Group of the University of Granada).

[1] Kimberley N, et al. J Pediatr Adolesc Gynecol. 2012;25:54-58
[2] Lin WC, et al. Hum Reprod. 2003;18:604-07
[3] Garzón I, et al. Stem Cells Transl Med. 2013;2(8): 625-32

Poster presentation: Session 2. Topic: Tissue Engineering. Code: 5817

Histology and Histopathology
From Cell Biology to Tissue Engineering

Hematological quality control of decellularized peripheral nerves used in a model of sciatic nerve defect

Chato-Astrain J.[1], García-García O.D.[1], El Soury M.[1,2], Campos F.[1], Sáez-Moreno J.A.[3], Philips C.[4], Campos A.[1] and Carriel V.[1]

[1]Tissue Engineering Group, Department of Histology, University of Granada and Instituto de Investigación Biosanitaria ibs, Granada, Spain, [2]Department of Clinical and Biological Sciences, University of Torino, Italy, [3]Division of Clinical Neurophysiology, University Hospital San Cecilio, Granada, Spain, [4]Department of Basic Medical Sciences, Ghent University, Belgium

The regenerative potential of nerve substitutes is often determined by clinical-functional and histological assessments [1,2]. However, biochemical and haematological parameters are poorly studied, despite the potential information that can be obtained with these parameters, which are crucial in the daily clinical practice. In this context, the aim of this study was to compare the haematological and biochemical profiles of three different decellularized nerve allografts and autografts grafted in laboratory animals.

In this study, 24 Wistar rats were anaesthetized and 10-mm sciatic nerve defect was created and repaired by using three different nerve substitutes generated by decellularization of native nerves using three different protocols (RSN, HD and SD) [3]. Native autografts were used as controls (n=6 each). After 12 weeks, biochemical and hematological parameters were determined with a Cobas c311 clinical chemistry analyzer. Furthermore, HE staining of grafted tissues were performed to correlate laboratory findings with histological parameters.

The quantitative hematological and biochemical analyses revealed changes, as compared to normal range, in some parameters of both profiles at 12 weeks after surgery. Interestingly, hematological analyses revealed changes in neutrophils (NEUT), mixed leucocytes (MXD) and platelets (MPV) values but not in hemoglobin and red blood cell count (RBC). In the case of biochemical profile, significant alterations were observed in the alanine transaminase (ALT), aspartate aminotransferase (ASP), urea (UREA) and in creatine kinase (CK).

Histology confirmed an active peripheral nerve regeneration in all groups, which was composed by a variable amount of newly-formed nerve fascicles without signs of inflammation. Furthermore, histology confirmed different degrees of muscle atrophy.

This study demonstrated that different decellularized allografts and autografts can elicit significant alterations in some hematological and biochemical parameters. These modifications could be related to the decellularization protocols used to generate the decellularized nerve allografts or due to the surgical procedure or tissue regeneration. Finally, our study highlights the usefulness of hematological and biochemical tests as quality controls in peripheral nerve repair.

This study was Supported by Plan Nacional de Investigación Científica, Desarrollo e Innovación Tecnológica (I+D+I) from the Spanish Ministry of Economy and Competitiveness (Instituto de Salud Carlos III), grant FIS PI17/0393 (co-financed by ERDF-FEDER, EU).

[1] Carriel V, et al. Expert Rev Neurother. 2014;14, 301–318
[2] Chato-Astrain J, et al. Front Cell Neuros. 2018;12, 501
[3] Philips C, et al. Ann Biomed Eng. 2018;46 (11):1921-1937

Poster presentation: Session 2. Topic: Tissue Engineering. Code: 5818

Histology and Histopathology
From Cell Biology to Tissue Engineering

Analysis of biocompatibility and mechanical properties of nanostructured hydrogels for use in tissue engineering

Campos F.[1], Díaz-Ramos M.[1], García-García O.D.[1], Sánchez-Quevedo M.C.[1], Fernández-Valadés R.[1,2], Alaminos M.[1], Garzón I.[1] and Carriel V.[1]

[1]Tissue Engineering Group, Department of Histology, University of Granada and Instituto de Investigación Biosanitaria ibs, Granada, Spain, [2]Division of Pediatric Surgery, University Hospital Virgen de las Nieves, Granada, Spain

Hydrogels can be defined as three-dimensional polymeric network structures, which can absorb and retain considerable amounts of water. Among the hydrogels that are most commonly used for the generation of bioartificial tissues by tissue engineering, collagen and fibrin-agarose biomaterials show excellent properties for their use as matrices or scaffolds, especially when nanostructuration methods are applied to these hydrogels.

In this study, we compared the *ex vivo* biocompatibility and biomechanical properties of nanostructured fibrin-agarose hydrogels (NFAH) and nanostructured fibrin-collagen hydrogels (NFCH) to determine their adequateness and potential usefulness for the generation of bioartificial tissues by tissue engineering.

First, hydrated hydrogels based on fibrin-agarose and type-I collagen were fabricated in the laboratory and subjected to a nanostructuration protocol based on plastic compression in order to generate acellular NFAH and NFCH. Then, human fibroblasts were cultured on top of both structures and cell viability was assessed by WST-1 and Live/Dead techniques after 24, 48, 72 and 96h of culture. In addition, these bioartificial tissues were subjected to tensile test to determine the main biomechanical parameters including Young's module, strain at fracture and stress at fracture values as previously described [1, 2].

Live/Dead *ex vivo* biocompatibility analysis revealed high cell viability and functionally in both tissue types, being these consistently higher in NFCH over the time. In addition, the WST-1 test showed a progressive increase of cell metabolic activity over the time in both groups, being these results considerably higher in NFAH, especially from 72 to 96 hrs. Finally, biomechanical analyses showed that some parameters were significantly higher in NFAH as compared to NFCH ($p<0.05$).

These results suggest that both types of bioartificial tissues fulfill the criteria for use in tissue engineering, including adequate biocompatibility ex vivo and proper biomechanical behavior, especially in the case of NFAH. Future studies should determine the potential usefulness of these biomaterials in tissue engineering of specific tissues and organs such as the human peripheral nerve, cornea, oral mucosa and palate.

Supported by the Spanish Plan Nacional de Investigación Científica, Desarrollo e Innovación Tecnológica (I+D+i) from the Spanish Ministry of Economy and Competitiveness (Instituto de Salud Carlos III), Grants FIS PI17/0393, FIS PI17/0391, FIS PI18/0331 and FIS PI18/0332 (cofinanced by FEDER funds, European Union).

[1] Campos F, et al. Biomed Mater. 2016;11(5):055004
[2] Campos F, et al. 2018;13(2):025021

Poster presentation: Session 2. Topic: Tissue Engineering. Code: 5819

Histology and Histopathology
From Cell Biology to Tissue Engineering

In vivo evaluation of fibrin-agarose hydrogels functionalized with magnetic nanoparticles

Rodríguez I.A.[1,2], Carriel V.[1], Bonhome A.[3], López-López M.T.[3], Voltes-Martinez A.[1], Garzón I.[1], Fernández-Valadés R.[1,4] and Campos A.[1]

[1]Tissue Engineering Group, Department of Histology, University of Granada and Instituto de Investigación Biosanitaria ibs, Granada, Spain, [2]Cátedra de Histología B, School of Dentistry, National University of Cordoba, Argentina, [3]Department of Applied Physics, University of Granada and Instituto de Investigación Biosanitaria ibs, Granada, Spain, [4]Division of Pediatric Surgery, University Hospital Virgen de las Nieves, Granada, Spain

Magnetic nanoparticles (MNPs) have recently used in biomedicine and several applications have been proposed [1]. Our research group developed a novel nanomagnetic tissue-like structure by combining fibrin-agarose hydrogels (FAH) and MNPs. Preliminary results showed that the incorporation of MNPs in the hydrogels resulted in a significant improvement of all major biomechanical properties of the biomaterial [2]. However, studies focused on the analysis of these novel FAH-MNPs should determine whether or not these biomaterials fulfill the *in vitro* and *in vivo* biocompatibility criteria established for biomaterials for medical use according to the European regulation [3].

The objective of this study, is to evaluate the in vivo behavior (biodistribution and biocompatibility) of novel FAH-MNPs as part of the required quality control process focused on the future clinical translation of these tissue-like structures.

FAH-MNPs were generated in the laboratory using human plasma and commercially-available MNPs. These combined biomaterials were then subcutaneously implanted in 5 adult Wistar rats. As controls, FAH biomaterials without MNPs were implanted in a control group. Biodistribution and biocompatibility analyses were performed after 1 and 12 weeks of the surgical procedure by magnetic resonance imaging (MRI) and hematological, biochemical and histological analyses. For MRI, animals were deeply anesthetized with isoflurane and subjected to a whole-body scanning using a Bruker Biospec TM70/20 USR device. For the hematological and biochemical tests, a blood sample was collected in heparin-containing tubes and several parameters related to liver and kidney functions were determined. For histology, animals were euthanatized and samples were obtained and fixed in paraffin using routine methods.

MRI analysis of animals in the study group showed hyperintense areas in the region of FAH-MNPs implantation at 1 and 12 weeks of follow-up, but signs of the presence of MNPs were not observed in distal organs. Hematological and biochemical studies revealed that most of the parameters evaluated in both groups of study resulted comparable to the range observed in healthy non-operated animals. Histology showed the presence of Perl's positive areas in the FAH-MNPs group and confirmed a high amount of MNPs in the region of implantation, but not in distal organs. However, a local macrophage and lymphoplasmocytic-rich inflammatory reaction was observed around the implants in both study groups after 1 week, but this inflammatory reaction decreased after 12 weeks. In all cases, the structural analysis of organs (liver, kidney, spleen and lymph nodes) was compatible with normal organs, with a complete absence of damage or morphological changes.

In vivo quality control assessment of animals with the novel tissue-like structures demonstrated that MNPs are not able to significantly migrate to distal organs after 12 weeks of implantation, although future studies using complementary tests should confirm these preliminary findings. The proper results related to the hematological, biochemical and histological analyses suggest that the use of FAH-MNPs is safe and opens the door to the generation of tissue-like structures based on these biomaterials.

Supported by the Spanish Plan Nacional de Investigación Científica, Desarrollo e Innovación Tecnológica (I+D+i) from the Spanish Ministry of Economy and Competitiveness (Instituto de Salud Carlos III), Grants FIS PI17/393, FIS PI18/0332 and FIS PI18/0331 (cofinanced by FEDER funds, European Union).

[1] Lee GY, et al. ACS Nano. 2013;7:2078-2089
[2] Lopez-Lopez MT, et al. PLoS One. 2015;10:e0133878
[3] Carriel V, et al. J Neural Eng. 2013;10:026022

Poster presentation: Session 2. Topic: Tissue Engineering. Code: 5821

Histology and Histopathology
From Cell Biology to Tissue Engineering

Development of bioactive microaggregate tissues using human mesenchymal stem cells

Sánchez-Porras D.[1], Albaladejo-García V.[1], Durand-Herrera D.[1], Campos F.[1], Domingo-Roa V.[2], Nygren-Jimenez E.[1], García J.M.[1] and Carriel V.[1]

[1]Tissue Engineering Group, Department of Histology, University of Granada and Instituto de Investigación Biosanitaria ibs, Granada, Spain, [2]Experimental Unit, Instituto de Investigación Biosanitaria ibs, Granada, Spain

Cell microaggregates can be generated by human cells cultured under specific 3D cell conditions inducing cell-cell attachment. In this milieu, the increasing applications of human mesenchymal stem cells (MSC) in tissue engineering make these cells excellent candidates for use in tissue engineering protocols. MSC are immunoprivileged and have high proliferation and differentiation capabilities in vitro and in vivo.

In the present work, we have analyzed the capability of three different sources of MSC to form cell microaggregate tissues (microtissues) with potential usefulness in tissue engineering.

Wharton Jelly Stem Cells (WJSC), Bone Marrow Stem Cells (BMSC) and Adipose Stem Cells (ADSC) primary cell cultures were generated from human tissue biopsies as previously reported [1]. Then, $5x10^4$ cells of each type were seeded on previously elaborated agarose chips formed by 256 micro-wells with an average size of 400x800µm [2]. Microtissues formation was daily controlled by phase contrast microscopy. The cell viability (as determined by live/dead, WST-1 and DNA release methods), structure and histological properties of these microspheres were analyzed at 4, 7, 14, 21, 28 days of ex vivo culture.

Microscopic images showed that WJSC, BMSC and ADSC were able to self-assemble and form microtissues from day 1 onward, adopting a clearly different organization for the different cell types. ADSC and BMSC microtissues did not remain stably aggregated through the entire culture period and tended to desegregate. BMSC formed the less compact microtissues from the beginning, showing less peripheral cohesion. WJSC produced an abundant extracellular matrix and cells tended to adopt a peripheral distribution. For the viability analyses, microtissues were mainly composed by viable cells that remained viable during the whole culture period. The WST-1 assay showed similar cell metabolic activity levels for the different cells, although WJSC showed slightly lower activity levels at the final stages of the study as compared to ADSC and BMSC.

WJSC, BMSC and ADSC were able to form stable viable microtissues consisting of a variable amount of extracellular matrix surrounded by living cells. Further histological and molecular studies are still needed to determine the functionality and the synthesis of essential extracellular matrix molecules by these microtissues, but these preliminary results point out the potential usefulness of these biological structures in tissue engineering.

Supported by CS PI-0257-2017, Regional Ministry of Health, Junta de Andalucia, Spain.

[1] Martín-Piedra MA, et al. Eur Cell Mater. 2019;37:233-249
[2] Durand-Herrera D, et al. Histochem Cell Biol. 2018;150(4):379-393

Poster presentation: Session 2. Topic: Tissue Engineering. Code: 5822

Histology and Histopathology
From Cell Biology to Tissue Engineering

Epithelial cell culture using biocompatible coating biomaterials for tissue engineering

Irastorza-Lorenzo A.[1], Blanco-Elices C.[1], Chato-Astrain J.[1], Oyonarte S.[1,2], Alaminos M.[1], Fernández-Valadés R.[1,3], Sánchez-Quevedo M.C.[1] and Garzón I.[1]

[1]Tissue Engineering Group, Department of Histology, University of Granada and Instituto de Investigación Biosanitaria ibs, Granada, Spain, [2]Cell and Tissue Bank of Granada-Almería, Spain, [3]Division of Pediatric Surgery, University Hospital Virgen de las Nieves, Granada, Spain

Expansion of primary cell cultures is a crucial step for the generation of human tissues by tissue engineering. However, efficient culture of human epithelial cells is challenging, especially when epithelial cells are subcultured. The use of 3T3 feeder layers has been extensively used to support epithelial cell attachment and proliferation [1]. Nevertheless, the use of xenogeneic cells and products should be avoided in order to ensure the clinical translation of bioengineered tissues.

The aim of this work is to characterize different biomaterials that could act as attachment substrates allowing an efficient culture of human epithelial cells without the need of using feeder layers.

Eight different commercially available materials were tested as culture surfaces coating materials: collagen coating solution (CCS), type-I rat tail collagen, Geltrex, fibronectin, Attachment Factor, type A gelatine (1%), Poly-L-lysine and human plasma fibrin. Human epithelial keratinocytes were isolated and cultured for 7 days on the different surfaces. Live/Death, WST-1 and DNA quantification assays were performed at 24h, 4 days and 7 days to determine the efficacy of the different biomaterials.

Cell viability results based on the WST-1 showed that CCS was the most supportive biomaterial, followed by Attachment Factor and Type A gelatine at 24h. The lower viability was found for cells cultured on Geltrex and fibronectin. After 4d, the best results were found for CCS, fibronectin and fibrin, whilst poly-L-lysine showed the lowest viability. At 7 days, CCS showed the highest results, whereas type-I rat tail collagen had the lowest values. For the DNA quantification, the best results at 24h were found for type-I rat tail collagen, type A gelatin and poly-L-lysine, with fibronectin and fibrin showing the worst results. After 4 days, the best cell viability corresponded to CCS, type A gelatine and Geltrex, and poly-L-lysine and fibrin had the poorest results. At day 7, the best results corresponded to both collagen types and Geltrex, and the worst results were found for fibrin and attachment factor. In summary, collagen tends to be the most supportable biomaterial for epithelial cell attachment and survival. The presence of collagen in the epithelial cell basement membrane could contribute to explain these results.

The results obtained in the present work suggest that human epithelial cell cultures can be efficiently supported by the use of specific surface coating solutions. Although further studies should be performed, our results open the door to the use of coating solutions for the generation of primary cultures of epithelial skin, cornea, oral mucosa and palate cells for use in tissue engineering.

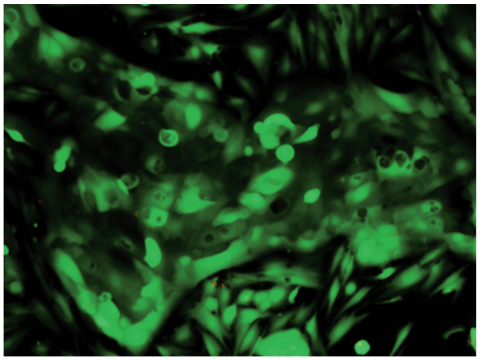

Figure 1. Live/Death analysis of epithelial cells cultured for 24h on CCS.

Supported by the Spanish Plan Nacional de Investigación Científica, Desarrollo e Innovación Tecnológica (I+D+i) from the Spanish Ministry of Economy and Competitiveness (Instituto de Salud Carlos III), Grants FIS PI17/0391, FIS PI18/0331 and FIS PI18/0332 (cofinanced by FEDER funds, European Union) and AC17/00013 (NanoGSkin) by ISCIII thorough AES 2017 and within the EuroNanoMed framework.

[1] Suzuki D, et al. Wound Repair Regen. 2017;25(3):526-531

Poster presentation: Session 2. Topic: Tissue Engineering. Code: 5823

Histology and Histopathology
From Cell Biology to Tissue Engineering

Generation of a biomechanically suitable tissue-like stroma for tissue engineering applications

Chato-Astrain J.[1], Carriel V.[1], Oyonarte S.[1,2], Tercero-Hidalgo J.R.[1], España-López A.[3], Fernández-Valadés R.[1,4], Garzón I.[1] and Campos A.[1],

[1]Tissue Engineering Group, Department of Histology, University of Granada and Instituto de Investigación Biosanitaria ibs, Granada, Spain, [2]Cell and Tissue Bank of Granada-Almería, Spain, [3]Craniofacial Malformations and Cleft Lip and Palate Management Unit, University Hospital Virgen de las Nieves, Granada, Spain, [4]Division of Pediatric Surgery, University Hospital Virgen de las Nieves, Granada, Spain

Biomaterials play a key role in tissue engineering as they provide the essential 3D environment to promote cell adhesion, migration and proliferation [1]. Gelatin is a biomaterial whose high collagen content could contribute to the construction of more biomimetic artificial tissues, although its biomechanical properties are typically suboptimal. In this regard, different chemical cross-linking techniques have been used to improve the biomaterials physical properties. The aim of this study is to evaluate the effects of the crosslinker agent glutaraldehyde (GA) applied to gelatin to determine its potential application in tissue engineering.

Gelatin hydrogels were generated by following previously described protocols [2]. After 10 min of stirring, three different GA concentrations (2.5%, 5% and 8%) was added to the gelatin as a crosslinker agent. Macroscopic evaluation included a thermal test performed at 37ºC for 24h. Microscopic characterization was performed with hematoxylin-eosin histological staining and ultrastructural evaluation was analyzed by scanning electron microscopy (SEM).

Our results demonstrated that gels treated with 5% and 8% GA concentrations were thermostable at physiological conditions. However, hydrogels crosslinked with 8% GA showed a heterogeneous appearance. Hematoxylin-eosin staining revealed a majority of basophil structures in all the experimental groups. An organized structure with fibers aligned in parallel was only found in 2.5% GA crosslinked hydrogels, whereas a typical porous pattern was found in the other experimental groups (5% and 8%).

In this study, we tested the potential of crosslinked gelatin in tissue engineering. Optimal conditions were only found in 5% GA crosslinked hydrogels. Still, interesting findings were obtained that could be helpful to design scaffolds with controlled properties regarding its crosslinked degree that would facilitate the production of more suitable tissue-like products for tissue engineering applications.

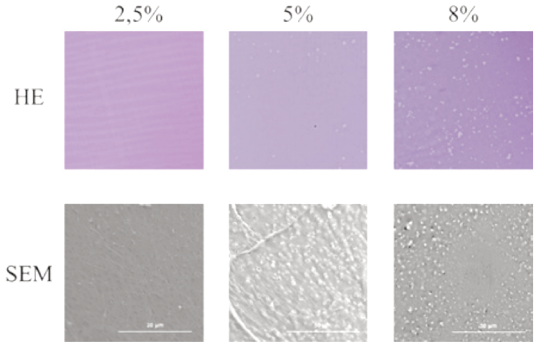

Figure 1: Microscopic analysis of crosslinked gelatin hydrogels. HE: Hematoxylin-eosin staining 200X. SEM: scanning electron microscopy.

Supported by the Spanish Plan Nacional de Investigación Científica, Desarrollo e Innovación Tecnológica (I+D+i) from the Spanish Ministry of Economy and Competitiveness (Instituto de Salud Carlos III), Grants FIS PI17/0393, PI18/0331 and PI18/0332 (cofinanced by FEDER funds, European Union).

[1] O'Brien FJ. Materials Today. 2011;14(3):88-95
[2] Coester CJ, et al. Microencapsul. 2000;17(2):187-93

Poster presentation: Session 2. Topic: Tissue Engineering. Code: 5839

Histology and Histopathology
From Cell Biology to Tissue Engineering

Direct suture versus tubulation for decellularized prostheses grafting in experimental neurectomy repair

Mesuro N.[1], Gayoso S.[2,3], Martín-Ferrero M.A.[4], Rodríguez C.[4], Garrosa M.[2,3] and Gayoso M.J.[2,3]

[1]Hospital of Medina del Campo. Valladolid. Spain, [2]Department of Cell Biology, Histology and Pharmacology, Faculty of Medicine, University of Valladolid, [3]Institute of Neurosciences of Castile y Leon, University of Valladolid, Spain, [4]University Clinical Hospital of Valladolid, Spain

Traumatisms in peripheral nerves are caused by traffic, labour and domestic accidents. In addition to their medical relevance, these lesions have an important economic effect. Complete nervous sections (neurotmesis) usually is not spontaneously recovered because an important retraction between both stumps of the neurectomy occurs. In these cases, it is necessary to bridge the proximal and distal stumps with an adequate prosthesis, a large number of natural or synthetic substances having been used to fill the gap. At the present moment, decellularized nerve segments are the preferred prostheses. An open question is how the union between the graft and the nerve are made, being discussed whether a direct suture or tubulation must be performed

We analysed the regeneration outcome obtained when the graft is direct sutured to the distal and proximal stumps as compared with the tubulation. We used albino Wistar rat handled under the national and international rules for laboratory animals use, housing and care. After being anesthetised, the sciatic nerve was exposed and a 5-mm neurectomy was performed to be repaired by grafting a decellularized isogenic nerve segment. Grafts were harvested from isogenic nerve segment treated with triton x100 and sodium deoxicolate. The tubes were made with polilactic coglicolic acid (PLCG) or Ɛ-caprolactone (Ɛ-CL). Rats were distributed in three groups. The graft in animals in group 1 (G1) consisted in a decellularized isogenic nerve segment directly sutured, whereas in groups 2 (G2) and 3 (G3) the grafts were protected by tubulation with a synthetic tube made out of PLCG (G2) or Ɛ-CL (G3). After a survival time of 3 weeks, the animals were euthanased, the grafts were removed and cut in 2-mm pieces for histological study. The limit of regeneration was decided by the presence of myelinated fibres as seen in semithin cross sections stained with toluidine blue.

The results show that the length reached by the regenerating nerve fibres in animals of the G1 group (8.5 mm.) is higher than in the other groups G2 (4 mm) and G3 (4 mm). Nevertheless, the surgical difficulties of the tubulation technics may contribute to cause worst results in the tubulation experimental groups.

The direct suture of nerve grafts renders better results for neural regeneration than when tubulation of the graft is used, either with PLCG or Ɛ-CL tubes.

Supported by Grants of Junta de Castilla y León for Regenerative Medicine Network and of the University of Valladolid for Neurobiology GIR (2018-19).

Poster presentation: Session 2. Topic: Tissue Engineering. Code: 5840

Histology and Histopathology
From Cell Biology to Tissue Engineering

Multilinear differentiation of adipose tissue-derived mesenchymal stem cells in a model of bone regeneration

Gayoso J.[1], Garrosa M.[1,2], Gayoso S.[1,2] and Gayoso M.J.[1,2]

[1]Department of Cell Biology, Histology and Pharmacology. Faculty of Medicine. University of Valladolid, [2]Institute of Neurosciences of Castile and Leon. University of Valladolid, Spain

The cellular mechanism of bone regeneration is at the base of a large number of medical processes in traumatology, orthopedics, stomatology and plastic surgery. The “critically sized osteotomy model” has been widely used for the study of bone regeneration.

In our experiments, an osteotomy (4 mm in diameter) was performed on Wistar rat jaw and covered with perforated titanium foil (Ti foil) that supported a culture of adipose tissue-derived stem cells (AMSC), this cell culture facing the outer surface of the osteotomy. The Ti foil with the cell culture was applied covering the osteotomy without any fixation system, then the wound sutured by tissue planes. After one month of survival, the animals, under deep anesthesia, were transcardially perfused with 4% buffered paraformaldehyde. Use of animals always followed the legal guidelines concerning the protection of laboratory animals.

Despite the absence of union between the Ti foil and the mandibular bone, bone regeneration occurred closing the osteotomy. Bone growth showed a variety of shapes, from flattened to domed appearance. In these implants, the internal cells differ from a morphology of mesenchymal cells to osteoblasts and osteocytes. The newly formed bone is distinguished from the old bone because the former has more trabecular spaces that are filled with bone marrow tissue. However, their element composition detected by microanalysis is similar. We also found areas with other well differentiated cell types: adipocytes and skeletal muscle cells. The adipocytes showed their characteristic morphology, while the muscle cells had the normal striate appearance, but with a less evident organization of the sarcomeres.

The AMSC in a prosthesis implanted to repair an experimental osteotomy of critical size in rats, produces, after one month, bone growth, but also the cells can differentiate into other non-osteogenic mesenchymal cell types such as adipocytes and striate muscle.

Supported by Grants of Junta de Castilla y León for Regenerative Medicine Network and of the University of Valladolid for Neurobiology GIR (2018-19).

Poster presentation: Session 2. Topic: Tissue Engineering. Code: 5857

Histology and Histopathology
From Cell Biology to Tissue Engineering

Tissue response and tolerance to a designed 3D porous scaffold composed of nanocrystaline carbonate-hydroxyapatite and agarose as preliminary step in bone repair and regeneration

Ortega M.A.[1,2], Coca A.[1], Trejo C.[3], Román J.[4], Peña J.[4], Cabañas M.V.[4], Vallet Regi M.[2,4], García-Honduvilla N.[1,2,5] and Buján J[1,2]

[1]Departments of Medicine and Medical Specialties, Faculty of Medicine and Health Sciences, University of Alcalá, Alcalá de Henares, Madrid, Spain, Ramón y Cajal Institute of Sanitary Research (IRYCIS), Madrid, Spain [2]Networking Biomedical Research Center on Bioengineering, Biomaterials and Nanomedicine (CIBER-BBN), Madrid, Spain, [3]Research Group on Stem Cells and Tissue Engineering (GICTIT), Laboratory of Research in Dentistry Almaraz, FES Iztacala, UNAM, Mexico. [4]Department of Inorganic and Bioinorganic Chemistry, Faculty of Pharmacy, UCM, Institute of Health Research Hospital 12 de Octubre i + 12, Spain, [5]Defense University Center of Military Central Academy (CUD-ACD), Madrid, Spain

Advances in the development and compatibility of biomaterials are crucial milestones in the progress of tissue engineering and, in particular, regenerative medicine. The improvements should be directed especially towards the use of biomaterials as substitutes and/or inductors in the repair of different tissues, such as bone. In this work, we evaluated the tissue response and tolerance to a porous scaffold designed in 3D.

The materials used in this work were generated with nanocrystalline carbonate hydroxyapatite (nCHA) and polysaccharide agarose. The nCHA/agarose macro-porous scaffolds, at a weight ratio of 80/20, were manufactured with a porosity designed using the GELPOR3D method. In this study were used rats Wistar females (n=24) between 4-4.5 months of age and with a weight of 235±15 g. These scaffolds were implanted subcutaneously in rats, which were sacrificed at different times. The animals were slaughtered after 7, 14, 21 and 30 days (6 rats per group). The presence of proinflammatory cells (lymphocytes CD4+ and CD8+) and macrophage cells (ED1+) was determined by immunofluorescence techniques. The samples were stained with vascular endothelial growth factor (VEGF) to determine the angiogenic capacity of the scaffold and Osteopontine (OPN), Osteocalcin (OC), RunX2 and tartrate resistant acid phosphatase (TRAP) to determine the capacity of Osteoinduction of the scaffold. CD4+, CD8+ and ED1+ cells were evaluated as measurements of inflammatory reaction and tolerance.

We observed a certain inflammatory response early after subcutaneous implantation. 3D interconnected porosity increased the integration of the scaffold through the formation of granulation tissue and the generation of a fibrous capsule around the scaffold. The capsule is formed initially by collagen that progressively invades the scaffold, creating a network that supports the settlement of connective tissue and generates a compact structure. The moment of onset of the populations of CD4+ and CD8+ cells is in accordance with the inflammatory response resolved. The emergence of macrophage activity evidences a slow and gradual degradation activity. Degradation began with the agarose component of the scaffold, but the nano-apatite remained intact for up to 30 days. The scaffold's fundamental properties would provide mechanical support and facilitate bone mobilization, which is of great importance in the masticatory system or large bones.

These results support the usefulness of these apatite/agarose scaffolds as a potential material for applications in guided bone regeneration. We can conclude that the 3D scaffolding of nano-apatite/agarose improves connective integration while slowing down the degradation of apatite. Thus, this biomaterial would lead to rapid bone mobilization.

The authors would like to thank the Instituto de Salud Carlos III (PI 15/00978), Ministerio de Economía y Competitividad, (MEC), (Project MAT2015-64831-R) and IMIDEF-2014 and Madrid Provide (B2017/BMD-3804. MITIC-CM) for supporting this work. Funding from the European Research Council through the Advanced Grant VERDI (ERC-2015 AdG Proposal no.694160) is gratefully acknowledged.

Poster presentation: Session 2. Topic: Tissue Engineering. Code: 5858

Histology and Histopathology
From Cell Biology to Tissue Engineering

Polylatic-co-glycolic acid microspheres as a vehicle for the release of antibiotics in a preclinical environment of bone contamination

Ortega M.A.[1,2,6], García-García J.[3], Azua G.[4], Ibarra B.[1], De la Torre B.[1,5], Vázquez-Lasa B.[6,7], Asúnsolo A.[1,2], San Román J.[6,7], Buján J.[1,2,6] and García-Honduvilla N.[1,2,6]

[1]Departments of Medicine and Medical Specialities/Surgery, Medical and Social Sciences, University of Alcala, Spain, [2]Ramón y Cajal Institute of Sanitary Research (IRYCIS), Madrid, Spain, [3]Service of Orthopedic Surgery of University Hospital Principe de Asturias, Madrid, Spain, [4]Service of Traumatology of University Hospital of Guadalajara, Spain, [5]Service of Traumatology of University Hospital Ramón y Cajal, Madrid, Spain, [6]Networking Biomedical Research Center on Bioengineering, Biomaterials and Nanomedicine (CIBER-BBN), Madrid, Spain, [7]Institute of PolymerScience and Technology (ICTP-CSIC), Madrid, Spain

The prevalence rates of hip arthroplasty and knee arthroplasty were 0.83% and 1.52%, respectively. Infection and aseptic loosening, hip instability, and periprosthetic fracture are the most important causes of failure. Joint prostheses are an essential element to improve quality of life. However, prostheses may fail due to several factors, including the most frequent cause, S. aureus infection. The aim of this study is to evaluate the response of bone tissue in rabbits after introduction of a hydroxyapatite-coated titanium rod with a commercial fixative cement (Palacos®) compared to a modified experimental cement (EC) containing polylactic-co-glycolic acid (PLGA) microspheres in the presence or absence of contaminating germs treated or nor with antibiotics.

This study used 20 New Zealand rabbits (2.5-3 kg) divided into 4 groups, depending on the cement (commercial or experimental) and the antibiotic (vancomycin, daptomycin or linezolid) used to control a bone infection caused by S. aureus. The commercial cement is Palacos® R and the experimental cement has been achieved by adding PLGA microspheres to the solid phase of Palacos® R cement. A novel histological staging method based on bone histoarchitecture has been used.

If we compare the control groups, that is, the rod groups without contaminating with contaminated rods, we observed that in the groups of cement without PLGA, the presence of bacteria contributes to a structural loss of the bone. However, in the groups in which cement has been used supplemented with PLGA, it seems that PLGA protects the bone from infection thus maintaining the structure of the bone itself, even in the presence of bacteria. In groups of contaminated rods, when we doped PALACOS cement with antibiotics, the used antibiotics, protected the bone from the action of them, maintaining better bone structure, especially when Vancomycin or Daptomycin were present. The treatment with Linezolid seems to be clearly less effective against this type of bacteria and fails to protect the structure of the bone reaching values as high as the rod with contaminated control PACACOS. When the rod is cemented with PALACOS/PLGA, it seems that the PLGA is sufficient to maintain bone structure regardless of the efficacy of the different antibiotics against the type of bacteria used for the infection. The macrophage increased with the use of EC with PLGA microspheres against the Palacos® commercial cement, including the non-contaminated and contaminated groups. The percentage of macrophages varied exclusively depending on the antibiotic used, and was higher in the vancomycin groups.

The new formulation of PALACOS cement with the introduction of microspheres of PLGA, induces a clear and significant preservation of the bone structure before infection and opens a pathway for the maintenance and prolonged release of local antibiotic.

MINECO: MAT2014-51918-C2-1-R, MAT-201784277-R. MITIC-CM (Community of Madrid); /BMD-3804 and SECOT (Spanish Society of Orthopedic Surgery and Traumatology): 2016/0055.

Poster presentation: Session 2. Topic: Tissue Engineering. Code: 5886

Histology and Histopathology
From Cell Biology to Tissue Engineering

Histological evaluation of the tissue integration process of reticular hybrid meshes following intraperitoneal abdominal wall implant

Pérez-Köhler B.[1,3,4], Gómez-Gil V.[2,3], Rodríguez M.[2,3,4], Benito-Martínez S.[2,3,4], García-Moreno Nisa F.[2,3,4] and Pascual G.[1,3,4]

[1]Department of Medicine and Medical Specialities, Faculty of Medicine and Health Sciences, University of Alcalá, Madrid, Spain, [2]Department of Surgery, Medical and Social Sciences, Faculty of Medicine and Health Sciences, University of Alcalá, Madrid, Spain, [3]Biomedical Networking Research Centre on Bioengineering, Biomaterials and Nanomedicine (CIBER-BBN), Madrid, Spain, [4]Ramón y Cajal Health Research Institute (IRYCIS), Madrid, Spain

Reticular hybrid biomaterials, composed of a reticular mesh coated or interwoven with inert compounds, are being developed as candidate prostheses to be used in intraperitoneal abdominal hernia repair. The aim of the present study is to evaluate the host tissue integration of two reticular hybrid meshes versus two conventional hernia repair materials, in a rabbit intraperitoneal implant model.

Two reticular polypropylene hybrid meshes, TiMESH (titanium-coated) and DynaMesh (polyvinylidene fluoride-interwoven), plus two conventional materials Surgipro (reticular polypropylene) and Preclude (laminar expanded polytetrafluoroethylene) were tested. Meshes (5x3.5 cm) were sutured on the intact parietal peritoneum of New Zealand white rabbits (n=6 each). By day 14, animals were euthanized, and host tissue incorporation was assessed in terms of implant collagenization (picrosirius red staining; collagen type I/III immunolabeling; col1/col3 qRT-PCR) and macrophage reaction (RAM11 immunolabeling).

By day 14, implants receiving Preclude were partially encapsulated due to its laminar architecture. Contrary, the reticular materials Surgipro, TiMESH and DynaMesh exhibited loose neoformed connective tissue that infiltrated the mesh pores surrounding the filaments. At the protein level, the neoperitoneum developed in all these implants displayed a more extensive expression of collagen type III compared to collagen type I. At the gene expression level, the col1 mRNA expression was higher for both hybrid meshes DynaMesh ($p<0.05$) and TiMESH ($p<0.01$) compared to Preclude and Surgipro. For col3, the lowest mRNA expression was recorded for Preclude and the highest for TiMESH, although not reaching statistical relevance. The highest col1/col3 ratio was observed in Preclude implants. Macrophages and foreign body giant cells were limited to the peri-filamentary region with reticular meshes and lined the biomaterial in the laminar material, showing TiMESH the highest macrophage reaction which was only significant compared to Preclude ($p<0.05$).

In this model, the three reticular meshes analyzed showed excellent incorporation into host tissues and similar macrophage response. The two hybrid meshes DynaMesh and TiMESH provoked an increase in mRNA col1 expression in the implant area compared to that of the conventional reticular or laminar materials tested.

Grant SAF2017-89481-P from the Spanish Ministry of Science, Innovation and Universities

Poster presentation: Session 2. Topic: Tissue Engineering. Code: 5922

Histology and Histopathology
From Cell Biology to Tissue Engineering

Alginate-chitosan scaffolds modified by gold nanoparticles for cardiac tissue engineering

Vaquero-Hernández D.[1], Campos-Terán J.[2], García-Lorenzana M.[3] and Beltran N.E.[2]

[1]Licenciatura en Ingeniería Biológica, Departamento de Procesos y Tecnología, Universidad Autónoma Metropolitana-Cuajimalpa, [2]Departamento de Procesos y Tecnología, Universidad Autónoma Metropolitana-Cuajimalpa, [3]Departamento de Biología de la Reproducción, Universidad Autónoma Metropolitana-Iztapalapa. Ciudad de México, México
vaquero.h.daniela@gmail.com, jcampos@correo.cua.uam.mx, mglo@xanum.uam.mx, nbeltran@correo.cua.uam.mx

Alginate-chitosan hydrogels has been used in tissue engineering due to its low toxicity and stability; however, its application for cardiac tissue engineering has not been well reported. Porous scaffolds facilitate rapid nutrient and oxygen transfer and provide a 3D microenvironment for cardiac cells. The aim of this work is to evaluate if gold nanoparticles improve permeability and swelling in alginate-chitosan scaffolds to be used in cardiac tissue engineering.

Two formulations were synthesized, characterized, functionalized with two concentrations of gold nanoparticles (1:10 and 1:20), and compared to evaluate their permeability and swelling. The porous scaffolds were obtained using 2 solutions with different concentrations (alginate 0.75% w/v and chitosan 1.25% w/v, alginate 1% w/v and chitosan 1% w/v) by lyophilization. Permeability and swelling of the scaffolds, with and without nanoparticles, were evaluated. Falling head permeability test was used. Swelling behavior was evaluated by weighing the dry and wet scaffolds.

The combination of chitosan 1.25% w/v and alginate 0.75% w/v had the best permeability ($4.55x10^{-12}\pm3.32x10^{-14}$ m^2) and swelling (1826±380% at 48 h). Swelling had a significant increase with a concentration of 1:20 gold nanoparticles with ultrapure water pre-wetting (2205±248%), whereas PBS buffer pre-wetting has a swelling of 1740±293. A decrease in permeability was observed when more nanoparticles were added to the scaffolds. The combination of chitosan 1.25% w/v and alginate 0.75% w/v had permeability stabilization.

The proposed alginate 0.75% w/v and chitosan 1.25% w/v scaffolds functionalized with 1:20 gold nanoparticles had better permeability and swelling properties for cardiac tissue engineering applications.

Poster presentation: Session 2. Topic: Techniques. Code: 4729

Histology and Histopathology
From Cell Biology to Tissue Engineering

New direct progressive hematoxilin for the application in routine and special techniques

Garrido-Fariña G.I. and López-Pérez V.M.
Laboratory of Support to Histology and Biology, Department of Biological Sciences, School of Higher Studies Cuautitlán, Universidad Nacional Autónoma de México, Mexico
isaurogafa@yahoo.com.mx

Hematoxilins are used to evidencing most of the elements in living matter, some of their variants are still cosmopolitan, these formulations can be used to dye with general methods but only few resist topographical stains, the latter must resist baths in aggressive mixtures of dyes and baths in very acidic solutions. This work presents a new formulation that has been applied in general and special stains with success.

In the LAHB of the FES-Cuautitlán, UNAM, has been applied for 1 year routinely, to collections for teaching and permanent preparations for diagnosis (including decalcification), histochemistry, nuclear contrast in immunohistochemistry and cell culture. The results of the new formula were compared with those obtained routinely using hematoxylin from Harris, Ehrlich and Weigert.

Hematoxylin	1.64 g
Ammonium alum	24.00 g.
Absolute ethyl alcohol	122.00 ml.
Glycerin	32.20 ml.
Distilled water	232.20 ml.
Glacial acetic acid	20.00 ml.
Sodium iodate	0.180 g.

Preparation: The hematoxylin is dissolved in alcohol, the alum in water and heated to 50 °C, the two solutions are mixed, glycerin, iodate, acetic acid is added and it is heated again to 60 °C, cooled quickly by immersion and ilter to dye immediately. Its duration is more than 48 months.

For routine techniques such as eosin and PAS, nuclear staining is between 3 and 5 minutes; for topographic stains (Masson, Gomori, Groat, Gieson, Casson, Pianesse) 20 minutes. For immunohistochemistry it has been diluted up to 1:4 with excellent results. After nuclear dyeing, it is washed with water and the lacquer is stabilized in a 1.7% aqueous solution of lithium carbonate for one minute, washed and can be continued with the chosen technique.

This new formulation was applied in material fixed in different mixtures and was processed by the routine paraffin inclusion method. Resistant nuclear stains were observed in the topographic techniques, great sharpness in the most delicate nuclear structures, simple preparation, avoids in its formulation toxic elements such as mercury and has a prolonged useful life. As time passed (6 months) the aging improved the nuclear staining.

This new formulation has been integrated into the work for diagnosis, research and teaching in our faculty, with good results. Some advantages are: dyed properly and supported all the applied techniques, including trichromic protocols. Dilutions to stain cell culture and immunocytochemistry worked properly. Throughout its testing time, samples of any origin, fixation or processes, such as decalcification, were used. This new variant of hematoxylin formulation favors the nuclear staining process, for routine and topographic techniques.

Poster presentation: Session 2. Topic: Techniques. Code: 5542

Histology and Histopathology
From Cell Biology to Tissue Engineering

Standardization of morphometry and stereology techniques in liver of fish of the species *Astyanax altiparanae*

Pereira B.F.[1] and Pitol D.L.[2]

[1]Federal University of São Paulo - Campus of Diadema - SP – Brazil, [2]University of São Paulo - FORP - Ribeirão Preto - SP - Brazil

In fish, morphological studies are directed to different organs, especially the liver, which is directly affected by several agents such as pollutants, unbalanced feed, toxins, parasites, and microorganisms. This organ is responsible for the detoxification of toxins, drugs, heavy metals, pesticides. Therefore, it is necessary to create methodologies for the study of changes in the structure and morphology of the organ, taking into account quantitative data that can generate more robust results and methodologies more sensitive to variables capable of identifying changes that would hardly be reported in qualitative analysis. Within this scenario, morphometry and stereology emerge as efficient tools for pathological and toxicological studies; however, they require adaptations for experimental models such as fish. So, the data obtained can be reliable and replicable, being one of the main factors to be considered in this type of approach is the number of samples and/or cells, for example, to be measured to have a result as close to reality as possible.

Liver samples from 15 individuals of the species *A. altiparanae* (chosen for being a neotropical model of easy manipulation for pathology and toxicology studies), were fixed in buffered formalin and included in historesin. Initially, the liver samples were measured and fragmented in 1mm portions. Subsequently, 5 fragments from each individual were randomly selected to obtain serial sections and submitted to hematoxylin-eosin reaction. Analyzes of the total number of hepatocytes, relative number or numerical density (Nv), the latter referring to the number of cells per unit volume; cytoplasmic area; diameter, area, and form coefficient of the nucleus and diameter of the capillaries in longitudinal sections were mesured. To obtain the standardization of the number of samples to be used in experiments, the sections of the same fragment, then of different fragments, and finally between different individuals were compared. All these analyses were performed with the help of the ImageJ program. The data were submitted to the Shapiro-Wilk test to verify the normality of the groups and later to ANOVA/Tukey test for parametric data and Kruskal-Wallis/Dunn for non-parametric data to determine the significance of the results.

As samples were extremely homogeneous, both within the same individual and between different individuals. With this initially, taking into account the number of sections to be considered per individual, 6 would be sufficient, both to obtain morphometric and stereological results as well as for statistical analysis; as well as the analyzes of vessels and cells, a sample of 20-50 cells are already representative for the model. Regarding the location in which the fragment should be obtained in the collection, our results showed that this factor does not interfere in the final result, and one fragment per individual is enough.

The neotropical *Astyanax altipanae* model proved to be reliable for morphological tests in toxicology and pathology, as well as the patterns presented here make the results of future experiments more robust and reliable.

Poster presentation: Session 2. Topic: Techniques. Code: 5741

Histology and Histopathology
From Cell Biology to Tissue Engineering

Morphohistochemical investigation of the feeding, digestive and reproductive systems of female dog ticks in rapid feeding stage

Furkim K.C.S.[1], Camargo-Mathias M.I.[1] and Benvindo C.J.[2]

[1]Biology Department, Bioscience Institute, UNESP, Rio Claro, S.P., Brazil, [2]Laboratory of Applied Immunology to Animal Sanity nº 205, Biotechnology Center, UFRGS, Porto Alegre, R.S., Brazil

Rhipicephalus sanguineus is one of the most important hematophagous ectoparasites, having the dog as preferential host, thus living in human dwellings in several regions. In ticks, the feeding process stimulates the synthesis of ecdysteroids, hormones capable of promoting morphophysiological changes in the development of the salivary, intestinal and reproductive systems, especially in females. In this sense, the salivary secretion allows blood feeding by modulating the hemostatic and immune-inflammatory systems of the hosts. The blood ingested by the ectoparasite is digested extracellularly in the midgut lumen, and the nutrients are absorbed by the tissues and systems. Consequently, the females produce oocytes that will originate new individuals.

The study group BCSTM (Brazilian Central of Studies on Ticks Morphology) has been successfully using morphohistological techniques to investigate how ticks are internally organized; therefore, the present study brought unprecedented information on morphohistochemical modifications on the salivary glands, on the midgut and on the ovary of female *R. sanguineus* in rapid feeding stage.

For this, 25 females fed on host rabbits for 4 days. Then, the salivary glands, midgut and ovary of the ticks were removed, fixed and histologically processed.

Hematoxylin-eosin, carbohydrate, protein and calcium markers (PAS: Periodic Acid Schiff, bromophenol blue and von Kossa) showed that the salivary glands presented cells in full secretory activity (glycoprotein and calcium), storing secretory granules in the cytoplasm. The midgut digestive cells were filled with granules, which have the function of digesting the blood. The ovary was in the initial developmental phase, i.e., presenting oocytes I and II stained by the techniques described herein.

Therefore, the results of this study indicate that the bioactives produced in the salivary glands of *R. sanguineus* in this feeding stage favor rapid blood intake and stimulate ovary development. These relevant data signalize that the rapid feeding stage would be the ideal phase to apply strategies to control these ectoparasites, considering that blood feeding inhibition would: a) minimize aggressive host spoliation; b) significantly decrease pathogen transmission (pathogens are carried by the saliva during intense feeding); and c) interfere in the ovary development, inhibiting vitellogenesis, and, consequently, the capacity to generate new individuals.

Financial support: CNPq

Poster presentation: Session 2. Topic: Techniques. Code: 5750

Histology and Histopathology
From Cell Biology to Tissue Engineering

Quantification of protein expression by immunohistology: comparison of two different techniques

Junceda S.[1], Navarro A.[2], Tolivia J.[2], Cruz-Alonso M.[3], Fernández B.[3], Astudillo A.[4] and Pereiro R.[3]

[1]Anatomopathological Service, Hospital Valle del Nalón, Asturias, [2]Department of Morphology and Cell Biology, University of Oviedo, [3]Department of Analytical Chemistry, University of Oviedo, [4]Anatomopathological Service, Hospital Universitario Central de Asturias, España

One of the problems of conventional immunohistochemistry (IHC) approaches is related to the quantitative interpretation of the results, which may vary according to the subjective criteria of the observer. So far, several strategies have been developed using some programs that can help us in the densitometric analysis, but only give values of level instead of concentrations. In contrast, a detection with the LA-ICP-MS technique, that has previously been described, avoids the risks of biased results and also opens the door to obtain absolute concentrations. In this work, the ferroportin (FPN) absolute quantitative distribution in hippocampus, obtained by a previous publicated LA-ICP-MS method, was compared to FPN densitometric analysis provided by conventional IHC localization.

Samples of hippocampus for controls (n=4) and Alzheimer's patients (n=4) were provide by National Network of Biobanks. Tissues were fixed in 4% phosphate-buffered formaldehyde, embedded in paraffin and sectioned. Classical immunohistochemistry (IHC) was performed for FPN in hippocampus sections of 5-μm thickness and visualized with diaminobencidine. Quantitative valuation of the chromogen signal on histological sections was performed using Photoshop and Image Fiji according with a technique published previously by our group. In parallel, AuNanoComplex (AuNC) with 314 gold atoms per AuNC was used to mark the antibody (Ab) in sections in order to achieve an amplified Au detection by LA-ICP-MS. Quantitative images of FPN were obtained after an IHC procedure with AuNCs in CA1 hippocampal region of human brain sections. The proposed format with the AuNCs attached to Ab and the Au detection by LA-ICP-MS made it possible to obtain the absolute quantification of the protein in CA1 selected areas.

Qualitative two dimensional images were obtained by microscopy and LA-ICP-MS for $^{197}Au+$ (FPN) after IHC with Ab-AuNCs bioconjugate. The analysis of human brain tissue provided absolute values (in μg to FPN g-1) in the selected area of the hippocampus (CA1). In the same way, the relative values (arbitrary units of measurement) of the density of labeled FPN in the IHC were obtained in the same area. The combined representation of both values has shown that there is a direct and consistent correspondence.

Although LA-ICP-MS provides more adjusted and real values of the amount of proteins, the technique is still very expensive and inaccessible for many researchers. In this preliminary study, we have demonstrated that the IHC labelling quantification, although providing relative values, is a powerful and reliable tool to study the changes and trends of the quantity of proteins presents in tissue samples in a cheaper and accessible way.

This work was supported by FISS Instituto de Salud Carlos III and FEDER (Fondo Europeo de Desarrollo Regional) (PI15/00601) grant.

Poster presentation: Session 2. Topic: Techniques. Code: 5779

Histology and Histopathology
From Cell Biology to Tissue Engineering

Histological detection of the F-actinin cytoskeleton comparing paraffin-embedded versus frozen sections of xenografted tumors

Garcia-Sanmartin J., Vilariño M. and Martínez A.
Centro de Investigación Biomédica de La Rioja (CIBIR) Logroño, Spain

The cytoskeleton is a dynamic network of protein rods that defines the structure and motility of the cell. The eukaryotic cytoskeleton is composed mainly of microfilaments, intermediate filaments, and microtubules. Microfilaments are composed of linear actin polymers, intermediate filaments are composed of a variety of different fibrilary proteins, and microtubules are structures composed of the globular protein, tubulin. The cytoskeleton contributes to biological processes such as sensing environmental forces, internalizing membrane vesicles, moving over surfaces, and dividing the cell. Beside this, cytoskeleton remodeling is essential for cell invasion and migration, and plays a major role in cancer cell metastasis. So, cytoskeleton changes are crucial to study cancer progression.

The pathology laboratory from hospitals or research centers routinely prepares and preserves tissues through paraffin embedding. Formalin-fixed paraffin-embedded tissue can be stored long term at room temperature whereas frozen tissue can only be stored at -80 °C. Only when a specific stain requires a different type of tissue preservation, samples are prepared and kept through cryopreservation. Therefore, the conservation method must be planned carefully before performing a procedure not to waste time and samples. In this study, we analyzed how the preparation method influences actin detection in human and mouse sections.

A xenograft experiment was set up using human lung cancer cell line A549 injected ($10x10^6$ cells per mouse) into the flank of immunodeficient mice (NOD *scid* gamma). Ten weeks after initial cell injection, tumors were excised, divided in small fragments, and fixed in 10% formalin. Some fragments were paraffin embedded whereas others were cryoprotected and frozen. In addition, kidneys from normal mice were fixed and embedded in the same way to be used as controls. Changes in the organization of actin and tubulin were observed and studied using immunofluorescence and confocal microscopy. F-actinin was labeled with Bodipy-phallacydin.

The actin-binding toxin phallacydin is routinely used to detect the F-actinin in cells in culture. When we tried to do the same thing with paraffin-embedded sections of xenografted tumors, we could not get any specific staining. We hypothesized that the embedding procedure may preclude an adequate binding of the toxin and thus we tested the staining in frozen sections. The phallacydin pattern became intense in the tumor-associated fibroblasts and in the cytoplasm of the tumor cells in samples that had not been subjected to the paraffin embedding, suggesting that this manipulation is detrimental for the toxin binding. To demonstrate that this is a common phenomenon, we also studied mouse kidneys prepared in both ways. Again, staining was only present when using frozen sections. Phallacydin binding sites in the kidney were mainly found in glomerular podocytes and in the brush border and basal membrane of convoluted tubules.

Although Bodipy-phallacydin commercial datasheet information indicates that it can be used in paraffin-embedded samples, we recommend to prepare the tissues through cryopreservation and cryostat sectioning to obtain a more realistic pattern of the F-actinin distribution.

Poster presentation: Session 2. Topic: Tissue Biology. Code: 5709

Histology and Histopathology
From Cell Biology to Tissue Engineering

Co-localization of IGF1 and cholinergic receptors in neurons of the basal forebrain. implication in physiological conditions

Chaves-Coira I.[1] and Núñez A.[1]

[1]Department of Anatomy, Histology and Neuroscience, Medical School, Universidad Autónoma de Madrid, Madrid, Spain

It has been indicated that basal forebrain (BF) is a heterogeneous area that include different nuclei and different neuronal types with distinct projection pattern to the cortex that may control cortical information processing. The BF cholinergic neurons provide the main source of acetylcholine to the cortex. They facilitate cortical activity. These neurons are the first neurons degenerating in some pathological processes such as Alzheimer disease (AD). In Alzheimer patients not only cognition is deteriorated but altered mood (depression) and disturbed arousal (sleep patterns) are commonly present. The insulin-like growth factor I (IGF-I) is also involved in cognition and mood regulation. Taking all these in account our objective is to study if there is a co-localization in the expression of IGF1 receptors in the BF.

C57 mice were used to study the IGF-I and acetylcholine receptor expression in neurons of different BF nuclei. Brains were processed for immunoassay for visualization of cholinergic neurons and IGF-I receptor expression. Brain sections were studied under confocal microscope.

Positive double-labelled immunostaining for cholinergic neurons and IGF1 receptors were found in all different BF nuclei showing a IGF-I ubiquitous expression IGF-I receptors were also observed in non-cholinergic neuronal types.

The co-localization of IGF-I receptors in different neuronal types of the BF may contribute to the pathology observed in neurodegenerative diseases and dysfunctional neuronal activity providing a connection between mood disturbances and cognitive loss in AD.

This work has been supported by the Spanish Ministerio de Economía y Competitividad Grant SAF2016-76462

Poster presentation: Session 2. Topic: Tissue Biology. Code: 5711

Histology and Histopathology
From Cell Biology to Tissue Engineering

Free software applied to automated digital analysis of CD34 expression in human meningioma

Santonja N.[1], Navarro L.[1], Megías J.[2,3], López-Ginés C.[2,3], Cerdá-Nicolás M.[2,3] and San-Miguel T.[2,3]

[1]Consorcio Hospital General Universitario, Servicio de Anatomía Patológica, Valencia, España, [2]Universitat de València, Departamento de Patología, Valencia, España, [3]Instituto de Investigación Hospital Clínico INCLIVA, Valencia, España

Many papers based on Digital Pathology (DP) have been published in recent years. However, DP usually requires multidisciplinary collaboration, including bioinformaticians to develop new software. The aim of this work was to explore free-available software for developing easy-to-use algorithms of DP analysis available to any researcher, without the need of high level computer skills. The second goal was to apply these methods to study CD34-immunostaining in a highly vascularized tumor as the meningioma.

Samples from 50 patients diagnosed of meningioma in HCUV were used to build tissue-microarrays (TMAs). TMAs were sectioned and HE stained. We carried out CD34 immunostaining (Agilent, Spain) and we digitalized the slides with Ventana iScan-HT (Roche Diagnostics). We made a comparison among free-software available in order to find the friendliest one to de-array TMA images. We chose QuPath software and FIJI/ImageJ. In order to find the most accurate way to analyze the CD34 landscape, different macros were developed. Key steps for automation of the process were color deconvolution into DAB/hematoxilyn, *AutoThreshold* with the *MaxEntropy* method, iterations of *dilate/erode* and *fill holes*. Deconvoluted pictures were saved. Particle analysis was made and objects under 400 pixel (diameter <9.2 μm) were not measured. CSV-files were combined and statistical analysis was done by PSPP statistics software.

The files obtained from digital scanners show a limited compatibility, arising from its format and size. Many software was tested. Three softwares were compatibles with almost every scanning system. QuPath was selected because it allows semi-automated de-arraying. It also cooperates with FIJI/ImageJ and allows to save the pixel size for downstream applications. The macros developed analyzed each pack of 50x4 pictures in about 15 minutes. FIJI particle analysis revealed significant differences between grade I-meningiomas and higher grades meningiomas. The main differences were found in the percentage of positive areas, its deviations and in some particle properties as feret-distance or circularity. Analysis of grade I meningiomas, depending on their clinical outcome, also showed statistically significant results, related to standard deviation of the areas measured.

Once de-arraying is made, FIJI automated analysis is easy, fast and it does not require any special hardware. The algorithms here developed can be copy-pasted and applied to any immunohistochemical marker with little modifications according to the shape of the objects generated by the technique. The CD34-positivity automatically measured suggests that grade I meningioma could be better vascularized than higher grade meningiomas. The higher deviation detected in meningiomas that recurred could evidence that their vessels are more angiodisplastic than the ones detected in non-recurrent meningiomas. Further analyses are necessary to improve statistical management of these measurements, but our results suggest a prognostic potential of digital imaging automation in meningioma.

This work has been supported by grant GV/2018/130 from Generalitat Valencia.

Poster presentation: Session 2. Topic: Tissue Biology. Code: 5763

Histology and Histopathology
From Cell Biology to Tissue Engineering

Cumulus cells projections on ZP coated beads

Hamze J.G.[1], Romar R.[2] and Jiménez-Movilla M.[1]

[1]Department of Cell Biology and Histology, School of Medicine, University of Murcia, Campus Mare Nostrum and IMIB-Arrixaca, Murcia, Spain, [2]Department of Physiology, Faculty of Veterinary, University of Murcia, Campus Mare Nostrum and IMIB-Arrixaca, Murcia, Spain

A novel *in vitro* 3D model to study gamete interaction in mammals has been developed in the last years (1,2). The generation of this model could help elucidate the molecular mechanisms of fertilization and gamete interaction, which remains unclear (3,4). During ovulation, the cumulus oocyte complexes (COCs) composed by the oocyte surrounded by a glycoprotein matrix termed zona pellucida (ZP) and cumulus cells are released from the ovary into the female reproductive tract. The cumulus cells communicate with the oocyte by means of gap junctions, paracrine signals, transzonal projections (TZP), and possibly extracellular vesicles (5). The objective of this experiment was to observe if when adding cumulus cells to the 3D model, these cells were able to interact and develop cell projections on the surface of the model.

To obtain the model, porcine recombinant zona pellucida (ZP) proteins (ZP2, ZP3 and ZP4) were conjugated to groups of 30-40 magnetic Sepharose® beads (B). Then, cumulus cells from *in vitro* matured porcine oocytes were co-incubated 24 h with the B_{ZP} to allow its adhesion. After co-incubation period, B_{ZP} surrounded by the attached cumulus cells were fixed in 4% paraformaldehyde and permeabilized with 1% Triton X-100. The samples were stained with Rhodamine Phalloidin 1:50 (v/v) and 0.01 mM Hoechst 33342. Samples were observed in a confocal microscope. Partially denuded porcine *in vitro* matured oocytes were used as a positive control.

All B_{ZP} models ($B_{ZP2,}$ B_{ZP3} and B_{ZP4}) presented more than 89% of the beads with at least one cumulus cell bound. Cell projections grew from cumulus cells to B_{ZP} similar as the TZP observed in all *in vitro* matured oocytes evaluated by confocal microscopy. These results are preliminary.

As a conclusion, this model recreates the size and shape of native porcine oocytes and its layers, the first one with the recombinant ZP proteins and the second one with the cumulus cells. Furthermore, the attached cumulus cells are able to emit projections towards the $B_{ZP.}$ Therefore, this model could be implemented in the future to study gamete interaction under *in vitro* conditions as an alternative to classic *in vitro* experiments.

Supported by MINECO and FEDER (AGL2015-70159-P), Fundación Seneca-Agencia de Ciencia y Tecnología de la Región de Murcia (20887/PI/18, Ayudas a proyectos para el desarrollo de investigación científica y técnica por grupos competitivos).

1. Hamze, JG, et al. Porcine sperm bind to beads conjugated to ZP2 protein under in vitro conditions. Animal Reprod 2016.
2. Hamze JG, et al. In vitro assessment of acrosomal status of boar sperm bound to beads conjugated to ZP proteins. Animal Reprod 2017.
3. Avella MA, et al. A single domain of the ZP2 zona pellucida protein mediates gamete recognition in mice and humans. J Cell Biol. 2014.
4. Yonezawa N, et al. Porcine zona pellucida glycoprotein ZP4 is responsible for the sperm-binding activity of the ZP3/ZP4 complex. Zygote 2012.
5. Del Collado M, et al. Fatty Acid Binding Protein 3 And Transzonal Projections Are Involved In Lipid Accumulation During In Vitro Maturation Of Bovine Oocytes. Sci Rep 2017.

Poster presentation: Session 2. Topic: Tissue Biology. Code: 5786

Histology and Histopathology
From Cell Biology to Tissue Engineering

A scanning electron microscopy study of heifer cervical mucus

Cortés M.E.[1], López-Castro R.[2], González F.[3], Salgado A.M.[4] and Vigil P.[4-6]

[1]Departamento de Ciencias Químicas y Biológicas, Universidad Bernardo O'Higgins, Santiago, Chile, [2]Escuela de Kinesiología, Universidad Bernardo O'Higgins, Santiago, Chile, [3]Departamento de Ciencias Animales, Facultad de Agronomía e Ingeniería Forestal, Pontificia Universidad Católica de Chile, Santiago, Chile, [4]Laboratorio Clínico, Fundación Médica San Cristóbal, Santiago, Chile, [5]Biomedical Division, Reproductive Health Research Institute, Santiago, Chile, [6]Vicerrectoría de Comunicaciones, Pontificia Universidad Católica de Chile Santiago, Chile

Cervical mucus is a heterogeneous mixture of water, electrolytes, plasma, locally derived proteins and mucous glycoproteins (mucins), among other compounds. Its water content is predominant, representing 92-95%. This secretion plays critical roles in the reproductive process of several mammals, facilitating sperm ascent or acting as a filter for sperm, among other functions. Some researchers have reported that cervical mucus ultrastructure comprises a meshwork of parallel fibrillar subunits, while others suggest it comprises a mesh of interconnected filaments. In view of this, the purpose of this work was to study the ultrastructure of heifer cervical mucus.

The animals studied were 6 healthy Holstein Friesian heifers (15 months old) from the herd at the Experimental Station the Faculty of Agronomy and Forestry Engineering of the Pontificia Universidad Católica de Chile has in Pirque (33°40'12.0"S-70°35'05.7"W), Chile. This research considered all aspects concerning animal welfare and the approval of the respective bioethical committee. Samples of cervical mucus were obtained from heifers at oestrus using a 50-mL sterile plastic tube and stored at 4ºC to be analysed later. For SEM procedure, cervical mucus samples were aspirated using cannulae, and they were cut into 1-cm segments and fixed in a solution of 3% pentane-1,5-dial (glutaraldehyde) prepared in Na-cacodylate (0.24 mol/L; pH 7.3), where they were kept at 4°C for 48 h to prevent morphological changes and, thereby, any alterations in the structures under observation. After the fixation period, the cannula segments containing the mucus samples were washed twice for 10 min in distilled water to remove any remains of fixer. Next, the mucus samples contained in the cannula segments were dehydrated by placing them in solutions of increasing propanone (acetone) concentrations (50%, 70%, 95%, 100% and 100% v/v), remaining in each solution for 10 min. Final dehydration was performed using a critical point drying apparatus. Later, cervical mucus samples were gently removed from the cannula segments and mounted on metallic specimen holders to be shaded with palladium-gold for 3 min at 18 mA using a vacuum sputter coater, for subsequent observation through SEM.

Ultrastructures observed for 4 heifers are characterised by having a mesh-like arrangement with a fine latticework. Micrographs clearly showed that, at oestrus stage, the ultrastructure of cervical mucus consists mainly of a three-dimensional mesh of interconnected filaments with a large number of small pores (range: 0.10-1.5 µm). Large and small filaments can be observed, which are interconnected to one another. None of the SEM micrographs revealed arrangements with zones formed by parallel fibrillar subunits in the cervical mucus ultrastructures observed. For 2 heifers, cervical mucus micrographs showed spherical or sponge-like structures which, most probably, correspond to artifacts originated in the critical point drying process or in the metallic coating prior to SEM observation.

Considering the aforementioned results, it can be concluded that the ultrastructure of heifer cervical mucus obtained at oestrus stage consists mainly of a three-dimensional mesh of interconnected filaments in which a large number of small pores are present.

Poster presentation: Session 2. Topic: Tissue Biology. Code: 5787

Histology and Histopathology
From Cell Biology to Tissue Engineering

Four glycoproteins (ZP1, ZP2, ZP3 and ZP4) are expressed in *Mus mattheyi* and *Mus pahari's ovaries: ZP4* pseudogenization is restricted to the subgenus *mus*

Moros-Nicolás C.[1], Chevret P.[2], Veyrunes F.[3], Guillén-Martínez A.[1], Ballesta J.[1], Izquierdo-Rico M.J.[1] and Avilés M.[1]

[1]Department of Cell Biology and Histology, Faculty of Medicine, University of Murcia, Campus Mare Nostrum and IMIB-Arrixaca, Murcia, Spain, [2]Laboratoire de Biométrie et Biologie Evolutive - UMR CNRS 5558, Université Claude Bernard-Lyon 1, Villeurbanne, France, [3]Institut des Sciences de l'Evolution, UMR5554 CNRS/ Université Montpellier II, Montpellier, France

The zona pellucida (ZP) is an extracellular coat that surrounds mammalian oocytes. This matrix is implicated in gamete interaction, induction of the acrosome reaction, block to polyspermy and protection of the preimplantation embryo. In eutherian mammals, this coat is formed by three or four glycoproteins (ZP1 to ZP4). The lab mouse (*Mus musculus,* subgenus *Mus*) has been used as a model to study the ZP since more than 35 years. Its ZP is formed by three glycoproteins (ZP1, ZP2, and ZP3), *ZP4* being a pseudogene. However, four glycoproteins (ZP1, ZP2, ZP3 and ZP4) have been reported in rat oocytes (*Rattus norvegicus*). As the rat and the mouse belong to the same subfamily of rodents (the Murinae), *ZP4* has probably been lost after their divergence around 12 million years ago (MYA).

The aim of our study was to determine when this event took place during the history of the Murinae subfamily.

mRNA expression and proteomic analysis of ZP1, ZP2, ZP3 and ZP4 were performed, in two rodents belonging to the same genus as *Mus musculus*, but different subgenera: *Mus mattheyi* (subgenus *Nannomys*) and *Mus pahari* (subgenus *Coelomys*). Total RNA was isolated from ovaries and cDNA was synthesized with oligo-dT as primer and the amplicons were automatically sequenced. For proteomics, partially purified ZP from 50 ovaries (25 females) were used for HPLC-MS/MS analysis. Full-length of *Mus mattheyi* and *Mus pahari* ZP1 and ZP4 cDNAs were obtained and submitted to GenBank with the following accession numbers (ZP1: MH822869.1; ZP4: MH822867.1) and (ZP1: MH822870.1;

ZP4: MH822868.1) for *Mus mattheyi* and *Mus pahari*, respectively. Moreover, partial amplifications of ZP2 and ZP3 were made in both species to probe the presence of the four transcripts.

The percentage identity between the amplicons and the corresponded sequences in other rodents (*Mus musculus*, *Mus caroli*, *Rattus norvegicus*, etc.) was high (95%-89%). The results showed several peptides corresponding with ZP1 and ZP4 proteins: for ZP1, two peptides were detected in both species, and for ZP4, twelve and six peptides were identified for *Mus mattheyi* and *Mus pahari*, respectively. Obtaining a ZP4 coverage of 30.99% for *Mus mattheyi* and 16.74% for *Mus pahari*.

These results suggest that ZP1, ZP2, ZP3 and ZP4 proteins are expressed in *Mus mattheyi* and *Mus pahari's* ovaries and indicate that *ZP4* pseudogenization is restricted to the subgenus *Mus*, that diverged from the three other subgenera around 6 MYA.

This work has been funded with support from the Spanish MICINN (AGL2015-7159, PGC2018-094781-B- 100) and FEDER.

Poster presentation: Session 2. Topic: Tissue Biology. Code: 5834

Histology and Histopathology
From Cell Biology to Tissue Engineering

Copy number load: quantification and role in high risk neuroblastoma tumors

Fernández-Blanco B.[1], Berbegall A.P.[1,2], Martín-Vañó S.[1,2] and Noguera R.[1,2]

[1]Department of Pathology, Medical School, University of Valencia-INCLIVA, Valencia, Spain, [2]CIBERONC, Madrid, Spain

Neuroblastoma tumor (NBT) is a pediatric tumor predominantly driven by copy number chromosome aberrations. Apart from clinical, and histopathologic information, molecular characterization at diagnosis remains crucial to prognosis. Five-year survival probability within high-risk (HR) patients remains poor. HR group is associated with *MYCN* amplification (MNA) and 11q deletion (11q-). Few other specific alterations such as *ATRX*, *TERT* and *ALK* alterations have been related to HR. Despite all this genetic knowledge, it is not clear what is the influence of the contribution of the genetic net gained and lost material that results from segmental chromosomal aberrations (SCA). Therefore, we aimed to study the contribution of SCA load in a group of primary HR NBT to add valuable information to current patient stratification classifications.

Genomic profiles were analyzed for 132 primary HR NBT SNP array platforms (Illumina and Affymetrix). SCAs (>2Mb) were considered to quantify the kilobases (Kb) of net genetic material. NBT were classified into three groups according to their net of genetic material resulting from the subtraction of lost kb from gained kb: i) balanced, ii) gained or iii) lost. MNA, 11q- and *ATRX* and *TERT* alterations were also considered for subgrouping NBT.

Most of NBT (68%) were classified into net gained group. Compared to net lost group these NBT showed a higher mean of SCA (9 vs 6) and also presented higher absolute net value (202897 vs 77006 kb). This distribution was more pronounced in nonMNA 11q than in MNA non11q-, (73% vs 61% belonged to net gained group respectively). Within these groups, poorly differentiated NBT showed higher net gain than undifferentiated (121763 vs 220653 for nonMNA 11q- and 103390 vs 167486 for MNA non11q-). In non MMA 11q- *ATRX* and *TERT* alterations were mainly present in the net gain group, while the few *TERT* alterations in MNA not11q- (20%) were equally distributed into net gained and lost groups. Net gained and lost genetic material were higher in the absence of *TERT* or *ATRX* alterations and even higher when MNA was absent too. Main difference observed in the frequency of typical SCA between net gain and loss groups was related to a higher presence of 1q gain in net gained nonMNA 11q- NBT and MNA non 11q- NBT compared to net lost of these groups (56% vs 14% and 36% vs 7%).

Net gained and lost genetic material could aid to better define genomic instable groups within HR NBT, since net gain could be related to poor prognosis factors in NBT (high number of SCA, *ATRX* and *TERT* alterations, 1q gain). Study of association with clinical data and patients from net gained and net lost subgroups is warranted and ongoing.

CIBERONC (CB16/12/00484) and FIS (PI17/01558), Institute of Health Carlos III (Madrid) cofounded with ERDF; Association NEN-NicoContraElCáncer 2017-19 (Spain).

Poster presentation: Session 2. Topic: Tissue Biology. Code: 5875

Histology and Histopathology
From Cell Biology to Tissue Engineering

Fractality in crystallisation of heifer cervical mucus

Cortés M.E.[1] and Vigil P.[2,3]

[1]Departamento de Ciencias Químicas y Biológicas, Universidad Bernardo O'Higgins, Santiago, Chile, [2]Biomedical Division, Reproductive Health Research Institute, Santiago, Chile, [3]Vicerrectoría de Comunicaciones, Pontificia Universidad Católica de Chile Santiago, Chile
cortesmanuel@docente.ubo.cl, pvigil@uc.cl

A fractal is defined as a structure comprised of smaller parts that resemble the whole in a smaller scale. During the last decades, fractality has emerged as a feature of the organisation of some complex natural systems. Various biological secretions show fractal-like patterns for their crystallisation phenomena; however, their presence in crystallisations of heifer cervical mucus has been poorly studied. The aim of this study was to assess fractality in crystallisations of heifer cervical mucus.

Samples of cervical mucus were taken from six heifers at oestrus, their crystalline patterns photographed and its morphology analysed using *Fractalyse 2.4.1*.

Among the many images obtained for cervical mucus crystallisations, some of them had highly symmetrical geometric arrangements, possessing zones characterised by arboriform structures, evidencing a remarkable similarity among them. Moreover, fractal dimensions obtained for these zones were similar when analysed by *Fractalyse 2.4.1*.

In summary, this work shows that some patterns of crystallisation of heifer cervical mucus at oestrus possess a fractal-like organisation.

We thank Prof Fernando González DVM (PUCCh) and Mr Roberto Hauyón MSc (UChile) for their valuable comments about this research.

Poster presentation: Session 2. Topic: Tissue Biology. Code: 5889

Histology and Histopathology
From Cell Biology to Tissue Engineering

Quantification of glycosaminoglycans in paired neuroblastoma samples as a prognostic factor of aggressiveness

Tarazona C.[1], López-Carrasco A.[1,2], Burgos-Panadero R.[1,2], Tadeo I.[1,2], Gamero E.[1,2], Navarro S.[1,2] and Noguera R.[1,2]

[1]Department of Pathology, Medical School, University of Valencia/INCLIVA, [2]CIBER of Cancer (CIBERONC), Madrid, Spain

Neuroblastoma (NB) is the most frequent pediatric extracranial solid tumor, being responsible for 8-10% of all childhood malignancies. This embryonal tumor of the sympathetic nervous system is highly heterogeneous with various clinical courses that range from spontaneous regression to aggressive and therapy-resistant progression. Patient's outcome is strongly influenced by genomic aberrations in neuroblastic cells, but the organization and composition of the tumor microenvironment (TME), including the extracellular matrix (ECM) also plays an important role in tumor progression, metastasis and therapeutic resistance. Glycosaminoglycans (GAGs) have an essential role in ECM and are responsible for retaining water and providing viscosity and low compressibility.

The aims of the present study were: i) to look for patterns of a relationship between the content of GAGs of tumoral-ECM in paired-samples; ii) to establish the utility of the tissue microarray tool (TMAs) in digital histopathological analysis, being representative of the complete tumor sections of paraffinized samples (CS-FFPE).

Paired-samples of primary and non-primary NB (relapse, metastasis and post-chemotherapy) of 10 patients were selected. As GAGs content controls, we used 99 primary-NB from patients without known relapse withmore than 65 months of follow-up (C1) and 75 unpaired non-primary NBs (C2). In the case of paired-tumors, we analyzed the GAGs content of the CS-FFPE and also of 1mm^2 cores of TMAs corresponding to areas selected by the pathologist, being *a priori* representative of the FFPE. For the controls, only cores of TMAs were analyzed. A 3 µm section of each TMA core or CS-FFPE was cut and stained with Alcian Blue pH 2.5, a solution used for the histological staining of acidic GAGs that are carboxylated or sulfated. The percentage of stained-area by GAGs was quantified with an algorithm that we programmed and included in Image-ProPlus 6.0, and evaluated by optical microscopy.

We have detected a lower content of GAGs in the primary paired-samples (mean:1,10%, median: 1.0%) than in the C1 group (mean: 3.21%, median:1.62%). Contrary, the non-primary paired-samples (mean: 2.58%, median: 1.0%) and the C2 group (mean: 5.3%, median: 3.7%) had a high amount of GAGs. On the other hand, we have observed that the TMAs' cores are representative of the CS-FFPE in 70% of the cases. The results were validated by optical microscopy evaluation.

The lower density of GAGs in the primary paired-samples have probably contributed to the tumor greater relapse capacity. The high content in GAGs of non-primary tumors (paired and unpaired samples) reflects the characteristics of the different tumor microenviorment niches. A largest cohort of paired-tumors is needed to validate the amount of GAGs as a pronostic parameter. By the other side, the quantification of GAGs by our algorithm was similar to that estimated visually by two researchers, which implies a great validity for the histopathological digital analysis. Finally, our results revealed the TMAs as a representative material, allowing a faster digital-analysis and less use of digital storage space.

CIBERONC (CB16/12/00484) and FIS (PI17/01558), Institute of Health Carlos III (Madrid) cofounded with ERDF; Association NEN-NicoContraElCáncer 2017-19 (Spain).

Poster presentation: Session 2. Topic: Tissue Biology. Code: 5905

Histology and Histopathology
From Cell Biology to Tissue Engineering

Comparison between ZP resistance to trypsin digestion and ZP structure of carnivores (canine and feline) using polarized light microscopy (polscope)

Cots-Rodríguez P.[1], Sánchez-Férez J.[2], Gómez E.[3], López-Fortún N.[1], González-Brusi L.[1], Moros-Nicolás C.[1], Izquierdo-Rico M.J.[1] and Avilés M.[1]

[1]Department of Cell Biology and Histology, University of Murcia, IMIB-Arrixaca CMN, Murcia, Spain, [2]IMFER, Murcia, Spain, [3]SERIDA, Gijón, Spain

The Zona Pellucida (ZP) is a multilaminar matrix surrounding mammalian oocytes and it is involved in relevant roles during folliculogenesis and fertilization. Regarding to carnivores, feline ZP consists of four different glycoproteins (ZP1, ZP2, ZP3 and ZP4) while in canines ZP1 is absent.

The aim of this study was to compare the ZP resistance to trypsin digestion and the ZP structure between feline oocytes (n=50) and canine oocytes (n=30) using Polscope microscopy. Oosight Meta® software (CRI, USA) was used to analyse birefringence and structural parameters of the ZP. The same oocytes were incubated with trypsin solution (5mg/mL in PBS) at 37ºC, and the time required to digest the ZP was recorded. Pearson's correlation between parameters was analysed.

According to ZP resistance to trypsin digestion, canine oocytes required 35.73±0.59 min to be completely digested, compared to the 18.64±0.75 min required by feline oocytes. Using Polscope microscopy, dog oocytes consisted of three differentiated layers (3L), while cat oocytes were classified in two groups depending on the presence of three (3L) or two layers (2L). The thickness of the 3L canine ZP is 21.21±0.87µm, while the thickness of feline ZP is 23.17±1.00µm in 2L oocytes and 28.88±0.87µm in 3L oocytes. Regarding to the relative thickness of layers in 3L oocytes, canine ZP presents a similar inner and outer layer, thicker than the middle layer (IL 43%; ML 15%; OL 42%). In 3L feline oocytes, the outer layer is thicker than the inner and the middle layer (IL 27%; ML 12%; OL 61%). According to birefringence, in both species the inner layer was the most birefringent (feline, 2.03±0.18nm; canine, 4.79±0.78nm), followed by the outer layer (feline, 1.22±0.08nm; canine, 2.50±0.21nm) and the middle layer (feline, 0.29±0.14nm; canine, 0.47±0.01nm). However, in all cases dog ZP was more birefringent than cat ZP. Finally, the birefringence of the inner layer of canine oocytes was correlated (Pearson's correlation 0.70, $p<0.05$) with digestion time, suggesting that there is a linear relationship between both parameters. This correlation was not found in feline oocytes.

In conclusion, despite the fact that carnivore oocytes are similar through light microscopy, the polscope indicates structural differences between species and oocytes of the same species. The reason underlying such differences remains unknown, but it could be related with different protein composition between the two species and perhaps the maturation stage of the oocytes. Further studies are required to confirm these preliminary results.

Supported by MINECO AGL2015-70159-P, FEDER and AGL2016-81890-REDT.

Poster presentation: Session 2. Topic: Tissue Biology. Code: 5706

Histology and Histopathology
From Cell Biology to Tissue Engineering

Osteoarthritis induced by papain and monoiodoacetate in rabbit temporomandibular joints: a microscopic study

Alves N.[1,2,3], Deana N.F.[4], Molinet M.[1,5] and Vasconcelos A.[6]

[1]Master Program in Sciences, mention Morphology, Faculty of Medicine, Universidad de La Frontera, Temuco, Chile, [2]Applied Morphology Research Centre (CIMA), Faculty of Dentistry, Temuco, Chile, [3]Center of Excellence in Surgical and Morphological Research (CEMyQ), Faculty of Medicine, Temuco, Chile, [4]Center for Research in Epidemiology, Economics and Oral Public Health (CIEESPO), Faculty of Dentistry, Universidad de La Frontera, Temuco, Chile, [5]Escuela de Tecnología Médica, Universidad Austral de Chile, Sede Puerto Montt, Chile, [6]Department of Basic Sciences, Faculty of Medicine, Chile

Osteoarthritis (OA) is a chronic, progressive degenerative pathology, characterised by cartilage degradation, formation of osteophytes, narrowing of the joint space, synovitis, remodelling of the subchondral bone, and chronic pain. Many inducers have been used in order to generate morphological alterations similar to OA in animal model, however there are few comparative studies among different inducers. Pre-clinical studies to induce OA in the temporomandibular joints (TMJ) is useful for studying the pathology and testing the effectiveness of new treatments.

The aim of this study was to determine the effectiveness of these two chemical inductors (papain and monoiodoacetate - MIA) in generating microscopic changes compatibles with OA in rabbit TMJ.

Twenty-two adult male rabbits were used in the experiment. The rabbits were divided at random into 3 groups: a control group (n=4) and two experimental groups, MIA (n=9) and papain (n=9). OA induction was carried out by arthrocentesis in both TMJs of the rabbits. An intra-articular injection of 3 mg of MIA dissolved in 50 µl of sterile saline solution was performed in the first experimental group in a single dose; in the second experimental group the papain was administered together with L-cysteine activator, in 3 doses of 0.1 ml of solution 1.6% on days 1, 4 and 7. The progress of the OA was analysed at 15, 30 and 45 days after chemical induction. Histological analysis was carried out of the joint disc and the mandibular condyle. The most evident changes were expressed in the condyle and disc of joints with OA induced by MIA. The severity grade of OA was evaluated by qualitative analysis. For statistical analysis, Kruskal Wallis test, Mann-Whitney U test, Cohen's kappa were used, software SPSS 22.0, considering significance level of 5%.

In the histological analysis of both experimental groups, we observed that the condyles presented fissures, deformation, and loss of joint surface, the chondrocytes lost their morphology and organization. In more advanced stages there was loss of the mid zone of the joint disc. The effects of papain were associated with condyle deformation, disorientation of the chondrocytes in the middle layer, and proliferation in deep zones; there was also an increase in the extracellular matrix. The severity grade of OA presented by the MIA group was higher than the papain group after 45 days of induction.

Both inductors generated changes in the TMJ and its joint surfaces after 15 days of induction. At 45 days after induction, MIA produced a moderate degree of severity, while papain produced slight changes. The MIA is a good chemical inducer that can be used as a suitable model for experiments aimed at inducing OA in TMJ of rabbits.

HISTOLOGY AND HISTOPATHOLOGY

This Journal is supported by

SOCIEDAD ESPAÑOLA DE HISTOLOGIA E INGENIERÍA TISULAR

UNIVERSITY OF MURCIA

University of Murcia

Indexed in: Science Citation Index, Science Citation Index Expanded (SciSearch), Journal Citation Reports/Science Edition, PubMed, Medline, SCOPUS, EMBASE, Chemical Abstracts Service (CAS), Google Scholar, EBSCO, CSA, CAB International, Biological Abstracts, BIOSIS, CAB Abstracts, Current Contents/ Life Sciences, SCImago, Zoological Record

Published by "Sercrisma International S.L." - Murcia, Spain

ISSN 0213-3911

Printed by "Jiménez Godoy, S.A." D.L. MU-33-1986 - Murcia, Spain